AN ABSTRACT OF THE DISSERTATION OF

Sheila A. Kitchen for the degree of Doctor of Philosophy in Zoology presented on January 29, 2016.

Title: Onset and Breakdown of Cnidarian-Dinoflagellate Symbiosis: A Survey of the Host Transcriptomic Response and Characterization of the Sphingosine Rheostat during Symbiont Colonization and Hyperthermal Stress

Abstract approved: _____
Virginia M. Weis

The symbiosis between cnidarians, such as corals and sea anemones, and photosynthetic dinoflagellates belonging to the genus *Symbiodinium* spp. is one of the most productive in the marine environment. This mutualistic endosymbiosis allow reef-building corals to lay down the foundation of coral reef ecosystems, which supports a highly biodiverse community of marine organisms. The relationship between the cnidarian host and algal symbiont changes over time, from the initial contact through symbiont removal. The breakdown of the partnership can be brought on by numerous environmental stressors; most notably by elevated temperatures associated with climate change. The cellular and molecular mechanisms underlying these key events in cnidarian-dinoflagellate symbiosis are still poorly understood. Lipids play a central role in symbiosis by providing cellular structure, energy storage, signaling platforms. Specifically, the signaling lipids from the sphingosine rheostat, sphingosine and sphingosine-1-phosphate (S1P), play a pivotal role in determining cell fate. Increased sphingosine drives apoptotic activity within the cell while S1P promotes cell survival. The research presented in this dissertation addresses (1) the role of signaling sphingolipids at different stages of cnidarian-dinoflagellate symbiosis and (2) the transcriptional patterns of coral larvae undergoing onset of symbiosis while exposed to elevated seawater temperatures. In Chapter 2, the proposed cnidarian sphingosine rheostat model was functionally characterized in the sea anemone *Aiptasia pallida*. This study identified differential response of the sphingosine rheostat with symbiont

recolonization and long-term symbiont maintenance, suggesting a role in host-symbiont interactions. In Chapter 3, a heat stress experiment revealed a biphasic sphingosine rheostat response in *A. pallida* where acute stress inhibits rheostat expression and activity that is recovered and shifted toward cell death with longer-term heat stress. This response was not linked to symbiont loss, but has implications for a more generalized heat stress response for long-term acclimation in cnidarians. In Chapter 4, coral *Acropora digitifera* larvae displayed different phenotypes and transcriptional profiles with the combined stress of elevated temperature and symbiont uptake. Larval survival, symbiont colonization and algal density were highly reduced from this treatment. These transcriptional patterns indicate immune suppression, membrane reorganization and oxidative stress. Furthermore, sphingolipid signaling differed at the onset of heat stress. Overall, the work presented here indicates that the sphingosine rheostat mediates host-symbiont interactions until symbiosis dysfunction and that the determinants of symbiosis can be altered with climate-induced stress.

Onset and Breakdown of Cnidarian-Dinoflagellate Symbiosis: A Survey of the Host Transcriptomic Response and Characterization of the Sphingosine Rheostat during Symbiont Colonization and Hyperthermal Stress

by
Sheila A. Kitchen

A DISSERTATION

submitted to

Oregon State University

in partial fulfillment of
the requirements for the
degree of

Doctor of Philosophy

Presented January 29, 2016
Commencement June 2016

Doctor of Philosophy dissertation of Sheila A. Kitchen presented on January 29, 2016

APPROVED:

Major Professor, representing Zoology

Chair of the Department of Integrative Biology

Dean of the Graduate School

I understand that my dissertation will become part of the permanent collection of Oregon State University libraries. My signature below authorizes release of my dissertation to any reader upon request.

Sheila A. Kitchen, Author

ACKNOWLEDGEMENTS

I would like to express sincere appreciation for the encouragement and support of my advisor, Dr. Virginia Weis. Over the course of my time in the Weis Lab, she continued to "fill my glass" with her optimism and insights. She has made significant strides to improve my scientific communication and deepen my understanding of symbiosis. Furthermore, she provided many opportunities for me to explore my interests leading to a collaboration with researchers in Japan that allowed me to do field work, developing curriculum for invertebrate biology and symbiosis classes and engaging in non-dissertation projects.

I would like to thank my committee members Drs. Jerri Bartholemew, Dee Denver, John Fowler, and Barb Taylor for their feedback and technical assistance throughout my time at OSU. Additionally, I would like to specially thank Drs. Eli Meyer, Chuya Shinzato and Duo Jiang for their significant contributions to my scientific training. Both Eli and Chuya generously allowed me to work in their lab spaces and were instrumental to my bioinformatic training that allowed me to analyze the high-throughput sequencing data in this dissertation and other various collaborative projects. Duo played an important role in building my confidence with statistical analyses of small and big datasets and our conversations contributed greatly to the analyses in Chapter 4.

A special thanks to the Weis Lab members, past and present, that have created a collaborative and productive working environment. From the lab, I would like to recognize Angela Poole, Cammie Crowder, Trevor Tivey and Nate Kirk, all of whom have kept me sane throughout graduate school and research woes. Angela not only made significant contributions to my transition in the lab with training on all things *Aiptasia* and our various collaborative projects, but she has been the most supportive and thoughtful friend outside of the lab. I would like to thank Cammie, Trevor and Nate for allowing me to bother them with scientific and often non-scientific questions. In addition, I would like to thank a couple undergraduates that contributed to my research projects: Jessica Flesher helped with the experimental design and execution of *Aiptasia* bleaching

in Chapter 3 and Jamie Jo McGraw contributed to the *Symbiodinium* RNA extraction protocol in Chapter 2.

Finally, I want to show my appreciation for the continued support from my friends and family during this long process. Their reassurance and optimism in my abilities to succeed did not go unnoticed. I cannot thank them enough for providing happy distractions when I was overwhelmed.

CONTRIBUTION OF AUTHORS

Dr. Angela Z. Poole assisted in the experimental design, collection and analysis of the symbiotic state and colonization qPCR data from Chapter 2. Dr. Poole also significantly contributed to preparation of the Appendix.

Dr. Duo Jiang provided feedback on the statistical approaches used to analyze symbiont colonization, algal density and gene expression data in Chapter 4. Moreover, she performed the analysis of the survival data.

Dr. Saki Harii assisted in both designing and performing the 2013 and 2014 larval colonization experiment. She performed pilot studies in 2013 on temperature tolerance of *A. digitifera* larvae, facilities for rearing adult colonies and larvae, and *Symbiodinium* cultures.

Dr. Noriyuki Satoh provided laboratory equipment, reagents and financial support for high-throughput sequencing at Okinawa Institute of Science and Technology.

Dr. Chuya Shinzato contributed significantly to the design, execution and analysis of the larval colonization experiment in Chapter 4. He assisted in the collection of samples, preparation of sequencing libraries, and provided resources from the *A. digitifera* genome necessary to perform RNASeq.

Dr. Virginia M. Weis contributed significantly to the experimental design of each chapter. She provided equipment, reagents and space to complete Chapters 2 and 3, and computational resources to analyze the data from Chapter 4. In addition, her feedback was influential in the development and writing of each chapter.

TABLE OF CONTENTS

TABLE OF CONTENTS (Continued)

Page

LIST OF FIGURES

LIST OF FIGURES (Continued)

Figure Page

LIST OF FIGURES (Continued)

Figure Page

LIST OF TABLES

LIST OF ABBREVIATIONS

ABC	ATP-binding cassette
AH	aposymbiotic larvae, high temperature
AL	aposymbiotic larvae, low temperature
ANOVA	analysis of variance
A-SMase	acidic sphingomyelinase
ASW	artificial seawater
bicor	biweight midcorrelation
BLAST	basic local alignment search tool
BSE	brine shrimp extract
CAEP	ceramide aminoethylphosphonate
cDNA	complementary DNA
CGRB	Center for Genome Research and Biocomputing
CH	colonized larvae, high temperature
Chl *a*	chlorophyll *a*
CL	colonized larvae, low temperature
C_t	threshold cycle
CTAB	cetyl trimethylammonium bromide
CUBSD	CUB and sushi domain-containing protein
CV	coefficient of variance
DEG	differentially expressed gene
Edg	endothelial differentiation gene
EEF1A1	eukaryotic elongation factor 1, alpha 1
eNOS	endothelial nitric oxide synthase
ERK	extracellular-regulated kinase

LIST OF ABBREVIATIONS (Continued)

ESI MS/MS	electron spray ionization tandem mass spectrometry
FASW	filtered artificial seawater
FSW	filtered seawater
FSWA	filtered seawater + antibiotics
FISH	fluorescent *in situ* hybridization
GAPDH	glyceraldehyde 3-phosphate dehydrogenase
GFP	green fluorescent protein
GLMM	generalized mixed effects model
GLS	glycosphingolipids
GO	Gene Ontology
GOI	gene of interest
GMP	Gisele Muller-Parker *Aiptasia pallida* population
GPCR	G protein-coupled receptor
HPLC	high performance liquid chromatography
HSR	heat stress response
HTS	high-throughput sequencing
ITS	internal transcribed spacer
iNOS	inducible nitric oxide synthase
KEGG	Kyoto Encyclopedia of Genes and Genomes
L10	ribosomal large subunit 10
L12	ribosomal large subunit 12
LC MS/MS	liquid chromatography tandem mass spectrometry
LPA	lysophosphatidic acid
LPP	lipid phosphate phosphohydrolyase

LIST OF ABBREVIATIONS (Continued)

LPS	lipopolysaccharide
MAPK	mitogen-activate protein kinase
MAMP	microbial-associated molecular pattern
MASP	mannose-associated serine protease
NCBI	National Center for Biotechnology Information
NF-κB	nuclear factor kappa-light-chain-enhancer of activated B cells
NO	nitric oxide
NOD	nucleotide-binding oligmerization domain-containing protein
N-SMase	neutral sphingomyelinase
PABP	poly-A binding protein
PBS	phosphate buffered saline
PRR	pattern recognition receptor
PSII	photosystem II
qPCR	quantitative polymerase chain reaction
RACE	rapid amplification of cDNA ends
rDNA	ribosomal DNA
ROS	reactive oxygen species
RNS	reactive nitrogen species
S1P	sphingosine-1-phosphate
S1PR	sphingosine-1-phosphate receptor (1-5)
SGPP	sphingosine-1-phosphate phosphatase
SM	sphingomyelin
SNP	single nucleotide polymorphism
Sph	sphingosine

LIST OF ABBREVIATIONS (Continued)

SPHK	sphingosine kinase
SST	sea surface temperature
TNF	tumor necrosis factor
TRAF	TNF receptor associated factor
VWA	Virginia Weis *Aiptasia pallida* population A
WGCNA	Weighted Gene Co-Expression Network Analysis

1. INTRODUCTION

The symbiosis between cnidarians and photosynthetic dinoflagellates is one of the most important symbioses in marine environments. These partnerships create the foundation of coral reef ecosystems as structural units providing complex and varied habitats for a diverse range of marine organisms. The cnidarian-dinoflagellate endosymbiosis begins with engulfment of free-living dinoflagellates that are subsequently phagocytosed into membrane-bound vesicles called symbiosomes within host endodermal cells lining the gastric cavity (Venn *et al.*, 2008, Wooldridge, 2010, Davy *et al.*, 2012). In the host symbiosomes, the photosynthetic dinoflagellates are efficient at light capture and carbon dioxide fixation thereby producing photosynthate that is donated to the host cells (Kellogg *et al.*, 1983, Patton *et al.*, 1983, Whitehead *et al.*, 2003, Yellowlees *et al.*, 2008, Wooldridge, 2010). In return, the cnidarian host provides a high light environment, a refuge from herbivory, and inorganic nutrient waste that will promote high productivity from the algae (Kellogg *et al.*, 1983, Patton *et al.*, 1983, Whitehead *et al.*, 2003, Yellowlees *et al.*, 2008, Wooldridge, 2010). Wooldridge describes the cnidarian host as 'active farmers' for their ability to optimize energy coupling from their captive symbionts (Wooldridge, 2010). Within cnidarians, symbiosis can range from facultative mutualism, where survival of the cnidarian host is independent of the algal partnership, or obligate mutualism, where survival of the cnidarian host, algae or both are exclusively dependent on living as a unit. In our lab, we study a facultatively symbiotic sea anemone, *Aiptasia pallida* (also known as *Exaiptasia pallida* (Grajales *et al.*, 2014)), as well as a variety of obligately symbiotic corals including the coral model *Acropora digitifera*. Using both systems, I investigated cnidarian immune responses during symbiosis establishment and subsequent effector responses as a result of symbiosis breakdown following an internal and/or external disturbance.

1.1 Initiation and establishment of cnidarian-dinoflagellate symbiosis

Cnidarian innate immunity is an emerging field of study. Immunity is an evolutionarily conserved system divided into the innate immune and adaptive immune systems. Cnidarians and other invertebrates mediate interactions with foreign microbes

and heal wounds with innate immunity, but lack adaptive immune systems found in vertebrates (Palmer *et al.*, 2012, Oren *et al.*, 2013). The innate immune response to invading microorganisms involves an immediate reaction to the presence of a non-self threat or compromised tissue integrity and is separated into three phases: recognition of the microbe, signaling activation of defense mechanisms, and effector responses to remove the microbe (Hoffmann *et al.*, 1999, Palmer *et al.*, 2012). Numerous immune activators such as parasites (Burge *et al.*, 2013), allorecognition (Rosengarten *et al.*, 2011, Puill-Stephan *et al.*, 2012), and infectious disease (Kvennefors *et al.*, 2010, Vidal-Dupiol *et al.*, 2011) can initiate the innate immune response in the cnidarian host. However, innate immunity is not only activated for the removal of threatening microbes, but also facilitates colonization of beneficial microorganisms within the cnidarian host whereby tolerogenic signaling between the host and symbiont promotes suitable living arrangements to form a partnership (Dunn, 2009, Detournay *et al.*, 2012).

There are several phases of symbiosis establishment: (1) host-symbiont contact, (2) symbiont colonization (also known as infection) and (3) sorting of the symbionts within the host (Davy *et al.*, 2012). Initiation of cnidarian symbiosis includes phagocytosis, the same pathway used for digestion and a vital part of cnidarian innate immunity. Phagocytosis is a multi-staged process, starting with recognition and opsonination of the microbial target, to microbe engulfment, and ultimately phagosome-lysosome maturation, leading to microbe destruction. These stages include extensive lipid remodeling, vesicular trafficking, acidification, reactive oxygen species (ROS) production and accumulation of proteolytic enzymes on the lysosome (Steinberg *et al.*, 2008, Nunes *et al.*, 2010). During host-symbiont contact, microbe-associated molecular patterns (MAMPs) on the symbiont trigger pattern recognition receptors (PRRs) on the host that orchestrate cytoskeletal and membrane remodeling events to engulf the algae and create the phagosome, or symbiosome (Dunn, 2009, Davy *et al.*, 2012). Stabilization of the partnership is accomplished through these complex recognition interactions, termed “winnowing” (Nyholm *et al.*, 2004, Dunn *et al.*, 2009). Algae must suppress or evade host innate immune pathways (Chen *et al.*, 2005, Rodriguez-Lanetty *et al.*, 2006, Miller *et al.*, 2007, Dunn, 2009, Kvennefors *et al.*, 2010, Wooldridge, 2010) and defense

mechanisms (Shinzato *et al.*, 2012) to prevent lysosomal fusion and phagosomal maturation. Genomic resources for cnidarians have provided evidence of many host-microbe signaling pathways and cellular responses that are homologous to higher animal systems and suggest similar functionality (Putnam *et al.*, 2007, Chapman *et al.*, 2010, Shinzato *et al.*, 2011, Baumgarten *et al.*, 2015). The underlying mechanisms, however, remain unresolved although there is great interest in discovering how the algae are able to avoid or prevent intracellular digestion and persist within the symbiosome.

1.2 Breakdown of cnidarian-dinoflagellate symbiosis in a changing world

Symbiotic cnidarians are threatened with worldwide decline, primarily due to elevated seawater temperatures caused by global climate change (Hughes *et al.*, 2003, Weis, 2010). Under prolonged heat stress, the cnidarian host undergoes destructive cellular processes that lead to the collapse of their mutualistic symbiosis with *Symbiodinium* spp. resulting in a bleaching event. Bleaching refers to a loss of symbionts and their pigmentation from host tissues (Venn *et al.*, 2008). The typical bleaching threshold is 1-2°C above the mean summer maximum temperature and is predicted to be chronically exceeded over the next 50 years (Hoegh-Guldberg, 1999, Hughes *et al.*, 2003). Bleaching events can result in decreased growth, increased susceptibility to disease and increased coral mortalities, leaving the reef ecosystem at risk of decline (Weis *et al.*, 2008, Weis, 2010). Global reef ecosystems account for 25% of marine biodiversity and have already lost extensive coral cover due to global warming and anthropogenic influences (Roberts *et al.*, 2002). Although the evidence linking climate change to increased coral bleaching is irrefutable (Douglas, 2003, Venn *et al.*, 2008), the sub-cellular events underlying symbiosis dysfunction resulting in symbiont loss remains poorly understood.

Under ambient conditions, the cnidarian-dinoflagellate partnership is highly productive. Nutrients are exchanged between the algal cells and cnidarian host cells promoting a stable partnership (Davy *et al.*, 2012). The partnership is disassembled when environmental changes impair algal photosynthetic capability and consequently nutrient exchange to the host. Specifically, photosystem II (PSII) in the algal photosynthetic machinery is compromised during elevated heat stress, with a dramatic decrease in

efficiency (Warner *et al.*, 1996), and degradation of protein D1, the Achilles heel of PSII (Warner *et al.*, 1999). In addition, the thylakoid membrane damage from elevated temperatures causes an increase in electron transport in PSII while the quantum yield decreases in the reaction center (Tchernov *et al.*, 2004). This results in increased oxygen generation that is then further reduced by photosystem I into ROS (Venn *et al.*, 2008, Weis, 2008). The overabundance of ROS is harmful to both the symbiont and host, causing damage to proteins, DNA and membrane integrity (Venn *et al.*, 2008, Weis, 2008). In addition, both the host (Perez *et al.*, 2006) and *Symbiodinium* spp. (Hawkins *et al.*, 2013) produce nitric oxide, a reactive nitrogen species (RNS), under heat stress. Host protection mechanisms to reduce the effects of cytotoxic ROS and RNS are incapable of managing the dramatic elevations of these harmful byproducts with heat stress (Douglas, 2003, Venn *et al.*, 2008). Therefore, ROS and RNS production have become established components of the coral bleaching response.

Teasing apart the harmful effects of the algae on the cnidarian host in the context of thermal stress has been the focus of many cnidarian symbiosis studies and is an active area of research. The proposed mechanisms for symbiont removal (see the review by Weis (2008)) include host cell detachment (Gates *et al.*, 1992b), exocytosis (Brown *et al.*, 1995, Fang *et al.*, 1997, Fang *et al.*, 1998), programmed cell death (Dunn *et al.*, 2007, Dunn *et al.*, 2009, Detournay *et al.*, 2011, Paxton *et al.*, 2013), autophagy (Dunn *et al.*, 2007, Hanes *et al.*, 2013) and uncontrolled cell death (Dunn *et al.*, 2004) (Fig. 1.1). These different symbiont removal strategies are active in cnidarians with heat stress, but the severity of the stress, the symbiont type, duration of the stress and/or the combination of these interrelated factors can affect which mechanism is prevalent in the bleaching response through time (Weis, 2008). Transcriptional studies on hyperthermal stress in symbiotic cnidarians indicate that components of multiple symbiont removal mechanisms are upregulated and are likely to co-occur (DeSalvo *et al.*, 2008, Starcevic *et al.*, 2010, Kenkel *et al.*, 2013, Pinzón *et al.*, 2015). Despite the numerous studies on cnidarian bleaching mechanisms, our understanding of dynamic molecular and cellular events preceding symbiont loss is still limited.

1.3 Lipids are regulators of symbiosis

Lipids play a central role in symbiosis, providing both cellular structure, compartmentalization and energy storage, but little is known about the role of lipids as cell signalers between the cnidarian host and algal symbiont during symbiosis. In the first study to examine the lipid differences between symbiotic states in *A. pallida,* lipid profiles were found to differ between symbiotic anemones and aposymbiotic anemones, suggesting that that symbiotic anemones are not the sum of host and symbiont, but rather that the lipids present varied as a result of symbiosis (Garrett *et al.,* 2013). Investigating the individual components of the lipid profiles used in lipid metabolism and modification could provide novel information on symbiosis regulation.

The focus of Chapters 2 and 3 is on the role of sphingolipids, a ubiquitous class of membrane lipids composed of a long chain sphingoid-base backbone linked to a fatty acid tail and polar head group (Olivera *et al.,* 2001, Chen *et al.,* 2010), in cnidarian-dinoflagellate symbiosis. Sphingolipids constitute the major lipid component in lipid rafts, which are tightly compacted compartments in the membrane involved in diverse cellular processes including protein and receptor trafficking (Chen *et al.,* 2010, Ali *et al.,* 2011). The biosynthesis of sphingolipids is highly conserved among eukaryotes with key enzymes found in budding yeast *Saccharomyces cerevisiae* (Jenkins *et al.,* 1997, Cowart *et al.,* 2007), sea anemone *Anthopleura elegantissma* (Rodriguez-Lanetty *et al.,* 2006), nematode *Caenorhaditis elegans* (Mendel *et al.,* 2003, Oskouian *et al.,* 2004), fruit fly *Drosophila melanogaster* (Renault *et al.,* 2002, Phan *et al.,* 2007), and Pacific oyster *Crassostrea gigas* (Timmins-Schiffman *et al.,* 2012). Sphingolipids are not only influential in providing cellular structural support but also as essential signaling molecules within cells for stress response, cell proliferation, apoptosis and pathogenesis (Maceyka *et al.,* 2002, Spiegel *et al.,* 2003, Heung *et al.,* 2006). One common evasion strategy of pathogens is the ability to either co-opt or disrupt host sphingolipid metabolism to modulate phagosomal maturation (Steinberg *et al.,* 2008). However, there is little information regarding the function and metabolism of these lipids in invertebrates that form beneficial symbioses.

Building upon other well-studied animal-microbe partnerships, we can draw comparisons from microbial pathogens and parasites that demonstrate evasion tactics by controlling host phagocytosis and immune cellular pathways *via* sphingolipid metabolism (Koul *et al.*, 2004, Heung *et al.*, 2006, Davy *et al.*, 2012). The self-associative properties of glycosphingolipids form lipid rafts that play essential roles in cell adhesion, motility of phagocytes, and microbe recognition through PRR clustering (Miyazaki *et al.*, 1995, Cherukuri *et al.*, 2001, Mañes *et al.*, 2003, Bryan *et al.*, 2015). Disruption of lipid rafts lowered phagocytic uptake of fungi *Cryptococcus* (Bryan *et al.*, 2014) and HIV entry (Dykstra *et al.*, 2003). Furthermore, inhibition of sphingolipid synthesis in the moth *Galleria mellonella* and mice, both models systems to study fungal infections, followed by exposure to the fungal pathogen *Candida albicans* increased mortality in *G. mellonella* (Fallon *et al.*, 2012) and impaired the phagocytosis by macrophages in mice (Tafesse *et al.*, 2015).

Of particular interest to this study is the involvement of sphingosine kinase (SPHK) that produces pro-survival signaling lipid sphingosine-1 phosphate (S1P) in mediating host-microbe interactions. The coupled enzymatic activities of SPHK and S1P phosphatase (SGPP) create the sphingosine rheostat (Cuvillier *et al.*, 1996) (Fig. 1.2) that has a hypothesized role in the maintenance of cnidarian-dinoflagellate symbiosis (Rodriguez-Lanetty *et al.*, 2006, Detournay *et al.*, 2011). Mycobacterial infection of macrophages requires SPHK translocation to the phagosomal membrane to create a pro-inflammatory environment to kill pathogenic and non-pathogenic mycobacteria (Malik *et al.*, 2003, Thompson *et al.*, 2005, Yadav *et al.*, 2006, Prakash *et al.*, 2010). Infected macrophages with the benign *Mycobacterium smegmatis* had increased S1P levels that resulted in elevated RNS generation and tumor necrosis factor α (TNF-α) secretions, both important for reducing infections (Prakash *et al.*, 2010). On the other hand, pathogenic *Mycobacterium tuberculosis* can avoid phagosomal maturation by inhibiting SPHK translocation and activity (Malik *et al.*, 2003, Thompson *et al.*, 2005). The respiratory syncytical virus that is not dependent on phagocytosis for cellular entry, stimulates SPHK activity to generate pro-survival signal S1P, delay host cell death and facilitate viral replication (Monick *et al.*, 2004). Thus, SPHK-mediated response is dependent of the

mode of invasion and signaling modification by the microorganism. These results indicate an activation of SPHK in favor of a pro-inflammatory environment. These are just a few of many examples where the disruption of lipids enhances survival of microorganisms within a host.

In cnidarians, SGPP was downregulated in the symbiotic state of the sea anemone *A. elegantissma*, suggesting a shift in the rheostat toward increased S1P levels and increased cell survival (Rodriguez-Lanetty *et al.*, 2006). Detournay and Weis (2011) incubated *A. pallida* in sphingolipid metabolites and then exposed them to an immune challenge and hyperthermal stress (discussed in detail in Chapters 2 and 3). S1P incubations reduced host RNS production to the immune challenge and reduced bleaching with heat stress (Detournay *et al.*, 2011). The results of these studies suggested that sphingolipid metabolism plays a functional role in cnidarian pathogenesis and symbiosis dysfunction. However, the endogenous sphingolipid metabolism of cnidarians as a response two key events in cnidarian symbiosis, colonization and breakdown, have not been addressed.

1.4 *A. pallida* and *A. digitifera*: Two model systems used to investigate cnidarian-dinoflagellate symbiosis

To investigate the cellular and molecular mechanisms involved in the initiation, establishment and breakdown of symbiosis in cnidarians, I used two model cnidarian systems. First, the anemone *A. pallida* was used to investigate sphingolipid metabolism at a molecular level. *A. pallida* has proven to be a good laboratory model for studying cnidarian symbiosis because it can undergo both asexual and sexual reproduction, grows rapidly in the laboratory, has available molecular resources (Lehnert *et al.*, 2012, Lehnert *et al.*, 2014, Baumgarten *et al.*, 2015) and engages in a facultative mutualistic relationship with *Symbiodinium* spp. similar to those found in corals (Weis *et al.*, 2008, Voolstra, 2013). In addition, *A. pallida* can be maintained in aposymbiotic state, allowing for recolonization experiments.

Second, larvae from the branching coral *A. digitifera* were used to investigate the host phenotypic and transcriptomic changes with the combination of symbiont colonization and elevated temperature. During the 1998 global bleaching event, the

abundance and percent cover of *A. digitifera* adult colonies in Okinawan reefs were completely decimated, and therefore considered a 'loser' of climate change (Loya *et al.*, 2001). However, thermal stress did not affect developmental stages of *A. digitifera* uniformly, with higher survival in juveniles (< 5cm) compared to adult colonies (Loya *et al.*, 2001). A decade later, *A. digitifera* completely recovered pre-bleaching numbers, suggesting that although they might be short-term losers, they can rapidly recover following a bleaching event, most likely from recruitment of larvae from nearby reefs (van Woesik *et al.*, 2011). Therefore, the response of early developmental stages to heat stress is important the resilience of this species. In addition to the differential thermal sensitivity of *A. digitifera* at different developmental stages, spawning is predictable (Richmond, 1990), aposymbiotic larvae that can be reared in the lab, and symbiosis can be established experimentally (Harii *et al.*, 2009). Furthermore, the genome is sequenced (Shinzato *et al.*, 2011).

Using these two cnidarian systems, I addressed how the cnidarian sphingosine rheostat functions during symbiont colonization in *A. pallida* (Chapter 2), how the rheostat changes during environmental disturbance leading to symbiosis dysfunction and collapse in *A. pallida* (Chapter 3) and how *A. digitifera* larvae respond to the onset of symbiosis with hyperthermal stress (Chapter 4).

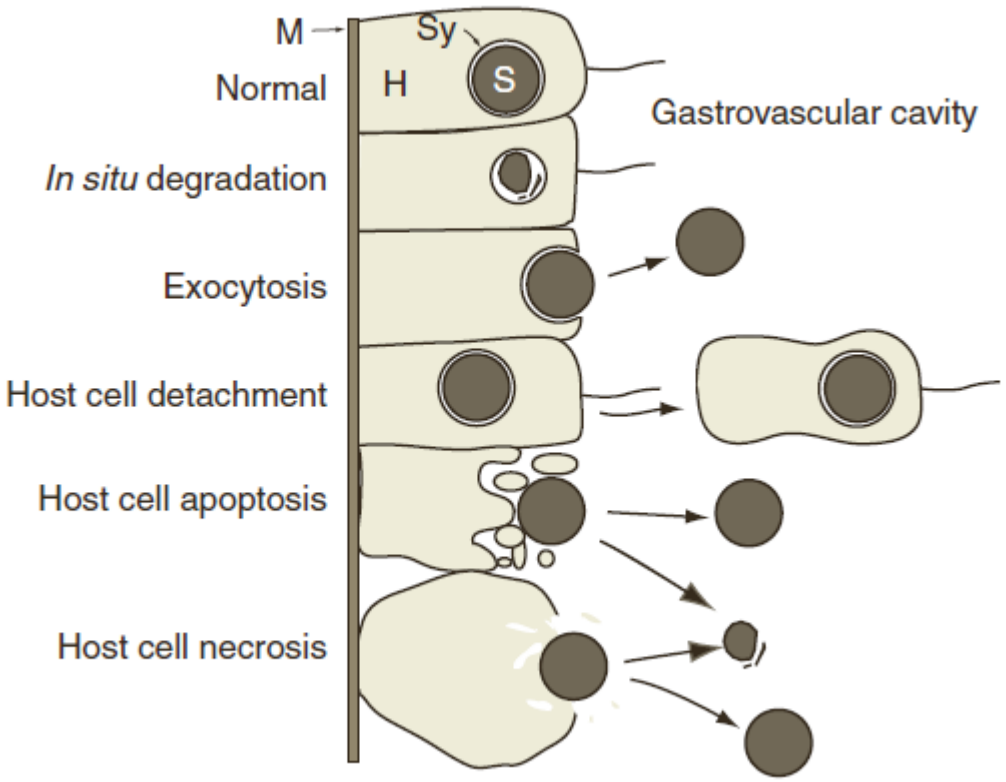

Figure 1.1 Proposed cellular mechanisms for symbiont loss from the cnidarian host tissue. The symbionts are held within the vacuoles or symbiosome (Sy) of host cells that line the gastrovascular cavity. Autophagy of the host cell leads to *in situ* degradation and digestion of symbionts. In host cell exocytosis, intact symbionts are released within the gastrovascular cavity. Detachment of the host cell containing symbionts from the mesoglea (M) and other host cells leads to floating host cells in the gastrovascular cavity. Programmed cell death (apoptosis) and uncontrolled cell death (necrosis) cause the host cell morphology to change and results in loss of unharmed or degraded symbionts. Figure from Weis (2008).

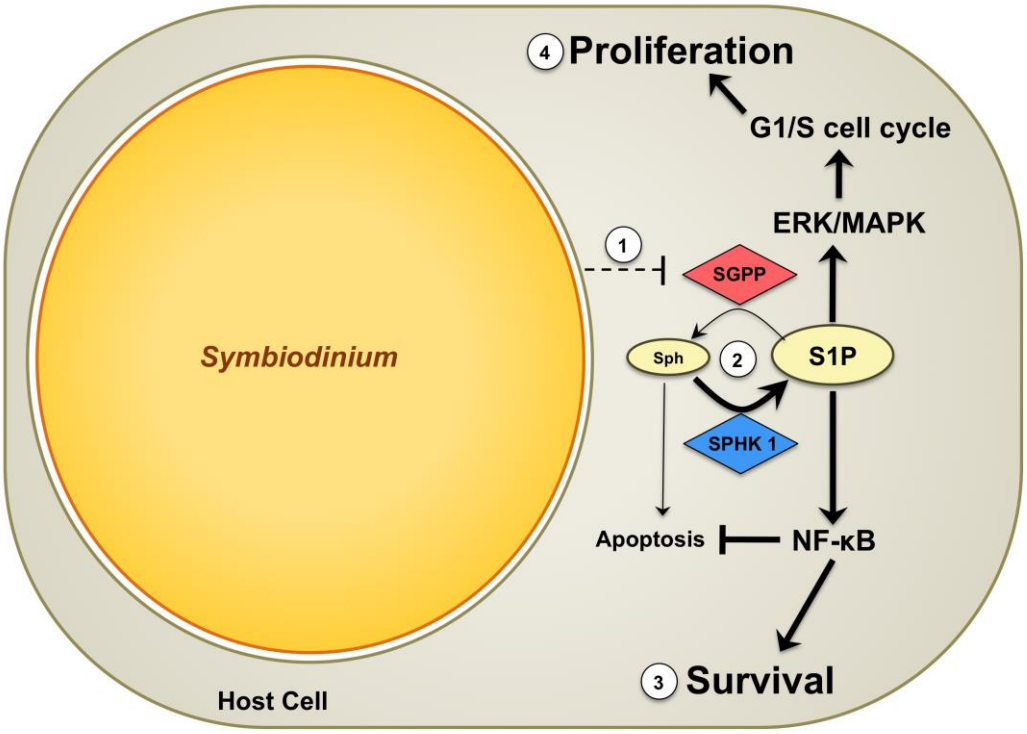

Figure 1.2 Proposed cnidarian sphingosine rheostat model. In the cnidarian-dinoflagellate symbiosis, down-regulation of SGPP from an uncharacterized tolerogenic signal from the alga is predicted to increase S1P over Sph cellular levels (1). Decreased Sph would then suppress sphingolipid-induced apoptosis (2) while increased S1P activates NF-κB (3) which decreases apoptosis and enhances cell survival. Increased levels of S1P also activates ERK/MAPK pathways and expedites G1/S cell cycle transition that promotes cell proliferation (4). This figure was adapted from Rodriguez-Lanetty *et al.* (2006)**.**

1.5 References

Ali, H.Z., Harding, C.R. and Denny, P.W. (2011). Endocytosis and sphingolipid scavenging in *Leishmania mexicana* amastigotes. *Biochemistry Research International* **2012**.

Baumgarten, S., Simakov, O., Esherick, L.Y., Liew, Y.J., Lehnert, E.M., Michell, C.T., *et al.* (2015). The genome of *Aiptasia*, a sea anemone model for coral symbiosis. *Proc. Natl. Acad. Sci. USA* **112,** 11893-11898.

Brown, B., Le Tissier, M. and Bythell, J. (1995). Mechanisms of bleaching deduced from histological studies of reef corals sampled during a natural bleaching event. *Mar. Biol.* **122,** 655-663.

Bryan, A.M., Del Poeta, M. and Luberto, C. (2015). Sphingolipids as regulators of the phagocytic response to fungal infections. *Mediators Inflamm.* **2015,** 640540.

Bryan, A.M., Farnoud, A.M., Mor, V. and Del Poeta, M. (2014). Macrophage cholesterol depletion and its effect on the phagocytosis of *Cryptococcus neoformans*. *J. Vis. Exp.***,** e52432-e52432.

Burge, C.A., Mouchka, M.E., Harvell, C.D. and Roberts, S. (2013). Immune response of the Caribbean sea fan, *Gorgonia ventalina*, exposed to an *Aplanochytrium* parasite as revealed by transcriptome sequencing. *Front. Physiol.* **4**.

Chapman, J.A., Kirkness, E.F., Simakov, O., Hampson, S.E., Mitros, T., Weinmaier, T., *et al.* (2010). The dynamic genome of *Hydra*. *Nature* **464,** 592-596.

Chen, M.C., Hong, M.C., Huang, Y.S., Liu, M.C., Cheng, Y.M. and Fang, L.S. (2005). ApRab11, a cnidarian homologue of the recycling regulatory protein Rab11, is involved in the establishment and maintenance of the *Aiptasia* - *Symbiodinium* endosymbiosis. *Biochem. Biophys. Res. Commun.* **338,** 1607 - 1616.

Chen, Y., Liu, Y., Sullards, M.C. and Merrill Jr, A.H. (2010). An introduction to sphingolipid metabolism and analysis by new technologies. *Neuromolecular Med.* **12,** 306-319.

Cherukuri, A., Dykstra, M. and Pierce, S.K. (2001). Floating the raft hypothesis: lipid rafts play a role in immune cell activation. *Immunity* **14,** 657-660.

Cowart, L.A. and Obeid, L.M. (2007). Yeast sphingolipids: recent developments in understanding biosynthesis, regulation, and function. *Biochim. Biophys. Acta* **1771,** 421-431.

Cuvillier, O., Pirianov, G., Kleuser, B., Vanek, P.G., Coso, O.A., Gutkind, J.S. and Spiegel, S. (1996). Suppression of ceramide-mediated programmed cell death by sphingosine-1-phosphate. *Nature* **381,** 800-803.

Davy, S.K., Allemand, D. and Weis, V.M. (2012). Cell biology of cnidarian-dinoflagellate symbiosis. *Microbiol. Mol. Biol. Rev.* **76,** 229-261.

DeSalvo, M.K., Voolstra, C.R., Sunagawa, S., Schwarz, J.A., Stillman, J.H., Coffroth, M.A., *et al.* (2008). Differential gene expression during thermal stress and bleaching in the Caribbean coral *Montastraea faveolata*. *Mol. Ecol.* **17,** 3952-3971.

Detournay, O., Schnitzler, C.E., Poole, A. and Weis, V.M. (2012). Regulation of cnidarian–dinoflagellate mutualisms: Evidence that activation of a host TGFβ innate immune pathway promotes tolerance of the symbiont. *Dev. Comp. Immunol.* **38,** 525-537.

Detournay, O. and Weis, V.M. (2011). Role of the sphingosine rheostat in the regulation of cnidarian-dinoflagellate symbioses. *Biol. Bull.* **221,** 261-269.

Douglas, A.E. (2003). Coral bleaching - how and why? *Mar. Pollut. Bull.* **46,** 385-392.

Dunn, S.R. (2009). Immunorecognition and immunoreceptors in the Cnidaria. *Isj* **6,** 7-14.

Dunn, S.R., Schnitzler, C.E. and Weis, V.M. (2007). Apoptosis and autophagy as mechanisms of dinoflagellate symbiont release during cnidarian bleaching: every which way you lose. *Proc. R. Soc. Lond., Ser. B: Biol. Sci.* **274,** 3079-3085.

Dunn, S.R., Thomason, J.C., Le Tissier, M.D.A. and Bythell, J.C. (2004). Heat stress induces different forms of cell death in sea anemones and their endosymbiotic algae depending on temperature and duration. *Cell Death Differ.* **11,** 1213-1222.

Dunn, S.R. and Weis, V.M. (2009). Apoptosis as a post-phagocytic winnowing mechanism in a coral-dinoflagellate mutualism. *Environ. Microbiol.* **11,** 268-276.

Dykstra, M., Cherukuri, A., Sohn, H.W., Tzeng, S.-J. and Pierce, S.K. (2003). Location is everything: lipid rafts and immune cell signaling. *Annu. Rev. Immunol.* **21,** 457-481.

Fallon, J., Kelly, J. and Kavanagh, K. (2012) *Galleria mellonella* as a model for fungal pathogenicity testing. In *Host-Fungus Interactions*. Springer, pp. 469-485.

Fang, L.-S., Wang, J.-T. and Lin, K.-L. (1998). The subcellular mechanism of the release of zooxanthellae during coral bleaching. *Proc. Natl. Sci. Counc. Rep. China Pt. B Life Sci.* **22,** 150-158.

Fang, L.S., Huang, S.P. and Lin, K.L. (1997). High temperature induces the synthesis of heat-shock proteins and the elevation of intracellular calcium in the coral *Acropora grandis*. *Coral Reefs* **16,** 127-131.

Garrett, T.A., Schmeitzel, J.L., Klein, J.A., Hwang, J.J. and Schwarz, J.A. (2013). Comparative lipid profiling of the cnidarian *Aiptasia pallida* and its dinoflagellate symbiont. *PLoS One* **8,** e57975.

Gates, R.D., Baghdasarian, G. and Muscatine, L. (1992b). Temperature stress causes host cell detachment in symbiotic cnidarians: Implications for coral bleaching. *Biol. Bull.* **182,** 324-332.

Grajales, A. and Rodriguez, E. (2014). Morphological revision of the genus *Aiptasia* and the family Aiptasiidae (Cnidaria, Actiniaria, Metridioidea). *Zootaxa* **3826,** 55-100.

Hanes, S.D. and Kempf, S.C. (2013). Host autophagic degradation and associated symbiont loss in response to heat stress in the symbiotic anemone, *Aiptasia pallida*. *Invertebr. Biol.* **132,** 95-107.

Harii, S., Yasuda, N., Rodriguez-Lanetty, M., Irie, T. and Hidaka, M. (2009). Onset of symbiosis and distribution patterns of symbiotic dinoflagellates in the larvae of scleractinian corals. *Mar. Biol.* **156,** 1203-1212.

Hawkins, T.D., Bradley, B.J. and Davy, S.K. (2013). Nitric oxide mediates coral bleaching through an apoptotic-like cell death pathway: evidence from a model sea anemone-dinoflagellate symbiosis. *FASEB J.* **27,** 4790-4798.

Heung, L.J., Luberto, C. and Del Poeta, M. (2006). Role of sphingolipids in microbial pathogenesis. *Infect. Immun.* **74,** 28-39.

Hoegh-Guldberg, O. (1999). Climate change, coral bleaching and the future of the world's coral reefs. *Marine and Freshwater Research* **50,** 839-866.

Hoffmann, J.A., Kafatos, F.C., Janeway, C.A. and Ezekowitz, R.A.B. (1999). Phylogenetic perspectives in innate immunity. *Science* **284,** 1313-1318.

Hughes, T.P., Baird, A.H., Bellwood, D.R., Card, M., Connolly, S.R., Folke, C., *et al.* (2003). Climate change, human impacts, and the resilience of coral reefs. *Science* **301,** 929-933.

Jenkins, G.M., Richards, A., Wahl, T., Mao, C., Obeid, L. and Hannun, Y. (1997). Involvement of yeast sphingolipids in the heat stress response of *Saccharomyces cerevisiae*. *J. Biol. Chem.* **272,** 32566-32572.

Kellogg, R.B. and Patton, J.S. (1983). Lipid droplets, medium of energy exchange in the symbiotic anemone *Condylactis gigantea*: a model coral polyp. *Mar. Biol.* **75,** 137-149.

Kenkel, C., Meyer, E. and Matz, M. (2013). Gene expression under chronic heat stress in populations of the mustard hill coral (*Porites astreoides*) from different thermal environments. *Mol. Ecol.* **22,** 4322-4334.

Koul, A., Herget, T., Klebl, B. and Ullrich, A. (2004). Interplay between mycobacteria and host signalling pathways. *Nat Rev Micro* **2,** 189-202.

Kvennefors, E.C.E., Leggat, W., Kerr, C.C., Ainsworth, T.D., Hoegh-Guldberg, O. and Barnes, A.C. (2010). Analysis of evolutionarily conserved innate immune components in coral links immunity and symbiosis. *Dev. Comp. Immunol.* **34,** 1219-1229.

Lehnert, E.M., Burriesci, M.S. and Pringle, J.R. (2012). Developing the anemone *Aiptasia* as a tractable model for cnidarian-dinoflagellate symbiosis: the transcriptome of aposymbiotic *A. pallida*. *BMC Genomics* **13,** 271.

Lehnert, E.M., Mouchka, M.E., Burriesci, M.S., Gallo, N.D., Schwarz, J.A. and Pringle, J.R. (2014). Extensive differences in gene expression between symbiotic and aposymbiotic Cnidarians. *G3: Genes| Genomes| Genetics* **4,** 277-295.

Loya, Sakai, Yamazato, Nakano, Sambali and Van, W. (2001). Coral bleaching: the winners and the losers. *Ecol. Lett.* **4,** 122-131.

Maceyka, M., Payne, S.G., Milstien, S. and Spiegel, S. (2002). Sphingosine kinase, sphingosine-1-phosphate, and apoptosis. *Biochim. Biophys. Acta* **1585,** 193 - 201.

Malik, Z.A., Thompson, C.R., Hashimi, S., Porter, B., Iyer, S.S. and Kusner, D.J. (2003). Cutting edge: *Mycobacterium tuberculosis* blocks Ca2+ signaling and phagosome maturation in human macrophages via specific inhibition of sphingosine kinase. *J. Immunol.* **170,** 2811-2815.

Mañes, S., del Real, G. and Martínez-A, C. (2003). Pathogens: raft hijackers. *Nat. Rev. Immunol.* **3,** 557-568.

Mendel, J., Heinecke, K., Fyrst, H. and Saba, J.D. (2003). Sphingosine phosphate lyase expression is essential for normal development in *Caenorhabditis elegans*. *J. Biol. Chem.* **278,** 22341-22349.

Miller, D.J., Hemmrich, G., Ball, E.E., Hayward, D.C., Khalturin, K., Funayama, N., *et al.* (2007). The innate immune repertoire in Cnidaria-ancestral complexity and stochastic gene loss. *Genome Biol.* **8,** R59.

Miyazaki, Y., Oka, S., Yamaguchi, S., Mizuno, S. and Yano, I. (1995). Stimulation of phagocytosis and phagosome-lysosome fusion by glycosphingolipids from *Sphingomonas paucimobilis*. *J. Biochem.* **118,** 271-277.

Monick, M.M., Cameron, K., Powers, L.S., Butler, N.S., McCoy, D., Mallampalli, R.K. and Hunninghake, G.W. (2004). Sphingosine kinase mediates activation of extracellular signal–related kinase and Akt by Respiratory Syncytial Virus. *Am. J. Respir. Cell Mol. Biol.* **30,** 844-852.

Nunes, P. and Demaurex, N. (2010). The role of calcium signaling in phagocytosis. *J. Leukoc. Biol.* **88,** 57-68.

Nyholm, S.V. and McFall-Ngai, M. (2004). The winnowing: establishing the squid–*Vibrio* symbiosis. *Nat. Rev. Microbiol.* **2,** 632-642.

Olivera, A. and Spiegel, S. (2001). Sphingosine kinase: a mediator of vital cellular functions. *Prostaglandins Other Lipid Mediat.* **64,** 123-134.

Oren, M., Paz, G., Douek, J., Rosner, A., Amar, K.O. and Rinkevich, B. (2013). Marine invertebrates cross phyla comparisons reveal highly conserved immune machinery. *Immunobiology* **218,** 484-495.

Oskouian, B. and Saba, J.D. (2004). Death and taxis: what non-mammalian models tell us about sphingosine-1-phosphate. *Semin. Cell Dev. Biol.* **15,** 529-540.

Palmer, C.V. and Traylor-Knowles, N. (2012). Towards an integrated network of coral immune mechanisms. *Proc. R. Soc. Lond., Ser. B: Biol. Sci.* **279,** 4106-4114.

Patton, J.S. and Burris, J.E. (1983). Lipid synthesis and extrusion by freshly isolated zooxanthellae (symbiotic algae). *Mar. Biol.* **75,** 131-136.

Paxton, C.W., Davy, S.K. and Weis, V.M. (2013). Stress and death of cnidarian host cells play a role in cnidarian bleaching. *J. Exp. Biol.* **216,** 2813-2820.

Perez, S. and Weis, V. (2006). Nitric oxide and cnidarian bleaching: an eviction notice mediates breakdown of a symbiosis. *J. Exp. Biol.* **209,** 2804-2810.

Phan, V.H., Herr, D.R., Panton, D., Fyrst, H., Saba, J.D. and Harris, G.L. (2007). Disruption of sphingolipid metabolism elicits apoptosis-associated reproductive defects in *Drosophila*. *Dev. Biol.* **309,** 329-341.

Pinzón, J.H., Kamel, B., Burge, C.A., Harvell, C.D., Medina, M., Weil, E. and Mydlarz, L.D. (2015). Whole transcriptome analysis reveals changes in expression of immune-related genes during and after bleaching in a reef-building coral. *R. Soc. Open Sci.* **2,** 140214.

Prakash, H., Luth, A., Grinkina, N., Holzer, D., Wadgaonkar, R., Gonzalez, A.P., *et al.* (2010). Sphingosine kinase-1 (SphK-1) regulates *Mycobacterium smegmatis* infection in macrophages. *PLoS One* **5,** e10657.

Puill-Stephan, E., Seneca, F.O., Miller, D.J., van Oppen, M.J. and Willis, B.L. (2012). Expression of putative immune response genes during early ontogeny in the coral *Acropora millepora*. *PLoS One* **7,** e39099.

Putnam, N.H., Srivastava, M., Hellsten, U., Dirks, B., Chapman, J., Salamov, A., *et al.* (2007). Sea anemone genome reveals ancestral eumetazoan gene repertoire and genomic organization. *Science* **317,** 86-94.

Renault, A.D., Starz-Gaiano, M. and Lehmann, R. (2002). Metabolism of sphingosine 1-phosphate and lysophosphatidic acid: a genome wide analysis of gene expression in *Drosophila*. *Mech. Dev.* **119,** S293-S301.

Richmond, R.H. (1990). Reproduction and recruitment of corals : comparisons among the Caribbean, the tropical Pacific, and the Red Sea. *Mar. Ecol. Prog. Ser.* **60,** 185-203.

Roberts, C.M., McClean, C.J., Veron, J.E.N., Hawkins, J.P., Allen, G.R., McAllister, D.E., *et al.* (2002). Marine biodiversity hotspots and conservation priorities for tropical reefs. *Science* **295,** 1280-1284.

Rodriguez-Lanetty, M., Phillips, W. and Weis, V. (2006). Transcriptome analysis of a cnidarian - dinoflagellate mutualism reveals complex modulation of host gene expression. *BMC Genomics* **7,** 23.

Rosengarten, R.D. and Nicotra, M.L. (2011). Model systems of invertebrate allorecognition. *Curr. Biol.* **21,** R82-R92.

Shinzato, C., Hamada, M., Shoguchi, E., Kawashima, T. and Satoh, N. (2012). The repertoire of chemical defense genes in the coral *Acropora digitifera* genome. *Zool. Sci.* **29,** 510-517.

Shinzato, C., Shoguchi, E., Kawashima, T., Hamada, M., Hisata, K., Tanaka, M., *et al.* (2011). Using the *Acropora digitifera* genome to understand coral responses to environmental change. *Nature* **476,** 320-323.

Spiegel, S. and Milstien, S. (2003). Sphingosine-1-phosphate: An enigmatic signaling lipid. *Nat. Rev. Mol. Cell Biol.* **4,** 397 - 407.

Starcevic, A., Dunlap, W.C., Cullum, J., Shick, J.M., Hranueli, D. and Long, P.F. (2010). Gene expression in the scleractinian Acropora microphthalma exposed to high solar irradiance reveals elements of photoprotection and coral bleaching. *PLoS One* **5,** e13975.

Steinberg, B.E. and Grinstein, S. (2008). Pathogen destruction versus intracellular survival: the role of lipids as phagosomal fate determinants. *J. Clin. Invest.* **118,** 2002-2011.

Tafesse, F.G., Rashidfarrokhi, A., Schmidt, F.I., Freinkman, E., Dougan, S., Dougan, M., *et al.* (2015). Disruption of sphingolipid biosynthesis blocks phagocytosis of *Candida albicans*. *PLoS Path.* **11,** e1005188.

Tchernov, D., Gorbunov, M.Y., de Vargas, C., Yadav, S.N., Milligan, A.J., Häggblom, M. and Falkowski, P.G. (2004). Membrane lipids of symbiotic algae are diagnostic of sensitivity to thermal bleaching in corals. *Proc. Natl. Acad. Sci. USA* **101,** 13531-13535.

Thompson, C.R., Iyer, S.S., Melrose, N., VanOosten, R., Johnson, K., Pitson, S.M., *et al.* (2005). Sphingosine kinase 1 (SK1) is recruited to nascent phagosomes in human

macrophages: inhibition of SK1 translocation by *Mycobacterium tuberculosis*. *J. Immunol.* **174,** 3551-3561.

Timmins-Schiffman, E. and Roberts, S. (2012). Characterization of genes involved in ceramide metabolism in the Pacific oyster (*Crassostrea gigas*). *BMC Res. Notes* **5,** 502.

van Woesik, R., Sakai, K., Ganase, A. and Loya, Y. (2011). Revisiting the winners and the losers a decade after coral bleaching. *Mar. Ecol. Prog. Ser.* **434,** 67-76.

Venn, A.A., Loram, J.E. and Douglas, A.E. (2008). Photosynthetic symbioses in animals. *J. Exp. Bot.* **59,** 1069-1080.

Vidal-Dupiol, J., Ladrière, O., Destoumieux-Garzón, D., Sautière, P.-E., Meistertzheim, A.-L., Tambutté, E., *et al.* (2011). Innate immune responses of a scleractinian coral to vibriosis. *J. Biol. Chem.* **286,** 22688-22698.

Voolstra, C.R. (2013). A journey into the wild of the cnidarian model system *Aiptasia* and its symbionts. *Mol. Ecol.* **22,** 4366-4368.

Warner, M.E., Fitt, W.K. and Schmidt, G.W. (1996). The effects of elevated temperature on the photosynthetic efficiency of zooxanthellae *in hospite* from four different species of reef coral: a novel approach. *Plant, Cell Environ.* **19,** 291-299.

Warner, M.E., Fitt, W.K. and Schmidt, G.W. (1999). Damage to photosystem II in symbiotic dinoflagellates: a determinant of coral bleaching. *Proc. Natl. Acad. Sci. USA* **96,** 8007-8012.

Weis, V.M. (2008). Cellular mechanisms of Cnidarian bleaching: stress causes the collapse of symbiosis. *J. Exp. Biol.* **211,** 3059-3066.

Weis, V.M. (2010). The susceptibility and resilience of corals to thermal stress: adaptation, acclimatization or both? *Mol. Ecol.* **19,** 1515-1517.

Weis, V.M., Davy, S.K., Hoegh-Guldberg, O., Rodriguez-Lanetty, M. and Pringle, J.R. (2008). Cell biology in model systems as the key to understanding corals. *Trends Ecol. Evol.* **23,** 369-376.

Whitehead, L.F. and Douglas, A.E. (2003). Metabolite comparisons and the identity of nutrients translocated from symbiotic algae to an animal host. *J. Exp. Biol.* **206,** 3149-3157.

Wooldridge, S.A. (2010). Is the coral-algae symbiosis really 'mutually beneficial' for the partners? *Bioessays* **32,** 615-625.

Yadav, M., Clark, L. and Schorey, J.S. (2006). Macrophage's proinflammatory response to a mycobacterial infection is dependent on sphingosine kinase-mediated activation of

phosphatidylinositol phospholipase C, protein kinase C, ERK1/2, and phosphatidylinositol 3-kinase. *J. Immunol.* **176,** 5494-5503.

Yellowlees, D., Rees, T.A.V. and Leggat, W. (2008). Metabolic interactions between algal symbionts and invertebrate hosts. *Plant, Cell Environ.* **31,** 679-694.

2. SPHINGOLIPIDS IN CNIDARIAN-DINOFLAGELLATE INTERACTIONS: INVESTIGATING THE ROLE OF THE SPHINGOSINE RHEOSTAT DURING ONSET OF SYMBIOSIS AND AT STEADY-STATE IN *AIPTASIA PALLIDA*

Sheila A. Kitchen

Angela Z. Poole

Virginia M. Weis

Formatted for *Cellular Microbiology*

John Wiley and Sons, INC.

350 Main Street

Malden, MA 02148

USA

2.1 Summary

Lipids play a central role in symbiosis, providing both cellular structure and energy storage, but little is known about how signaling lipids participate in the symbiosis between cnidarians and dinoflagellates of the genus *Symbiodinium.* The balance of signaling lipids, sphingosine (Sph) and sphingosine-1-phosphate (S1P) through catalytic activities of sphingosine kinase (SPHK) and sphingosine-1-phosphatase (SGPP) creates the sphingosine rheostat. Exogenously applied sphingolipids can alter the cnidarian-*Symbiodinium* partnership, however endogenous host regulation of the rheostat in symbiosis has not been characterized. In this study, we examined rheostat function in the sea anemone *Aiptasia pallida* in different symbiotic states and during host recolonization by symbionts. For recolonization, aposymbiotic *A. pallida* were inoculated with *Symbiodinium* and relative symbiont uptake was quantified using qRT-PCR. Through a survey of the *A. pallida* genome, 54 genes involved in sphingolipid metabolism and signaling were identified, including complete *de novo* synthesis, salvage, rheostat and degradation pathways. *A. pallida* rheostat enzymes, AP-SPHK and AP-SGPP, were further characterized for their function in recognition and establishment of cnidarian-*Symbiodinium* symbiosis by measuring gene expression, protein production, and sphingolipid metabolites. Symbiotic anemones had higher basal AP-SPHK expression and protein levels than did aposymbiotic animals, suggesting differing physiological demands between symbiotic and aposymbiotic lifestyles. AP-SPHK and AP-SGPP were upregulated over the first day of symbiont recolonization suggesting a potential role of the rheostat in host-symbiont recognition. Differences in S1P and Sph lipid levels were not observed until three days post-inoculation. Collectively, these data support the regulatory role of sphingolipid signaling in cnidarian-*Symbiodinium* symbiosis and symbiont colonization.

2.2 Introduction

The symbiosis between cnidarians and photosynthetic dinoflagellates of the genus *Symbiodinium* is one of the most important symbioses in the marine environment. These partnerships create the foundation of coral reef ecosystems as structural units that provide complex and varied habitats for a diverse range of marine organisms (Bellwood *et al.*,

2001). The cnidarian-*Symbiodinium* endosymbiosis begins with host cnidarian phagocytosis of *Symbiodinium* spp. into membrane-bound vesicles called symbiosomes within host gastrodermal cells lining the gastric cavity (Venn *et al.*, 2008, Wooldridge, 2010, Davy *et al.*, 2012). The symbiosome compartment occupies a large volume of the host cell (Davy *et al.*, 2012), requiring substantial investment in remodeling and biosynthesis of host lipids (Rodriguez-Lanetty *et al.*, 2006, Steinberg *et al.*, 2008, Garrett *et al.*, 2013). These lipids play integral roles in regulating phagocytosis and symbiosis including in recruitment and retention of phagocytic proteins (Yeung *et al.*, 2007, Flannagan *et al.*, 2012), providing cellular structure and energy storage (Dunn *et al.*, 2012, Garrett *et al.*, 2013, Revel *et al.*, 2016), and in generation and transduction of cellular signals (Yeung *et al.*, 2007, Steinberg *et al.*, 2008). Fatty-acid composition (Yamashiro *et al.*, 1999, Imbs *et al.*, 2010, Dunn *et al.*, 2012, Imbs, 2014, Revel *et al.*, 2016) and endosymbiosis-specific lipid bodies (Simon *et al.*, 1967, Kellogg *et al.*, 1983, Peng *et al.*, 2011, Chen *et al.*, 2015) have been investigated in symbiotic cnidarians, but these studies provide very little information on lipid classes or the role of lipids in signaling between the cnidarian host and algal symbiont.

Sphingolipids are a family of membrane lipids that provide important cellular structure, and also act as signaling molecules that mediate host-microbe interactions (Heung *et al.*, 2006, An *et al.*, 2011, Bryan *et al.*, 2015). These lipids are composed of a long-chain sphingoid base linked to a fatty acid tail and polar head group, which can be modified to form an array of complex sphingolipids through *de novo* synthesis and complex hydrolysis (Fig. 2.1) (Olivera *et al.*, 2001, Chen *et al.*, 2010). The assembly of sphingolipids with cholesterol, receptors and signaling molecules forms sphingolipid-enriched platforms, known as lipid rafts or microdomains, that act as membrane-reactive centers for diverse cellular processes (Hakomori *et al.*, 1998, Dykstra *et al.*, 2003). The biological outcomes of sphingolipid signaling are numerous, including cell proliferation, apoptosis, inflammation and pathogenesis (Maceyka *et al.*, 2002, Spiegel *et al.*, 2003, Heung *et al.*, 2006). Interactions between an animal host and microbe can be regulated by sphingolipids derived from one or both partners. In the host, sphingolipids are part of a rapid innate immune response that responds to non-self molecules, where they participate

in distinguishing beneficial from harmful microbes (Cinque *et al.*, 2003, Rivera *et al.*, 2008, Spiegel *et al.*, 2011, Bryan *et al.*, 2015). To evade host immune responses or to obtain a new function to enhance survival and promote virulence, microorganisms lacking sphingolipids can co-opt host lipids (reviewed by Heung *et al.* (2006)) or acquire their own *de novo* synthesis machinery through horizontal gene transfer from their host (Wilson *et al.*, 2005). In other cases, both microbe and host sphingolipids are involved in the crosstalk between partners (Heung *et al.*, 2006, Ali *et al.*, 2011, An *et al.*, 2014). Although varied approaches are employed, in all cases, the modulation of sphingolipids by the microbe, host or both partners alters the ability of a microbe to colonize a host.

The relative amounts of the bioactive sphingolipids sphingosine (Sph) and sphingosine-1-phosphate (S1P) play pivotal roles in determining cell fate and host-microbe partnerships through the coupled enzymatic activities of sphingosine kinase (SPHK) and sphingosine-1-phosphate phosphatase (SGPP), known as the 'sphingosine rheostat' (Fig. 2.1) (Cuvillier *et al.*, 1996, Mandala *et al.*, 1998). Both SPHK and SGPP act to maintain S1P balance by clearing metabolic byproducts and therefore have some constitutive expression and activity under normal conditions (Spiegel *et al.*, 2003, Chan *et al.*, 2013). Activation of the two closely related SPHK enzymes, SPHK1 and SPHK2, from external stimuli such as cytokines, growth factors and environmental agents results in the phosphorylation of Sph into S1P (Maceyka *et al.*, 2005). SPHK is considered the key regulator of the rheostat with rapid generation of S1P gradients(Alemany *et al.*, 2007). S1P can have pleiotropic actions through activation of intracellular signaling cascades (Olivera *et al.*, 2003) or autocrine and paracrine receptor-mediated activation of downstream effectors by a repertoire of extracellular G-protein-coupled sphingosine-1-phosphate receptors ($S1PR_{1-5}$; Fig. 2.1) (An *et al.*, 1997, Goetzl *et al.*, 1998, Lee *et al.*, 1998). Elevated cellular S1P promotes cell survival and proliferation in numerous ways (reviewed in Olivera *et al.* (2001), Spiegel *et al.* (2003), van Brocklyn *et al.* (2012). For example, increased S1P activates transcription factors with the extracellular-regulated kinase/mitogen-activated protein kinase (ERK/MAPK) pathways thereby increasing DNA synthesis and accelerating cell cycle G1/S transitions (Olivera *et al.*, 1999). The reversible dephosphorylation of S1P to Sph by SGPP and accumulation of Sph and

ceramide, the Sph precursor, drives pro-apoptotic activity within the cell and halts cell proliferation (Mandala *et al.*, 1998, Olivera *et al.*, 1999). In addition to their important role in growth and survival, the rheostat lipids act as secondary messengers in the host immune response. When specific cytokines or microbe-associated molecular patterns (MAMPs) bind to host receptors, SPHK1 is activated through an unknown mechanism, translocates to plasma or phagosomal membranes and produces S1P that ultimately causes intrinsic activation of transcription factors such as NF-κB, an immune response mediator (Xia *et al.*, 2002, Seo *et al.*, 2011, Spiegel *et al.*, 2011). Furthermore, inside-out S1P signaling through S1PRs is fundamental to immune cell migration, barrier integrity, and immune molecule expression (reviewed by Spiegel *et al.* (2011)). Under normal conditions, constitutive levels of S1P in tissues are relatively low from the enzymatic balance of generation and rapid degradation or dephosphorylation (Fig. 2.1) (Schwab *et al.*, 2005, Chan *et al.*, 2013). Thus, the dynamic flux of these two signaling lipids is an important indicator of homeostatic imbalance, environmental perturbation and ultimately cell fate of the host, which in turn dictates the survival of the microbes.

The cnidarian sphingosine rheostat model for symbiosis regulation was proposed following the discovery of downregulation of SGPP in the symbiotic sea anemone *Anthopleura elegantissima* from a transcriptome study comparing symbiotic states (Rodriguez-Lanetty *et al.*, 2006). This transcriptional response to symbiosis suggested a shift in the rheostat toward increased S1P levels, which would correspond to increased cell survival and symbiont proliferation. However, empirical evidence of cnidarian SPHK, the central enzyme for a functioning rheostat, and of sphingolipids has not been documented. A subsequent study by Detournay and Weis (2011) explored the potential role of sphingolipid metabolism in cnidarian immunity by incubating the anemone *Aiptasia pallida* (*sensu Exaiptasia pallida* (Grajales *et al.*, 2014)) in the lipid metabolites Sph, S1P and FTY720, an S1P agonist, and exposing anemones to lipopolysaccharide (LPS), an immune-eliciting MAMP. Anemones incubated in S1P and FTY720 followed by LPS challenge exhibited decreased levels of the cytotoxic nitric oxide (NO), a proxy for an immune response, compared to controls (Detournay *et al.*, 2011). Conversely, LPS challenge of anemones incubated in Sph led to an increase in the NO signal. Moreover,

elevated Sph led to increased caspase activity, an indicator of a programmed cell death response (Detournay *et al.*, 2011). Isolated ceramides from other cnidarians have also demonstrated both anti-microbial and anti-inflammatory activity when challenged with immune elicitors (Cheng *et al.*, 2009, Al-Lihaibi *et al.*, 2010, Wei *et al.*, 2013). These results suggest a functional role of sphingolipid metabolism in cnidarian pathogenesis and immunity, although the linkage between host sphingolipid-mediated responses in the presence of algal symbionts needs further investigation. Moreover, the involvement of the rheostat during the initial stages of symbiosis from recognition to successful colonization (also referred to as infection) has not been explored.

In this study we further characterize cnidarian sphingolipids with the molecular identification and quantification of endogenous sphingolipid metabolism in the sea anemone *A. pallida*. *A. pallida* is an established laboratory model system for the study of cnidarian symbiosis (Weis *et al.*, 2008, Voolstra, 2013) as it engages in a facultative relationship with *Symbiodinium* spp. and can be maintained without symbionts (aposymbiotic state). We expanded upon the proposed sphingosine rheostat model with quantification of SPHK and SGPP gene expression, SPHK protein abundance and rheostat lipid concentrations in different symbiotic states and newly recolonized animals. Overall, the functional role of the sphingosine rheostat in regulating cnidarian-*Symbiodinium* symbiosis was enhanced by the identification and characterization of key components of sphingolipid metabolism from onset of symbiosis through stable associations in *A. pallida*.

2.3 Results and Discussion

2.3.1 Sphingolipid metabolic pathways are conserved in Aiptasia pallida

There is little information regarding the function and metabolism of sphingolipids in cnidarians. To gain insights into biosynthesis, regulation and evolution of sphingolipid metabolic pathways, we examined the gene repertoire in the *A. pallida* genome. A survey of KEGG-annotated sequences identified 54 genes in the sphingolipid metabolism (ko00600) and signaling (ko04071) KEGG pathways (Table 2.1). All genes necessary for *de novo* synthesis of sphingolipids, recycling of Sph and ceramide in the salvage

pathway, and irreversible degradation of S1P are present in *A. pallida*. However, several enzymes involved in complex hydrolysis of ceramide into sphingomyelin (SM) or glycosphingolipids (GLSs) are apparently missing from the *A. pallida* genome (Table 2.1). These missing genes are part of lysosomal processing of complex GLS and include alpha-galactosidase, galactosylceramidase, arylsufatase A and sialidase (Li *et al.*, 1999, Bartke *et al.*, 2009). Sialidase hydrolyzes sialic acid from glycolipids and is found in deutrostomes and symbiotic microorganisms (commensals to pathogens), but was thought to be lost in most other animal groups (Roggentin *et al.*, 1993, Koles *et al.*, 2004). However, an absence of sialidase in *A. pallida* genome could result from incomplete draft genome assembly or from a lineage specific loss because a sialidase homolog is present in genomes of the sea anemone *Nematostella vectensis* (Sullivan *et al.*, 2007) and coral *Acropora digitifera* (Shinzato *et al.*, 2011).

Sphingolipid signaling was thought to be receptor-independent in early metazoans (Metpally *et al.*, 2005, Nordström *et al.*, 2008). To date, S1P-specific G protein-coupled receptor (GPCR) have only been identified in the ascidian *Botryllus schlosseri* (Kassmer *et al.*, 2015) but not in other invertebrates. Surprisingly, one of the five G-coupled S1P receptor types, $S1PR_2$, used for extracellular S1P signaling was recovered from BLAST homology to the KEGG database (Table 2.1). The two genes, AIPGENE11572 and AIPGENE11573, matched *Danio rerio,* $S1PR_2$ (SwissProt; Q918k8, E value= 4e-35 for both) with 35.2% similarity (Baumgarten *et al.*, 2015). We performed independent homology searches with BLASTp to NCBI non-redundant database (ncbi.nlm.nih.gov) and identified protein domains with InterProScan (Jones *et al.*, 2014). The best match in the NCBI database was to *D. rerio* lysophosphatidic acid (LPA) receptor 2b (NCBI: NP_001032783.1; E value = 4e-39 and 7e-39, respectively) with 33% similarity to both *A. pallida* genes. Comparison of the gene models with the InterPro database indicates that these homologs belong to the GPCR rhodopsin-like family, a broad group encompassing both LPA and S1P receptors. LPAs are also lipid signalers that have similar biological functions to S1P-mediated signaling, and have been shown to counteract each other *in vivo* (Nakanaga *et al.*, 2014). LPA receptors share 35% similarity with SIPRs and both belong to the endothelial differentiation gene (Edg) family of GPCRs (Chun *et al.*, 2002).

Further characterization of this putative GPCR in *A. pallida* will help reveal its role in mediating extracellular LPA, S1P or both lipids in extrinsic cell signaling and more broadly expand on the evolution of rhodopsin-like GPCRs in basal metazoans.

The rheostat enzymes SPHK and SGPP, like the components of sphingolipid metabolism, are highly conserved across eukaryotes, occurring in both cnidarian and dinoflagellate genomes. One AP-SPHK and one AP-SGPP gene was recovered from the *A. pallida* transcriptome (Lehnert *et al.*, 2012) and matched BLAST queries with 43% (E value= 3e-43) and 83% (E value= 9e-63) coverage, respectively. These partial transcripts were RACE-amplified and then searched against the *A. pallida* and *Symbiodinium minutum* genomes that became available after this study began (Fig. 2.2 and 2.3). From the *A. pallida* genome, two putative SPHK genes, AIPGENE12769 and AIPGENE12827, and one SGPP, AIPGENE2150, were identified (Baumgarten *et al.*, 2015) (Table 2.1). In the *S. minutum* genome, one SPHK homolog was recovered [symbB1.v1.2.011198.t1, E value= 7e-41], but none were recovered for SGPP. Using the plant *Arabidopsis thaliana* SGPP as a query [NCBI: NP_191408], however, two homologs were identified from *S. minutum* [symbB1.v1.2.002394.t1 (E value = 4e-32) and symbB1.v1.2.027512.t1 (E value= 3e-18)] that contained a phosphatidic acid phosphatase type 2 domain found in SGPP and a larger group of lipid phosphate phosphohydrolyases (LPPs). Based on protein sequence similarity, AP-SPHK and *S. minutum* SPHK share just 25.3% pairwise identity (Fig. 2.2B). Therefore, both partners have the molecular machinery necessary to cycle S1P and Sph, but the enzymes are highly divergent at the protein level.

In mammals, there are two SPHK isoenzymes, SPHK1 and SPHK2, which differ in cellular location, leading to some overlapping and opposing functions (reviewed by Maceyka *et al.* 2005, Alemany *et al.* 2007, and Chan *et al.* 2013). SPHK1- and SPHK2-like genes have also been identified in slime mold *Dictostylium discoideum*, yeast *S. cervisiae*, and fruit fly *D. melanogaster* (Alemany *et al.*, 2007). It is unclear if the two SPHK enzymes arose from a common ancestor or are the result of lineage-specific gene duplication and diversification. To determine if the predicted gene models recovered from the genome were two distinct SPHKs, AP-SPHK sequence was compared to the gene models. A nucleotide pairwise comparison resulted in 98.3% identity to

AIPGENE12769 and 61.8% identity to AIPGENE12827 (Fig. 2.4). However, both SPHK sequences were found adjacent to one another on the same scaffold (Fig. 2.5). This arrangement can arise from segmental duplications during genome draft assembly of diploid organisms with heterozygous allele copies, especially those in highly divergent regions (Kelley *et al.*, 2010). Given that only one transcript has been identified in the transcriptome, RACE amplification and other cnidarian resources (Table 2.2), we suggest that the two gene models identified in the genome originate from sequence mis-assembly rather than from gene duplication. Therefore, the results presented in this study are based on the full length RACE-amplified AP-SPHK transcript. To determine if AP-SPHK was more similar to the cytosolic SPHK1 or membrane bound SPHK2 identified in mammals, we compared the protein translation of AP-SPHK to *R. norvegicus* SPHK1 and SPHK2 using a multiple protein sequence alignment (Fig. 2.2B). AP-SPHK did not share the hallmark features of membrane-bound SPHK2 which include a 200 aa proline-rich insert between domains 4 and 5 (Liu *et al.*, 2000), four transmembrane segments (Liu *et al.*, 2000) and a nuclear localization sequence at the N terminal (Igarashi *et al.*, 2003) (hydropathy data not shown).

Two SGPP genes were first characterized in yeast (Mandala *et al.*, 1998) and then mammals (Le Stunff *et al.*, 2002, Ogawa *et al.*, 2003), with three conserved domains between them (Fig. 2.3) (Spiegel *et al.*, 2003). We compared AP-SGPP to *R. norvegicus* SGPP1 and SGPP2 using a multiple protein sequence alignment (Fig. 2.3) and found 33.2% and 31.6% pairwise identity, respectively. The low sequence similarity observed is comparable to the predicted homolog in oyster *Crassostrea gigas* (Timmins-Schiffman *et al.*, 2012). Therefore, the AP-SGPP and *C. gigas* homologs could represent ancestral SGPPs. SGPPs belong to a larger group of LPPs including those that process LPAs, but share little homology with known LPPs (Stukey *et al.*, 1997, Chun *et al.*, 2002). Most LPPs are bound to the plasma membrane and mediate extracellular events, but SGPPs localize to the endoplasmic reticulum (Le Stunff *et al.*, 2002, Ogawa *et al.*, 2003). LPPs have been identified in *D. melanogaster* (Starz-Gaiano *et al.*, 2001) and *B. schlosseri* (Kassmer *et al.*, 2015), with a suggested role in sphingolipid metabolite recycling. Identification of two putative *S. minutum* LPP homologs suggests a non-specific

mechanism for S1P dephosphorylation, important to the recycling of Sph, ceramide and glycosphingolipid production. Unlike LPPs, SGPPs are substrate-specific for S1P and similar SPHK byproducts (Ogawa *et al.*, 2003). Measuring substrate-specificity of both *S. minutum* LPPs and AP-SGPP in the future will resolve the catalytic properties of these enzymes and further characterize their classification.

2.3.2 A. pallida *sphingosine rheostat changes with symbiotic state*

A regulatory role for the rheostat in maintaining cnidarian-dinoflagellate symbiosis has been hypothesized (Rodriguez-Lanetty *et al.*, 2006). Here, we tested this hypothesis empirically through quantification of the genes AP-SPHK and AP-SGPP expression, SPHK protein quantities and enzymatic products S1P and Sph concentrations in different symbiotic states of *A. pallida*.

Based on the findings of Rodriguez-Lanetty *et al.* (2006), the change in steady state expression of rheostat enzymes between symbiotic states suggests differing physiological demands on the host to maintain a stable association. Using a host-specific qPCR assay (see Experimental Procedures), we quantified gene expression of AP-SGPP and AP-SPHK in symbiotic and aposymbiotic anemones. AP-SGPP was 2-fold lower in symbiotic compared to aposymbiotic state suggesting a pro-survival cellular response in symbiotic *A. pallida* (Fig. 2.6A; Mann Whitney test, $p = 0.05$) and consistent with SGPP expression in symbiotic *A. elegantissma* previously reported (Rodriguez-Lanetty *et al.*, 2006). Although AP-SPHK expression demonstrates the opposite pattern under different symbiotic states, the difference was not significant (Mann Whitney U test, $p = 0.2$).

The relative quantity of SPHK in symbiotic anemones, detected in immunoblots was 49% higher than in aposymbiotic animals, however the difference was not significant (Mann Whitney test, $p = 0.1$; Fig. 2.6B). From the AP-SPHK transcript, the predicted molecular weight is 61 kDa based on *in silico* estimates, however the polyclonal SPHK1 antibody (anti-SPHK1) labeled a band with an approximate molecular weight of 75 kDa (Fig. 2.7B). Anti-SPHK1 labeled a single 49 kDa band in mouse heart homogenate positive control as previously reported (data not shown, (Kohama *et al.*, 1998, Olivera *et al.*, 1998, Murate *et al.*, 2001)). Post-translational modification such as phosphorylation, palmitoylation and other protein interactions with SPHK1 and SPHK2 has been

demonstrated in multiple studies on yeast ((Iwaki *et al.*, 2005, Kihara *et al.*, 2005)) and vertebrates (reviewed in Chan *et al.* (2013)), and could account for the higher observed molecular weight of AP-SPHK. Isolation of the 75 kDa band and characterization of the protein sequence is needed to confirm the modification of AP-SPHK.

These modest changes in SPHK expression and protein quantities could be sufficient to generate differences in cellular S1P levels between symbiotic states. It has been shown that slight enhancement of SPHK expression and activity by just 1.5 to 2-fold results in rapid S1P production (Pitson *et al.*, 2000, Pitson *et al.*, 2003). This upregulation of AP-SPHK expression and protein production at resting state in symbiotic anemones reflects a new regulatory mechanism to mediate symbiont interactions possibly through elevated S1P production that is not present in aposymbiotic state.

To assess the functioning of the rheostat and if it changes with symbiotic state, we quantified S1P and Sph concentrations in two populations of *A. pallida*, Virginia Weis lab population VWA collected from various sources and Gisele Muller-Parker lab population GMP collected from Walsingham Pond, Bermuda, in different symbiotic states. The mean Sph concentration was three times higher than S1P in VWA anemones (Mann Whitney test, $p = 0.010$), but there was no difference between sphingolipids in the GMP population (Fig. 2.7C). Sph concentrations in VWA anemones in both symbiotic states are similar to those in human fibroblast and keratinocytes under normal conditions reported to range from 50 to 200 pmol/mg (Lieser *et al.*, 2003). We predicted that the constitutively higher AP-SPHK expression in symbiotic anemones (Fig. 2.6A) would result in elevated cellular S1P concentrations. However, there was no detectable change in S1P concentrations between populations or symbiotic states (Fig. 2.6C). Upregulation of AP-SPHK expression and elevated protein production in symbiotic anemones could build up a reserve of mature SPHK enzymes that can be activated more readily to mediate host-symbiont interactions, but does not contribute to persistent enzymatic activity in the presence of symbionts. Although sphingolipids did not differ in symbiotic anemones from either population, mean VWA Sph concentration was slightly lower in the symbiotic than the aposymbiotic state (Fig 2.6C). Reduced Sph concentrations correspond to the reduced AP-SGPP gene expression in symbiotic anemones, again

suggesting enhanced protection against apoptosis when symbionts are present. In contrast, mean Sph concentration in VWA aposymbiotic anemones was significantly higher than S1P by an average of 108 pmol/mg (Mann Whitney test, $p = 0.014$). This difference in the aposymbiotic VWA is consistent with studies in other organisms where S1P can be $1/100^{th}$ the concentration of Sph under stable conditions (Maceyka *et al.*, 2005, Hannun *et al.*, 2008, Lloyd-Evans *et al.*, 2008, Shaner *et al.*, 2009).

2.3.3 The presence of symbionts modulates host rheostat gene expression and sphingolipids during recolonization

We predicted that the rheostat would shift toward pro-survival during onset of the beneficial cnidarian-*Symbiodinium* symbiosis based on the observed differences in sphingosine rheostat under differing symbiotic states discussed above and the role of the rheostat in eliciting an immune response in *A. pallida* (Detournay *et al.*, 2011). To assess changes in gene expression during onset of symbiosis, we needed to measure expression levels of our GOIs as well as symbiont abundance in our samples. These experiments were performed on a set of animals that was also used in a study on the role of the complement system in cnidarian symbiosis (Poole et al, submitted). The treatments used for repopulation of *A. pallida* are described in Table 2.3.

The expression of AP-SPHK and AP-SGPP displayed significant interactions of time and colonization, and time and light treatments in the respective comparison groups (Table 2.4) but did not differ with anemone size or brine shrimp feeding stimulus (ANOVA, $p > 0.05$; Table 2.4). AP-SPHK mean expression increased by 2.09- and 6.22-fold in the recolonization with light (+L) treatment group at 12 h and day one, respectively (Fig. 2.7A, Tukey *post-hoc* $p < 0.001$). This dynamic change in AP-SPHK with onset of symbiosis suggests that this enzyme is playing a role in host-symbiont recognition. AP-SPHK expression in the +L group returned to the same levels of the aposymbiotic with light (–L) anemones after day one. Therefore, initial symbiont-induced elevations of AP-SPHK subsided after recognition. AP-SGPP expression also increased in the +L anemones at 12 h and day one, but only by 1.16 and 2.15 times that of the –L group (Fig. 2.7B, Tukey *post-hoc* $p= 0.007$). The increase in both AP-SPHK and AP-SGPP expression at day one post-inoculation could indicate the presence of a selection

mechanism where the host cells discriminates between compatible and incompatible partners. Compatible symbionts will drive the host sphingosine rheostat towards cell survival, while incompatible symbionts, determined by host innate immune mechanisms, shifts the rheostat toward cell death and symbiont removal. At day three in the light, AP-SPHK expression did not change but AP-SGPP was significantly upregulated by 1.97-fold (Fig. 2.7B, Tukey *post-hoc* $p < 0.001$). Elevated AP-SGPP expression could be a result of cytosolic S1P imbalance following increased SPHK activity with onset of symbiosis with compatible symbionts, whereby AP-SGPP brings S1P levels back to constitutive levels. On the other hand, increased AP-SGPP expression could be a continuation of host selection of compatible symbionts as part of the winnowing process.

In addition to measuring symbiont recolonization and rheostat modulation in the light, we investigated how incubation in the dark influenced *A. pallida* recolonization. The exchange of photosynthetic products is the basis for the cnidarian-*Symbiodinium* symbiosis. Therefore, uptake of symbionts in the dark would be less favorable for symbiosis establishment. Previous studies of symbiosis-linked genes such as sym32 (Ganot *et al.*, 2011) and complement C3, Factor B and mannose-associated serine protease (MASP) (Poole *et al.*, submitted) have identified light-induced expression patterns. The downregulation of AP-SPHK and AP-SGPP in recolonizing animals in the dark (+D) significantly differed at 12 h post-inoculation from their respective +L groups (Fig. 2.7, Tukey *post-hoc* $p < 0.001$). Expression of both genes was then upregulated at day one, but significantly less than in the +L groups (Fig. 2.7). Elevation of expression in the dark by the presence of symbionts suggests that rheostat regulation is not solely dependent on light and is related to the presence of symbionts.

The qPCR methods developed for measurement of symbiont abundance and the symbiont colonization results for these samples are described in detail in Poole *et al.* (submitted). In that study, the relative abundance of symbionts from the recolonized anemones used for qPCR significantly increased after three days post-inoculation in both +L and +D treatment groups compared to aposymbiotic anemones (Poole *et al.* submitted, see Appendix). In addition, the relative symbiont abundance of anemones in the +L group continued to increase between days one and three, whereas the +D group

decreased slightly (Poole *et al.* submitted). Prolonged incubation in darkness repressed both symbiont abundance and rheostat gene expression, suggesting that light and likely photosynthetic performance by the algae is required for the symbiont population to increase and for the symbiosis ultimately reach a dynamic stable state. Considering the lower symbiont abundance in the dark by day three, anemones undergoing colonization in the dark might be under more cellular stress resulting in lower symbiont abundance and rheostat expression.

To compare the sphingosine rheostat expression to activity, we quantified S1P and Sph concentrations in +L and -L treatment groups at one and three days of recolonization and calculated a ratio of +L/-L. Mean S1P levels were lower in +L anemones compared to the -L group at all sampled time points (Fig. 2.8). Enhanced SPHK gene expression in the light at day one did not correspond with a simultaneous increase in S1P levels (Fig. 2.8). However, at day three post-inoculation in +L, the mean S1P ratios increased slightly ($p = 0.114$) and mean Sph ratios decreased significantly (Mann Whitney test, $p = 0.029$; Fig. 2.8). Using the qPCR method for symbiont quantification, the symbiont abundance at day three post-inoculation of +L anemones used in the lipid analysis significantly increased, but was 4.6-fold lower than the +L samples used to measure GOI expression (Mann Whitney test, $p = 0.032$). The lag in changes in Sph lipid concentrations following changes in rheostat gene expression could be the result of multiple factors, for example: (1) low symbiont abundance in this experiment could have delayed initiation of AP-SPHK expression and activity, (2) desphosphorylation and degradation enzymes could be more active at day one in +L to maintain homeostasis but becomes overwhelmed at day three by AP-SPHK activity, or (3) the time scale (over days) used to capture transient S1P signaling could be too long. Other studies, for example, detect measureable differences in sphingolipids over hours (Zhang *et al.*, 1991, Xia *et al.*, 2002, Döll *et al.*, 2005, Lloyd-Evans *et al.*, 2008, Prakash *et al.*, 2010). While the underlying mechanisms for the delay in S1P production need to be addressed in future studies, this modest amplification of S1P levels may trigger multiple cellular responses that promote symbiont acquisition.

In conclusion, the findings from this study demonstrate acute modulation of the host sphingosine rheostat at the onset of symbiosis that could be playing a role in symbiosis regulation. A genomic survey identified a conserved gene repertoire for sphingolipid metabolism, intrinsic, and extrinsic cell signaling, the latter of which was thought to be limited to chordates. We provide further support for symbiosis regulation by the cnidarian sphingosine rheostat with persistent upregulation of SPHK gene expression and protein production in the symbiotic state. Although we did not observe significant differences in sphingolipids in symbiotic compared to aposymbiotic animals, the slight reduction of the pro-apoptotic signaler Sph in symbiotic animals suggests a dynamic shift in resting concentrations in favor of cell survival in the presence of *S. minutum*. This pattern is also observed during symbiont recolonization in the light, suggesting a role for the host rheostat in controlling *S. minutum* colonization during initial contact and phagocytosis. Sphingolipid metabolism has been linked to macrophage phagocytosis of other microbes (Thompson *et al.*, 2005, Tafesse *et al.*, 2015) pointing to a conserved mechanism for microbe recognition and sorting in metazoans. The offset of expression and detectable differences in lipid levels needs to be explored in future investigations. Direct measurements of enzymatic activity under both light conditions and symbiotic states will help resolve the timing of S1P production and its importance in symbiont recognition.

2.4 Experimental Procedures

2.4.1 Maintenance of Aiptasia pallida *and* Symbiodinium minutum

Symbiotic *A. pallida* from the Weis Lab population (VWA, Grajales *et al.* (2016)) and Gisele Muller-Parker population (GMP, Grajales *et al.* (2016)) were maintained in artificial seawater (ASW) at room temperature (RT, ~ 25 °C) under 40 µmol quanta m^{-2} s^{-1} on a 12 h light:12 h dark photoperiod. GMP anemones were used only for lipid extraction and quantification (see Section 2.4.9). For the recolonization experiment, aposymbiotic anemones were generated by subjecting symbiotic anemones to a series of cold-shock treatments at 4 °C for 6 h twice a week for six weeks to remove algal symbionts (Muscatine *et al.*, 1991). Aposymbiotic anemones were kept in the dark for at

least two months prior to experimentation to prevent symbiont repopulation. Symbiotic and aposymbiotic anemones were fed *Artemia* sp. nauplii twice a week up to two weeks prior to the commencement of experiments, after which time they were starved. In the recolonization experiment, aposymbiotic VWA anemones were inoculated with homologous symbionts, *S. minutum s*train CCMP830 (type B1, Bigelow Laboratory for Ocean Science, ME) previously isolated from *A. pallida* (Lesser, 1996). CCMP830 was grown in sterile f/2 media (Guillard *et al.*, 1962) at 25 °C at an irradiance of 40 µmol quanta m^{-2} s^{-1} on a 12-h light:12-h dark cycle.

2.4.2 Recolonization experiments

To explore the role of sphingosine rheostat enzymes (AP-SPHK and AP-SGPP) and lipids (S1P and Sph) in onset of symbiosis, symbiont recolonization in anemones was examined over three days. Anemones were plated in 6-well dishes in 10 ml of 0.45 µm filtered ASW (FASW) two weeks prior to recolonization. Water was changed daily. For the first recolonization experiment used for the qPCR assay, oral and pedal disc diameter (mean 3.93 ± 0.16 and 4.08 ±0.15, respectively) for each anemone was measured with calipers to estimate animal size and randomly placed into one of four treatment groups: (1) light, - symbionts, + brine shrimp extract (feeding stimulant, BSE) (-L); (2) light, + symbionts, + BSE (+L); (3) light, - symbionts, - BSE (-BSE); and (4) dark, + symbionts, + BSE (+D, Table 2.2). In the second recolonization experiment for lipid quantification, total host protein was measured using a Bradford assay described below (Section 2.4.9) and randomly assigned to treatments -L and +L. In both qPCR and lipid experiments, the culture of CCMP830 strain was concentrated and quantified as described by Poole *et al.* ((submitted); see Appendix). Treatments +L and +D were inoculated with 2.19 x 10^5 ml^{-1} of CCMP830 in exponential growth phase, and treatments -L, +L and +D received 40 µl of BSE, a known feeding stimulus in cnidarians (Schwarz *et al.*, 1999, Weis *et al.*, 2002, Harii *et al.*, 2009). Treatments without symbionts (–BSE and –L) were brought to the same volume as those that received symbionts with the addition of one ml of FASW. Treatments –L, +L, and -BSE were then placed in an incubator at 25 °C on a 12 h: 12 h light-dark cycle at a light intensity of 40 µmol quanta m^{-2} s^{-1}. Treatment +D was placed in

the dark at room temperature (rt; aposymbiotic husbandry conditions). After 24 h, anemones were washed with FASW to remove residual symbionts and collected at various time points (0, 0.5, 1, 2 and 3 days post-inoculation; qPCR n = 3; lipids n = 4), flash-frozen in liquid nitrogen, and stored at -80 °C for processing.

2.4.3 Symbiont quantification

To confirm the uptake of symbionts by *A. pallida* in the recolonization experiments, algal density was quantified using a relative qPCR assay based on the delta C_t method (Livak *et al.* (2001), Poole *et al.* (submitted); see Appendix for details). Previous quantification methods (eg. hemocytometer counts and chlorophyll *a* concentration) failed to provide accurate measurements of symbiont abundance at low concentrations during onset of symbiosis in this study. Therefore, the qPCR assay was designed to compare gene copies of 28S from symbiont nuclear rDNA using clade B1-specific primers (Correa *et al.*, 2009) after samples were normalized to host copies of nuclear ribosomal protein L10 ((Poole *et al.*, submitted); Appendix). Samples for the symbiotic-state and recolonization experiments were previously analyzed by Poole *et al.* (submitted). For recolonized anemones used for lipid analysis, DNA was extracted at 3 days (n = 3) using a modified CTAB protocol described by Coffroth et al. (1992). Each sample was run in triplicate on a MasterCycler RealPlex^4 machine (Eppendorf, Hamburg, Germany) using 20 ng μl^{-1} genomic DNA, 0.4 μM of the gene-specific forward and reverse primers and SensiFAST SYBR Hi-ROX master mix (Bioline USA, Boston, MA) according to the manufacturer's protocol. The cycle threshold, or C_t, values were used to calculate relative quantities of 28S rDNA as previously described (Poole *et al.*, submitted).

2.4.4 RNA extraction and cDNA synthesis

Total RNA was extracted from each anemone using an extraction protocol with TRIzol Reagent (Invitrogen, CA) and an RNeasy Mini kit (Qiagen, CA) described by Poole *et al.* (submitted). Briefly, the TRIzol extraction was followed through phase separation according to the manufacturer's protocol, and then the aqueous phase was washed with an equal volume of 100% cold ethanol. The mixture was applied to an

RNeasy spin column, processed to elute RNA following the manufacturer's protocol and stored at -80 °C.

To assess primer specificity for AP-SPHK and AP-SGPP with the qPCR assay, we tested amplification of CCMP830 cDNA. RNA was extracted using a combination of protocols from Rosic and Hoegh-Guldberg (2010) and an RNeasy Mini Kit (Qiagen, CA). Briefly, 15 ml of CCMP830 cells in exponential growth phase at a concentration of 10^6 ml^{-1} were pelleted by centrifugation at 13,000 x g for 5 min. The pellet was resuspended in 1.5 ml of f/2 media, transferred to a FastPrep screw-top tube (MP Biomedical, CA), and repelleted at 14,000 x g for 30 sec. The supernatant was removed and pellet frozen in liquid nitrogen. Acid-washed 0.45-0.6 mm glass beads (Sigma, MO) and 0.5 ml TRIzol were added to the pellet, and placed in the FastPrep FP120 cell disruptor (MP Biomedical, CA) at the low speed (4.0 s) for two 20 sec pulses. The homogenate was then processed as described above for the anemone samples using a combination of TRIzol protocol through phase separation followed by the RNeasy Mini kit (Qiagen, CA).

RNA quality and quantity was assessed by gel electrophoresis and the NanoDrop ND-1000 (NanoDrop Products, DE), respectively. Samples with a NanoDrop 260/230 ratio less than 1.5 underwent RNA purification protocol described by Poole *et al.* (Submitted). Then, each sample was treated with the DNA-*free* kit (Ambion, CA) or TURBO DNA-*free* kit (Ambion, CA) to remove residual genomic DNA contamination. RNA concentrations were then re-quantified. cDNA was synthesized using SuperScript III First- Strand Synthesis System (Invitrogen, CA) with 500-750 ng of RNA and 50 µM oligo $(dT)_{20}$ primer. Each cDNA sample was diluted to a final concentration of 300 ng μl^{-1} before use in qPCR reactions. Symbiotic *A. pallida* (n=6) and CCMP830 (n=1) cDNA was tested for amplification of the symbiont-specific peridinin chlorophyll protein using previously published primers (Amar *et al.*, 2008) following the GoTaq Flexi polymerase (Promega, WI) protocol.

2.4.5 RACE amplification of SPHK and SGPP sequences

Partial transcripts of AP-SPHK and AP-SGPP were identified from the *A. pallida* transcriptome (Lehnert *et al.*, 2012) using tBLASTn with an expect value (E value) ≤ e-20 in Geneious v5.4.3 (Altschul *et al.*, 1990, Kearse *et al.*, 2012). The query protein sequences used were *Rattus norvegicus* SPHK1 [NCBI: ABF30968.1] and *Homo sapiens* SGPP [NCBI: CAC17772.1]. To generate full-length cDNA sequences, we performed rapid amplification of the cDNA ends (RACE) using FirstChoice RLM- RACE kit (Invitrogen, CA) and RNA template from symbiotic *A. pallida*. Nested gene-specific primers (Table 2.1) were designed by hand for the 3' and 5' ends following the manufacturer's guidelines. Successful PCR products detected by gel electrophoresis were ligated into plasmids with the pGEM-T easy vector system (Promega, WI) overnight at 4 °C and cloned into MAX Efficiency DH5α competent cells (Invitrogen, CA) following the manufacturer's protocol. Plasmids were purified using the QIAprep Spin Miniprep kit (Qiagen, CA), product size verified with FastDigest EcoRI (Thermo Scientific, MA) or rapid digestion with Promega EcoRI (Promega, WI), and Sanger sequenced on the ABI 3730 capillary machine at the Center for Genome Research and Biocomputing (CGRB) at Oregon State University (OSU). Sequence products from RACE were assembled with the transcriptome fragments using Geneious v 5.4.3 (Kearse *et al.*, 2012). We searched for conserved protein domains (Kohama *et al.*, 1998, Mandala *et al.*, 2000), nuclear localization sequence of SPHK2 (Igarashi *et al.*, 2003) and transmembrane segments using Consensus Constrained TOPology prediction web server (Dobson *et al.*, 2015).

2.4.6 **A. pallida** *and* **S. minutum** *genome comparisons*

While this project was in process, the *A. pallida* genome (v1.0) was sequenced and is now publicly available (Baumgarten *et al.*, 2015). The predicted gene models from the genome were searched using the full-length transcripts of AP-SPHK and AP-SGPP (generated as described above) as BLASTx queries to identify homologs. Moreover, given that SPHK and SGPP proteins are highly conserved across eukaryotes, *A. pallida* sequences from this study were also compared to the *S. minutum* genome [OIST: symb_aug_v1.120123] using BLASTx with an E value ≤ e-10. DNA sequences of AP-

SPHK and AP-SGPP from this study were aligned with BLAST hits from the *A. pallida* genome using MUSCLE (Fig 2.2; (Edgar, 2004)) or converted to predicted protein in Geneious v5.4.3 (Kearse *et al.*, 2012) and aligned with representative proteins from *A. pallida*, *S. minutum*, and mammalian model *R. norvegicus* [SPHK1: NCBI ABF30968.1; SPHK2: NCBI AAH79120.1; SGPP1: UniProt Q99P55.2; SGPP2: UniProt F1LZ44] using MUSCLE ((Edgar, 2004), Fig. 2.4 and 2.5) Finally, to gain a broader understanding of sphingolipids in the *A. pallida* genome, genes with KEGG (Kyoto Encyclopedia of Genes and Genomes) annotations were scanned for sphingolipid metabolism (ko00600) and signaling (ko04071) pathways.

2.4.7 SPHK and SGPP Relative qPCR

Before developing the qPCR assay, the full-length transcripts from RACE amplification were surveyed for single nucleotide polymorphisms (SNPs), which have been shown to interfere with amplification and quantification of PCR products if they occur within primer annealing sites (Taris *et al.*, 2008). SNP primers for the genes of interests (GOI) AP-SPHK and AP-SGPP (Table 2.4) were designed with Primer3 software v 2.3.4 (Rozen *et al.*, 1999) and verified with cDNA from six symbiotic anemones using cloning and sequencing methods described in Section 2.4.5 (data not shown). qPCR primers were designed to exclude SNPs and amplify a product ranging in size from 100-200 bp (Table 2.4, Fig. 2.2 and 2.5). The *A. pallida* samples used for qPCR analysis in this study have been analyzed previously to measure gene expression of complement genes, a recognition pathway in innate immunity (Poole *et al.*, submitted).

Given that homologs of SPHK and SGPP/LPPs were identified in *A. pallida* and *S. minutum* genomes, we developed a host-specific qPCR assay that excluded amplification of the symbiont enzymes. During RNA extraction, symbiotic anemones had varying amounts of accompanying symbiont RNA. This contamination was confirmed with amplification of a *Symbiodinium*-specific protein, peridinin chlorophyll protein, from sample cDNA. Therefore, we tested the specificity of the *A. pallida* qPCR primers for amplification of *S. minutum* (strain CCMP830) cDNA. Symbiont cDNA failed to amplify a product with AP-SPHK qPCR primers, but did amplify a product with AP-

SGPP qPCR primers at a high C_t cycle of 34.208 ± 0.35. Although a product was detected with the AP-SGPP qPCR primers, this amplification was shifted by 7.2 cycles from *A. pallida* cDNA expression (C_t = 27.0.13 ± 0.19) and therefore considered to be a non-specific PCR product. These results indicated that the qPCR primers captured host-specific expression.

GOI were normalized to reference genes selected for stable expression during experimental treatments. Candidate reference genes included poly-A binding protein (PABP), ribosomal large subunit 10 and 12 (L10 and L12), and glyceraldehyde 3-phosphate dehydrogenase (GAPDH) obtained from the *A. pallida* transcriptome (Lehnert *et al.*, 2012) and a study on *A. pallida* reference gene selection (Rodriguez-Lanetty *et al.*, 2008). Primer pairs designed using Primer3 with amplicon sizes from 100-200 bp, were tested with standard PCR and verified by cloning and sequencing (Table 2.4; Poole *et al.* Submitted). The experimental stability of each potential reference gene was determined using cDNA from representative samples of the symbiotic-state and recolonization experiments (Poole *et al.*, submitted). Each sample was run in triplicate as 20 µl reactions of 10 µl *Power* SYBR® Green PCR master mix (Applied Biosystems, UK), 5 µmol of the forward and reverse primers, 0.5 µl of cDNA, and RNase-free H_2O on the ABI Prism 7500 Real-Time PCR machine (Applied Biosystems, UK) with standard settings for 40 cycles. A dissociation curve [95 °C for 15 s, 60 °C for 1 min, ramping temperature gradient (60-95 °C) for 20 min, and 95 °C for 30 s] for the final PCR product was performed to confirm single amplicon detection. Resulting C_t values were compared using NormFinder (Andersen *et al.*, 2004) and GeNorm (Vandesompele *et al.*, 2002), two programs that rank the reference genes based on their expression stability and variance (Table 2.5). The smaller the value the more stable the expression. A combination of PABP, L10 and L12 genes was used for all experiments based on stability values in Table 2.5.

All *A. pallida* samples were then run in triplicate using the same reagents and equipment described above. No-template, no-reverse transcriptase, and no-primer controls were included as well as at least one interplate calibrator per plate for the recolonization experiment. Mean PCR efficiencies for GOI and reference genes were

calculated in LinReg using raw fluorescence output from each run (Ramakers *et al.*, 2003). C_t values calculated by ABI 7500 software v2.0.6 (Applied Biosystems, UK) were imported into GenEx v5.3.7.332 (MultiD Analyses AB, Sweden) where values were adjusted for interplate variation and normalized to geometric mean of the reference genes. Normalized values (ΔC_t) were converted to relative quantities ($\log_2$) by the $\Delta\Delta C_t$ method (Livak *et al.*, 2001) with the selected reference samples for each experiment as follows: (1) aposymbiotic biological replicate with lowest expression (highest ΔC_t) for symbiotic-state comparison; (2) mean ΔC_t of treatment group -L at each time point (0, 0.5, 1, 2, and 3 days, n= 3 anemones) for recolonization in the light; and (3) mean ΔC_t of 0 h samples (n= 6, symbiotic-state anemones combined with experimental controls) for recolonization in the dark (+D). Relative quantities are presented on the $\log_2$ scale as the mean ± standard error.

2.4.8 Immunoblot of SPHK

Protein was extracted from aposymbiotic and symbiotic anemones (2 anemones per replicate, n = 3 replicates) by homogenization in an extraction buffer (100 mM Tris base, pH 7.4, 100 mM NaCl, 10 mM EDTA, pH 8.0 with cOmplete® protease inhibitor cocktail (Roche, Germany)) at a volume of 1 ml mg^{-1} of tissue. The supernatant was separated from cellular debris and symbionts through centrifugation 4 °C for 15 min at 14,000 x g. Protein concentrations of the supernatant were determined using a Bradford assay. Sample protein at a concentration of 15 µg was resuspended in Laemmli buffer (Bio-Rad, CA) with 5% 2-mercaptoethanol (Sigma, MO) and resolved on 10% Mini-PROTEAN® TGX gel (Bio-Rad, CA). Protein was transferred to a 0.45 µm nitrocellulose membrane at 4 °C for 90 min at 75 V using the Mini Trans-Blot unit (Bio-Rad, CA). Protein transfer was verified using Ponceau S stain in 5% acetic acid. The membrane was then blocked overnight at 37 °C with 5% non-fat milk in TBS-Tween (0.05%) solution, followed by 15 min wash in TBS-Tween. The membrane was incubated for 1 h at rt with anti-SPHK 1 (0.375 µg ml^{-1}, Caymen Chemical, MI, Fig. 2.2) and washed 5 times for 10 min each in TBS-Tween. The blot was then incubated in secondary goat anti-rabbit IgG HRP (0.005 µg ml^{-1}, Caymen Chemical, CA) at rt for 1 hr

followed by the same series of washes after primary incubation. Bands were detected with Clarity Western ECL substrate (Bio-Rad, CA) and exposure to audioradiography film. Relative band intensities were calculated compared to the 43 kDa actin band on the Ponceau S stained blot using ImageJ v1.48 (Rasband, 1997-2015).

2.4.9 Lipid extraction and LC-MS/MS of sphingolipids

Sample lipid extraction followed established protocols (Bligh *et al.*, 1959, Garrett *et al.*, 2013). VWA anemones (n=4 per group) were randomly assorted into 8 extraction groups. GMP anemones (n=3 per group) used in symbiotic-state comparison were processed separately in two extraction groups. For each group, the frozen anemones were homogenized in 0.5 ml of 1x phosphate buffered saline (PBS) and spun at 2,500 rpm for 3 min to gently pellet cellular debris and symbionts (Garrett *et al.*, 2013). For each sample, the supernatant was divided, with 100 µl set aside for protein quantification using a Bradford assay and the remainder transferred to a 13 mm borosilicate glass tube for lipid extraction. An internal standard mixture was added to the lipid portion consisting of 50 pmols of C17-base-D-*erythro*-sphingosine-1-phosphate (C17-S1P) and C17-base-D-*erythro*-sphingosine C17 (C17-Sph; Avanti Polar Lipids, AL). A 1:2 chloroform:methanol mixture was added to each sample, agitated by vortexing for 20 sec, and incubated at rt for 5 min. Then, equal volumes of chloroform and PBS were added to the mixture. After centrifugation at 4 °C for 5 min at 3,000 rpm, a two-phase separation was visible. The lower organic phase was collected in a clean glass tube and dried under gentle nitrogen stream. Lipid residue was dissolved in LC-MS grade methanol:water:formic acid: ammonium formate (60:40:0.2:2mM v/v), and stored at -20 °C.

Peaks corresponding to target analytes (S1P and Sph) and C17 sphingolipid analogs were resolved on the Prominence XR system (Shimadzu, Japan) using a Targa C8 (5µ, 2.1x20 mm, Higgins Analytical, CA) column by the Lipidomics Core Facility at Wayne State University, Detroit, MI. The mobile phase consisted of a gradient between A: methanol-water-ammonium formate-formic acid (5:95:1mM:0.2 v/v) and B: methanol-ammonium formate-formic acid (100:2mM:0.2 v/v) with a flow rate of 0.5 ml/min. The HPLC eluate was introduced to ESI source of QTRAP5500 mass analyzer

(AB SCIEX, MA) in the positive ion mode and molecular ion – daughter ion transitions for each sphingolipid were detected using the multiple reaction monitoring (MRM) method. The MRM transition chromatograms were captured by Analyst v1.6.2 software (AB SCIEX, MA) and quantified by MultiQuant software (AB SCIEX, MA). Sample analytes that passed signal to noise thresholds and quality measures were quantified against internal standards and normalized to total protein. For the recolonization experiment, a fold change was calculated for each sample concentration of treatment group +L referenced to the mean of the concentrations of treatment group -L at each respective time point.

To assess the reproducibility of this method, coefficient of variance (CV) was calculated within and between extraction groups from the peak intensity of the internal standards (C17-S1P and C17-Sph). The C17 analogs should behave similarly to the target analytes during lipid extraction, therefore their peak intensities can be used to measure lipid extraction efficiency (Shaner *et al.*, 2009). For the ten extraction groups, Sph CV ranged from 0.9-59% and S1P CV varied from 4-62% (Fig. 2.9B). This variance is higher than previously reported values, which ranged from 15-25% for sphingoid bases (Lieser *et al.*, 2003, Shaner *et al.*, 2009). This high CV in sphingoid base recovery from total lipids has been attributed to low cellular concentrations, or organismal variation associated with cellular signaling events (Shaner *et al.*, 2009). In addition, the raw intensity peaks for each internal sample per sample was correlated to the sample's total protein using a linear regression model. Size did not appear to correspond to C17-S1P intensity peaks (Fig. 2.9C). However, we found that C17-S1P recovery was higher in the aposymbiotic anemones, which were smaller than the symbiotic samples (Fig. 2.9D). It is unclear if size or symbiotic state contributed to the loss of C17-Sph in the extraction method, and requires further investigation.

2.4.10 Statistical analysis

The normality, homoskedasticity and outlier identification for each respective assay was evaluated using statistical software R v3.03 (RCoreTeam, 2013). For symbiont quantification, symbiotic-state qPCR, protein and lipid analyses, and sphingolipid fold changes from recolonized anemones, statistical significance was tested using a non-

parametric Mann Whitney test. Relative quantities (log_2) from the recolonization qPCR assay were analyzed using a multi-factor analysis of variance (ANOVA) with factors including oral disc size (continuous), brine shrimp extract (2 levels= + BSE or – BSE), light (2 levels= light or dark), symbiont (2 levels= + symbionts or – symbionts) and time (5 levels= 0, 0.5, 1, 2, and 3). The final statistical model for each enzyme was determined through stepwise model tests using the AIC criterion. A separate model was fit with the data for each sphingolipid enzyme mRNA (AP-SPHK and AP-SGPP) and Tukey's HSD post hoc test was performed on ANOVA factors with > two levels. In all test, the statistical significant threshold was a p-values ≤ 0.05.

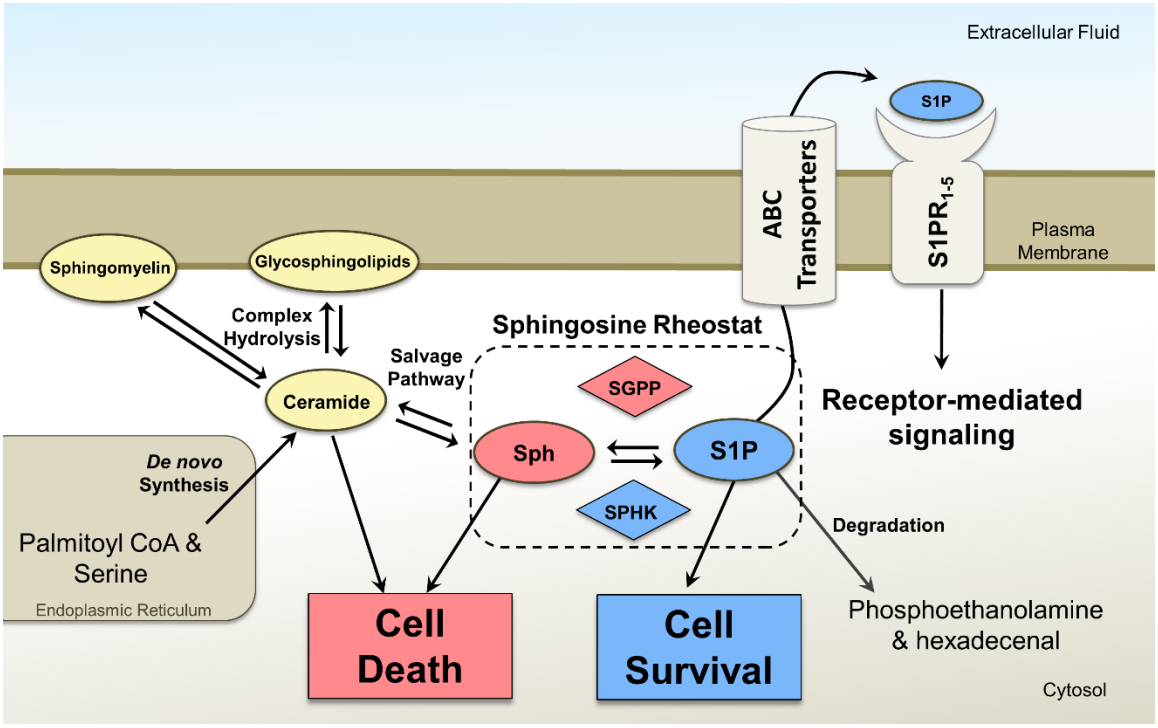

Figure 2.1 Schematic drawing of sphingolipid metabolism in a mammalian cell. *De novo* synthesis of sphingolipids takes place on the cytosolic surface of the endoplasmic reticulum (ER) and ER-associated membranes. The lipid intermediate ceramide is then incorporated into complex sphingolipids such as sphingomyelin in the Golgi apparatus and trafficked to the plasma membrane. Catabolism of ceramide releases the bioactive lipid sphingosine (Sph), and both contribute to activation of pro-apoptotic cellular cascades. Phosphorylation of Sph by SPHK produces the potent signaler sphingosine-1-phosphate (S1P), with extra- and intracellular signaling targets. Extracellular S1P is translocated by ABC transporters and is bound by substrate-specific G protein-coupled S1P receptors 1-5. Elevated cytosolic S1P enhances cell survival and proliferation. S1P can be dephosphorylated by SGPP or irreversibly degraded into phosphoethanolamine and hexadecenal. The enzymatic interconversion of S1P and Sph is known as the sphingosine rheostat (dashed box). Sphingolipids (ovals): Sph (red) = sphingosine, S1P (blue) = sphingosine-1-phosphate, ceramide, sphingomyelin, glycosphingolipids; enzymes (diamonds): SPHK 1 (blue) = sphingosine kinase, SGPP (red) = sphingosine-1-phosphate phosphatase.

Table 2.1 *A. pallida* genes recovered from sphingolipid metabolism (ko00600) and signaling (ko04071) KEGG pathways categorized into *de novo* synthesis, salvage, rheostat, extracellular signaling, complex hydrolysis, and degradation (see Fig 2.1).

Pathway	KEGG ID	Description	Gene ID
De Novo Synthesis	K00654	serine palmitoyltransferase	AIPGENE3105
			AIPGENE15671
	K04708	3-dehydrosphinganine reductase	AIPGENE4706
	K04711	dihydroceramidase	AIPGENE3830
			AIPGENE26941
			AIPGENE6073
			AIPGENE19985
	K04712	sphingolipid delta-4 desaturase	AIPGENE11788
			AIPGENE11883
Salvage	K12348	acid ceramidase	AIPGENE20488
			AIPGENE19389
	K12349	neutral ceramidase	AIPGENE19216
	K01441	alkaline ceramidase	AIPGENE13017
	K04710	ceramide synthetase	AIPGENE20100
			AIPGENE9390
			AIPGENE25238
	K04715	ceramide kinase	AIPGENE17788
			AIPGENE957
			AIPGENE18625
	K01080	phosphatidate phosphatase	AIPGENE7194
			AIPGENE15711
			AIPGENE15709
			AIPGENE15703
			AIPGENE21968
Sphingosine Rheostat	K04716	S1P phosphatase 1 (SGPP1)	AIPGENE2150
	K04717	S1P phosphatase 2 (SGPP2)	NF
	K04718	sphingosine kinase (SPHK)	AIPGENE12769
			AIPGENE12827
Extracellular Signaling	K04288	S1P receptor 1 ($S1PR_1$)	NF
	K04292	S1P receptor 2 ($S1PR_2$)	AIPGENE11572
			AIPGENE11573
	K04290	S1P receptor 3 ($S1PR_3$)	NF
	K04293	S1P receptor 4 ($S1PR_4$)	NF
	K04295	S1P receptor 5 ($S1PR_5$)	NF

NF- not found

Table 2.1 (Continued)

Pathway	KEGG	Description	Gene ID
Extracellular Signaling	K05641	ATP-binding cassette, subfamily A	AIPGENE23551
			AIPGENE23554
			AIPGENE23550
			AIPGENE23552
			AIPGENE23549
			AIPGENE23548
			AIPGENE23553
	K05665	ATP-binding cassette, subfamily C	AIPGENE20688
			AIPGENE25090
			AIPGENE25127
	K05681	ATP-binding cassette, subfamily G	AIPGENE7771
			AIPGENE25234
			AIPGENE25233
			AIPGENE21249
Complex Hydrolysis	K00720	ceramide glucosyltransferase	AIPGENE27284
	K01201	glucosylceramidase	AIPGENE4062
			AIPGENE3973
	K17108	non-lysosomal glucosylceramidase	AIPGENE27398
			AIPGENE27398
	K05991	endoglycosylceramidase	AIPGENE1599
	K01019	galactosylceramide sulfotransferase	AIPGENE4055
			AIPGENE16984
	K01202	galactosylceramidase	NF
	K01189	alpha-galactosidase	NF
	K04628	2-hydroxyacylsphingosine 1-beta-galactosyltransferase	AIPGENE25843
			AIPGENE25848
			AIPGENE3411
			AIPGENE7513
			AIPGENE7524
			AIPGENE13973
	K01134	arylsulfatase A	NF
	K01186	sialidase-1	NF
	K12357	sialidase-2/3/4	NF
	K07553	beta-1,4-galactosyltransferase 6	NF

NF- not found

Table 2.1 (Continued)

Pathway	KEGG	Description	Gene ID
	K12309	beta-galactosidase	AIPGENE10572
			AIPGENE17172
	K04714	sphingomyelin synthase	AIPGENE20052
	K12350	sphingomyelin phosphodiesterase (acid sphingomyelinase)	AIPGENE10332
	K12351	sphingomyelin phosphodiesterase 2 (neutral sphingomyelinase 2)	AIPGENE18038
	K12352	sphingomyelin phosphodiesterase 3 (neutral sphingomyelinase 2)	NF
	K12353	sphingomyelin phosphodiesterase 4 (neutral sphingomyelinase 3)	AIPGENE17030
	K12354	ectonucleotide pyrophosphatase/ phosphodiesterase family member7 (alkaline sphingomyelinase)	NF
Degradation	K01634	sphinganine-1-phosphate lyase	AIPGENE12684

NF- not found

Figure 2.2 Protein sequence alignment of predicted SPHKs from *A. pallida*. Representative SPHKs were selected from *R. norvegicus* domains (D1-5) shown in yellow (A). The nuclear localization sequence (NLS= red), sequence insert between D4 and D5, and transmembrane segments (TM=blue) distinguish the two enzymes (Spiegel *et al.*, 2003). Visualization of protein structure between SPHK1 and SPHK2 was made using Domain Graph (DOG) v2.0 (Ren *et al.*, 2009). Multiple sequence alignment of isoenzymes SPHK1 and SPHK2 with predicted AP-SPHK, *A. pallida* and *S. minutum* genome homologs was produced using MUSCLE in Geneious v8.0.3 (B). Binding sites for primers used for qPCR (purple) and SPHK1 antibody (teal) are indicated on the sequence alignment. Sequence similarity was determined using a Blosum62 score matrix (Henikoff *et al.*, 1992) where > 60% is white, 60-80% is light grey, 80 to 99% is dark grey, and 100% is black.

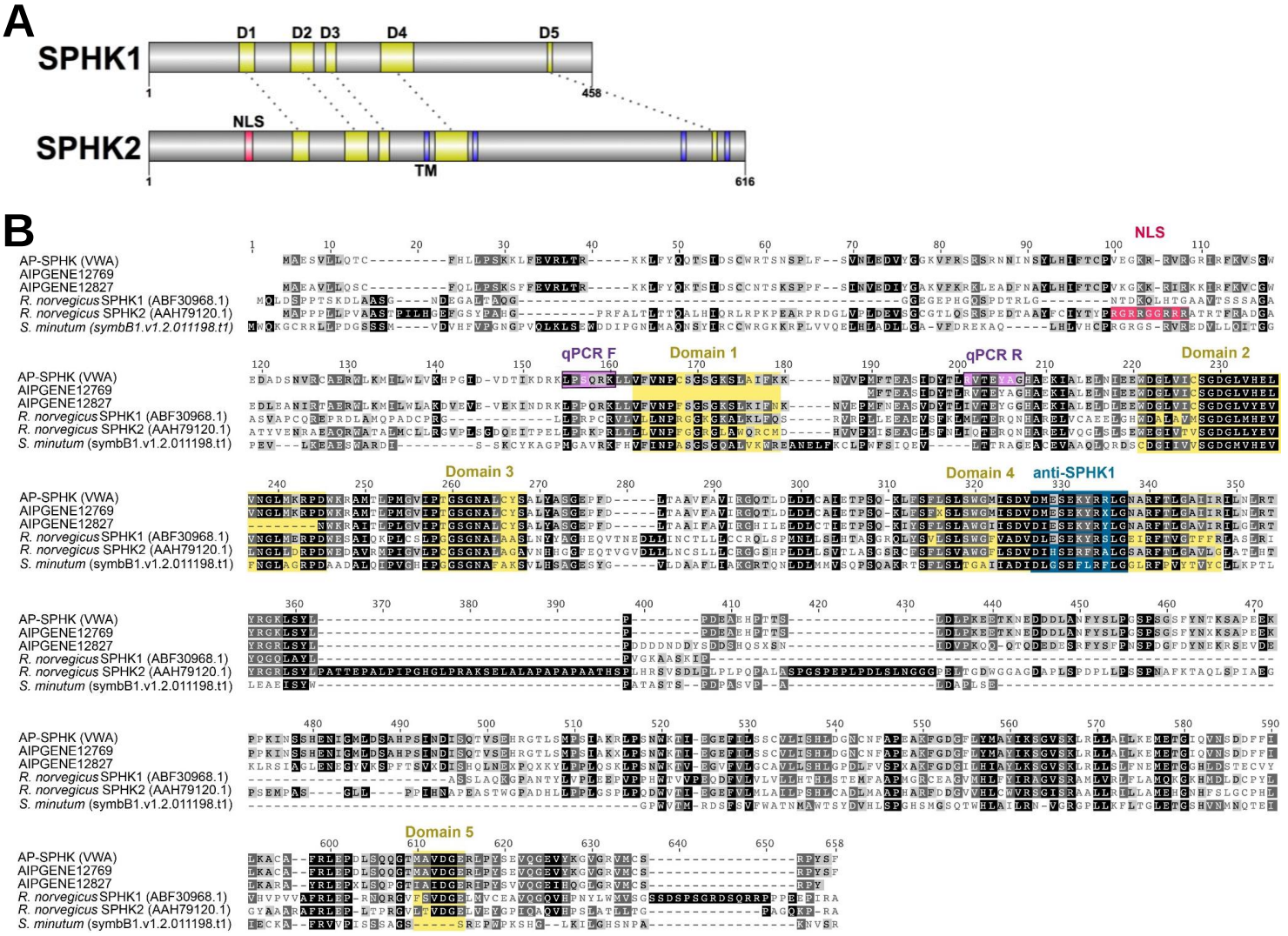
A
SPHK1
D1
D2
D3
D4
D5
1
458
SPHK2
NLS
TM
1
616
B
NLS
qPCR F
Domain 1
qPCR R
Domain 2
Domain 3
Domain 4
anti-SPHK1
Domain 5
AP-SPHK (VWA)
AIPGENE12769
AIPGENE12827
R. norvegicus SPHK1 (ABF30968.1)
R. norvegicus SPHK2 (AAH79120.1)
S. minutum (symbB1.v1.2.011198.t1)

Figure 2.2

Figure 2.3 Protein sequence alignment of the putative SGPP from *A. pallida*. Representative SGPP1 and SGPP2 from *R. norvegicus* were aligned with AP-SGPP using MUSCLE in Geneious v8.0.3. Conserved domains (D1-3) are highlighted yellow. Binding sites for primers used for qPCR (purple) are indicated on the sequence alignment. Sequence similarity was determined using a Blosum62 score matrix as described in Fig. 2.2 (Henikoff *et al.*, 1992).

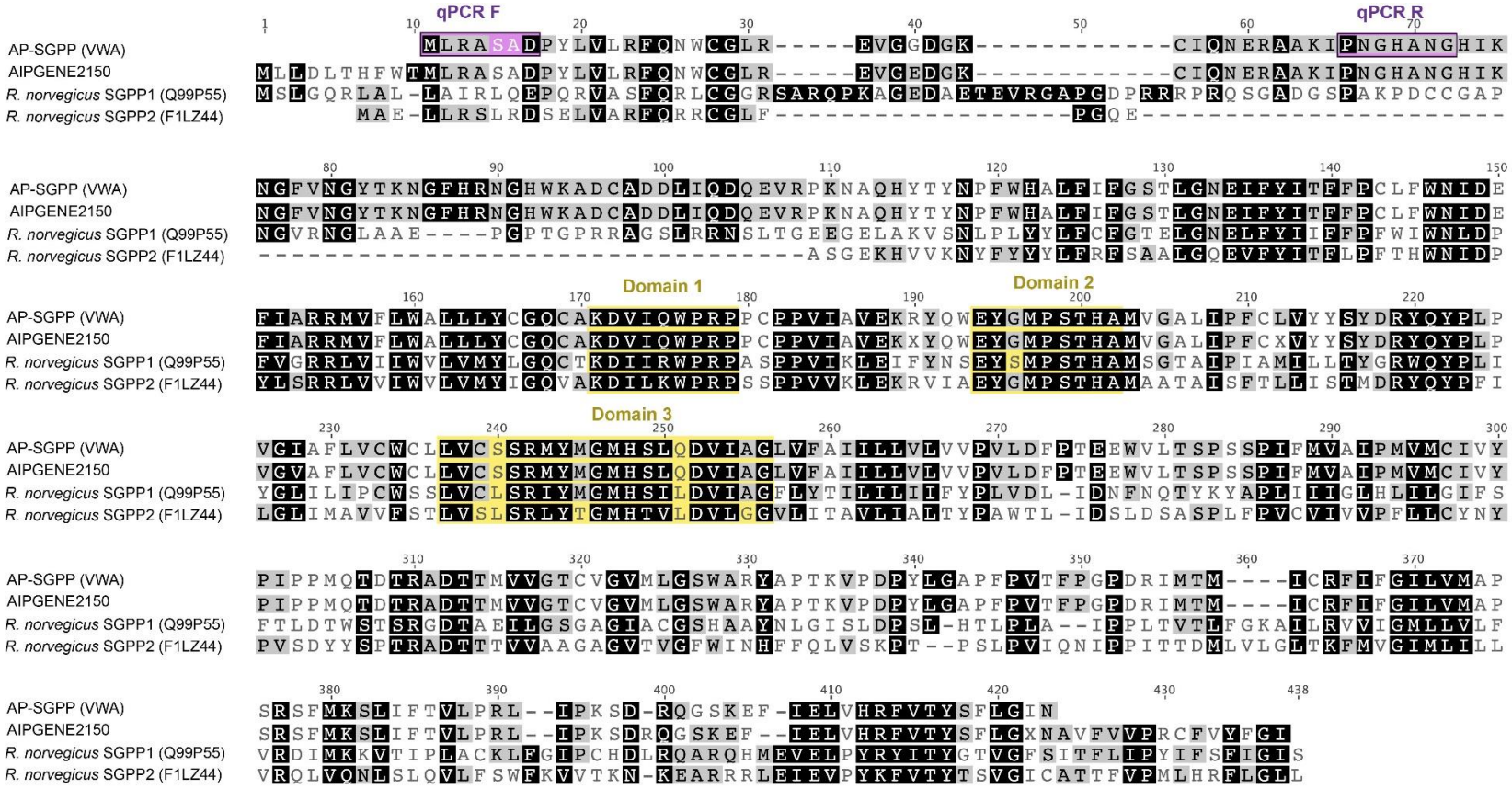
qPCR F
qPCR R
AP-SGPP (VWA)
AIPGENE2150
R. norvegicus SGPP1 (Q99P55)
R. norvegicus SGPP2 (F1LZ44)
Domain 1
Domain 2
Domain 3

Figure 2.3

Figure 2.4 Nucleotide sequence alignment of SPHKs from *A. pallida*. Nucleotide sequences of the proteins in Fig. 2.2 were aligned using MUSCLE in Geneious v8.0.3. Binding sites for primers used for qPCR (purple) are indicated on the sequence alignment. Sequence similarity was determined using a Blosum62 score matrix as described in Fig. 2.2 (Henikoff *et al.*, 1992).

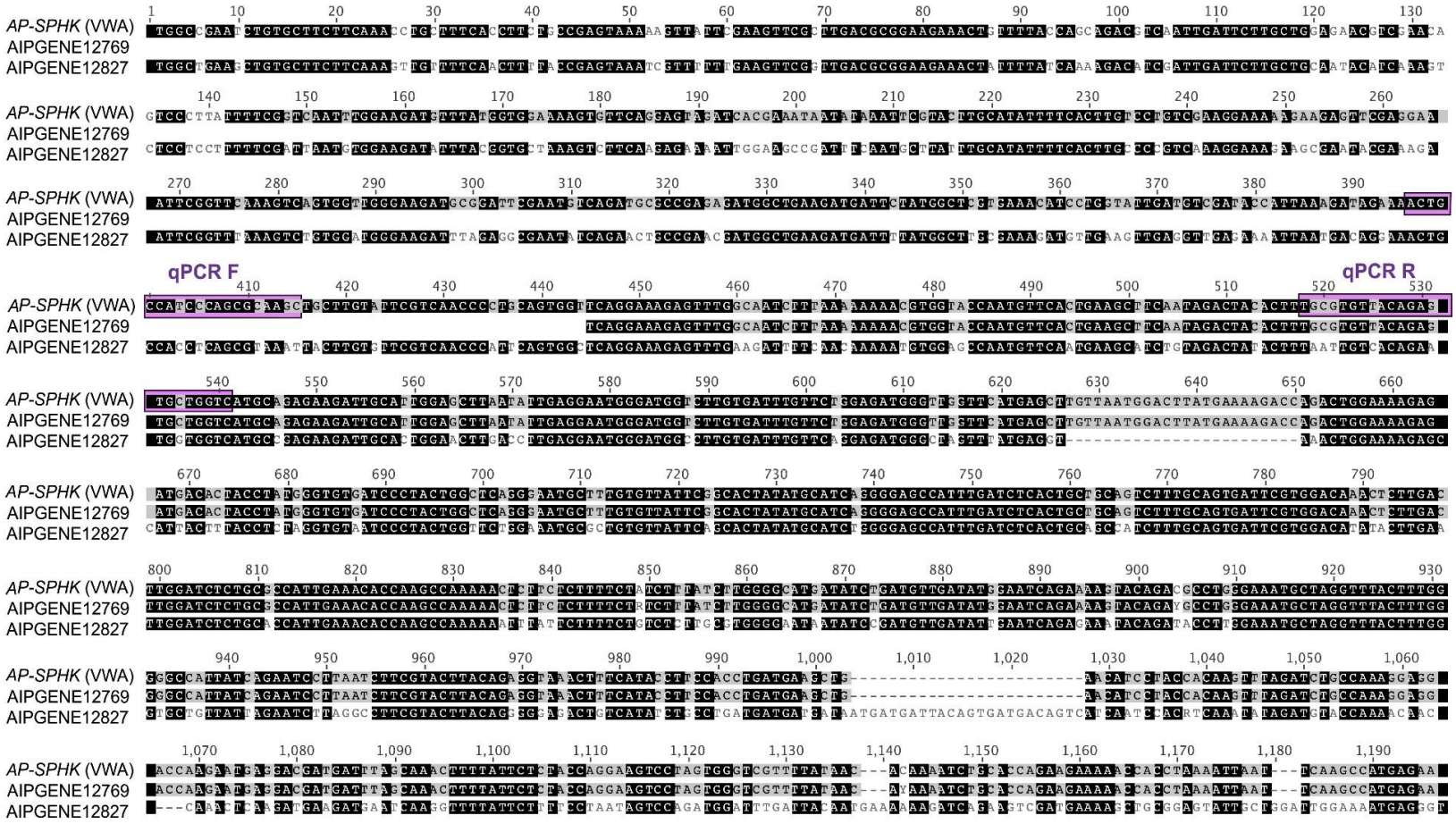

Figure 2.4

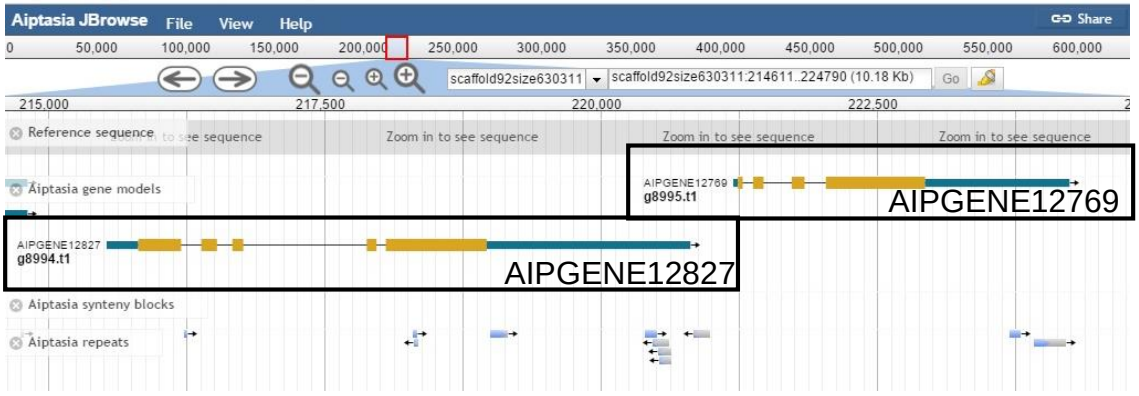

Figure 2.5 Screenshot of the two AP-SPHK gene models in the *Aiptasia* genome browser.

Table 2.2 Predicted SPHK homologs identified from publically available cnidarian genome or transcriptomes using *R. norvegicus* SPHK1 (NCBI: ABF30968) as the query.

Class	Species	Accession ID	E value	Resource
Anthozoa	*Acropora digitifera*	aug_v2a.11507.t1	3e-29	(Shinzato *et al.*, 2011)
	Aiptasia pallida	JV079020.1	3e-43	(Lehnert *et al.*, 2012)
	Anthopleura elegantissma	comp146758_c0_seq1	4e-48	(Kitchen *et al.*, 2015)
	Fungia scutaria	comp154870_c0_seq1	4e-47	(Kitchen *et al.*, 2015)
	Montastrea cavernosa	comp92849_c0_seq1	3e-66	(Kitchen *et al.*, 2015)
	Nematostella vectensis	XP_001632121.1	8e-82	(Putnam *et al.*, 2007)
	Porites australiensis	FX463324.1	1e-58	(Shinzato *et al.*, 2014)
	Seriatopora hystrix	comp210758_c0_seq1	3e-48	(Kitchen *et al.*, 2015)
	Stylophora pistillata	GARY01028221.1	1e-62	(Liew *et al.*, 2014)
Hydrozoa	*Hydra vulgaris*	GAOL01020445	5e-48	(Juliano *et al.*, 2014)
	Hydractinia symbiolongicarpus	GAWH01039148	2e-51	(Sanders *et al.*, 2014)
Myxozoa	*Polypodium hydriforme*	GBGH01016640	3e-22	(Shpirer *et al.*, 2014)
	Thelohanellus kitauei	KII70896.1	4e-16	(Yang *et al.*, 2014)
Scyphozoa	*Aurelia aurita*	GBRG01155343	8e-37	(Brekhman *et al.*, 2015)

Figure 2.6 Rheostat gene expression, immunodetection and lipid concentration of *A. pallida* in different symbiotic states. RNA, protein and lipid extracts were extracted from symbiotic (grey) or aposymbiotic (white) VWA anemones in steady-state. (A) Synthesized cDNA from sample RNA was used to quantify relative mRNA quantities (log_2) of AP-SPHK and AP-SGPP with qPCR (n=3 anemones per group). AP-SGPP and AP-SPHK expression was lower and higher respectively in symbiotic compared to aposymbiotic anemones. (B) An immunoblot of anemones in different states (n= 3) was probed with rabbit polyclonal antibody against SPHK1, upper panel. The band intensity of SPHK1 (75 kDa) was calculated relative to the actin band, 43 kDa, in the Ponceau S (Pon-S) stained blot (n=2 blots), lower panel. (C) *A. pallida* lipid extracts were collected from VWA (n= 4 anemones) and GMP (n=3 anemones) populations. Lipid concentrations (pmols/mg protein) were quantified after HPLC resolution ESI-tandem MS/MS, then normalized to internal standards (pmols) and host protein (mg). Sph differed from S1P in the aposymbiotic state and all VWA anemones (*). Boxplots (A and C) display the distribution of the data with the solid line in the box is the median, the box is the upper and lower quartiles and bracketed lines are maximum and minimum values. Differences in lowercase letters indicate significant differences between groups determined with 1-tailed Mann Whitney tests.

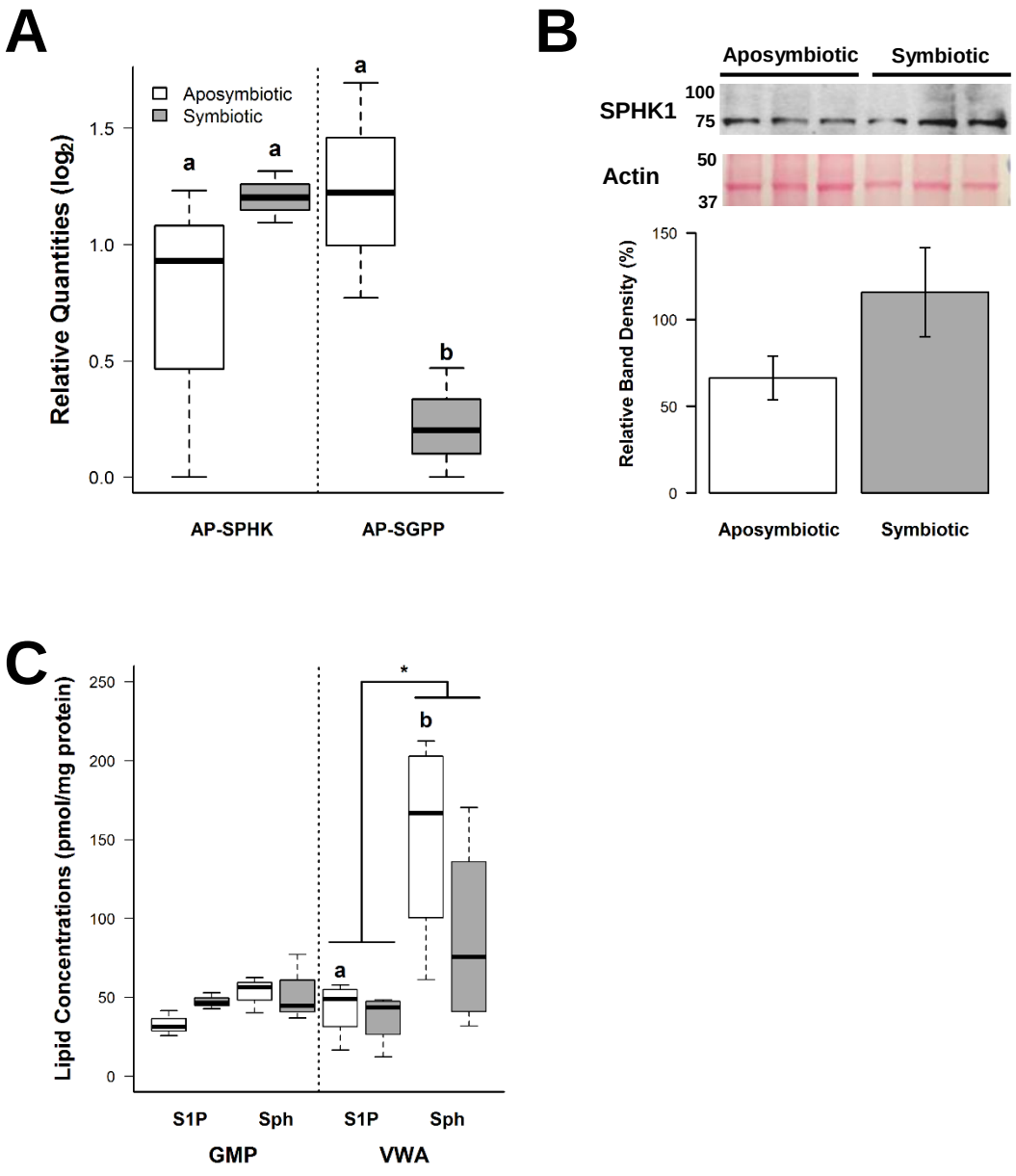
A
Aposymbiotic
Symbiotic
Relative Quantities (log2)
1.5
1.0
0.5
0.0
a
a
a
b
AP-SPHK
AP-SGPP
B
Aposymbiotic
Symbiotic
SPHK1
100
75
Actin
50
37
Relative Band Density (%)
150
100
50
0
Aposymbiotic
Symbiotic
C
Lipid Concentrations (pmol/mg protein)
250
200
150
100
50
0
*
b
a
S1P
Sph
S1P
Sph
GMP
VWA

Figure 2.6

Table 2.3 Recolonization experimental treatment groups.

Treatment Group	-L	+L	-BSE	+D
Light	+	+	+	–
Symbionts	–	+	–	+
Brine Shrimp Extract	+	+	–	+

Table 2.4 Analysis of variance results for gene expression of AP-SPHK and AP-SGPP during recolonization experiment. Factors were selected based on AIC criterion for statistical model testing. Sum of squares (SS), degrees of freedom (*df*), *F*-statistics and p-values were rounded to the nearest hundredth.

Gene	Comparisons	Factors	SS	*df*	*F*	p-value
AP- SPHK	+L *vs.* -L	Time	54.25	4	41.57	< 0.001
		Symbiont	23.27	1	71.33	< 0.001
		BSE	0.09	1	0.287	0.60
		Time:Symbiont	42.64	3	45.79	< 0.001
	+L *vs.* +D	Time	136.76	4	59.26	< 0.001
		Light	27.68	1	47.97	< 0.001
		Oral Disc	2.00	1	3.47	0.08
		Time:Light	6.34	3	3.67	0.03
AP-SGPP	+L *vs.* -L	Time	6.96	4	14.38	< 0.001
		Symbiont	10.12	1	83.60	< 0.001
		BSE	0.37	1	3.17	0.09
		Time:Symbiont	4.45	3	12.68	< 0.001
	+L *vs.* +D	Time	21.28	4	30.05	< 0.001
		Light	3.89	1	21.98	< 0.001
		Time:Light	9.46	3	17.81	< 0.001

Figure 2.7 Symbiont uptake in the light and dark modulates AP-SPHK and AP-SGPP expression. Aposymbiotic *A. pallida* were inoculated with 10^5 *S. minutum* strain CCMP830 (type B1) and washed 24 h post-inoculation. Relative mRNA quantities (log2) of (A) AP-SPHK and (B) AP-SGPP were quantified over time using qPCR with recolonized anemone cDNA from light only (-L, ◆), symbiont + light (+L, ●) and symbiont + dark (+D, ■) treatment groups. Relative quantities are presented as mean ± standard error, n=3 anemones for each time point within each treatment group. Results of the Tukey post hoc comparisons from the ANOVA test in Table 2.4 are presented above (A) and (B). Comparisons that were not significant (n.s.) did not pass the $p \leq 0.05$ threshold.

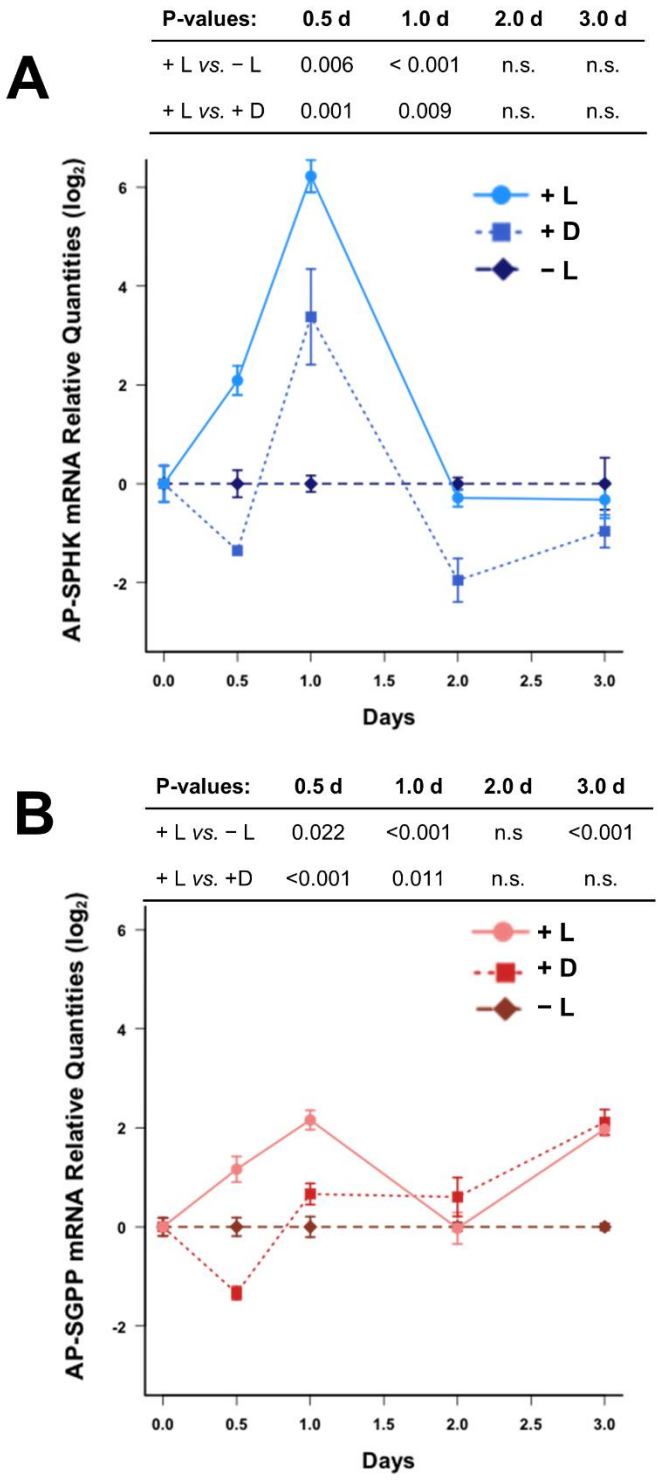
A
P-values: 0.5 d 1.0 d 2.0 d 3.0 d
+ L vs. − L 0.006 < 0.001 n.s. n.s.
+ L vs. + D 0.001 0.009 n.s. n.s.
AP-SPHK mRNA Relative Quantities (log2)
+ L
+ D
− L
Days
B
P-values: 0.5 d 1.0 d 2.0 d 3.0 d
+ L vs. − L 0.022 <0.001 n.s <0.001
+ L vs. +D <0.001 0.011 n.s. n.s.
AP-SGPP mRNA Relative Quantities (log2)
+ L
+ D
− L
Days

Figure 2.7

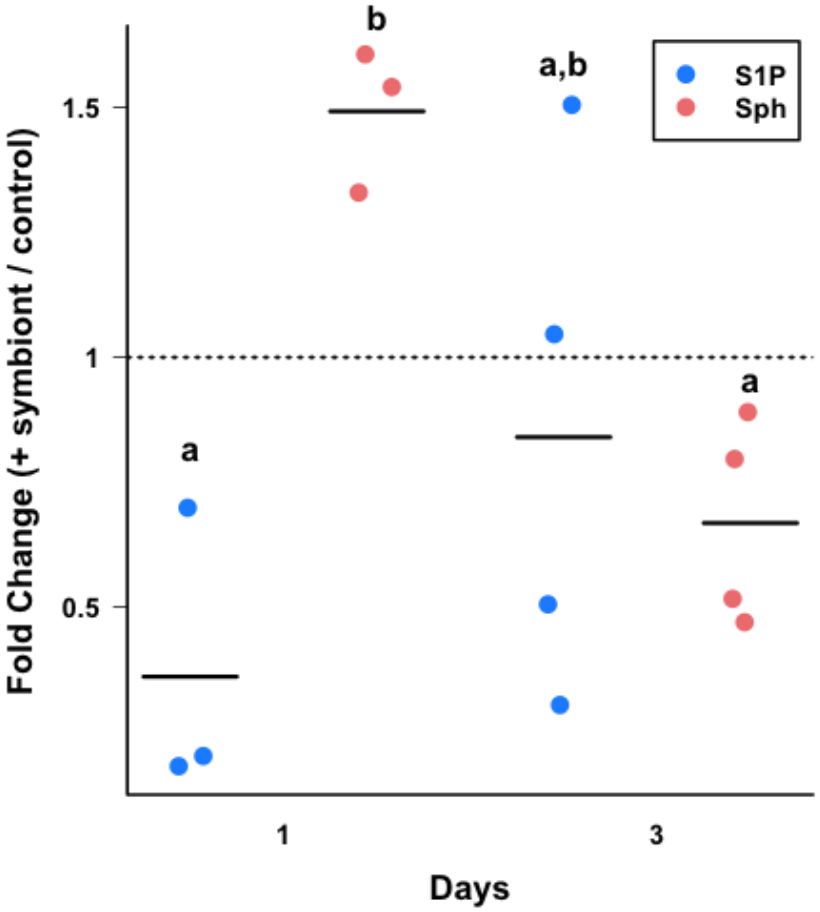

Figure 2.8 Recolonization in the light shifts ratios of *A. pallida* sphingolipids. Lipids extracts were quantified with HPLC ESI tandem-MS/MS, normalized to internal standards and total protein. Calculated fold changes of S1P (blue) and Sph (red) for treatment groups +L/-L at day one and three were analyzed with 1-tailed Mann Whitney test. Black bars show the mean fold change for each metabolite at the separate days. Groups not sharing a letter (a or b) significantly differ ($p \leq 0.05$).

Table 2.5 Oligonucleotide primers used in RACE, SNP detection and qPCR.

Gene	Application	Primers
Sphingosine kinase (AP-SPHK)	3' end RACE	F 5' ATG CTA GAC AGT GCG CAT CCA TCA 3'
	5' end RACE	R 5' ACC CAA CCA CTG ACT TTG AAC CGA 3'
	SNP detection	F 5' TCT TGC TGG AGA ACG TCG AAC AGT 3' R 5' ATG GCG CAG AGA TCC AAG TCA AGA 3'
	qPCR GOI	F 5' ACT GCC ATC CCA GCG CAA GC 3' R 5'GAC CAG CAT ACT CTG TAA CAC GCA 3'
Sphingosine-1-phosphatase (AP-SGPP)	5' end RACE	R 5' AAG TGC GTG CCA GAA GGG GTT GT 3'
	SNP detection	F 5' AAT GCT GCG TGC TTC AGC GGA T 3' R 5' ACG CGA TGG AGC CAT CAC AAG A 3'
	qPCR GOI	F 5' AAT GCT GCG TGC TTC AGC GGA T 3' R 5' TCC GTT AGC ATG GCC GTT TGG A 3'
Ribosomal large subunit 10 (L10)*	qPCR reference	F 5' ACG TTT CTG CCG TGG TGT CCC 3' R 5' CGG GCA GCT TCA AGG GCT TCA 3'
Ribosomal large subunit 12 (L12)*	qPCR reference	F 5' ACA TCG CCA AGA CAA TGC GTC C 3' R 5' GAC GTC ATG GGG CGG CTG TC 3'
Poly-A binding protein (PABP)*	qPCR reference	F 5' GTG CAA GGA GGC GGA CAG CG 3' R 5' TTG GCT GAT TGC GGG TTG CC 3'
Glyceraldehyde 3-phosphate dehydrogenase (GAPDH)*	qPCR reference	F 5' AAG GCT GCT AAG GCA ATC GGC 3' R 5' TCG CAC GGT TAA GTC CAA GAC 3'
Elongation factor 1 alpha 1 (EEF1A1)*	qPCR reference	F 5' TGC TCG ACA AAC TCA AGG CCG A 3' R 5' TGC GAA GTG CCG GTG ATC ATG T 3'

* qPCR reference genes were also used in the previous study by Poole *et al.* (submitted)

Table 2.6 Stability values of reference genes tested for symbiotic-state and colonization experiments with GeNorm (Vandesompele *et al.*, 2002) and NormFinder (Andersen *et al.*, 2004).

Gene	GeNorm (M)	NormFinder
L10	0.866	0.202
L12	0.967	0.225
PABP	0.959	0.228
GAPDH	1.077	0.394

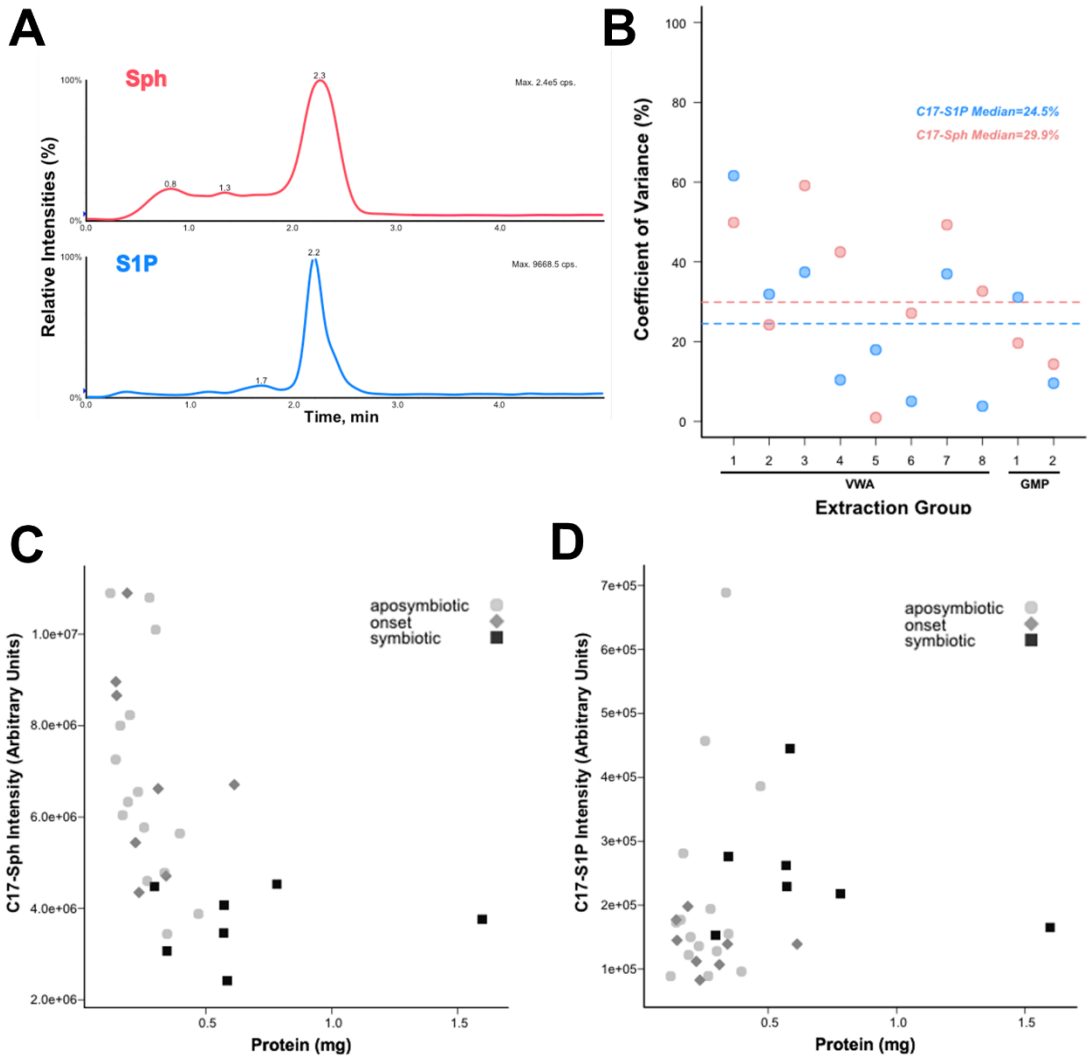

Figure 2.9 Lipid extraction variations between groups and steady state or colonization treatment. (A) Representative chromatograms of Sph (red) and S1P (blue) used for quantification show peak relative intensities over time. (B) The coefficient of variance was calculated from the C17 internal standard peak intensity for each analyte in each extraction group. Dashed lines indicate median percent CV for each metabolite. Recovery was examined by comparing relative intensity of C17 internal standards for (C) Sph and (D) S1P to animal size (total protein) by treatment groups: aposymbiotic = ●, onset of symbiosis = ◆, and symbiotic = ■.

2.5 References

Al-Lihaibi, S.S., Ayyad, S.-E.N., Shaher, F. and Alarif, W.M. (2010). Antibacterial sphingolipid and steroids from the black coral *Antipathes dichotoma*. *Chem. Pharm. Bull. (Tokyo)* **58,** 1635-1638.

Alemany, R., van Koppen, C.J., Danneberg, K., Ter Braak, M. and Meyer zu Heringdorf, D. (2007). Regulation and functional roles of sphingosine kinases. *Naunyn-Schmiedeberg's Arch. Pharmacol.* **374,** 413-428.

Ali, H.Z., Harding, C.R. and Denny, P.W. (2011). Endocytosis and sphingolipid scavenging in *Leishmania mexicana* amastigotes. *Biochemistry Research International* **2012**.

Altschul, S.F., Gish, W., Miller, W., Myers, E.W. and Lipman, D.J. (1990). Basic local alignment search tool. *J. Mol. Biol.* **215,** 403-410.

Amar, K.-O., Douek, J., Rabinowitz, C. and Rinkevich, B. (2008). Employing of the amplified fragment length polymorphism (AFLP) methodology as an efficient population genetic tool for symbiotic cnidarians. *Mar. Biotechnol.* **10,** 350-357.

An, D., Na, C., Bielawski, J., Hannun, Y.A. and Kasper, D.L. (2011). Membrane sphingolipids as essential molecular signals for *Bacteroides* survival in the intestine. *Proc. Natl. Acad. Sci. USA* **108,** 4666-4671.

An, D., Oh, S.F., Olszak, T., Neves, J.F., Avci, F.Y., Erturk-Hasdemir, D., *et al.* (2014). Sphingolipids from a symbiotic microbe regulate homeostasis of host intestinal natural killer T cells. *Cell* **156,** 123-133.

An, S., Bleu, T., Huang, W., Hallmark, O.G., Coughlin, S.R. and Goetzl, E.J. (1997). Identification of cDNAs encoding two G protein-coupled receptors for lysosphingolipids. *FEBS Lett.* **417,** 279-282.

Andersen, C.L., Jensen, J.L. and Ørntoft, T.F. (2004). Normalization of real-time quantitative reverse transcription-PCR data: A model-based variance estimation approach to identify genes suited for normalization, applied to bladder and colon cancer data sets. *Cancer Res.* **64,** 5245-5250.

Bartke, N. and Hannun, Y.A. (2009). Bioactive sphingolipids: metabolism and function. *J. Lipid Res.* **50,** S91-S96.

Baumgarten, S., Simakov, O., Esherick, L.Y., Liew, Y.J., Lehnert, E.M., Michell, C.T., *et al.* (2015). The genome of *Aiptasia*, a sea anemone model for coral symbiosis. *Proc. Natl. Acad. Sci. USA* **112,** 11893-11898.

Bellwood, D.R. and Hughes, T.P. (2001). Regional-scale assembly rules and biodiversity of coral reefs. *Science* **292,** 1532-1535.

Bligh, E.G. and Dyer, W.J. (1959). A rapid method of total lipid extraction and purification. *Can. J. Biochem. Physiol.* **37,** 911-917.

Brekhman, V., Malik, A., Haas, B., Sher, N. and Lotan, T. (2015). Transcriptome profiling of the dynamic life cycle of the scypohozoan jellyfish *Aurelia aurita*. *BMC Genomics* **16,** 74.

Bryan, A.M., Del Poeta, M. and Luberto, C. (2015). Sphingolipids as regulators of the phagocytic response to fungal infections. *Mediators Inflamm.* **2015,** 640540.

Chan, H. and Pitson, S.M. (2013). Post-translational regulation of sphingosine kinases. *Biochim. Biophys. Acta* **1831,** 147-156.

Chen, H.-K., Song, S.-N., Wang, L.-H., Mayfield, A.B., Chen, Y.-J., Chen, W.-N.U. and Chen, C.-S. (2015). A compartmental comparison of major lipid species in a coral-*Symbiodinium* endosymbiosis: Evidence that the coral host regulates lipogenesis of its cytosolic lipid bodies. *PLoS One* **10,** e0132519.

Chen, Y., Liu, Y., Sullards, M.C. and Merrill Jr, A.H. (2010). An introduction to sphingolipid metabolism and analysis by new technologies. *Neuromolecular Med.* **12,** 306-319.

Cheng, S., Wen, Z., Chiou, S., Tsai, C., Wang, S., Hsu, C., *et al.* (2009). Ceramide and cerebrosides from the octocoral *Sarcophyton ehrenbergi*. *J. Nat. Prod.* **72,** 465-468.

Chun, J., Goetzl, E.J., Hla, T., Igarashi, Y., Lynch, K.R., Moolenaar, W., *et al.* (2002). International union of pharmacology. XXXIV. Lysophospholipid receptor nomenclature. *Pharmacol. Rev.* **54,** 265-269.

Cinque, B., Di Marzio, L., Centi, C., Di Rocco, C., Riccardi, C. and Cifone, M.G. (2003). Sphingolipids and the immune system. *Pharmacol. Res.* **47,** 421-437.

Coffroth, M.A., Lasker, H.R., Diamond, M.E., Bruenn, J.A. and Bermingham, E. (1992). DNA fingerprints of a gorgonian coral: a method for detecting clonal structure in a vegetative species. *Mar. Biol.* **114,** 317-325.

Correa, A.M., McDonald, M.D. and Baker, A.C. (2009). Development of clade-specific *Symbiodinium* primers for quantitative PCR (qPCR) and their application to detecting clade D symbionts in Caribbean corals. *Mar. Biol.* **156,** 2403-2411.

Cuvillier, O., Pirianov, G., Kleuser, B., Vanek, P.G., Coso, O.A., Gutkind, J.S. and Spiegel, S. (1996). Suppression of ceramide-mediated programmed cell death by sphingosine-1-phosphate. *Nature* **381,** 800-803.

Davy, S.K., Allemand, D. and Weis, V.M. (2012). Cell biology of cnidarian-dinoflagellate symbiosis. *Microbiol. Mol. Biol. Rev.* **76,** 229-261.

Detournay, O. and Weis, V.M. (2011). Role of the sphingosine rheostat in the regulation of cnidarian-dinoflagellate symbioses. *Biol. Bull.* **221,** 261-269.

Dobson, L., Reményi, I. and Tusnády, G.E. (2015). CCTOP: a Consensus Constrained TOPology prediction web server. *Nucleic Acids Res.* **43,** W408-412.

Döll, F., Pfeilschifter, J. and Huwiler, A. (2005). The epidermal growth factor stimulates sphingosine kinase-1 expression and activity in the human mammary carcinoma cell line MCF7. *Biochim. Biophys. Acta* **1738,** 72-81.

Dunn, S.R., Thomas, M.C., Nette, G.W. and Dove, S.G. (2012). A lipidomic approach to understanding free fatty acid lipogenesis derived from dissolved inorganic carbon within cnidarian-dinoflagellate symbiosis. *PLoS One* **7,** e46801.

Dykstra, M., Cherukuri, A., Sohn, H.W., Tzeng, S.-J. and Pierce, S.K. (2003). Location is everything: lipid rafts and immune cell signaling. *Annu. Rev. Immunol.* **21,** 457-481.

Edgar, R.C. (2004). MUSCLE: multiple sequence alignment with high accuracy and high throughput. *Nucleic Acids Res.* **32,** 1792-1797.

Flannagan, R.S., Jaumouillé, V. and Grinstein, S. (2012). The cell biology of phagocytosis. *Annu. Rev. Pathol.* **7,** 61-98.

Ganot, P., Moya, A., Magnone, V., Allemand, D., Furla, P. and Sabourault, C. (2011). Adaptations to endosymbiosis in a cnidarian-dinoflagellate association: differential gene expression and specific gene duplications. *PLoS Genet.* **7,** e1002187.

Garrett, T.A., Schmeitzel, J.L., Klein, J.A., Hwang, J.J. and Schwarz, J.A. (2013). Comparative lipid profiling of the cnidarian *Aiptasia pallida* and its dinoflagellate symbiont. *PLoS One* **8,** e57975.

Goetzl, E.J. and An, S. (1998). Diversity of cellular receptors and functions for the lysophospholipid growth factors lysophosphatidic acid and sphingosine 1-phosphate. *The FASEB Journal* **12,** 1589-1598.

Grajales, A. and Rodriguez, E. (2014). Morphological revision of the genus *Aiptasia* and the family Aiptasiidae (Cnidaria, Actiniaria, Metridioidea). *Zootaxa* **3826,** 55-100.

Grajales, A. and Rodríguez, E. (2016). Elucidating the evolutionary relationships of the Aiptasiidae, a widespread cnidarian–dinoflagellate model system (Cnidaria: Anthozoa: Actiniaria: Metridioidea). *Mol. Phylogenet. Evol.* **94,** 252-263.

Guillard, R.R.L. and Ryther, J.H. (1962). Studies of marine planktonic diatoms I. *Cyclotella nana* Hustedt and *Detonula confervacea* Cleve. . *Can. J. Microbiol.* **8,** 229-239.

Hakomori, S.I., Yamamura, S. and Handa, K. (1998). Signal transduction through glyco (sphingo) lipids: Introduction and recent studies on glyco (sphingo) lipid‐enriched microdomains. *Ann. N.Y. Acad. Sci.* **845,** 1-10.

Hannun, Y.A. and Obeid, L.M. (2008). Principles of bioactive lipid signalling: lessons from sphingolipids. *Nat. Rev. Mol. Cell Biol.* **9,** 139-150.

Harii, S., Yasuda, N., Rodriguez-Lanetty, M., Irie, T. and Hidaka, M. (2009). Onset of symbiosis and distribution patterns of symbiotic dinoflagellates in the larvae of scleractinian corals. *Mar. Biol.* **156,** 1203-1212.

Henikoff, S. and Henikoff, J.G. (1992). Amino acid substitution matrices from protein blocks. *Proc. Natl. Acad. Sci. USA* **89,** 10915-10919.

Heung, L.J., Luberto, C. and Del Poeta, M. (2006). Role of sphingolipids in microbial pathogenesis. *Infect. Immun.* **74,** 28-39.

Igarashi, N., Okada, T., Hayashi, S., Fujita, T., Jahangeer, S. and Nakamura, S.-i. (2003). Sphingosine kinase 2 is a nuclear protein and inhibits DNA synthesis. *J. Biol. Chem.* **278,** 46832-46839.

Imbs, A.B. (2014). Lipid class and fatty acid compositions of the zoanthid *Palythoa caesia* (Anthozoa: Hexacorallia: Zoanthidea) and its chemotaxonomic relations with corals. *Biochem. Syst. Ecol.* **54,** 213-218.

Imbs, A.B., Yakovleva, I.M. and Pham, L.Q. (2010). Distribution of lipids and fatty acids in the zooxanthellae and host of the soft coral *Sinularia* sp. *Fish. Sci.* **76,** 375-380.

Iwaki, S., Kihara, A., Sano, T. and Igarashi, Y. (2005). Phosphorylation by Pho85 cyclin-dependent kinase acts as a signal for the down-regulation of the yeast sphingoid long-chain base kinase Lcb4 during the stationary phase. *J. Biol. Chem.* **280,** 6520-6527.

Jones, P., Binns, D., Chang, H.-Y., Fraser, M., Li, W., McAnulla, C., *et al.* (2014). InterProScan 5: genome-scale protein function classification. *Bioinformatics* **30,** 1236-1240.

Juliano, C.E., Reich, A., Liu, N., Götzfried, J., Zhong, M., Uman, S., *et al.* (2014). PIWI proteins and PIWI-interacting RNAs function in *Hydra* somatic stem cells. *Proc. Natl. Acad. Sci. USA* **111,** 337-342.

Kassmer, S.H., Rodriguez, D., Langenbacher, A.D., Bui, C. and De Tomaso, A.W. (2015). Migration of germline progenitor cells is directed by sphingosine-1-phosphate signalling in a basal chordate. *Nat. Commun.* **6,** 8565.

Kearse, M., Moir, R., Wilson, A., Stones-Havas, S., Cheung, M., Sturrock, S., *et al.* (2012). Geneious Basic: an integrated and extendable desktop software platform for the organization and analysis of sequence data. *Bioinformatics* **28,** 1647-1649.

Kelley, D.R. and Salzberg, S.L. (2010). Detection and correction of false segmental duplications caused by genome mis-assembly. *Genome Biol.* **11,** R28.

Kellogg, R.B. and Patton, J.S. (1983). Lipid droplets, medium of energy exchange in the symbiotic anemone *Condylactis gigantea*: a model coral polyp. *Mar. Biol.* **75,** 137-149.

Kihara, A., Kurotsu, F., Sano, T., Iwaki, S. and Igarashi, Y. (2005). Long-chain base kinase Lcb4 Is anchored to the membrane through its palmitoylation by Akr1. *Mol. Cell. Biol.* **25,** 9189-9197.

Kitchen, S.A., Crowder, C.M., Poole, A.Z., Weis, V.M. and Meyer, E. (2015). *De novo* assembly and characterization of four anthozoan (Phylum Cnidaria) transcriptomes. *G3: Genes*| *Genomes*| *Genetics* **5,** 2441-2452.

Kohama, T., Olivera, A., Edsall, L., Nagiec, M.M., Dickson, R. and Spiegel, S. (1998). Molecular cloning and functional characterization of murine sphingosine kinase. *J. Biol. Chem.* **273,** 23722-23728.

Koles, K., Irvine, K.D. and Panin, V.M. (2004). Functional characterization of *Drosophila* sialyltransferase. *J. Biol. Chem.* **279,** 4346-4357.

Le Stunff, H., Peterson, C., Thornton, R., Milstien, S., Mandala, S.M. and Spiegel, S. (2002). Characterization of murine sphingosine-1-phosphate phosphohydrolase. *J. Biol. Chem.* **277,** 8920-8927.

Lee, M.-J., Van Brocklyn, J.R., Thangada, S., Liu, C.H., Hand, A.R., Menzeleev, R., *et al.* (1998). Sphingosine-1-phosphate as a ligand for the G protein-coupled receptor EDG-1. *Science* **279,** 1552-1555.

Lehnert, E.M., Burriesci, M.S. and Pringle, J.R. (2012). Developing the anemone *Aiptasia* as a tractable model for cnidarian-dinoflagellate symbiosis: the transcriptome of aposymbiotic *A. pallida*. *BMC Genomics* **13,** 271.

Lesser, M.P. (1996). Elevated temperatures and ultraviolet radiation cause oxidative stress and inhibit photosynthesis in symbiotic dinoflagellates. *Limnol. Oceanogr.* **41,** 271-283.

Li, Y.-T. and Li, S.-C. (1999). Enzymatic hydrolysis of glycosphingolipids. *Anal. Biochem.* **273,** 1-11.

Lieser, B., Liebisch, G., Drobnik, W. and Schmitz, G. (2003). Quantification of sphingosine and sphinganine from crude lipid extracts by HPLC electrospray ionization tandem mass spectrometry. *J. Lipid Res.* **44,** 2209-2216.

Liew, Y.J., Aranda, M., Carr, A., Baumgarten, S., Zoccola, D., Tambutté, S., *et al.* (2014). Identification of microRNAs in the coral *Stylophora pistillata*. *PLoS One* **9,** e91101.

Liu, H., Sugiura, M., Nava, V.E., Edsall, L.C., Kono, K., Poulton, S., *et al.* (2000). Molecular cloning and functional characterization of a novel mammalian sphingosine kinase type 2 isoform. *J. Biol. Chem.* **275,** 19513-19520.

Livak, K.J. and Schmittgen, T.D. (2001). Analysis of relative gene expression data using real-time quantitative PCR and the $2^{-\Delta\Delta CT}$ method. *Methods* **25,** 402-408.

Lloyd-Evans, E., Morgan, A.J., He, X., Smith, D.A., Elliot-Smith, E., Sillence, D.J., *et al.* (2008). Niemann-Pick disease type C1 is a sphingosine storage disease that causes deregulation of lysosomal calcium. *Nat. Med.* **14,** 1247-1255.

Maceyka, M., Payne, S.G., Milstien, S. and Spiegel, S. (2002). Sphingosine kinase, sphingosine-1-phosphate, and apoptosis. *Biochim. Biophys. Acta* **1585,** 193 - 201.

Maceyka, M., Sankala, H., Hait, N.C., Le Stunff, H., Liu, H., Toman, R., *et al.* (2005). SphK1 and SphK2, sphingosine kinase isoenzymes with opposing functions in sphingolipid metabolism. *J. Biol. Chem.* **280,** 37118-37129.

Mandala, S.M., Thornton, R., Galve-Roperh, I., Poulton, S., Peterson, C., Olivera, A., *et al.* (2000). Molecular cloning and characterization of a lipid phosphohydrolase that degrades sphingosine-1-phosphate and induces cell death. *Proc. Natl. Acad. Sci. USA* **97,** 7859-7864.

Mandala, S.M., Thornton, R., Tu, Z., Kurtz, M.B., Nickels, J., Broach, J., *et al.* (1998). Sphingoid base 1-phosphate phosphatase: a key regulator of sphingolipid metabolism and stress response. *Proc. Natl. Acad. Sci. USA* **95,** 150-155.

Metpally, R.P. and Sowdhamini, R. (2005). Cross genome phylogenetic analysis of human and *Drosophila* G protein-coupled receptors: application to functional annotation of orphan receptors. *BMC Genomics* **6,** 106.

Murate, T., Banno, Y., Keiko, T., Watanabe, K., Mori, N., Wada, A., *et al.* (2001). Cell type-specific localization of sphingosine kinase 1a in human tissues. *J. Histochem. Cytochem.* **49,** 845-855.

Muscatine, L., Grossman, D. and Doino, J. (1991). Release of symbiotic algae by tropical sea anemones and corals after cold shock. *Mar. Ecol. Prog. Ser.* **77,** 233-243.

Nakanaga, K., Hama, K., Kano, K., Sato, T., Yukiura, H., Inoue, A., *et al.* (2014). Overexpression of autotaxin, a lysophosphatidic acid-producing enzyme, enhances cardia bifida induced by hypo-sphingosine-1-phosphate signaling in zebrafish embryo. *J. Biochem.* **155,** 235-241.

Nordström, K.J., Fredriksson, R. and Schiöth, H.B. (2008). The amphioxus (*Branchiostoma floridae*) genome contains a highly diversified set of G protein-coupled receptors. *BMC Evol. Biol.* **8,** 9.

Ogawa, C., Kihara, A., Gokoh, M. and Igarashi, Y. (2003). Identification and characterization of a novel human sphingosine-1-phosphate phosphohydrolase, hSPP2. *J. Biol. Chem.* **278,** 1268-1272.

Olivera, A., Kohama, T., Edsall, L., Nava, V., Cuvillier, O., Poulton, S. and Spiegel, S. (1999). Sphingosine kinase expression increases intracellular sphingosine-1-phosphate and promotes cell growth and survival. *J. Cell Biol.* **147,** 545-558.

Olivera, A., Kohama, T., Tu, Z., Milstien, S. and Spiegel, S. (1998). Purification and characterization of rat kidney sphingosine kinase. *J. Biol. Chem.* **273,** 12576-12583.

Olivera, A., Rosenfeldt, H.M., Bektas, M., Wang, F., Ishii, I., Chun, J., *et al.* (2003). Sphingosine kinase type 1 induces G12/13-mediated stress fiber formation, yet promotes growth and survival independent of G protein-coupled receptors. *J. Biol. Chem.* **278,** 46452-46460.

Olivera, A. and Spiegel, S. (2001). Sphingosine kinase: a mediator of vital cellular functions. *Prostaglandins Other Lipid Mediat.* **64,** 123-134.

Peng, S.-E., Chen, W.-N.U., Chen, H.-K., Lu, C.-Y., Mayfield, A.B., Fang, L.-S. and Chen, C.-S. (2011). Lipid bodies in coral–dinoflagellate endosymbiosis: Proteomic and ultrastructural studies. *Proteomics* **11,** 3540-3555.

Pitson, S.M., Moretti, P.A., Zebol, J.R., Lynn, H.E., Xia, P., Vadas, M.A. and Wattenberg, B.W. (2003). Activation of sphingosine kinase 1 by ERK1/2-mediated phosphorylation. *EMBO J.* **22,** 5491-5500.

Pitson, S.M., Moretti, P.A., Zebol, J.R., Xia, P., Gamble, J.R., Vadas, M.A., *et al.* (2000). Expression of a catalytically inactive sphingosine kinase mutant blocks agonist-induced sphingosine kinase activation A dominant-negative sphingosine kinase. *J. Biol. Chem.* **275,** 33945-33950.

Poole, A.Z., Kitchen, S.A., Dow, E.G. and Weis, V.M. (submitted). The role of complement in cnidarian-dinoflagellate symbiosis and immune challenge in the sea anemone *Aiptasia pallida*. *Front. Microbiol.*

Prakash, H., Luth, A., Grinkina, N., Holzer, D., Wadgaonkar, R., Gonzalez, A.P., *et al.* (2010). Sphingosine kinase-1 (SphK-1) regulates *Mycobacterium smegmatis* infection in macrophages. *PLoS One* **5,** e10657.

Putnam, N.H., Srivastava, M., Hellsten, U., Dirks, B., Chapman, J., Salamov, A., *et al.* (2007). Sea anemone genome reveals ancestral eumetazoan gene repertoire and genomic organization. *Science* **317,** 86-94.

Ramakers, C., Ruijter, J.M., Deprez, R.H. and Moorman, A.F. (2003). Assumption-free analysis of quantitative real-time polymerase chain reaction (PCR) data. *Neurosci. Lett.* **339,** 62 - 66.

Rasband, W. (1997-2015) ImageJ. Bethesda, Maryland, USA, U. S. National Institutes of Health

RCoreTeam (2013) R: A language and environment for statistical computing. Vienna, Austria, R Foundation for Statistical Computing.

Ren, J., Wen, L., Gao, X., Jin, C., Xue, Y. and Yao, X. (2009). DOG 1.0: illustrator of protein domain structures. *Cell Res.* **19,** 271-273.

Revel, J., Massi, L., Mehiri, M., Boutoute, M., Mayzaud, P., Capron, L. and Sabourault, C. (2016). Differential distribution of lipids in epidermis, gastrodermis and hosted *Symbiodinium* in the sea anemone *Anemonia viridis*. *Comp. Biochem. Physiol., A: Mol. Integr. Physiol.* **191,** 140-151.

Rivera, J., Proia, R.L. and Olivera, A. (2008). The alliance of sphingosine-1-phosphate and its receptors in immunity. *Nat. Rev. Immunol.* **8,** 753-763.

Rodriguez-Lanetty, M., Phillips, W. and Weis, V. (2006). Transcriptome analysis of a cnidarian - dinoflagellate mutualism reveals complex modulation of host gene expression. *BMC Genomics* **7,** 23.

Rodriguez-Lanetty, M., Phillips, W.S., Dove, S., Hoegh-Guldberg, O. and Weis, V.M. (2008). Analytical approach for selecting normalizing genes from a cDNA microarray platform to be used in q-RT-PCR assays: a cnidarian case study. *J. Biochem. Biophys. Methods* **70,** 985-991.

Roggentin, P., Schauer, R., Hoyer, L.L. and Vimr, E.R. (1993). The sialidase superfamily and its spread by horizontal gene transfer. *Mol. Microbiol.* **9,** 915-921.

Rosic, N.N. and Hoegh-Guldberg, O. (2010). A method for extracting a high-quality RNA from *Symbiodinium* sp. *J. Appl. Phycol.* **22,** 139-146.

Rozen, S. and Skaletsky, H. (1999) Primer3 on the WWW for general users and for biologist programmers. In *Bioinformatics Methods and Protocols*. Springer, pp. 365-386.

Sanders, S.M., Shcheglovitova, M. and Cartwright, P. (2014). Differential gene expression between functionally specialized polyps of the colonial hydrozoan *Hydractinia symbiolongicarpus* (Phylum Cnidaria). *BMC Genomics* **15,** 406.

Schwab, S.R., Pereira, J.P., Matloubian, M., Xu, Y., Huang, Y. and Cyster, J.G. (2005). Lymphocyte sequestration through S1P lyase inhibition and disruption of S1P gradients. *Science* **309,** 1735-1739.

Schwarz, J.A., Krupp, D.A. and Weis, V.M. (1999). Late larval development and onset of symbiosis in the scleractinian coral *Fungia scutaria*. *Biol. Bull.* **196,** 70-79.

Seo, Y.-J., Alexander, S. and Hahm, B. (2011). Does cytokine signaling link sphingolipid metabolism to host defense and immunity against virus infections? *Cytokine Growth Factor Rev.* **22,** 55-61.

Shaner, R.L., Allegood, J.C., Park, H., Wang, E., Kelly, S., Haynes, C.A., *et al.* (2009). Quantitative analysis of sphingolipids for lipidomics using triple quadrupole and quadrupole linear ion trap mass spectrometers. *J. Lipid Res.* **50,** 1692-1707.

Shinzato, C., Inoue, M. and Kusakabe, M. (2014). A snapshot of a coral "holobiont": a transcriptome assembly of the scleractinian coral, *Porites*, captures a wide variety of genes from both the host and symbiotic zooxanthellae. *PLoS One* **9,** e85182.

Shinzato, C., Shoguchi, E., Kawashima, T., Hamada, M., Hisata, K., Tanaka, M., *et al.* (2011). Using the *Acropora digitifera* genome to understand coral responses to environmental change. *Nature* **476,** 320-323.

Shpirer, E., Chang, E.S., Diamant, A., Rubinstein, N., Cartwright, P. and Huchon, D. (2014). Diversity and evolution of myxozoan minicollagens and nematogalectins. *BMC Evol. Biol.* **14,** 205.

Simon, G. and Rouser, G. (1967). Phospholipids of the sea anemone: Quantitative distribution; absence of carbon-phosphorus linkages in glycerol phospholipids; structural elucidation of ceramide aminoethylphosphonate. *Lipids* **2,** 55-59.

Spiegel, S. and Milstien, S. (2003). Sphingosine-1-phosphate: An enigmatic signaling lipid. *Nat. Rev. Mol. Cell Biol.* **4,** 397 - 407.

Spiegel, S. and Milstien, S. (2011). The outs and the ins of sphingosine-1-phosphate in immunity. *Nat. Rev. Immunol.* **11,** 403-415.

Starz-Gaiano, M., Cho, N.K., Forbes, A. and Lehmann, R. (2001). Spatially restricted activity of a *Drosophila* lipid phosphatase guides migrating germ cells. *Development* **128,** 983-991.

Steinberg, B.E. and Grinstein, S. (2008). Pathogen destruction versus intracellular survival: the role of lipids as phagosomal fate determinants. *J. Clin. Invest.* **118,** 2002-2011.

Stukey, J. and Carman, G.M. (1997). Identification of a novel phosphatase sequence motif. *Protein Sci.* **6,** 469-472.

Sullivan, J., Kalaitzidis, D., Gilmore, T. and Finnerty, J. (2007). Rel homology domain-containing transcription factors in the cnidarian *Nematostella vectensis*. *Dev. Genes Evol.* **217,** 63-72.

Tafesse, F.G., Rashidfarrokhi, A., Schmidt, F.I., Freinkman, E., Dougan, S., Dougan, M., *et al.* (2015). Disruption of sphingolipid biosynthesis blocks phagocytosis of *Candida albicans*. *PLoS Path.* **11,** e1005188.

Taris, N., Lang, R.P. and Camara, M.D. (2008). Sequence polymorphism can produce serious artefacts in real-time PCR assays: hard lessons from Pacific oysters. *BMC Genomics* **9,** 234.

Thompson, C.R., Iyer, S.S., Melrose, N., VanOosten, R., Johnson, K., Pitson, S.M., *et al.* (2005). Sphingosine kinase 1 (SK1) is recruited to nascent phagosomes in human macrophages: inhibition of SK1 translocation by *Mycobacterium tuberculosis*. *J. Immunol.* **174,** 3551-3561.

Timmins-Schiffman, E. and Roberts, S. (2012). Characterization of genes involved in ceramide metabolism in the Pacific oyster (*Crassostrea gigas*). *BMC Res. Notes* **5,** 502.

van Brocklyn, J.R. and Williams, J.B. (2012). The control of the balance between ceramide and sphingosine-1-phosphate by sphingosine kinase: Oxidative stress and the seesaw of cell survival and death. *Comp. Biochem. Physiol. B Biochem. Mol. Biol.* **163,** 26-36.

Vandesompele, J., De Preter, K., Pattyn, F., Poppe, B., Van Roy, N., De Paepe, A. and Speleman, F. (2002). Accurate normalization of real-time quantitative RT-PCR data by geometric averaging of multiple internal control genes. *Genome Biol.* **3,** 1 - 11.

Venn, A.A., Loram, J.E. and Douglas, A.E. (2008). Photosynthetic symbioses in animals. *J. Exp. Bot.* **59,** 1069-1080.

Voolstra, C.R. (2013). A journey into the wild of the cnidarian model system *Aiptasia* and its symbionts. *Mol. Ecol.* **22,** 4366-4368.

Wei, W.-C., Sung, P.-J., Duh, C.-Y., Chen, B.-W., Sheu, J.-H. and Yang, N.-S. (2013). Anti-inflammatory activities of natural products isolated from soft corals of Taiwan between 2008 and 2012. *Mar. Drugs* **11,** 4083-4126.

Weis, V.M., Davy, S.K., Hoegh-Guldberg, O., Rodriguez-Lanetty, M. and Pringle, J.R. (2008). Cell biology in model systems as the key to understanding corals. *Trends Ecol. Evol.* **23,** 369-376.

Weis, V.M., Verde, E.A., Pribyl, A. and Schwarz, J.A. (2002). Aspects of the larval biology of the sea anemones *Anthopleura elegantissima* and *A. artemisia*. *Invertebr. Biol.* **121,** 190-201.

Wilson, W.H., Schroeder, D.C., Allen, M.J., Holden, M.T., Parkhill, J., Barrell, B.G., *et al.* (2005). Complete genome sequence and lytic phase transcription profile of a *Coccolithovirus*. *Science* **309,** 1090-1092.

Wooldridge, S.A. (2010). Is the coral-algae symbiosis really 'mutually beneficial' for the partners? *Bioessays* **32,** 615-625.

Xia, P., Wang, L., Moretti, P.A., Albanese, N., Chai, F., Pitson, S.M., *et al.* (2002). Sphingosine kinase interacts with TRAF2 and dissects tumor necrosis factor-α signaling. *J. Biol. Chem.* **277,** 7996-8003.

Yamashiro, H., Oku, H., Higa, H., Chinen, I. and Sakai, K. (1999). Composition of lipids, fatty acids and sterols in Okinawan corals. *Comp. Biochem. Physiol. B Biochem. Mol. Biol.* **122,** 397-407.

Yang, Y., Xiong, J., Zhou, Z., Huo, F., Miao, W., Ran, C., *et al.* (2014). The genome of the myxosporean *Thelohanellus kitauei* shows adaptations to nutrient acquisition within its fish host. *Genome Biol. Evol.* **6,** 3182-3198.

Yeung, T. and Grinstein, S. (2007). Lipid signaling and the modulation of surface charge during phagocytosis. *Immunol. Rev.* **219,** 17-36.

Zhang, H., Desai, N.N., Olivera, A., Seki, T., Brooker, G. and Spiegel, S. (1991). Sphingosine-1-phosphate, a novel lipid, involved in cellular proliferation. *J. Cell Biol.* **114,** 155-167.

3. SPHINGOSINE RHEOSTAT INVOLVED IN THE CNIDARIAN HEAT STRESS RESPONSE IS NOT LINKED TO CNIDARIAN-DINOFLAGELLATE SYMBIOSIS BREAKDOWN

Sheila A. Kitchen

Virginia M. Weis

Formatted for *Journal of Experimental Biology*

The Company of Biologists Limited

Bidder Building

Station Road

Histon

Cambridge

CB24 9LF

UK

3.1 Abstract

Marine organisms such as reef-building corals living in shallow waters are particularly vulnerable to elevated seawater temperature and high UV irradiance, two stressors that are increasing with climate change. Environmental stress activates general and stress-specific cellular signaling pathways in organisms. Sphingolipids play important roles in the heat stress response (HSR) and oxidative stress of many organisms by altering membrane fluidity, receptor clustering and gene expression. In particular, accumulation of signaling sphingolipids that make up the sphingosine rheostat, pro-apoptotic sphingosine (Sph) and pro-survival sphingosine-1-phosphate (S1P), is key to determining cell fate. In corals, elevations of temperature and UV also disrupt the photosynthetic machinery of their endosymbionts causing the partnership to collapse and loss of symbionts, a phenomenon known as coral bleaching. An earlier study demonstrated that exogenously applied Sph and S1P could alter heat-induced bleaching in the symbiotic anemone *Aiptasia pallida*, but the endogenous regulation of these lipids during heat stress is unknown. Here, we characterized the endogenous role of the sphingosine rheostat in the cnidarian HSR and the breakdown of cnidarian symbiosis. Expression of rheostat enzymes sphingosine kinase (AP-SPHK) and S1P phosphatase (AP-SGPP), and sphingolipid concentrations were quantified from *A. pallida* incubated at intermediate (27 and 30 °C) and hyperthermal (33 °C) seawater temperatures. In symbiotic anemones at 33 °C, modulation of rheostat expression and sphingolipids was detected after the majority of symbionts (~67%) were lost. Therefore, the sphingosine rheostat may not be an important mediator of the complex mechanisms underlying symbiont removal. However, a rheostat-mediated biphasic HSR was observed in symbiotic *A. pallida* where gene expression and lipid levels were suppressed at first, and then AP-SGPP and then by Sph levels increased with prolonged 33 °C exposure. During the first 12 h of heat stress, a difference in AP-SPHK gene expression was detected between symbiotic and aposymbiotic *A. pallida* indicating a different HSR in the presence of symbionts. Taken together, these results indicate that the activation of sphingosine rheostat expression and lipid production in symbiotic *A. pallida* does not align with symbiont loss, but occurs later after prolonged heat stress in the host.

3.2 Introduction

Reef-building corals are severely threatened by abiotic stressors associated with climate change, especially elevated temperature (Hoegh-Guldberg, 1999, Hughes *et al.*, 2003, Pandolfi *et al.*, 2003, Hoegh-Guldberg *et al.*, 2007). Many corals and other cnidarians form endosymbiotic associations with photosynthetic dinoflagellates in the genus *Symbiodinium* spp. These partnerships are based on the significant contribution of photosynthetically fixed carbon by the algal symbionts to the host in exchange for inorganic nutrients, shelter and a high light environment (Muscatine *et al.*, 1969). The algal photosynthetic apparatus is sensitive to climate-induced heat and light perturbations which results in photosystem II dysfunction (Warner *et al.*, 1996), and electron transport uncoupling in both photosystems (Tchernov *et al.*, 2004). The accumulation of electrons increases oxygen generation that is then further reduced in photosystem I into reactive oxygen species (ROS) (Venn *et al.*, 2008, Weis, 2008), thereby increasing ROS and reactive nitrogen species (RNS) in the algae (Lesser, 1996, Suggett *et al.*, 2008, Bouchard *et al.*, 2009, Hawkins *et al.*, 2012, McGinty *et al.*, 2012, Ross, 2014) and in turn oxidative stress in the host (Nii *et al.*, 1997, Perez *et al.*, 2006, Richier *et al.*, 2006, Hawkins *et al.*, 2013, Hawkins *et al.*, 2014). The overabundance of ROS or RNS is harmful to both the symbiont and host, causing damage to proteins, DNA and membrane integrity (Venn *et al.*, 2008, Weis, 2008, Hill *et al.*, 2009, Wang *et al.*, 2011). Corals have protective mechanisms to reduce the effects of reactive species including heat shock proteins, oxygen-scavenging enzymes and fluorescent proteins that absorb high light, but during heat stress, these mechanisms become overwhelmed (Douglas, 2003, DeSalvo *et al.*, 2008, Venn *et al.*, 2008). Ultimately, environmental stress leads to loss of symbionts from cnidarian hosts resulting in a loss of pigmentation referred to as cnidarian bleaching. There are several proposed mechanisms for symbiont removal (Gates *et al.*, 1992b, Weis, 2008), including programmed cell death (Dunn *et al.*, 2007, Dunn *et al.*, 2009, Detournay *et al.*, 2011, Paxton *et al.*, 2013) and autophagy (Dunn *et al.*, 2007, Hanes *et al.*, 2013). Although there have been extensive studies on removal mechanisms in a variety of corals and sea anemone model systems, our understanding of the cellular events preceding symbiont loss is limited. Given that lipids are co-directors of phagocytosis, the mode by

which *Symbiodinium* are acquired by hosts, and have roles in establishing symbiont colonization (see Chapter 2), symbiosis dysfunction could have significant impacts on lipid signaling, targeting and trafficking events.

Oxidative and heat stress are two cellular events mediated by bioactive sphingolipids in both eubacterial and eukaryotic cells (Jenkins *et al.*, 1997, An *et al.*, 2011, van Brocklyn *et al.*, 2012). The lipid messengers sphingosine (Sph) and sphingosine-1-phosphate (S1P) have antagonistic roles in the cell, where Sph initiates programmed cell death pathways and S1P activates cell survival and proliferation mechanisms (Olivera *et al.*, 2001, Spiegel *et al.*, 2003, Le Stunff *et al.*, 2004). The enzymatic activities of sphingosine kinase (SPHK) and sphingosine-1-phosphate phosphatase (SGPP) maintain the homeostatic balance of these sphingolipids in the 'sphingosine rheostat' (Cuvillier *et al.*, 1996, Mandala *et al.*, 1998). Heat stress studies in mammalian cell lines, yeast, and gut microbiome commensals *Bacteriodes* suggest an evolutionarily conserved sphingolipid-mediated heat stress response (HSR) (Chang *et al.*, 1995, Jenkins *et al.*, 1997, Jenkins *et al.*, 2002, An *et al.*, 2011). The HSR is a defense mechanism mediated through stress sensors and signal transduction pathways to offset deleterious effects of thermal stress (Hofmann *et al.*, 2010). In yeast and *Bacteroides*, elevated temperatures decreased cell viability in sphingolipid-deficient strains that was rescued with sphingolipid supplementation. Furthermore, in yeast and mammalian cells, synthesis of Sph and its precursor ceramide increased with heat stress (Chang *et al.*, 1995, Jenkins *et al.*, 1997). Elevated levels were reversed in yeast by deletion of the SGPP-like enzyme, which increased the cellular S1P-like metabolites, thereby enhancing survival (Mandala *et al.*, 1998, Mao *et al.*, 1999).

Oxidative stress is also linked to the sphingosine rheostat through modulation of S1P levels in yeast (Lanterman *et al.*, 1998, Jenkins *et al.*, 2001), nematodes (Deng *et al.*, 2008), fruit flies (Kawamura *et al.*, 2009), fish (Yabu *et al.*, 2008), and mammals (Gomez-Brouchet *et al.*, 2007, Pchejetski *et al.*, 2007, Ader *et al.*, 2008). The rheostat response is dependent on the severity of oxidative damage, with moderate ROS levels activating SPHK and increasing S1P levels (Ader *et al.*, 2008), while severe ROS levels degrade SPHK, reduce S1P and shift cells toward death (Gomez-Brouchet *et al.*, 2007,

Pchejetski *et al.*, 2007). Furthermore, the activation of endothelial nitric oxide synthase (NOS) by S1P causes production of an RNS, cytotoxic nitric oxide (NO), which at low cellular levels can inhibit pro-inflammatory cytokines (De Palma *et al.*, 2006). In contrast, immune elicitors and elevated ROS trigger inducible NOS, resulting in high cellular NO and NO-dependent elevations in ceramide through activation of lysosomal acidic sphingomyelinases (A-SMase) (Perrotta *et al.*, 2008). These findings suggest an active role for the sphinogsine rheostat in the cellular stress response, and led to Maceyka and coworkers (2007) to propose SPHK as a central enzyme in oxidative stress pathway in mammals. Its importance in the invertebrate stress response, however, needs to be investigated further.

In symbiotic cnidarians, the molecular crosstalk between the host and symbionts during the breakdown of symbiosis is still largely undescribed. In stable associations, symbionts are housed in host-derived vesicles, or symbiosomes, that resist phagosomal maturation (Chen et al., 2003, Chen et al., 2004, Chen et al., 2005). Transcriptional studies on symbiotic cnidarians exposed to elevated temperature or high irradiance stress indicate that symbiont removal mechanisms such as host apoptosis, innate immunity and exocytosis are upregulated (Richier *et al.*, 2006, DeSalvo *et al.*, 2008, Starcevic *et al.*, 2010). Modulation of sphingolipids could underlie these changes through activation of phagosomal maturation (Heung et al., 2006) and cell death (Maceyka *et al.*, 2002). The cnidarian sphingosine rheostat has been implicated in symbiont colonization (see Chapter 2), symbiosis maintenance (see Chapter 2, Rodriguez-Lanetty *et al.* (2006), Hemond *et al.* (2014)), immunity and the HSR (Detournay *et al.*, 2011). In the sea anemone *Aiptasia pallida* (also known as *Exaiptasia pallida* (Grajales et al., 2014)) exposure to an elevated temperature with the addition of exogenous Sph increased algal loss by 40%, whereas incubations in exogenous S1P reduced bleaching by nearly 50% (Detournay *et al.*, 2011). Moreover, elevated Sph led to increased host caspase activity, an indicator of programmed cell death. However, cytotoxic nitric oxide (NO) production, an RNS implicated in symbiosis breakdown (Perez *et al.*, 2006, Hawkins *et al.*, 2013, Ross, 2014) and functionally coupled to sphingolipid metabolism in other systems (Perrotta et al., 2008), was unaffected by Sph and S1P (Detournay *et al.*, 2011).

Given that exogenous sphingolipids altered the amount of symbiont loss and host cell death in *A. pallida* during heat stress, we predicted that endogenous transcriptional regulation of rheostat enzymes (AP-SPHK and AP-SGPP) and concomitant changes in sphingolipid metabolites contribute to symbiont loss and a host HSR. In this study we experimentally examined the response of the host sphingosine rheostat to elevated temperature through time by quantification of gene expression, sphingolipid concentrations and symbiont loss over prolonged a heat stress lasting seven days.

3.3 Materials and Methods

3.3.1 A. pallida *and* Symbiodinium *husbandry*

VWA anemones and algal cultures were maintained under the same conditions described in Chapter 2, pg. 33. Aposymbiotic anemones were kept in the dark to prevent repopulation of residual symbionts. Symbiotic anemones were kept in the light on a 12 h:12 h light-dark cycle at 40 μmol quanta m^{-2} s^{-1} intensity to promote symbiont photosynthesis and proliferation.

3.3.2 Elevated temperature treatment of A. pallida

Symbiotic and aposymbiotic anemones were randomly placed into 6-well plates (for qPCR= 3 symbiotic anemones per well or 1 aposymbiotic anemone per well, for lipid analyses = 1 anemone per well) with 10 ml of 0.45 μm filtered artificial seawater (FASW) one week prior to treatment. During the two weeks before and throughout the week of temperature exposure, the anemones were starved, given daily FASW changes and any expelled symbionts were removed. All experiments were carried out in temperature-controlled incubators. Three days before experimental temperature exposure, aposymbiotic anemones were placed at 40 μmol quanta m^{-2} s^{-1} intensity on the same 12 h:12 h light:dark cycles as symbiotic samples. For the qPCR assay, anemones (n=3 per time point) were exposed to a range of temperatures 25 (ambient), 27, 30 and 33 °C for 1 week. Anemones were sampled at 0, 0.5, 1, 2, 4 and 7 days. Additional samples were collected at 3 and 6 h for ambient and 33 °C to investigate very early expression differences at these experimental temperatures. The intermediate elevated temperatures

(27 and 30 °C) did not result in detectable gene expression differences (see Results), therefore only ambient and 33 °C-treated anemones (n=4 per time point) were used for quantification of sphingolipids. Anemones were sampled at 0, 1, 4 and 7 days based on gene expression results. At designated time points, anemones were rinsed in FASW before being frozen in liquid nitrogen and stored at -80 °C.

3.3.3 Bleaching quantification

To quantify symbiont loss from host tissues during exposure to elevated temperature, *S. minutum* chlorophyll autofluorescence was measured from the set of anemones that were destined for lipid analysis (n= 4 per time point). Measurements were taken from each individual until they were sacrificed at their designated time point. First, each anemone was captured under white light on the Zeiss Stemi 2000-c stereo-microscope (Zeiss, Germany) with standardized camera settings and 1 s exposure to determine well location and measure oral disc size. Autofluorescence was then detected using a long pass emission filter (> 665 nm) after excitation by 470 nm LED blue light at 130 µmol quanta m^{-2} s^{-1} intensity and digitally captured with a 25 s camera exposure. Mean fluorescence intensity was measured from the images from 10 random areas of the oral disc or base of the tentacles using ImageJ v1.47 software (Rasband, 1997-2015). Autofluorescence was normalized to the mean fluorescence intensity from five areas adjacent to the anemones considered to be background levels. The random effect of repeated measures of autofluorescence from the same individual accounted for 4% of total variance and inclusion in the statistical model was not significant (Chi Square goodness of fit test, p=0.514). Therefore, normalized values were fit with a regression model with fixed effects of time (continuous, quadratic fit) and temperature (factor, 2 levels). To determine if host size affected the loss of symbionts, the percent of symbiont loss calculated (100-(day 1 mean fluorescence/day 0 mean fluorescence))*100 was correlated to host protein using a Pearson's correlation test. Higher percent loss corresponds with greater difference in mean autofluorescence at day 1.

3.3.4 Relative qPCR of AP-SPHK and AP-SGPP

Total RNA extraction and cDNA synthesis was carried out as described in Chapter 2, pg. 35. qPCR reference genes in Table 2.5 (pg. 63) were tested on 25 and 33 °C-incubated samples at days 1 and 4 as described previously (Poole *et al.*, submitted). Based on stability values from GeNorm and NormFinder (Table 3.1), the combination of poly-A binding protein (PABP), ribosomal protein L10 and glyceraldehyde 3-phosphate dehydrogenase (GAPDH) genes were selected as references for elevated temperature-treated anemones. After reference gene selection, cDNA from each sample was run in triplicate 20 µl reactions of 10 µl *Power* SYBR® Green PCR master mix (Applied Biosystems, UK), 5 µmol of forward and reverse primer pair, 0.5 µl of cDNA, and RNase-free H_2O on the ABI Prism 7500 Real-Time PCR machine (Applied Biosystems, UK) with standard settings and an additional melt curve. No-template, no-reverse transcriptase, no-primers controls were included, as well as one interplate calibrator sample per plate. C_t values calculated by ABI 7500 software v2.0.6 (Applied Biosystems, UK) with a set baseline threshold of 0.2 were imported into GenEx v5.3.7.332 (MultiD Analyses AB, Sweden) to adjust interplate variation and normalize expression to reference genes. The $\Delta\Delta C_t$ method (Livak *et al.*, 2001) was used to calculate relative quantities for each treatment group (27, 30, and 33 °C) to the mean ΔC_t of 25 °C samples at each time point (n= 3 anemones), respectively. Relative quantities are presented on the $\log_2$ scale as the mean ± standard error. The best statistical model was determined through Chi-square goodness of fit tests for the fixed effects of time (7 levels) and temperature (4 levels = 25, 27, 30 and 33 °C), and random effect of well placement. Relative quantities of AP-SGPP from symbiotic anemones were fit to a generalized mixed effects model (GLMM) with the fixed effect of temperature and random effect of well placement, whereas AP-SPHK relative quantities were fit to an intercept model. *Post hoc* 2-tailed Student's T-tests were run for treated samples at each time point (n= 3 anemones) compared to the time-matched non-heat stressed control. P-values were adjusted for multiple-test comparisons using a Bonferroni correction. Comparisons of relative quantities of AP-SPHK and AP-SGPP between symbiotic states

at 6 and 12 h were analyzed using a Mann Whitney test. The significant threshold for all statistical tests was $p \leq 0.05$.

3.3.5 Lipid extraction and quantification

Lipid extraction and quantification methods were identical to those described in Chapter 2, pg. 41. S1P and Sph were resolved from symbiotic anemone lipid extracts using high performance liquid chromatography (HPLC) and electron spray ionization tandem mass spectrometry (ESI-MS/MS). The lipid concentrations were calculated from the ratio of the sample intensity peak to the respective internal odd carbon (C17) standard (C17-S1P and C17-Sph) for each sphingoid base and normalized to total protein, a proxy for anemone size. The relative intensity peaks for the internal standards were used to calculate variation between extractions and treatment conditions. Lipid recovery across the eight extraction groups resulted in median coefficient of variation of 21.9% for Sph and 23.5% for S1P (Fig. 3.1). No treatment effects were observed on internal standard recovery (Fig. 3.1). The fold change of each analyte was calculated as the 33 °C treated anemones referenced to the mean of the concentrations of control anemones at each respective time point. Fold changes were tested with a 1-way ANOVA with time (3 levels = 1, 4, and 7 days) followed by Tukey's *post hoc* test. In addition, each sample used for lipid extraction had recorded autofluorescence over the duration of temperature treatment, therefore, the lipid concentrations could be correlated to final mean fluorescence using a Pearson's correlation test.

3.4 Results

To test the hypothesis that the sphingosine rheostat is part of the immediate HSR in cnidarians, relative expression of rheostat genes AP-SPHK and AP-SGPP was measured in symbiotic anemones incubated in ambient (25 °C) and hyperthermal (27, 30 and 33 °C) temperatures at several time points. A range of temperatures was tested over one week to determine thermal and temporal activation of rheostat transcription. Relative quantities of AP-SGPP decreased by 0.8 fold in 33 °C-incubated anemones, but not with more moderate elevated temperatures (GLMM conditional $R^2 = 0.716$, $p = 0.003$) (Fig. 3.2). However, AP-SGPP expression was not downregulated over the entire time course.

It significantly declined between three hours and one day (*post hoc* T-test, 3 h: p= 0.008, 6 h: p=0.003, 12 h: p=0.012, 1 day: p= 0.031), began to increase by the second day and eventually exceeded control expression at one week (*post hoc* T-test, day 7: p= 0.011). In contrast, relative quantities of AP-SPHK did not differ between any of the four temperature treatments (linear regression R^2= 0.2037, p= 0.096) (Fig. 3.3). The *post hoc* test, however, revealed significantly decreased AP-SPHK expression at 12 h in 30 °C and day one in 33 °C compared to ambient temperature (*post hoc* T-test, 12 h: p= 0.002, day 1: p= 0.031). So, although there was no difference between hyperthermal temperatures on AP-SPHK expression over time, downregulation was observed for specific time points. By the end of one week, an opposing expression pattern of the rheostat genes emerged, although it was not significant for AP-SPHK (*post hoc* T-test, p= 0.112) (Fig. 3.2 and 3.3). Overall, the relative quantities of both rheostat genes were initially downregulated with acute hyperthermal stress and then shift to upregulation of AP-SGPP by the end of the experiment.

From the range of temperatures tested, the most extreme 33 °C hyperthermal treatment initiated a greater transcriptional response of the sphingosine rheostat than the intermediate hyperthermal treatments. Therefore, we only compared animals incubated at ambient and 33 °C in subsequent analyses. To examine the influence of symbiotic state on the rheostat under heat stress, AP-SPHK and AP-SGPP expression was also measured in aposymbiotic anemones and compared to the symbiotic anemones discussed above. Notably, the 33 °C treatment was lethal for some aposymbiotic anemones (1 at day one and 2 at day seven), limiting comparisons with symbiotic animals to the first 12 h. At 6 h and 12 h of heat stress, AP-SGPP expression was slightly higher (Fig. 3.4A, Mann Whitney test, p= 0.179) and AP-SPHK expression significantly higher (Fig. 3.4B, Mann Whitney test, p= 0.041) in aposymbiotic anemones compared to symbiotic anemones. These data suggest that the presence of symbionts can alter the transcriptional response of the rheostat genes in *A. pallida*, but extended time points are needed to draw conclusions on how these early differences affect physiological outcomes of the cnidarian HSR under different symbiotic states.

Although, transcriptional differences between rheostat genes were observed in symbiotic anemones were not observed until several days after the onset of heat stress, post-translational activation of AP-SPHK and AP-SGPP proteins could be part of the immediate HSR. Symbiotic anemones have higher constitutive AP-SPHK protein expression than aposymbiotic anemones (see Chapter 2, pg. 28). AP-SPHK could be recruited to mitigate the heat-induced cellular damage. We indirectly measured enzymatic activity of rheostat enzymes by quantifying their products, S1P and Sph. The mean fold change (concentrations at 33 °C/ambient) of Sph increased by 0.832 ± 0.30 between days four and seven (Fig. 3.5, Tukey *post hoc*, p= 0.05). Mean S1P fold change remained low throughout the experiment, but high sample variation at day one suggests that some anemones had elevated AP-SPHK activity (Fig. 3.5).

Next, we were interested to see if the timeline of symbiont loss corresponded to changes in sphingosine rheostat expression and activity during incubation at elevated temperature. Relative symbiont densities of anemones used for the lipid analysis were quantified by measuring mean chlorophyll autofluorescence periodically during the experiment (Fig. 3.6A). At elevated temperature, there was strong evidence for a non-linear change in symbiont autofluorescence over time (quadratic regression, adjusted R^2= 0.649, $p < 0.001$). For each additional day, mean autofluorescence was 0.12 times lower in heat-stressed anemones compared to control (quadratic regression, $p < 0.001$, Fig. 3.5B). The rapid loss of mean autofluorescence in the heat-stressed animals (49.42 ± 3.15%) at day one is consistent with previous studies that reported decreased *Symbiodinium* spp. pigment and density from a range of elevated temperatures (31.5 to 33.5 °C) (Dunn *et al.*, 2004, Perez *et al.*, 2006, Dunn *et al.*, 2007, Detournay *et al.*, 2011, Hawkins *et al.*, 2013). Relative symbiont loss was variable under hyperthermal stress. We compared the percent symbiont loss at day one with total protein, however, no correlation was detected between symbiont loss and anemone size (Pearson's correlation test, p= 0.08) (Fig. 3.6B).

Given that loss of symbionts varied across individuals, the severity of the hyperthermal stress on symbiosis breakdown was not uniform. More thermotolerant anemones (those with less symbiont loss) might therefore undergo regulation of

sphingolipid metabolism that contributes to bleaching resistance. To examine this, we correlated the mean fluorescence of ambient and 33 °C-treated anemones to their recovered sphingolipid concentrations. At 33 °C, there was suggestive, but not significant, evidence that S1P concentrations were negatively correlated with symbiont loss (Pearson's correlation test, R^2= -0.51, p= 0.089), and no relationship was found for Sph concentrations (Fig. 3.7A and B). This could indicate that S1P concentrations are lower in anemones with the greatest bleaching response, but larger sample sizes are required to definitively demonstrate such a correlation.

3.5 Discussion

We examined the activation of the sphingosine rheostat with heat stress as part of the signaling cascades involved in the cnidarian HSR and symbiosis breakdown. Our findings, summarized in Figure 3.8, suggest that although the rheostat is involved in the HSR, symbiosis breakdown precedes changes in the gene expression and activity of the rheostat. Therefore, there is no direct evidence that the rheostat is involved in cnidarian bleaching.

The HSR dynamically alters almost all cellular processes in a highly orchestrated fashion resulting in two response phases: acute (Phase I) and chronic (Phase II) (Balogh *et al.*, 2013, Chen *et al.*, 2013). In Phase I, processes required for immediate action include post-translational modifications of existing proteins, and rapid elevations in transcription and synthesis of heat shock and other stress responsive proteins coinciding with the downregulation of most non-essential cellular processes (Morimoto, 1993, Graner *et al.*, 2007). Therefore, the expression of heat shock proteins (HSPs) is an important biomarker for Phase I of the HSR in cnidarians. In previous studies of cnidarians, HSPs were shown to be upregulated as early as two to 24 hours after the onset of heat stress (Black *et al.*, 1984, Bosch *et al.*, 1988, Black *et al.*, 1995, Gates *et al.*, 1999, DeSalvo *et al.*, 2008, Rodriguez-Lanetty *et al.*, 2009, DeSalvo *et al.*, 2010), but were not detected on subsequent days (Voolstra *et al.*, 2009a, Bellantuono *et al.*, 2011, Mayfield *et al.*, 2011) (Fig. 3.8). Following Phase I, processes essential for slower, longer-term acclimatization are regulated by changes in gene expression, metabolism and membrane organization as part of Phase II (de Nadal *et al.*, 2011, Balogh *et al.*, 2013). The timing of

Phase II is dependent on the severity, duration of the stress and thermal tolerance of the partners, all of which contribute to the cnidarian HSR (Tchernov *et al.*, 2004, Hofmann *et al.*, 2010).

In *A. pallida*, symbiont loss is a rapid process associated with Phase I of the HSR (Fig. 3.8). We observed almost 50% loss after one day at 33 °C, a value consistent with other studies that noted significant symbiont expulsion after acute heat stress (Gates *et al.*, 1992b, Sawyer *et al.*, 2001, Dunn *et al.*, 2004, Perez *et al.*, 2006, Detournay *et al.*, 2011, Hawkins *et al.*, 2013, Paxton *et al.*, 2013, Tolleter *et al.*, 2013). Symbiosis dysfunction coincides with increased HSP synthesis, caspase activity, NO production and host cell death in anemones exposed to elevated temperatures from 31.5 to 33.5 °C (Black *et al.*, 1995, Detournay *et al.*, 2011, Hawkins *et al.*, 2012, Paxton *et al.*, 2013). The activity of the sphingosine rheostat, a regulator of host cell death and NO production, however, was not part of Phase I as we predicted. During Phase I, both rheostat genes and lipid concentrations were downregulated (Fig. 3.8). The pro-apoptotic enzyme AP-SGPP expression and subsequent elevations in Sph concentrations were induced by longer-term incubations at the highest temperature of 33 °C in symbiotic anemones, but not by moderately high temperatures of 27 and 30 °C. In a previous study, the slow heating of *A. pallida* revealed two peaks in proteolytic activity of caspase 3 and 9, two cysteine proteases essential in apoptosis, at day one and five at the maximal temperature (33 °C) (Hawkins *et al.*, 2013).The increase in Sph between days four and seven observed here could trigger pro-apoptotic mechanisms as part of the chronic HSR. Therefore in symbiotic anemones, symbiont loss is part of the acute response (Phase I) and sphingosine rheostat activation is part of the chronic response (Phase II) (Fig. 3.8).

Although additions of exogenous S1P and Sph altered bleaching in *A. pallida* (Detournay *et al.*, 2011), the endogenous rheostat did not change during rapid bleaching in Phase I. Increased symbiont loss appears to be independent of the sphingosine rheostat activation. Thus, the subprograms controlling the initial bleaching response might be functionally uncoupled from the rheostat. We measured the response of the whole animal to thermal stress, but it is important to consider that the microenvironment of gastrodermal tissue where the *Symbiodinium* spp. reside might be significantly different

than the rest of the animal. Further investigation into the tissue-specific effects of the rheostat using single cell expression profiling or fluorescently tagged sphingolipid localization will help reveal the involvement on sphingolipids in symbiosis breakdown.

Other components of the sphingolipid signaling and their downstream effectors may contribute to symbiont removal and increased apoptosis or NO production during the acute HSR. An important step in the mammalian HSR is the rapid accumulation of ceramide that precedes apoptosis in mammalian cell lines (Goldkorn *et al.*, 1991, Jenkins *et al.*, 2002, Nagai *et al.*, 2011). In addition to its role in cell death, ceramide can activate endothelial NOS leading to a high NO environment (Florio *et al.*, 2003). The metabolic pathways to produce ceramide in *A. pallida* are virtually unexplored, however *A. pallida* possess all of the necessary genes encoding the metabolic machinery (see Table 2.1 in Chapter 2, pg. 45-47). Future studies aimed at investigating ceramide levels and enzymatic activity of the various players involved in accumulating ceramide will enhance our understanding of the cnidarian HSR and HSR evolution in eukaryotes.

Our data also show that symbiotic state does affect the cnidarian HSR. Expression of AP-SPHK in aposymbiotic anemones was upregulated within the first 12 h, in contrast to its downregulation in symbiotic anemones, suggesting an accumulation of S1P. The lipid levels of aposymbiotic anemones should be quantified in the future to explore differences observed in the rheostat gene expression. In some aposymbiotic anemones hyperthermal stress was lethal after 12 h limiting the comparisons of the chronic HSR in *A. pallida*. To separate the physiological changes of heat stress from symbiosis breakdown, other non-symbiotic model cnidarians such as the anemone, *Nematostella vectensis* or hydrozoan, *Hydra vulgaris* would be good candidates for examining the role of the sphingosine rheostat in the HSR.

In summary, we showed that transcriptional activation and activity of the cnidarian sphingosine rheostat is part of the longer-term survival mechanisms with chronic heat stress. The modulation of the rheostat was dependent on the intensity and duration of cellular stress. Although the sphingosine rheostat plays a role in the establishment and maintenance of cnidarian-dinoflagellate symbiosis (see Chapter 2), it was not observed to be involved in symbiosis dysfunction. The presence of symbionts

did, however, alter the acute host response when comparing symbiotic states. Further examination of sphingolipid metabolism and signaling will broaden our understanding of its role in an evolutionarily conserved stress response and symbiosis breakdown.

Table 3.1 Stability values of reference genes tested for elevated temperature (33 °C) experiment in GeNorm (Vandesompele *et al.*, 2002) and NormFinder (Andersen *et al.*, 2004).

Gene	GeNorm (M)	NormFinder
L10	1.013	0.180
PABP	1.000	0.202
GAPDH	1.202	0.335
L12	1.387	0.580
EEF1A1	2.059	0.752

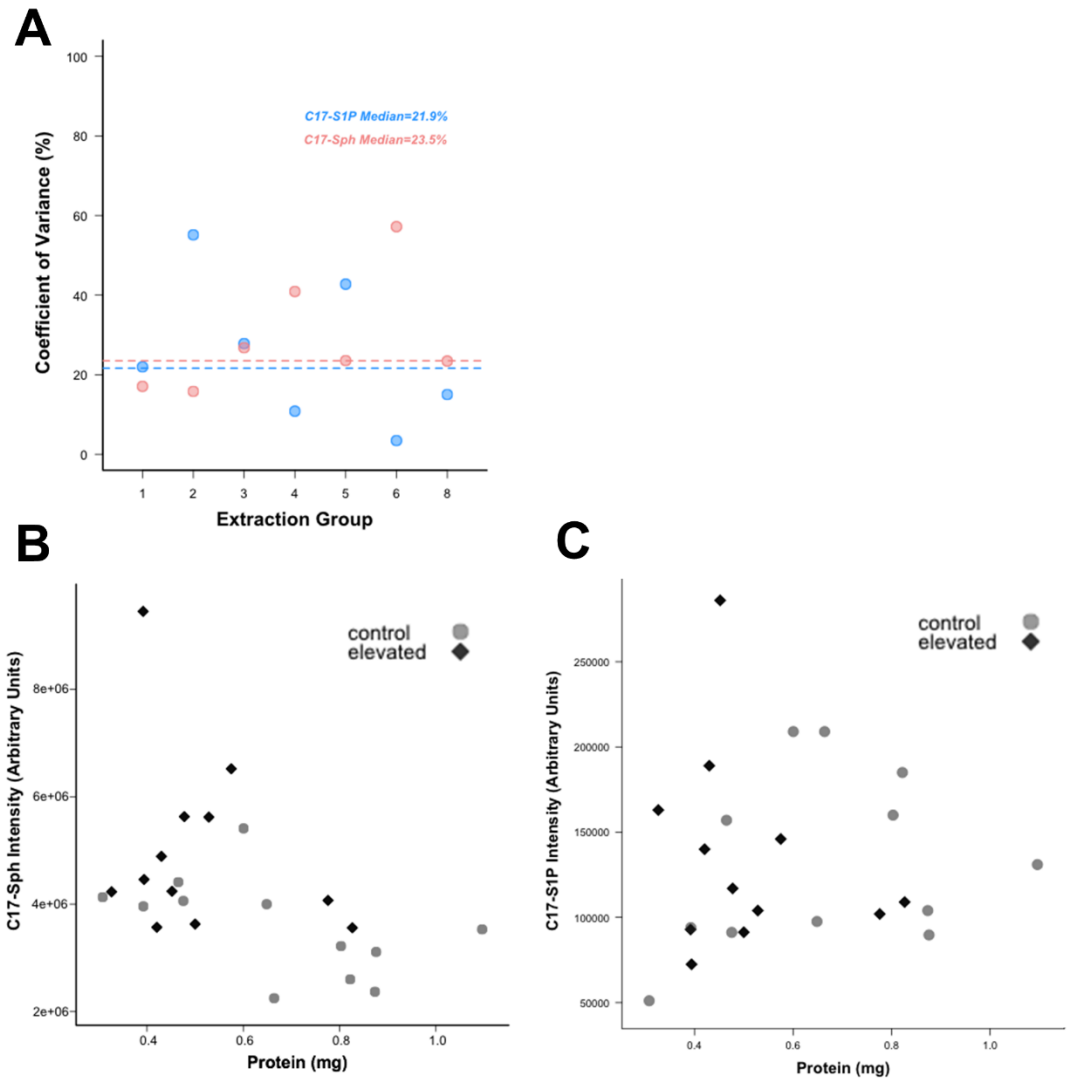

Figure 3.1 Lipid extraction recoveries by extraction group and temperature treatment. The coefficient of variance was calculated from the C17 internal standard peak intensity for each analyte in each extraction group (A). Dashed lines indicate median percent CV for each metabolite. Recovery was examined by comparing relative intensity of C17 internal standards for Sph (B) and S1P (C) to animal size (total protein) by treatment groups: 25 °C = ●, and 33 °C = ◆.

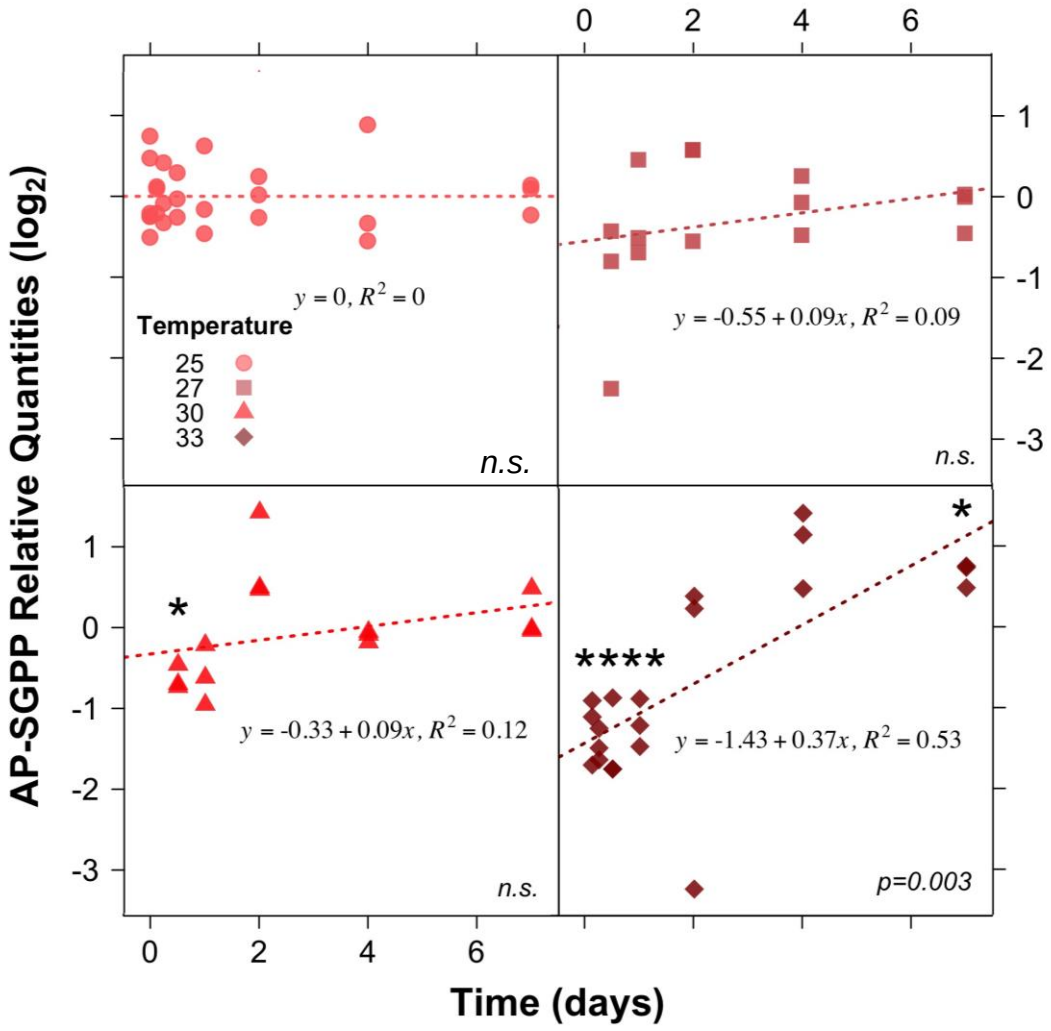

Figure 3.2 AP-SGPP expression in symbiotic *A. pallida* initially decreases and then increases with hyperthermal temperature after one week. Relative mRNA quantities (log_2) of AP-SGPP were measured using qPCR of ambient and heat-treated samples (n= 3 anemones per group). The proportion of variation explained by the model (R^2) and significance (not significant= n.s., $p \leq 0.05$) from the mixed effects model is displayed for each temperature. Heat-treated groups at each time point that significantly differed from their matched control group with *post hoc* Student T-test are indicated with an asterisk (*), $p \leq 0.05$. Treatment groups (clockwise): ambient = ●, 27 °C= ■, 30 °C= ▲, and 33 °C = ◆.

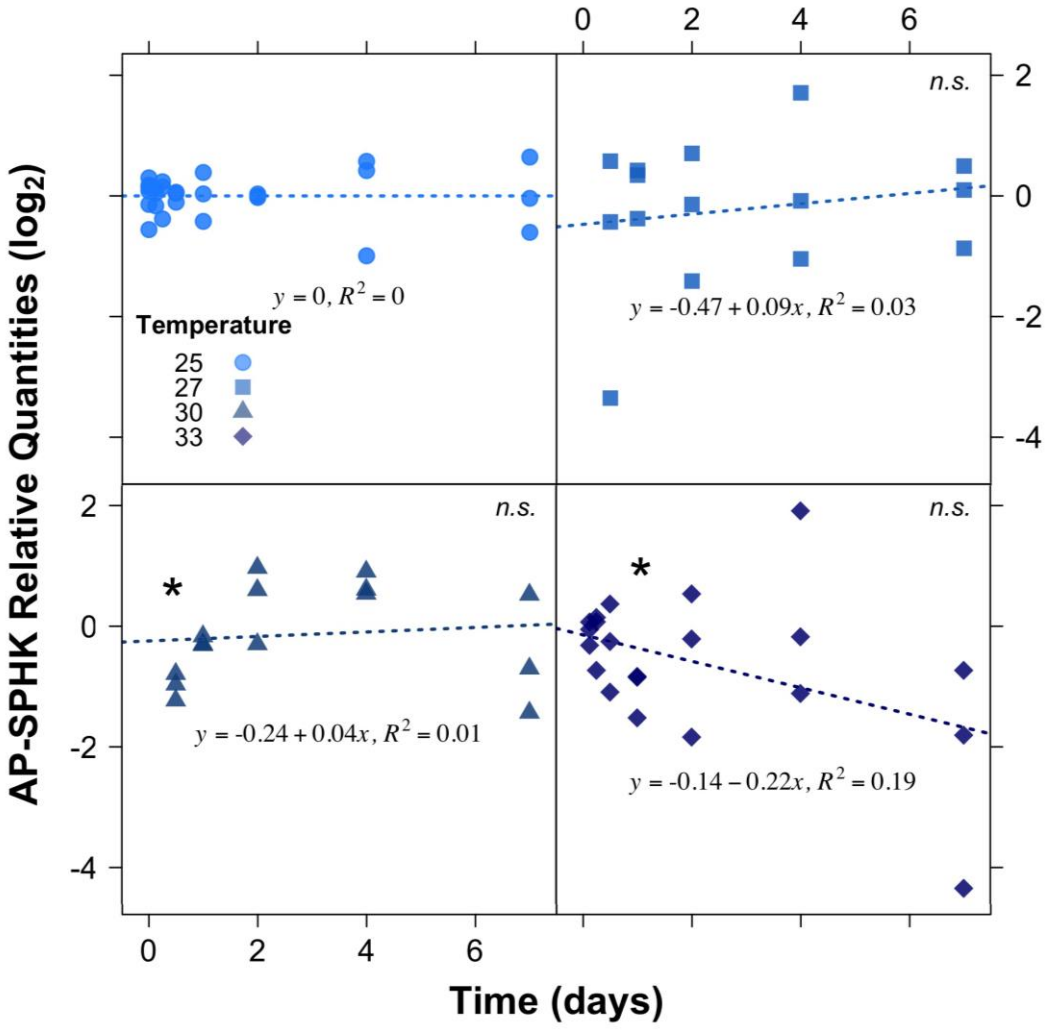

Figure 3.3 AP-SPHK expression in symbiotic *A. pallida* modestly decreases with hyperthermal temperature after one week. Synthesized cDNA from ambient (25 °C) and heat-treated samples (27, 30 and 33 °C) was used to quantify relative mRNA quantities (log_2) of AP-SPHK with qPCR (n= 3 anemones per group). The proportion of variation explained by the model (R^2) and significance (not significant= n.s., $p \leq 0.05$) from the linear regression is displayed for each temperature. Heat-treated groups at each time point that significantly differed from their matched control group with *post hoc* Student T-test are indicated with an asterisk (*), $p \leq 0.05$. Treatment groups (clockwise): ambient = ●, 27 °C= ■, 30 °C= ▲, and 33 °C = ◆.

Figure 3.4 Differential expression of AP-SPHK, but not AP-SGPP between symbiotic states in *A. pallida* during early heat stress but not AP-SGPP. Symbiotic (grey) and aposymbiotic (white) anemones were placed into ambient and hyperthermal temperature treatments and sampled at 6 and 12 h (n=3 anemones per time point and treatment). cDNA synthesized from collected anemones was used to calculate relative mRNA quantities (log_2) of AP-SGPP (A) and AP-SPHK (B) using qPCR. Expression of rheostat genes were analyzed using a Mann Whitney test, threshold $p \leq 0.05$ (not significant = n.s.). AP-SGPP expression was not significantly different between symbiotic states (A). AP-SPHK expression differed by symbiotic state, but not by individual time points (B).

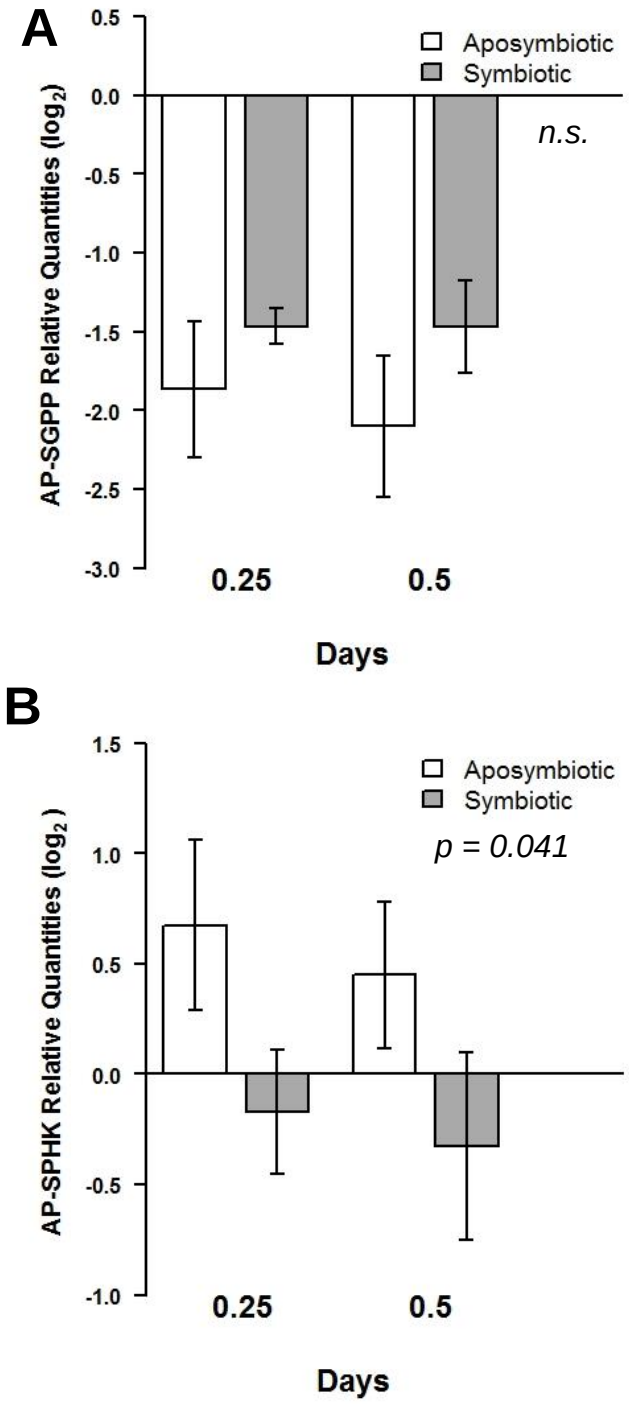
A
0.5
0.0
-0.5
-1.0
-1.5
-2.0
-2.5
-3.0
AP-SGPP Relative Quantities (log2)
Aposymbiotic
Symbiotic
n.s.
0.25
0.5
Days
B
1.5
1.0
0.5
0.0
-0.5
-1.0
AP-SPHK Relative Quantities (log2)
Aposymbiotic
Symbiotic
p = 0.041
0.25
0.5
Days

Figure 3.4

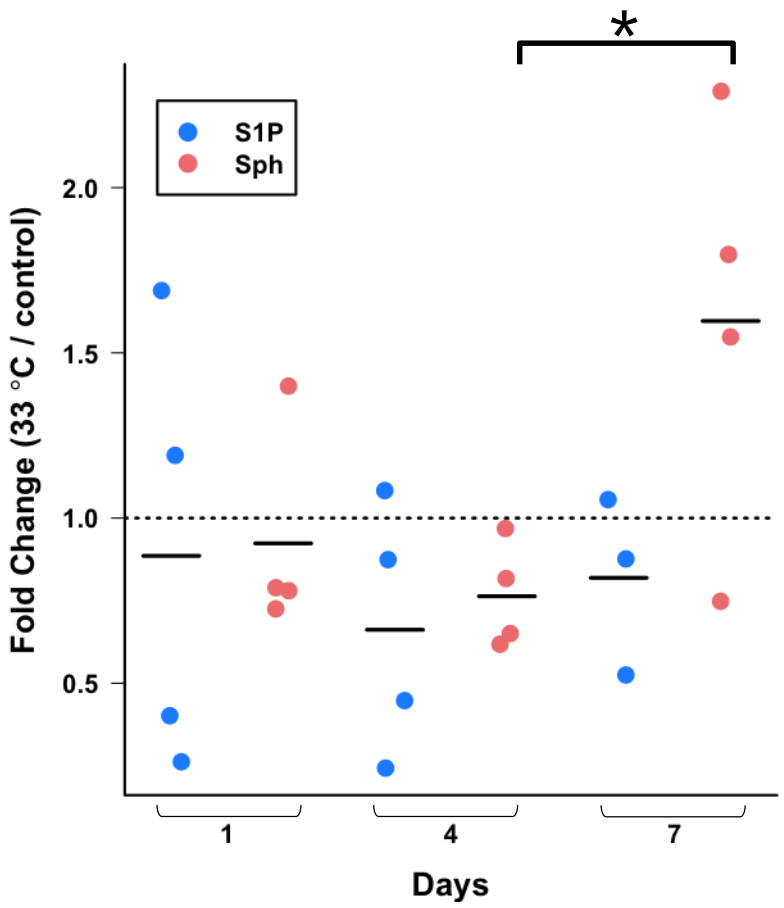

Figure 3.5 Cellular sphingolipid levels increased after one week at hyperthermal temperature. Sphingosine levels significantly increased, but there was no change in S1P levels through time. Lipids extracts were quantified with HPLC ESI-MS/MS, normalized to internal standards and total protein. Fold changes of S1P (blue) and Sph (red) were calculated at each time point as hyperthermal temperature (33 °C) over a time-matched non-heat stress control (25 °C), and then analyzed with 1-way ANOVA. Significance with Tukey *post hoc* test is indicated with an asterisk (*). Black bars show the mean fold change for each metabolite at the separate days.

Figure 3.6 Mean symbiont autofluorescence declines with elevated temperature. Symbiotic anemones were randomly placed into two temperatures, ambient (25 °C, n= 24) and hyperthermal (33 °C, n= 24), for one week. White light and fluorescent photographs were taken at indicated time points, where fluorescent emission was captured with a 665 nm bandpass filter following excitation with 470 nm LED light. Mean fluorescence from each anemone was calculated from 10 random areas of the oral disc and fit to quadratic regression over time (A, yellow dashed lines). Anemones were monitored until sacrificed at 1, 4, or 7 days. The change in autofluorescence from day 0 to day one (Δ fluorescence, dashed box in A) was compared to total anemone protein for the two temperatures (B). Positive values indicate lower autofluorescence at day one. Treatment groups: ambient = ●, and hyperthermal= ◆.

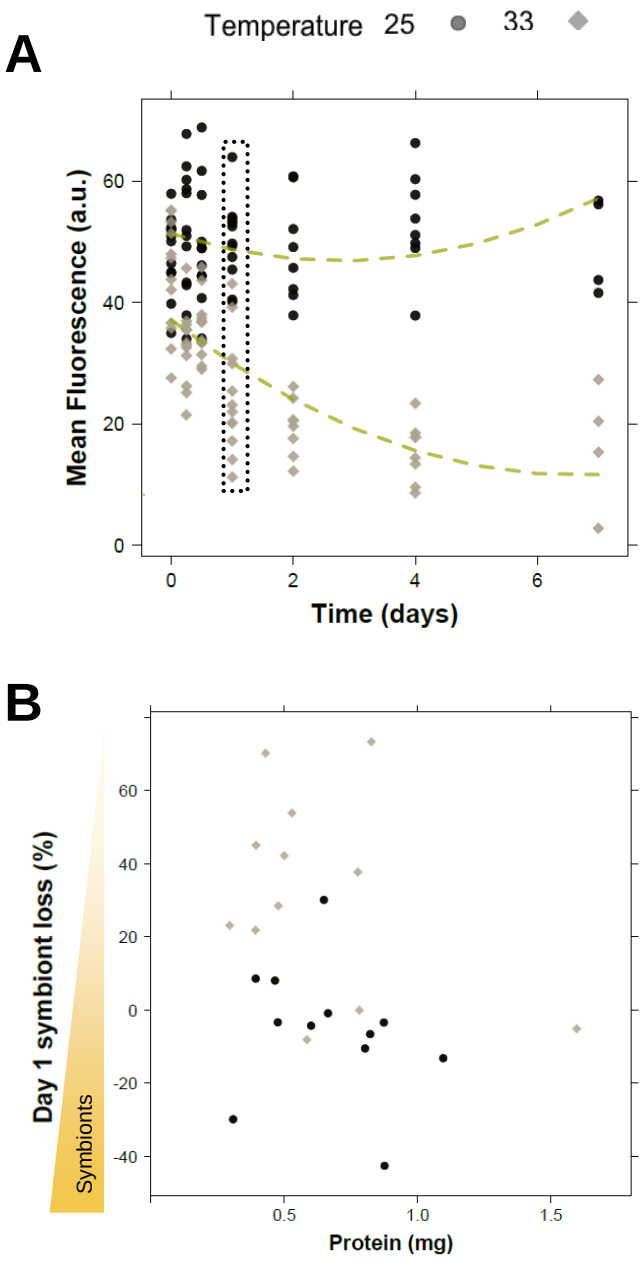
A
Temperature 25 33
Mean Fluorescence (a.u.)
0
20
40
60
0
2
4
6
Time (days)
B
Day 1 symbiont loss (%)
Symbionts
60
40
20
0
-20
-40
0.5
1.0
1.5
Protein (mg)

Figure 3.6

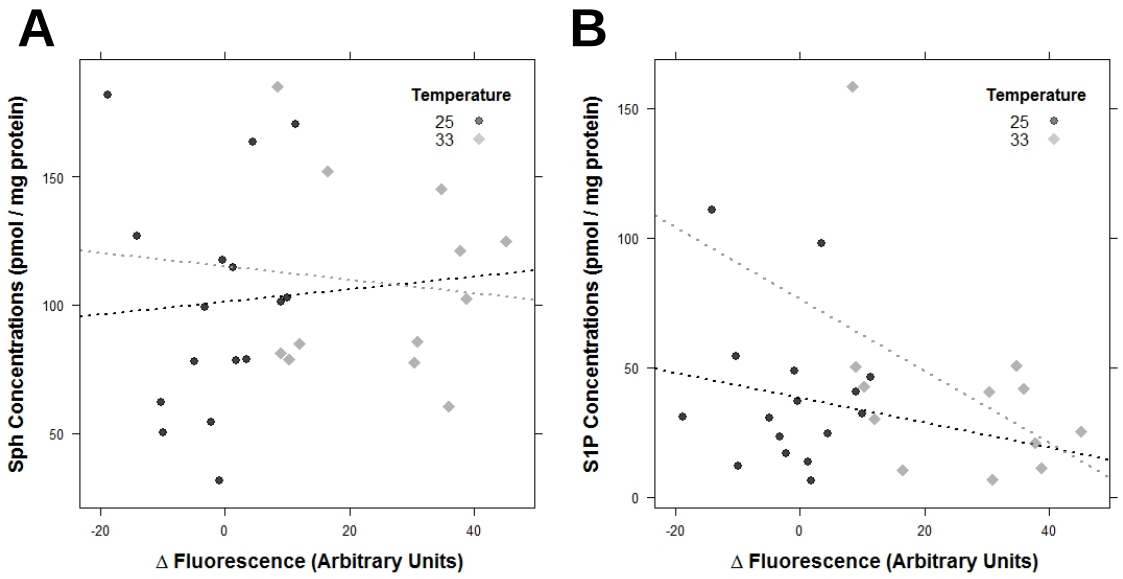

Figure 3.7 Loss of symbiont autofluorescence is not correlated with sphingolipid concentrations. Mean fluorescence was measured from anemones (n=4) used for lipid extraction, allowing for direct correlation of treatment conditions. Pearson's correlation analysis of sphingolipids Sph (A) and S1P (B) concentrations from symbiotic anemones found no evidence for a relationship of symbiont loss at hyperthermal temperatures (grey). Refer to Figure 3.5, Figure 3.6 and Materials and Methods for details on lipid and fluorescence quantification.

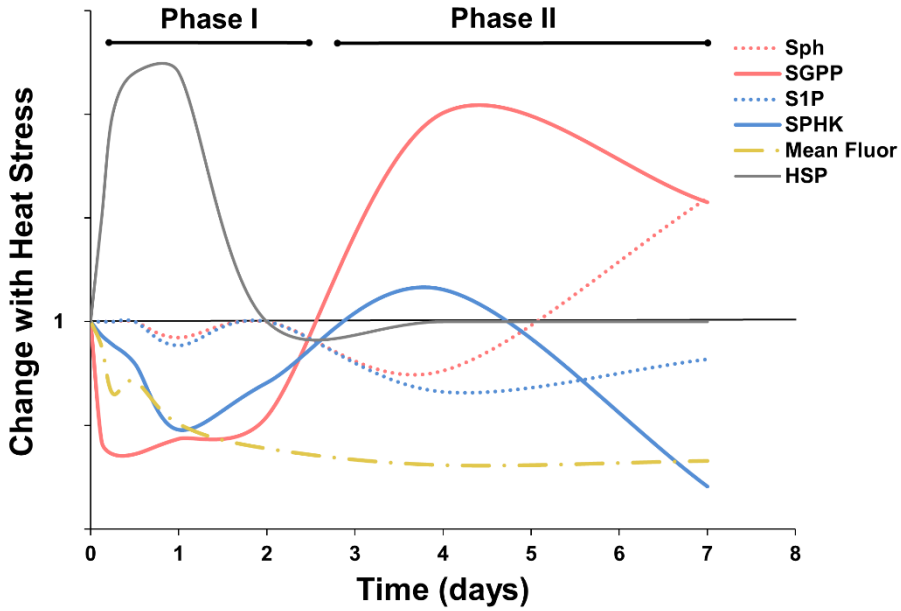

Figure 3.8 Summary of biphasic HSR in *A. pallida*. During phase I (three hours to two days), HSPs (grey) are upregulated (relative changes based on previously reported values (Black *et al.*, 1995, Gates *et al.*, 1999, Rodriguez-Lanetty *et al.*, 2009, Voolstra *et al.*, 2009b, DeSalvo *et al.*, 2010, Bellantuono *et al.*, 2011, Mayfield *et al.*, 2011)), symbiont density decreases by half (yellow), and the sphingosine rheostat transcriptional response and enzymatic activity are downregulated. After two days of heat treatment, AP-SPHK (blue) and AP-SGPP (red) expression are upregulated followed by altered lipid concentrations in phase II. To allow for comparisons between analyses, mean expression, lipid fold changes and fluorescence were scaled to initial values at 1. Expression was converted to linear fold changes and fluorescence to changes from initial for each time point.

3.6 References

Ader, I., Brizuela, L., Bouquerel, P., Malavaud, B. and Cuvillier, O. (2008). Sphingosine kinase 1: a new modulator of hypoxia inducible factor 1α during hypoxia in human cancer cells. *Cancer Res.* **68,** 8635-8642.

An, D., Na, C., Bielawski, J., Hannun, Y.A. and Kasper, D.L. (2011). Membrane sphingolipids as essential molecular signals for *Bacteroides* survival in the intestine. *Proc. Natl. Acad. Sci. USA* **108,** 4666-4671.

Andersen, C.L., Jensen, J.L. and Ørntoft, T.F. (2004). Normalization of real-time quantitative reverse transcription-PCR data: A model-based variance estimation approach to identify genes suited for normalization, applied to bladder and colon cancer data sets. *Cancer Res.* **64,** 5245-5250.

Balogh, G., Péter, M., Glatz, A., Gombos, I., Török, Z., Horváth, I., *et al.* (2013). Key role of lipids in heat stress management. *FEBS Lett.* **587,** 1970-1980.

Bellantuono, A.J., Hoegh-Guldberg, O. and Rodriguez-Lanetty, M. (2011). Resistance to thermal stress in corals without changes in symbiont composition. *Proc. R. Soc. Lond., Ser. B: Biol. Sci.* **279,** 1100-1107.

Black, N.A., Voellmy, R. and Szmant, A.M. (1995). Heat shock protein induction in *Montastraea faveolata* and *Aiptasia pallida* exposed to elevated temperatures. *Biol. Bull.* **188,** 234-240.

Black, R.E. and Bloom, L. (1984). Heat shock proteins in *Aurelia* (Cnidaria, Scyphozoa). *J. Exp. Zool.* **230,** 303-307.

Bosch, T., Krylow, S.M., Bode, H.R. and Steele, R.E. (1988). Thermotolerance and synthesis of heat shock proteins: these responses are present in *Hydra attenuata* but absent in *Hydra oligactis*. *Proc. Natl. Acad. Sci. USA* **85,** 7927-7931.

Bouchard, J.N. and Yamasaki, H. (2009). Implication of nitric oxide in the heat-stress-induced cell death of the symbiotic alga *Symbiodinium microadriaticum*. *Mar. Biol.* **156,** 2209-2220.

Chang, Y., Abe, A. and Shayman, J.A. (1995). Ceramide formation during heat shock: a potential mediator of alpha B-crystallin transcription. *Proc. Natl. Acad. Sci. USA* **92,** 12275-12279.

Chen, M.-C., Cheng, Y.-M., Hong, M.-C. and Fang, L.-S. (2004). Molecular cloning of Rab5 (ApRab5) in Aiptasia pulchella and its retention in phagosomes harboring live zooxanthellae. *Biochem. Biophys. Res. Commun.* **324,** 1024-1033.

Chen, M.-C., Cheng, Y.-M., Sung, P.-J., Kuo, C.-E. and Fang, L.-S. (2003). Molecular identification of Rab7 (ApRab7) in Aiptasia pulchella and its exclusion from phagosomes harboring zooxanthellae. *Biochem. Biophys. Res. Commun.* **308,** 586-595.

Chen, M.C., Hong, M.C., Huang, Y.S., Liu, M.C., Cheng, Y.M. and Fang, L.S. (2005). ApRab11, a cnidarian homologue of the recycling regulatory protein Rab11, is involved in the establishment and maintenance of the *Aiptasia - Symbiodinium* endosymbiosis. *Biochem. Biophys. Res. Commun.* **338,** 1607 - 1616.

Chen, P.-W., Fonseca, L.L., Hannun, Y.A. and Voit, E.O. (2013). Coordination of rapid sphingolipid responses to heat stress in yeast. *PLoS Comp. Biol.* **9,** e1003078.

Cuvillier, O., Pirianov, G., Kleuser, B., Vanek, P.G., Coso, O.A., Gutkind, J.S. and Spiegel, S. (1996). Suppression of ceramide-mediated programmed cell death by sphingosine-1-phosphate. *Nature* **381,** 800-803.

de Nadal, E., Ammerer, G. and Posas, F. (2011). Controlling gene expression in response to stress. *Nature Reviews Genetics* **12,** 833-845.

De Palma, C., Meacci, E., Perrotta, C., Bruni, P. and Clementi, E. (2006). Endothelial nitric oxide synthase activation by tumor necrosis factor α through neutral sphingomyelinase 2, sphingosine kinase 1, and sphingosine 1 phosphate receptors a novel pathway relevant to the pathophysiology of endothelium. *Arterioscler. Thromb. Vasc. Biol.* **26,** 99-105.

Deng, X., Yin, X., Allan, R., Lu, D.D., Maurer, C.W., Haimovitz-Friedman, A., *et al.* (2008). Ceramide biogenesis is required for radiation-induced apoptosis in the germ line of *C. elegans*. *Science* **322,** 110-115.

DeSalvo, M.K., Sunagawa, S., Voolstra, C.R. and Medina, M. (2010). Transcriptomic responses to heat stress and bleaching in the elkhorn coral *Acropora palmata*. *Mar. Ecol. Prog. Ser.* **402,** 97-113.

DeSalvo, M.K., Voolstra, C.R., Sunagawa, S., Schwarz, J.A., Stillman, J.H., Coffroth, M.A., *et al.* (2008). Differential gene expression during thermal stress and bleaching in the Caribbean coral *Montastraea faveolata*. *Mol. Ecol.* **17,** 3952-3971.

Detournay, O. and Weis, V.M. (2011). Role of the sphingosine rheostat in the regulation of cnidarian-dinoflagellate symbioses. *Biol. Bull.* **221,** 261-269.

Douglas, A.E. (2003). Coral bleaching - how and why? *Mar. Pollut. Bull.* **46,** 385-392.

Dunn, S.R., Schnitzler, C.E. and Weis, V.M. (2007). Apoptosis and autophagy as mechanisms of dinoflagellate symbiont release during cnidarian bleaching: every which way you lose. *Proc. R. Soc. Lond., Ser. B: Biol. Sci.* **274,** 3079-3085.

Dunn, S.R., Thomason, J.C., Le Tissier, M.D.A. and Bythell, J.C. (2004). Heat stress induces different forms of cell death in sea anemones and their endosymbiotic algae depending on temperature and duration. *Cell Death Differ.* **11,** 1213-1222.

Dunn, S.R. and Weis, V.M. (2009). Apoptosis as a post-phagocytic winnowing mechanism in a coral-dinoflagellate mutualism. *Environ. Microbiol.* **11,** 268-276.

Florio, T., Arena, S., Pattarozzi, A., Thellung, S., Corsaro, A., Villa, V., *et al.* (2003). Basic fibroblast growth factor activates endothelial nitric-oxide synthase in CHO-K1 cells via the activation of ceramide synthesis. *Mol. Pharmacol.* **63,** 297-310.

Gates, R.D., Baghdasarian, G. and Muscatine, L. (1992b). Temperature stress causes host cell detachment in symbiotic cnidarians: Implications for coral bleaching. *Biol. Bull.* **182,** 324-332.

Gates, R.D. and Edmunds, P.J. (1999). The physiological mechanisms of acclimatization in tropical reef corals. *Am. Zool.* **39,** 30-43.

Goldkorn, T., Dressler, K.A., Muindi, J., Radin, N.S., Mendelsohn, J., Menaldino, D., *et al.* (1991). Ceramide stimulates epidermal growth factor receptor phosphorylation in A431 human epidermoid carcinoma cells. Evidence that ceramide may mediate sphingosine action. *J. Biol. Chem.* **266,** 16092-16097.

Gomez-Brouchet, A., Pchejetski, D., Brizuela, L., Garcia, V., Altie, M.-F., Maddelein, M.-L., *et al.* (2007). Critical role for sphingosine kinase-1 in regulating survival of neuroblastoma cells exposed to amyloid-β peptide. *Mol. Pharmacol.* **72,** 341-349.

Grajales, A. and Rodriguez, E. (2014). Morphological revision of the genus *Aiptasia* and the family Aiptasiidae (Cnidaria, Actiniaria, Metridioidea). *Zootaxa* **3826,** 55-100.

Graner, M.W., Cumming, R.I. and Bigner, D.D. (2007). The heat shock response and chaperones/heat shock proteins in brain tumors: surface expression, release, and possible immune consequences. *J. Neurosci.* **27,** 11214-11227.

Hanes, S.D. and Kempf, S.C. (2013). Host autophagic degradation and associated symbiont loss in response to heat stress in the symbiotic anemone, *Aiptasia pallida*. *Invertebr. Biol.* **132,** 95-107.

Hawkins, T., Krueger, T., Becker, S., Fisher, P. and Davy, S. (2014). Differential nitric oxide synthesis and host apoptotic events correlate with bleaching susceptibility in reef corals. *Coral Reefs* **33,** 141-153.

Hawkins, T.D., Bradley, B.J. and Davy, S.K. (2013). Nitric oxide mediates coral bleaching through an apoptotic-like cell death pathway: evidence from a model sea anemone-dinoflagellate symbiosis. *FASEB J.* **27,** 4790-4798.

Hawkins, T.D. and Davy, S.K. (2012). Nitric oxide production and tolerance differ among *Symbiodinium t*ypes exposed to heat stress. *Plant Cell Physiol.* **53,** 1889-1898.

Hemond, E.M., Kaluziak, S.T. and Vollmer, S.V. (2014). The genetics of colony form and function in Caribbean Acropora corals. *BMC Genomics* **15,** 1133.

Heung, L.J., Luberto, C. and Del Poeta, M. (2006). Role of sphingolipids in microbial pathogenesis. *Infect. Immun.* **74,** 28-39.

Hill, R., Ulstrup, K.E. and Ralph, P.J. (2009). Temperature induced changes in thylakoid membrane thermostability of cultured, freshly isolated, and expelled zooxanthellae from scleractinian corals. *Bull. Mar. Sci.* **85,** 223-244.

Hoegh-Guldberg, O. (1999). Climate change, coral bleaching and the future of the world's coral reefs. *Marine and Freshwater Research* **50,** 839-866.

Hoegh-Guldberg, O., Mumby, P.J., Hooten, A.J., Steneck, R.S., Greenfield, P., Gomez, E., *et al.* (2007). Coral reefs under rapid climate change and ocean acidification. *Science* **318,** 1737-1742.

Hofmann, G.E. and Todgham, A.E. (2010). Living in the now: physiological mechanisms to tolerate a rapidly changing environment. *Annu. Rev. Physiol.* **72,** 127-145.

Hughes, T.P., Baird, A.H., Bellwood, D.R., Card, M., Connolly, S.R., Folke, C., *et al.* (2003). Climate change, human impacts, and the resilience of coral reefs. *Science* **301,** 929-933.

Jenkins, G.M., Cowart, L.A., Signorelli, P., Pettus, B.J., Chalfant, C.E. and Hannun, Y.A. (2002). Acute activation of de novo sphingolipid biosynthesis upon heat shock causes an accumulation of ceramide and subsequent dephosphorylation of SR proteins. *J. Biol. Chem.* **277,** 42572-42578.

Jenkins, G.M. and Hannun, Y.A. (2001). Role for de novo sphingoid base biosynthesis in the heat-induced transient cell cycle arrest of *Saccharomyces cerevisiae*. *J. Biol. Chem.* **276,** 8574-8581.

Jenkins, G.M., Richards, A., Wahl, T., Mao, C., Obeid, L. and Hannun, Y. (1997). Involvement of yeast sphingolipids in the heat stress response of *Saccharomyces cerevisiae*. *J. Biol. Chem.* **272,** 32566-32572.

Kawamura, H., Tatei, K., Nonaka, T., Obinata, H., Hattori, T., Ogawa, A., *et al.* (2009). Ceramide induces myogenic differentiation and apoptosis in *Drosophila* Schneider cells. *J. Radiat. Res. (Tokyo)* **50,** 161-169.

Lanterman, M. and Saba, J. (1998). Characterization of sphingosine kinase (SK) activity in *Saccharomyces cerevisiae* and isolation of SK-deficient mutants. *Biochem. J* **332,** 525-531.

Le Stunff, H., Milstien, S. and Spiegel, S. (2004). Generation and metabolism of bioactive sphingosine-1-phosphate. *J. Cell. Biochem.* **92,** 882 - 899.

Lesser, M.P. (1996). Elevated temperatures and ultraviolet radiation cause oxidative stress and inhibit photosynthesis in symbiotic dinoflagellates. *Limnol. Oceanogr.* **41,** 271-283.

Livak, K.J. and Schmittgen, T.D. (2001). Analysis of relative gene expression data using real-time quantitative PCR and the $2^{-\Delta\Delta CT}$ method. *Methods* **25,** 402-408.

Maceyka, M., Milstien, S. and Spiegel, S. (2007). Shooting the messenger: oxidative stress regulates sphingosine-1-phosphate. *Circ. Res.* **100,** 7-9.

Maceyka, M., Payne, S.G., Milstien, S. and Spiegel, S. (2002). Sphingosine kinase, sphingosine-1-phosphate, and apoptosis. *Biochim. Biophys. Acta* **1585,** 193 - 201.

Mandala, S.M., Thornton, R., Tu, Z., Kurtz, M.B., Nickels, J., Broach, J., *et al.* (1998). Sphingoid base 1-phosphate phosphatase: a key regulator of sphingolipid metabolism and stress response. *Proc. Natl. Acad. Sci. USA* **95,** 150-155.

Mao, C., Saba, J. and Obeid, L. (1999). The dihydrosphingosine-1-phosphate phosphatases of *Saccharomyces cerevisiae* are important regulators of cell proliferation and heat stress responses. *Biochem. J* **342,** 667-675.

Mayfield, A.B., Wang, L.-H., Tang, P.-C., Fan, T.-Y., Hsiao, Y.-Y., Tsai, C.-L. and Chen, C.-S. (2011). Assessing the impacts of experimentally elevated temperature on the biological composition and molecular chaperone gene expression of a reef coral. *PLoS One* **6,** e26529.

McGinty, E.S., Pieczonka, J. and Mydlarz, L.D. (2012). Variations in reactive oxygen release and antioxidant activity in multiple *Symbiodinium* types in response to elevated temperature. *Microb. Ecol.* **64,** 1000-1007.

Morimoto, R. (1993). Cells in stress: transcriptional activation of heat shock genes. *Science (New York, NY)* **259,** 1409.

Muscatine, L. and Cernichiari, E. (1969). Assimilation of photosynthetic products of zooxanthellae by a reef coral. *Biol. Bull.* **137,** 506-523.

Nagai, K.-i., Takahashi, N., Moue, T. and Niimura, Y. (2011). Alteration of fatty acid molecular species in ceramide and glucosylceramide under heat stress and expression of sphingolipid-related genes. *Advances in Biological Chemistry* **1,** 35-48.

Nii, C.M. and Muscatine, L. (1997). Oxidative stress in the symbiotic sea anemone *Aiptasia pulchella* (Carlgren, 1943): contribution of the animal to superoxide ion production at elevated temperature. *Biol. Bull.* **192,** 444-456.

Olivera, A. and Spiegel, S. (2001). Sphingosine kinase: a mediator of vital cellular functions. *Prostaglandins Other Lipid Mediat.* **64,** 123-134.

Pandolfi, J.M., Bradbury, R.H., Sala, E., Hughes, T.P., Bjorndal, K.A., Cooke, R.G., *et al.* (2003). Global trajectories of the long-term decline of coral reef ecosystems. *Science* **301,** 955-958.

Paxton, C.W., Davy, S.K. and Weis, V.M. (2013). Stress and death of cnidarian host cells play a role in cnidarian bleaching. *J. Exp. Biol.* **216,** 2813-2820.

Pchejetski, D., Kunduzova, O., Dayon, A., Calise, D., Seguelas, M.-H., Leducq, N., *et al.* (2007). Oxidative stress–dependent sphingosine kinase-1 inhibition mediates monoamine oxidase A–associated cardiac cell apoptosis. *Circ. Res.* **100,** 41-49.

Perez, S. and Weis, V. (2006). Nitric oxide and cnidarian bleaching: an eviction notice mediates breakdown of a symbiosis. *J. Exp. Biol.* **209,** 2804-2810.

Perrotta, C., De Palma, C. and Clementi, E. (2008). Nitric oxide and sphingolipids: mechanisms of interaction and role in cellular pathophysiology. *Biol. Chem.* **389,** 1391-1397.

Poole, A.Z., Kitchen, S.A., Dow, E.G. and Weis, V.M. (submitted). The role of complement in cnidarian-dinoflagellate symbiosis and immune challenge in the sea anemone *Aiptasia pallida*. *Front. Microbiol.*

Rasband, W. (1997-2015) ImageJ. Bethesda, Maryland, USA, U. S. National Institutes of Health

Richier, S., Sabourault, C., Courtiade, J., Zucchini, N., Allemand, D. and Furla, P. (2006). Oxidative stress and apoptotic events during thermal stress in the symbiotic sea anemone, *Anemonia viridis*. *FEBS J.* **273,** 4186-4198.

Rodriguez-Lanetty, M., Harii, S. and Hoegh-Guldberg, O.V.E. (2009). Early molecular responses of coral larvae to hyperthermal stress. *Mol. Ecol.* **18,** 5101-5114.

Rodriguez-Lanetty, M., Phillips, W. and Weis, V. (2006). Transcriptome analysis of a cnidarian - dinoflagellate mutualism reveals complex modulation of host gene expression. *BMC Genomics* **7,** 23.

Ross, C. (2014). Nitric oxide and heat shock protein 90 co-regulate temperature-induced bleaching in the soft coral *Eunicea fusca*. *Coral Reefs* **33,** 513-522.

Sawyer, S.J. and Muscatine, L. (2001). Cellular mechanisms underlying temperature-induced bleaching in the tropical sea anemone A*iptasia pulchella*. *J. Exp. Biol.* **204,** 3443-3456.

Spiegel, S. and Milstien, S. (2003). Sphingosine-1-phosphate: An enigmatic signaling lipid. *Nat. Rev. Mol. Cell Biol.* **4,** 397 - 407.

Starcevic, A., Dunlap, W.C., Cullum, J., Shick, J.M., Hranueli, D. and Long, P.F. (2010). Gene expression in the scleractinian Acropora microphthalma exposed to high solar irradiance reveals elements of photoprotection and coral bleaching. *PLoS One* **5,** e13975.

Suggett, D.J., Warner, M.E., Smith, D.J., Davey, P., Hennige, S. and Baker, N.R. (2008). Photosynthesis and production of hydrogene perxoide by *Symbiodinim* (Pyrrophyta) phylotypes with different thermal tolerances *J. Phycol.* **44,** 948-956.

Tchernov, D., Gorbunov, M.Y., de Vargas, C., Yadav, S.N., Milligan, A.J., Häggblom, M. and Falkowski, P.G. (2004). Membrane lipids of symbiotic algae are diagnostic of sensitivity to thermal bleaching in corals. *Proc. Natl. Acad. Sci. USA* **101,** 13531-13535.

Tolleter, D., Seneca, F.O., DeNofrio, J.C., Krediet, C.J., Palumbi, S.R., Pringle, J.R. and Grossman, A.R. (2013). Coral bleaching independent of photosynthetic activity. *Curr. Biol.* **23,** 1782-1786.

van Brocklyn, J.R. and Williams, J.B. (2012). The control of the balance between ceramide and sphingosine-1-phosphate by sphingosine kinase: Oxidative stress and the seesaw of cell survival and death. *Comp. Biochem. Physiol. B Biochem. Mol. Biol.* **163,** 26-36.

Vandesompele, J., De Preter, K., Pattyn, F., Poppe, B., Van Roy, N., De Paepe, A. and Speleman, F. (2002). Accurate normalization of real-time quantitative RT-PCR data by geometric averaging of multiple internal control genes. *Genome Biol.* **3,** 1 - 11.

Venn, A.A., Loram, J.E. and Douglas, A.E. (2008). Photosynthetic symbioses in animals. *J. Exp. Bot.* **59,** 1069-1080.

Voolstra, C., Schnetzer, J., Peshkin, L., Randall, C., Szmant, A. and Medina, M. (2009a). Effects of temperature on gene expression in embryos of the coral *Montastraea faveolata*. *BMC Genomics* **10,** 627.

Voolstra, C.R., Schwarz, J.A., Schnetzer, J., Sunagawa, S., Desalvo, M.K., Szmant, A.M., *et al.* (2009b). The host transcriptome remains unaltered during the establishment of coral–algal symbioses. *Mol. Ecol.* **18,** 1823-1833.

Wang, J., Meng, P., Sampayo, E., Tang, S. and Chen, C. (2011). Photosystem II breakdown induced by reactive oxygen species in freshly-isolated *Symbiodinium* from *Montipora* (Scleractinia; Acroporidae). *Mar. Ecol. Prog. Ser.* **422,** 51-62.

Warner, M.E., Fitt, W.K. and Schmidt, G.W. (1996). The effects of elevated temperature on the photosynthetic efficiency of zooxanthellae *in hospite* from four different species of reef coral: a novel approach. *Plant, Cell Environ.* **19,** 291-299.

Weis, V.M. (2008). Cellular mechanisms of Cnidarian bleaching: stress causes the collapse of symbiosis. *J. Exp. Biol.* **211,** 3059-3066.

Yabu, T., Imamura, S., Yamashita, M. and Okazaki, T. (2008). Identification of Mg2+-dependent neutral sphingomyelinase 1 as a mediator of heat stress-induced ceramide generation and apoptosis. *J. Biol. Chem.* **283,** 29971-29982.

4. HYPERTHERMAL STRESS ALTERS PHENOTYPIC AND TRANSCRIPTOMIC RESPONSES OF CORAL LARVAE AT THE ONSET OF SYMBIOSIS

Sheila A. Kitchen

Duo Jiang

Saki Harii

Noriyuki Satoh

Virginia M. Weis

Chuya Shinzato

Formatted for *Nature Climate Change*

The Macmillan Building

4 Crinan Street

London N1 9XW

United Kingdom

4.1 Summary

The mutualistic endosymbiosis between corals and their photosynthetic dinoflagellates collapses under prolonged hyperthermal stress associated with climate change and which in turn results in coral bleaching, or the loss of dinoflagellates from the host (Glynn, 1983, Hoegh-Guldberg, 1999). We are beginning to understand the physiological and molecular mechanisms underlying symbiosis dysfunction during bleaching in adult corals (Weis, 2008, Weis, 2010); however, very few studies have addressed the effects of temperature-induced stress during the onset and establishment of symbiosis in larval and juvenile corals. The capacity of larvae to buffer climate-induced stress while undergoing symbiont acquisition comes with physiological trade-offs altering larval behavior, development, settlement and survivorship (Baird, 2006, Munday *et al.*, 2009, Randall *et al.*, 2009a, Randall *et al.*, 2009b, Yakovleva *et al.*, 2009, Schnitzler *et al.*, 2011). Here we examined the joint effects of both thermal stress and onset of symbiosis on colonization of host larvae by symbionts, larval survival, and host global gene expression. Both temperature and symbiotic state affected larval survival rates, with increased mortality in larvae exposed to the combined treatment. Heat stress also decreased symbiont colonization by 50% and density by 98.5% after two weeks compared to non-stressed controls. Lastly, we identified 232 genes that were differentially expressed with the interaction of symbiont colonization and hyperthermal stress using RNASeq. The combination of treatments caused expression changes in immunity, cytoskeletal elements, oxidative stress and lipid metabolism. This study furthers our understanding of the physical environment and biotic pressures that mediate pre-settlement event in corals and describes novel transcriptional patterns in the coral molecular stress-response.

4.2 Manuscript Text

Reef building corals form endosymbiotic partnerships with photosynthetic dinoflagellates from the diverse set of dinoflagellates in the genus *Symbiodinium* spp. The colonization by symbionts in early developmental stages of corals may increase host survivorship and extend settlement competency periods, both of which play an important role in larval dispersal (van Oppen *et al.*, 2001, Harii *et al.*, 2009). As a taxon, corals

display two sexual reproductive modes, broadcast spawning and brooding, which influence symbiosis establishment. In most brooding species, symbiotic algae are usually transmitted directly from the parent colony to eggs or larvae. In contrast, broadcast spawners generally release gametes free of symbionts (aposymbiotic) (Richmond, 1990), and thus planula larvae and newly metamorphosed polyps must acquire symbionts from the surrounding environment by horizontal transmission (Babcock *et al.*, 1986, Schwarz *et al.*, 1999, Edmunds *et al.*, 2005, Harii *et al.*, 2009). Changes in the environment, for instance elevated temperatures or high irradiance, may therefore alter the availability of symbionts and mechanisms controlling symbiont colonization by the coral host.

Establishment of coral-*Symbiodinium* partnerships is accomplished through complex recognition events between the host and symbiont and modulation of the host immune pathways (Davy *et al.*, 2012). In aposymbiotic coral larvae, host-symbiont recognition mechanisms must be acquired or activated each generation (Babcock *et al.*, 1986). Numerous studies have demonstrated that coral larvae can establish symbiosis (Schwarz *et al.*, 1999, Weis *et al.*, 2001a, Little *et al.*, 2004, Harii *et al.*, 2009, Cumbo *et al.*, 2013), but the underlying mechanisms of symbiont recognition and maintenance in the larval host are just beginning to be understood. Furthermore, the impact of environmental conditions on these processes unexplored. Research on early developmental stages of corals demonstrates a variety of stress responses that are dependent on the duration of stress (hours to days) and symbiotic state. Studies of temperature-induced stress on larvae show detrimental effects on larval behavior, development, settlement and survivorship with more severe effects being observed in symbiotic compared to aposymbiotic larvae (Baird, 2006, Munday *et al.*, 2009, Randall *et al.*, 2009a, Randall *et al.*, 2009b, Yakovleva *et al.*, 2009, Schnitzler *et al.*, 2011). For example, in the larvae of the coral *Fungia scutaria* exposure to elevated temperatures impaired symbiosis establishment and the presence of symbionts greatly decreased larval survivorship with elevated temperature (Schnitzler *et al.*, 2011). Consequently, as sea surface temperatures (SST) continue to rise, physiologically compromised larvae devoid of symbionts could result in reduced larval dispersal and recruitment thereby hindering the development of healthy coral reefs.

There are numerous transcriptomic profiles of aposymbiotic larvae subjected to hyperthermal stress described, with evidence for modulation of genes involved in growth, development, structural support, cellular signaling, stress and immunity (DeSalvo *et al.*, 2008, Rodriguez-Lanetty *et al.*, 2009, Voolstra *et al.*, 2009a, Portune *et al.*, 2010, Schnitzler *et al.*, 2010, Meyer *et al.*, 2011, Meyer *et al.*, 2012). These transcriptomic studies reveal heat-induced molecular responses in larvae, however they exclude molecular responses related to symbiotic state, which could also influence larval health and survivorship. Previous transcriptional studies on coral larvae at the early stages of symbiosis with *Symbiodinium* spp. indicate that establishment of partnerships with appropriate symbiont strains do not elicit widespread host transcriptomic changes (Voolstra *et al.*, 2009b, Schnitzler *et al.*, 2010), in contrast to the formation of non-suitable partnerships which elicit notable expression differences (Voolstra *et al.*, 2009b). The few transcriptional patterns that emerged from these investigations suggest that acquiring homologous *Symbiodinium* spp. alters host gene expression related to protein metabolism and immunity (Voolstra *et al.*, 2009b, Schnitzler *et al.*, 2010). Thus, it is important to also examine transcriptional changes in symbiotic larvae, where symbiosis onset may become stressful when compounded with hyperthermal stress and could prevent successful symbiosis establishment. Presently, little is known about how altered environmental conditions impact molecular and cellular responses of coral larvae during the onset of symbiosis.

The research presented here extends the study of hyperthermal stress in coral larvae by examination of symbiont colonization, larval survival and high-throughput, unbiased transcriptional profiling when larvae are exposed simultaneously to elevated temperature and symbionts. We used a factorial experimental design to investigate the interaction of a low (L) and high (H) temperature on symbiotic state, either aposymbiotic (A) or during colonization by symbionts (C) (Table 4.1), on the branching coral *Acropora digitifera*, one of the most sensitive species to elevated SST on Okinawan reefs (Loya *et al.*, 2001). *A. digitifera* is a broadcast spawner releasing aposymbiotic gametes that develop into aposymbiotic larvae after fertilization (Richmond, 1990). Larvae can be reared in the lab and symbiosis can be established experimentally (Harii *et al.*, 2009). In

addition, the genome is sequenced (Shinzato *et al.*, 2011). Thus, *A. digitifera* in its early life stages is a relevant experimental system to study the molecular and cellular responses associated with climate change.

4.2.1 **A. digitifera** *larval colonization success, symbiont density and survival decreased in the colonization with high temperature (CH) treatment group*

In order to link the transcriptional patterns of *A. digitifera* larvae to the different experimental conditions over time, we first quantified the host phenotype for symbiont colonization and survival. Algal symbiont type is important for host recognition and specificity during symbiont colonization (Davy *et al.*, 2012), and can alter the sensitivity of corals to thermal stress (Hofmann *et al.*, 2010, Hume *et al.*, 2015, Silverstein *et al.*, 2015, Winkler *et al.*, 2015). The symbiont types initially acquired by developing stages of corals can differ from those found in adult (Coffroth *et al.*, 2001, Little *et al.*, 2004, Abrego *et al.*, 2009, Cumbo *et al.*, 2013). In adult *A. digitifera,* clade C1 *Symbiodinium* are the predominant symbiont type, however *A. digitifera* larvae can establish symbioses with multiple *Symbiodinium* types in the laboratory (Harii *et al.*, 2009, Suwa *et al.*, 2010, Cumbo *et al.*, 2013). For our colonization experiment, we used cultured *Symbiodinium tridacnidorum* (clade A3) that is preferentially taken up in early developmental stages of *A. digitifera* (Suwa *et al.*, 2010). Successful symbiont colonization was measured over time by scoring the presence or absence of symbiont chlorophyll autofluorescence using fluorescence microscopy (Figure 4.1A). There was a significant interaction of temperature and time on the odds of successful colonization (binomial generalized mixed effects model (GLMM), $p < 0.001$). Initially, more high temperature-treated larvae (CH) were colonized between 6 and 12 h compared to colonized larvae at the low temperature (CL) (binomial GLMM, $p= 0.001$ for both), however, at day one post-inoculation there was a dramatic divergence between temperature treatments. Starting at day one and for the remainder of the experiment just 50% of heat-treated larvae were colonized (Figure 4.1B). The odds of colonization in the CH treatment was 0.37 times lower (95% CI 0.2 to 0.68) than in the CL treatment, after accounting for time (binomial GLMM, $p =0.0016$). In contrast, nearly 95% of CL- treated larvae were colonized by day 14 and were 6.73 times (95% CI 2.3 to 19.7) more likely to be colonized compared to CH-treated larvae

(binomial GLMM, $p < 0.001$). The temporal increase in *S. tridacnidorum* colonization in CL larvae was slightly higher than a previous study that used homologous C1 symbionts to colonize *A. digitifera* larvae, which reached 80% colonization after 20 days (Harii *et al.*, 2009).

From the colonized larvae collected at each temperature, symbiont density was quantified from 20 randomly sampled larvae. The average algal density in larvae from the CL treatment relative to the CH treatment significantly increased with time (Figure 4.1C, quasi-poisson GLMM, $p < 0.001$). For each additional day, the average number of symbionts increased by 30.8% in CL-treated larvae (quasi-poisson GLMM, $p < 0.001$), while they remained low in CH-treated larvae (Figure 4.1C). These results suggest that elevated temperature severely limits *S. tridacnidorum* colonization of *A. digitifera* larvae and inhibits *S. tridacnidorum* proliferation in colonized larvae over time.

To address the impact of elevated temperature and symbiosis on larval survival, 300 larvae placed in the four treatment groups (Table 4.1) were counted at discrete time points over 14 days. By the end of the experiment, the larvae exposed to the CH treatment had the highest mortality (26.4 ± 6.09 %) while control larvae (aposymbiotic at 27 °C; AL) experienced minimal loss (8.83 ± 1.22%) (Figure 4.2). There was no significant temperature-colonization interaction on survival time (Weibull proportional hazard model, $p = 0.46$). Nevertheless, temperature (Weibull proportional hazard model, $p = 0.0028$) and colonization (Weibull proportional hazard model, $p = 0.040$) were significantly associated with survival time, and CH larvae displayed a rapid decline of survival probability with time (Figure 4.2). Notably, approximately 84% of the larvae survived more than 14 days irrespective of treatment. We predicted the probability of larvae in the different treatment groups to survive beyond 14 days using a GLMM with a binomial distribution. Survival beyond 14 days was also significantly affected by both temperature (binomial GLMM, $p = 8.0e\text{-}4$) and colonization (GLMM, $p = 0.025$), but not the interaction of these two treatments (binomial GLMM, p-value = 0.70). After controlling for the effects of colonization, elevated temperature decreased survival time by 0.097-fold (Weibull proportional hazard model, 95% CI 0.021 to 0.45) and the odds of

survival beyond 14 days at elevated temperature was estimated to be 40.1% lower than the odds under low temperature (binomial GLMM, 95% CI 24.3% to 69.0%).

Elevated temperature treatment reduces survival probability in larvae from two other Okinawan acroporids, *A. muricata* and *A. intermedia*, however only *A. intermedia* larvae showed a difference in survival time with symbiosis at elevated temperature (Baird, 2006, Yakovleva *et al.*, 2009). When comparing the survival probability of the three species at day three, symbiotic *A. digitifera* larvae exceeded both *A. muricata* (50%) and *A. intermedia* (60%) by roughly 20-30% (Figure 4.2). Therefore, co-occurring coral congeners can respond differently to the combination of elevated temperature and symbiosis and although *A. digitifera* larvae were negatively affected by the combination of these events, they might be less sensitive to SST elevations than other larval acroporids.

4.2.2 The combination of colonization and high temperature accelerates A. digitifera *development*

In addition to elevated temperature impacting larval survival and symbiont colonization, it can also affect host development. For example, studies have noted abnormal larval behavior (Randall *et al.*, 2009a), decreased settlement competence periods (Edmunds *et al.*, 2001, Nozawa *et al.*, 2007, Randall *et al.*, 2009b, Heyward *et al.*, 2010), and atypical floating polyps, i.e. individuals that had undergone metamorphosis without settlement onto a substrate (Putnam *et al.*, 2008), in response to elevated temperature. By day three of our experiment, we detected differential proportions of floating polyps in our samples for RNA extraction in our treatment conditions (Figure 4.3), which were was not present at day one. The percentages of floating polyps and planulae were calculated from 20 randomly selected individuals from each replicate (n=6) for the treatment group. The CH group had significantly more floating polyps (43.3 ± 1.96%) than the other three groups (Student T-test, p= 0.02). This result suggests that the presence of symbionts contributes to developmental cues that trigger metamorphosis. Similar results have been observed in symbiotic planulae of *Stylophora pistillata* and *Porites astreoides* (Edmunds *et al.*, 2001, Putnam *et al.*, 2008).

4.2.3 Gene expression in CH-treated larvae is not just the sum of colonization and high temperature effects, but instead reveals novel expression patterns

RNA samples were collected at day one (see grey bars in Figure 4.1) to capture early transcriptional differences between treatments prior to phenotypic differences in symbiont colonization success (Figure 4.1) and survival (Figure 4.2). The remaining RNA samples were collected on day three (see grey bars in Figure 4.1), based on the high percentage of metamorphosis observed (Figure 4.3) and differing larval phenotypes. We obtained paired-end 134 bp reads ranging from 8,725,968 to 71,485,978 in number for each sample from Illumina sequencing. On average, only 50% of the reads mapped to the *A. digitifera* v0.9 genome (Shinzato *et al.*, 2011) using TopHat v2.0.12 (Trapnell *et al.*, 2009) (Figure 4.4). Given that coral metamorphosis causes dramatic molecular, cellular and physiological reprogramming (Müller *et al.*, 2002, Grasso *et al.*, 2011, Hayward *et al.*, 2011), we explored the influence of metamorphosis on sample expression using a principle components analysis to ordinate the regularized log (rlog) transformed counts (Figure 4.5). Expression across the 23,526 gene models showed sample differences based on temperature and metamorphosis (Figure 4.5). Therefore, to account for the underlying variation of metamorphosis in our samples, we included it as a covariate in the statistical model. Altogether, we recovered 15,211 differentially-expressed genes (DEGs) using DESeq2 (Love *et al.*, 2014), 8,936 (58%) of which were significant with metamorphosis (Figure 4.4). Many of the DEGs important in metamorphosis also function in heat stress and symbiont colonization, however, because these patterns could not be separated, we excluded metamorphosis-linked DEGs from further analyses (Figure 4.4).

With the remaining DEGs, we identified 201 and 31 DEGs with the interaction of temperature and colonization at day one and three, respectively (Tables 4.2, 4.3 and 4.4). For these DEGs, the effects of colonization and temperature were not independent, but the effect of colonization, for example, on gene expression in *A. digitifera* larvae was dependent on the treatment temperature (low or high). From those, 149 DEGs from day one and 21 DEGs from day three had sequence similarity to genes in UniProt database (http://www.uniprot.org). To identify common biological processes and molecular functions among these DEGs, Gene Ontology (GO) terms assigned for each gene based

their match in the UniProt database were used in gene score (p-value) resampling GO-term enrichment method in ErmineJ (Lee *et al.*, 2005). The significant biological process GO-terms were unique to the interaction groups by day and not shared with the other treatment groups (Figure 4.6). At day one, genes were enriched for regulation of RNA metabolism (GO:0051254) and RNA transcription (GO:0045893), protein processing and localization (GO:0051220 and GO:0034934), actin organization (GO:0007015) and several genes with ankyrin repeat domains used as protein-protein interaction platforms in diverse cellular functions (part of compound eye photoreceptor cell differentiation, GO: 0001751). Day three genes were enriched for the synthesis and metabolism of amino acids. GO-terms categorized by molecular function were identified for all treatment groups except CH on day three (Figure 4.7). Oxidoreductase activity was common to all treatment groups and iron ion binding was shared by the CL and CH treatments. Groups that occurred in the CH treatment group included genes involved in actin crosslink formation (alpha-catenin binding, GO:0045294); Fc-gamma receptor I complex binding, GO: 0034988) and transcription factor binding (GO:0008134) were identified (Figure 4.7).

We performed an over-representation analysis (ORA) on DEGs with Kyoto Encyclopedia of Genes and Genomes (KEGG) annotations to predict cellular pathways involved in the AH, CL and CH treatments. On day one, the AH treatment had 19 over-represented KEGG pathways, 11 of which were shared with the CL treatment (Figure 4.8). By day three, just two pathways were shared between the CL- and AH-treated larvae, tight junction (ko04530) and viral carcinogenesis (ko05203), however, many of the same pathways in AH treatment at day one were still enriched at day three (Figure 4.8). One shared pathway in the AH-treated larvae between days that is interesting to note is cell cycle (ko04110) (Table 4.5). The overall expression patterns of DEGs associated with this pathway suggest that the AH-treated larvae were under cell cycle arrest on both days. For example, cyclin D2 (aug_v2a.16767), a regulatory component of the cell-cycle G1/S transition, was downregulated by 0.71-fold on day one and serine-protein kinase ataxia telangiectasia mutated (ATM; aug_v2a.14100), which acts as a DNA damage sensor, was upregulated by 1.04-fold on day three.

In the CH treatment, there were 86 and 12 KEGG-annotated DEGs on days one and three, respectively. The ORA recovered two pathways over-represented in the CH treatment on day one, RNA transport (ko03013) that was shared with the CL and AH treatments, and mRNA surveillance (ko03015) that was shared just with the AH treatment (Figure 4.8 and Table 4.5). Within these pathways, three common DEGs included a serine/arginine repetitive matrix protein (aug_v2a. 03929), RNA-binding protein with serine-rich domain (aug_v2a.16164), and polyadenylate-binding protein (aug_v2a.20361). These genes all function in messenger RNA processing and were upregulated in the CH-treated larvae. On day three, two DEGs were found in the one carbon pool by folate pathway (ko00670) (Figure 4.8 and Table 4.5). These included a 0.60-fold upregulation of 10-formyltetrahydrofolate dehydrogenase (aug_v2a.21013) and a 0.63-fold downregulation of methionine synthase (aug_v2a.11353), both of which are involved in the folate-dependent remethylation of the amino acid intermediate homocysteine to methionine (Anguera *et al.*, 2006, Blom *et al.*, 2011). These expression patterns suggest an accumulation of homocysteine over methionine, which has been linked to various diseases (Blom *et al.*, 2011), and more available methyl groups for DNA methylation that regulates gene expression (Anguera *et al.*, 2006).

In addition to the analyses performed above, we also highlighted some DEGs whose annotations suggest roles in symbiosis and stress. We illustrate how the effect of temperature on gene expression depends on colonization status in Figures 4.9 and 4.10 for samples collected on days one and three respectively. The CH-treatment resulted in dramatic expression shifts compared to the aposymbiotic larvae at 32 °C (AH) and the CL treatment.

For samples on day one, first, two pattern recognition receptor (PRRs) immunity genes, a transmembrane toll-like receptor (TLR) (Adi-IL1R-7, (Hamada *et al.*, 2012)) and an intracellular nucleotide-binding oligomerization domain-containing proteins (NOD)-like receptor (aug_v2a.08386)), that function to detect microbe-associated molecular patterns (MAMPs) and damage-associated molecular patterns (DAMPs) (Akira *et al.*, 2004, Hamada *et al.*, 2012) were examined in detail. Both were upregulated in AH, CL, and CH treatment groups (Figure 4.9A and B). In contrast, AL animals displayed low

expression. The expression of AH animals exceeded levels in colonized animals (Figure 4.9A and B), thus the combination of temperature and colonization reduced the effects of elevated temperature on the larvae (Table 4.3). These expression patterns suggest that an immune response is activated by temperature and colonization at day one, however, the CH combination did not magnify the response as we predicted. The upregulation of these PRRs in heat-stressed *A. digitifera* larvae could be associated with increased levels of DAMPs. Unlike previous expression studies of onset of symbiosis that found little to-no expression of these PRRs in CL-treated larvae (Voolstra *et al.*, 2009b, Schnitzler *et al.*, 2010), we found increased expression in colonized larvae from both temperature treatments. *A. digitifera* has extensive lineage-specific genomic expansion of novel genes with NOD (Hamada *et al.*, 2012) and TLR domains (Poole *et al.*, 2014) that are hypothesized to function in the initial stages of symbiosis establishment. Future functional studies on these two PRRs will help reveal their role in symbiont colonization and the heat stress response of the larvae.

Actin microfilaments play important roles in diverse cellular processes and their rearrangement is critical to phagocytosis of foreign objects (Flannagan *et al.*, 2012). Actin organization and crosslink formation identified from GO-enrichment were significant on day one (Figure 4.6). The expression of three filamin-A genes, actin-binding proteins that regulate actin cytoskeleton reorganization and cell signaling (Feng *et al.*, 2004), were significantly differentially expressed in the CH samples (Table 4. 3). The expression of the three filamin-A transcripts (exemplified by aug_v2a.03233) remained constant with CL and CH treatments, but was downregulated in the AH samples (Figure 4.9C). This could be linked to cell cycle arrest (Meng *et al.*, 2004) and is consistent with the over-represented KEGG cell cycle pathway in AH, but not CL or CH treatments (Figure 4.8).

Oxidative stress is an important indicator of heat stress and symbiosis dysfunction in corals (Lesser, 1996, Nii *et al.*, 1997, Richier *et al.*, 2006, Yakovleva *et al.*, 2009). Expression of an antioxidant gene, peroxidasin, differed with the colonization-by-temperature interaction at day one (Figure 4.9D). In this study, peroxidasin expression was downregulated in AH- and CL-treated samples compared to the AL animals,

however, expression of CH-treated larvae did not change (Figure 4.9D). Peroxidasin is a multifunctional gene with a role in apoptotic cell removal, extracellular matrix stabilization and oxidative stress reduction (Nelson *et al.*, 1994). In corals, studies have demonstrated that peroxidasin expression is upregulated with elevated temperature in juveniles (Voolstra *et al.*, 2009b, Polato *et al.*, 2010) and with white band disease in adults (Libro *et al.*, 2013). By day three, the expression of peroxidasin in AH animals was upregulated by 0.82-fold (Table 4.4) suggesting an increase in oxidative stress with time at elevated temperatures.

On day three, a tumor necrosis factor (TNF) receptor associated factor (TRAF6 homolog, aug_v2a. 06710), a NOD-like receptor (NLRC3, aug_v2a. 00365), a C-type lectin (aug_v2a.20323), the transcription factor AP-1 (aug_v2a.03150), a CUB and sushi domain (CUBSD) containing protein (aug_v2a.16069), and galatosylceramide sulfotransferase (aug_v2a.19379) were significant with the colonization-by-temperature interaction (Table 4.4 and Figure 4.10). TRAFs are intracellular secondary messengers that relay signals from extracellular TLRs after they bind to MAMPs or cytokines (Akira *et al.*, 2004). Specifically, TRAF6 can activate transcription factor AP-1 through mitogen-activated protein kinases (MAPK) signaling, causing increased pro-inflammatory cytokine production, cell differentiation and apoptosis (Akira *et al.*, 2004). In CH animals, the expression of TRAF remained low while the NLRC3 expression in CH animals returned to control levels, however, both were higher than expression in the AH animals (Figure 4.10A and B). TRAF homologs from adult coral *Orbicella faveolata* were suppressed in bleached colonies during and up to a year after a natural bleaching event (Pinzón *et al.*, 2015), suggesting that the immune suppression can persist even when the thermal stress is removed. In contrast, AP-1 had the opposite response and was higher in AH than in CH animals (Figure 4.10C), indicating that its upregulation was likely not mediated by TRAF but by some other intracellular pathway. The downregulation of immune genes with heat stress indicates that the immune response from day one had diminished by day three, and elevated AP-1 expression in both colonization and temperature suggests increased transcriptional activity.

Both C-type lectins and CUBSD proteins are involved in microbe recognition. C-type lectins are PRRs that bind glycans on the surface of microbes. Coral-isolated lectins have been shown to bind both pathogens and symbionts (Kvennefors *et al.*, 2010). C-type lectin was significantly downregulated and upregulated in CL and CH animals respectively (Figure 4.10D). During a natural bleaching event, adult coral *Acropora millepora* also had higher expression of C-type lectin (Seneca *et al.*, 2010), but aposymbiotic larvae display decreased levels compared to their symbiotic counterparts (Rodriguez-Lanetty *et al.*, 2009). This suggests that the presence of symbionts alters C-type lectin expression during thermal stress and could contribute to recognition and removal of symbionts. The CUBSD protein is involved in the activation of the complement system, an innate immune pathway that enhances clearance of foreign microbes (Palmer *et al.*, 2012). The complement system is functionally linked to lectin receptors as part of the lectin pathway (Palmer *et al.*, 2012) and has been shown to play a role in the onset of symbiosis in the sea anemone *Aiptasia pallida* (Poole *et al.*, submitted). The expression of CUBSD was lower in CH compared to CL animals (Figure 4.10E). This is in suprising contrast to the opposite regulation of C-type lectin (Figure 4.10D), a contrast that warrants further functional investigation in the future.

In addition to the immune response discussed above, *A. digitifera* larvae also had differences in sphingolipid metabolism on day three depending on colonization status and incubation temperature. Sphingolipids are important cell signalers that underlie the heat stress response in all eukaryotes (Jenkins, 2003) and their functional role in cnidarian heat stress response has been explored elsewhere in this thesis (see Chapter 3). We found that galatosylceramide sulfotransferase (aug_v2a.19379), an enzyme involved in complex sphingolipid synthesis, was downregulated in CH compared to CL animals (Figure 4.10F). Galactosylceramides sulfotransferase produce sulfatides that interact with the extracellular environment and function in protein trafficking, cell adhesion, and pathogen recognition (Bowman *et al.*, 1999). Increases in sulfatides can trigger the pathways that enhance transcriptional factor AP-1 binding and a pro-inflammatory response (Jeon *et al.*, 2008). The expression patterns of galactosylceramide sulfotransferase mirrored those of transcription factor AP-1 (Figure 4.10C). By reducing sulfatides under elevated

temperature with symbionts, the pro-death ceramide begins to accumulate unless it is converted to the pro-survival lipid sphingosine-1-phosphate by sphingosine kinase. There was no upregulation of sphingosine kinase at day three in the CH animals (data not shown). Altogether, the expression of immune-related genes across time points suggests that the interaction of hyperthermal stress and onset of symbiosis did not initiate an immune response or apoptosis by day three, but that host recognition of the symbiont might be enhanced.

4.2.4 Co-expression networks identify genes associated with colonization, temperature and the combination of the two treatments

Finally, to explore the expression patterns of the unannotated interaction genes, we constructed co-expression networks with Weighted Gene Co-Expression Network Analysis (WGCNA) (Langfelder *et al.*, 2008a). Information can be gained from studying co-expressed genes that are controlled by the same transcriptional regulatory program, functionally related, or members of the same pathway or protein complex (Carter *et al.*, 2004, Luo *et al.*, 2007). This analysis integrates and quantifies genome-scale interactions into modules of highly interconnected genes that are then correlated with sample phenotypes or experimental treatments (Langfelder *et al.*, 2008a). We identified 26 modules of genes with similar expression patterns (Figure 4.11). Correlation of the modules with experimental conditions identified six modules that were highly associated with elevated temperature and two modules that were moderately associated with colonization (Figure 4.11). The direction of the correlation indicates the module eigengene, or summarized expression, for that given trait. For example, expression of the genes in the M10 module was downregulated with elevated temperature (biweight midcorrelation (bicor) = -0.88, $p < 0.001$). A functional enrichment analysis was performed through DAVID Bioinformatic Database (hhtp://david.ncifcrf.gov) on significant modules with temperature and colonization (Table 4.6).

We selected three modules, M10, M13 and M21, to investigate further based on their correlation with the experimental conditions. The M21 module was positively correlated with temperature across samples (bicor = 0.84, $p < 0.001$, Figure 4.12) but showed no correlation with colonization. Thirty interaction genes were identified in this

module, seven of which lacked annotation. This module was enriched for TRAFs, calcium signaling and ankyrin repeats (Table 4.6) and the genes with the highest intramodular connectivity, or the hub genes, in the network were involved in redox activity, apoptosis, and response to stress (Figure 4.13). In contrast, module M10 was negatively correlated with temperature as mentioned earlier, and had only one interaction gene that also happened to be unannotated. The enrichment analysis recovered an abundance of genes associated with ion channel activity (Table 4.6 and Figure 4.13). The expression of the M10 module suggests that ion transport may be limited in the CH-treated animals (Figure 4.13). The M13 module had 28 interaction genes (seven without annotation) and was equally correlated with colonization and time (bicor= 0.47. $p< 0.001$, Figure 4.11). The M13 eigengene expression indicates that genes in the colonized samples were significantly upregulated at day one regardless of temperature treatment (Figure 4.12, Student's T-test). However, this relationship was not present at day three, suggesting that expression patterns on day one might be part of symbiont recognition. The functional enrichment of genes in this module was associated with endocytosis, cytoskeleton and ATP-binding (Table 4.6) and more hub genes with transcriptional or translational functions than the other two modules (Figure 4.13). By using this technique we were able to identify genes that were responsive to heat stress, onset of symbiosis, and in some cases both. This analysis also identifies unannotated genes that could be candidates for further functional study, such as yeast two-hybrid analyses to explore their role in symbiosis and stress response.

4.3 Conclusion

Our data show that *A. digitifera* larvae had low survivorship and failed to acquire and establish successful partnership with *S. tridacnidorum* when the partnership was initiated under elevated temperature conditions. CH treatment also caused premature metamorphosis. These results suggest that corals face severe challenges in recruitment, survivorship and therefore fitness in an era of climate change. The expression of molecular machinery used in metamorphosis strongly overlapped with both colonization and heat stress transcriptional responses, therefore reducing our ability to interpret the complete global expression patterns. However, the transcriptomic snapshots before and

after observable onset of symbiosis and hyperthermal stress revealed differences in transcriptional and translational processing, oxidoreductase activity, actin binding, immune modulation, and lipid metabolism. These findings expand our understanding of larval response to hyperthermal stress during the onset and establishment of symbiosis.

4.4 Methods

4.4.1. Collection and maintenance of coral larvae

Six coral colonies of *A. digitifera* were collected off Sesoko Island, Okinawa Prefecture, Japan (26 °39.1'N, 127°51.3'E) during the 2014 spawning season and placed into ambient temperature (26 °C) seawater tanks. After spawning, buoyant egg and sperm bundles were collected, pooled and mixed for 30 min by gentle agitation for fertilization. Fertilized embryos were washed twice with 0.22 μm filtered seawater (FSW) to remove any remaining sperm. Early developmental stages were maintained in ambient temperature FSW with an additional antibiotic mixture (0.12 mg ampicillin, 0.036 mg kanamycin, 0.007 mg streptomycin) (FSWA) and constant gentle agitation for six days. Larval health and development were monitored microscopically.

4.4.2 Symbiodinium *culture conditions*

To ensure successful onset of symbiosis at early time points, we inoculated larvae with *Symbiodinium tridacnidorum* sp. nov. (CCMP2465, type A3; recently named by (Lee *et al.*, 2015)) that are acquired more readily in early-life stages of *A. digitifera* than other symbiont clades (Suwa *et al.*, 2010, Yuyama *et al.*, 2012). Cultures of monoclonal *S. tridacnidorum* sp. nov. were grown in f/2 media at 25 °C under a 12h light: 12h dark cycle. The cultures were concentrated by centrifugation at 1,800 x g for 10 min and quantified with hemocytometer counts at the start of the experiment.

4.4.3 Experimental design

One day prior to starting the experiment (five days post-fertilization), larvae were moved to their respective treatment groups as indicated in Table 4.1 and placed in a multi-thermo Eyela MTI-201 incubator (Tokyo Rikakikai Co., Japan) at control temperature (26.69 ± 0.009 °C) and light intensity of 128.96 ± 2.34 lumens/ft^2. Larvae

were placed in 50 ml tubes (TPP, Switzerland) at a concentration of 6 larvae ml^{-1} FSW with 300, 300 and 50 larvae per replicate tube (n=6) for RNA extraction, symbiont density quantification and survivorship quantification, respectively. Aposymbiotic larvae at low temperature (AL) represented the steady-state transcriptional/behavioral state and was used as the baseline for comparison of the other treatment groups. Colonized larvae at low temperature (CL) and aposymbiotic larvae at high temperature (AH) were the positive controls for symbiotic state and elevated temperature, respectively. Finally, colonized larvae at high temperature (CH) tested the effects of the colonization-by-temperature interaction.

At six days post-fertilization, larvae, concentrated *S. tridacnidorum* and homogenized *Artemia* were pre-incubated for one hour in either control or elevated (31.98 ± 0.027 °C) temperature in the Eyela MTI-201 incubator (Schnitzler *et al.*, 2011, Yuyama *et al.,* 2012). The elevated temperature was selected from a pilot study in 2013 where a range of temperatures was tested on *A. digitifera* larval survival and only 32 °C, the highest temperature, caused a gradual decline in larvae survival (data not shown). The start of the experiment was chosen based on larval developmental programs. *A. digitifera* six days post-fertilization have fully formed mouths, allowing symbionts to be taken up during feeding (Harii *et al.,* 2009). Homogenized *Artemia* was prepared as described by (Schwarz *et al.,* 1999) and is a known feeding stimulant in *A. digitifera* larvae (Harii *et al.*, 2009). Following the pre-incubation period, *S. tridacnidorum* were added at a final concentration of 9 x 10^4 cells ml^{-1} to CL and CH larvae and homogenized *Artemia* at a 1:100 volume to all treatment groups (Table 4.1). All groups were washed daily with FSWA and incubated at their respective treatment temperatures. Throughout the experiment, temperature and light intensity of each chamber in the incubator was captured by HOBO Pendant data loggers (Onset Computer Co., MA, USA) submerged in water (Figure 4.14).

4.4.4 Monitoring survivorship

Survival time was calculated with visual counts of subsets of 50 larvae (n=6) between 12 h and 14 days. Metamorphosis (floating or settled polyps) when present was

noted. Coral larvae quickly dissolve after death, so any visible larvae were considered alive at each time interval (Richmond, 1990, Schnitzler *et al.*, 2011). The larvae that metamorphosed as well as larvae that remained alive at the end of the observation period were excluded from the statistical analysis. Preliminary analyses showed that, within treatment groups, survival time varied significantly across tubes. Therefore, tube variability (or replicate effect) was accounted for in the statistical analyses. To determine the survival probability of larvae under the different treatment conditions, we used a stratified Weibull proportional hazard model in the statistical R package survival (Therneau, 2013) to analyze the survival status data, where between-tube variability was accounted for by stratification. For this analysis, data collected from larvae were pooled across the replicates for each treatment group. In addition, we used a generalized mixed effects model (GLMM) to predict the success or failure of larvae from the different treatment groups to survive beyond the14 days of observation.

4.4.5 Quantification of colonization success and algal density

Symbiont colonization success was determined at multiple time points (3, 6, 12 h and 1, 2, 3, 7, and 14 days) from a subset of 20 larvae in CL and CH treatments (n=120 larvae total at each time point and treatment). The larvae were concentrated on a 40 µm filter, washed twice with 1x PBS and either processed immediately or fixed in 4% formalin in FSW and stored at 4 °C. Samples were processed by placing 3-4 larvae on a microscope slide and gently pressing down on them by removing excess fluid under the coverslip. Fluorescence from green fluorescent protein (GFP) of the larvae and chlorophyll autofluorescence of the symbionts was captured by Leica DFC310 FX camera (Leica, IL, USA) using a fluorescent Leica M205 FA stereo-microscope (Leica, IL, USA) with a GFP long pass emission filter. Larvae were scored for the presence or absence of symbionts and analyzed using a GLMM fitted to a binomial distribution with two factors, temperature and time, and a random effect of replicate tube (n=12) to account for repeated measures.

To determine the mean algal density at each time point, the number of symbionts in 20 randomly sampled colonized larva were quantified from images with the cell

counter plugin in ImageJ v1.47 software (Rasband, 1997-2015). The symbiont counts were analyzed with a GLMM using the same factors and random effect as colonization success but fit to a quasi-poisson distribution to account for overdispersion of the data.

4.4.6 RNASeq library preparation and sequencing

At one and three days post-inoculation, approximately 300 treated larvae from each replicate tube (n=6) under the four treatment conditions (Table 4.1) were concentrated on a 40 µm filter, frozen in liquid nitrogen and stored at -80°C. By day three, some samples metamorphosed, changing from swimming larvae (planula) to non-settled, floating polyps. The level of metamorphosis was assessed by removing a subset of 20 individuals from each replicate tube prior to concentrating and freezing. The individuals were scored visually for their developmental stage (polyp-like or planula) and compared with a Student's T-test.

Total RNA was extracted from frozen samples by tissue homogenization in TRIzol (Invitrogen, CA, USA) with the Polytron P1200 homogenizer (Kinematica, NY, USA), followed by the RNeasy extraction kit (Qiagen, CA, USA) (see Chapter 2, pg. 35) and purified with DNase I (Qiagen, CA, USA) treatment. RNA integrity was assessed using the Agilent 2100 Bioanalyzer (Agilent Technologies, CA, USA) and concentration quantified with the NanoDrop 1000 spectrophotometer (NanoDrop Products, DE, USA). Paired-end sequencing libraries were prepared with 2 µg of total RNA using the TruSeq RNA kit v2 (Illumina, CA, USA) following the manufacturer's protocol. Library quality was verified with the Aligent 2100 Bioanalyzer (Agilent Technologies, CA, USA) and quantity was calculated with the KAPA qPCR library quantification kit (KAPA Biosystems, MA, USA). Libraries were pooled and sequenced on the Illumina Genome Analyzer IIx (Illumina, CA, USA) by the Sequencing Section at Okinawa Institute for Science and Technology.

4.4.7 Gene expression, clustering and network analyses

Short 134 bp paired-end reads were checked for quality with FastQC v0.11.1 (Andrews, 2010)and adaptor contamination removed with cutadapt v1.6 (Martin, 2011). The high-quality sequences were then mapped against the annotated *A. digitifera* genome

(adi_v0.9.scaffold)(Shinzato *et al.*, 2011) using Bowtie v2.2.3.0 (Langmead *et al.*, 2012) and TopHat v2.0.12 (Trapnell *et al.*, 2009) (Figure 4.4). Read counts for each sample were exported using bedtools (Quinlan *et al.*, 2010) and differentially expressed genes (DEGs) were calculated with Wald tests using statistical R package DESeq2 (Love *et al.*, 2014) fitting the model: DEGs ~ β1 Temperature + β2 Colonization + β3 Time + β4 Metamorphosis + β5 Temperature * Colonization + β6 Temperature * Time + β7 Colonization * Time. Significant DEGs had Benjamini-Hochberg adjusted p-values ≤ 0.05 (Benjamini *et al.*, 1995). Fold changes were filtered by $\log_2$ values ≥ 0.6 or ≤ -0.6. Additional contrasts from the model were constructed to extract DEGs from CL and AH treatment groups on the separate days. For example within the AH group, we tested the difference of counts between AH and AL animals at day one (Table 4.2). Moreover, the model was tested twice to identify all the genes associated with developmental processes of metamorphosis, a side effect of the treatment conditions. First, metamorphosis for each sample was treated as a factor (yes or no), and second as a continuous covariate based on the proportion of floating polyps in each sample (Figure 4.3). All significant DEGs with metamorphosis from both models were discarded from subsequent analyses (Figure 4.4). To illustrate significant DEGs with temperature*colonization interaction, regularized log (rlog) transformation of the counts, which is normalized by library size, was used to calculate fold-changes for each treatment group.

To identify functionally-relevant gene sets from the remaining DEGs by treatment group, GO and KEGG annotations were analyzed using gene enrichment and over-representation tools, respectively. The GO-term enrichment was performed using gene score resampling (GSR) of negative-log-transformed p-values with 100,000 iterations in ErmineJ v3.0.2 (Lee *et al.*, 2005). Gene sets were limited to 3-150 genes, and when replicate transcripts were present, the best scoring replicate was included. The significance threshold for a gene set was determined by multiple test correction Benjamini-Hochberg false discovery rate < 0.1(Benjamini *et al.*, 1995). The over-representation of KEGG pathways in AH, CL and CH animals separated by day were tested using R package clusterProfiler v3.2 (Yu *et al.*, 2012) with a hypergeometric

distribution and p-values were adjusted for multiple comparisons using a Benjamini-Hochberg correction.

Lastly, DEGs were clustered by shared expression patterns using signed WGCNA v1.46 R package (Langfelder *et al.*, 2008a). A bicor matrix of variance stabilized transformed counts from DESeq2 (Love *et al.*, 2014) was transformed with a power function of 16 to generate a matrix of network connection strengths. Modules were assigned through unsupervised hierarchical clustering and refined with dynamic tree cutting of the dendrogram with a limit of 15 genes to a module (Langfelder *et al.*, 2008a, Langfelder *et al.*, 2008b). Module eigengenes, or the summarized gene expression profiles of the modules from principle component analysis, were correlated with sample traits (temperature, colonization, and time) using bicor and strength determined by corresponding Student asymptotic p-values. Gene significance (GS, correlation of expression of a gene to trait) and module membership (MM, correlation of expression from a gene to the module eigengene) were calculated for each gene. MM is similar to intramodular connectivity measurements used to find highly interconnected “hub” genes (Langfelder *et al.*, 2008a). To identify biological patterns in each module associated with a trait, we performed DAVID functional enrichment analyses using the gene symbols of annotated genes in each module, with a multiple test correction using the Benjamini-Hochberg algorithm (Benjamini *et al.*, 1995, Huang *et al.*, 2007). The top 50 genes from select networks with the highest MM were visualized using Cytoscape v3.3.0 software with an edge-weighted spring embedded network layout (Shannon *et al.*, 2003).

Table 4.1 Factorial treatment groups of elevated temperature and inoculation of symbionts at day six post-fertilization.

Treatment Group	AL	CL	AH	CH
Elevated Temperature (32 °C)	–	–	+	+
Symbionts	–	+	–	+

Figure 4.1 Symbiont colonization and density in *A. digitifera* larvae was decreased by elevated temperature. Larvae from 32 °C (orange) and 27 °C (black) treatment groups were inoculated with $9x10^4$ *S. tridacnidorum* at time 0. Samples were washed at 24 h (arrows) and collected at several time points (n=20 from each replicate tube). Chlorophyll autofluorescence of the symbionts (A) was used to quantify symbiont colonization (B) and density (C). The green fluorescent protein of the larvae and symbiont autofluorescence were both detected with a GFP long pass emission filter. The representative images in A are from 14 days post-inoculation in the different temperature treatments. (C) From the colonized larvae in B, 20 were randomly selected to quantify symbiont numbers using cell counter in ImageJ (Rasband, 1997-2015). Generalized mixed effects models with two factors (temperature and time) and random effect of replicate tube were fit with a binomial and quasi-poisson distribution for the colonization success and algal density data, respectively. The average of colonization success and density were calculated from 6 replicates and error bars represent the standard error. The asterisks denote statistical significance ($p \leq 0.05$). The shaded bars at day one and three indicate the sample collection days for RNASeq analysis.

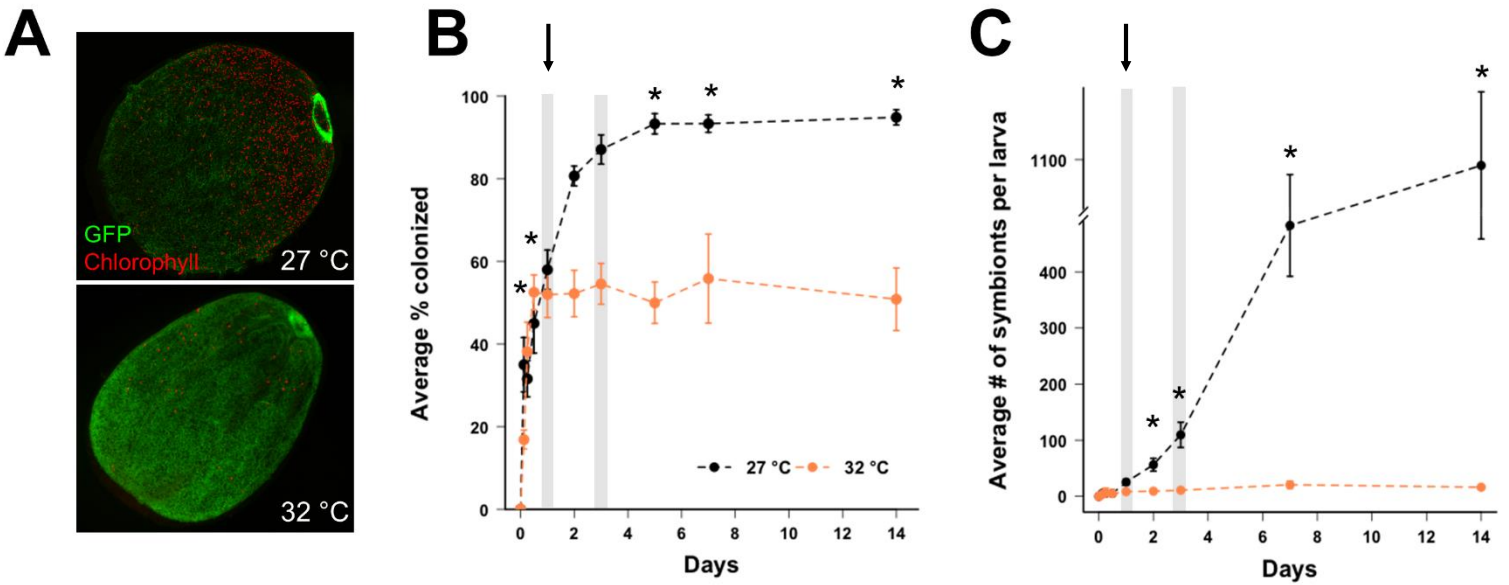
A
GFP
Chlorophyll
27 °C
32 °C
B
Average % colonized
Days
27 °C
32 °C
C
Average # of symbionts per larva
Days

Figure 4.1

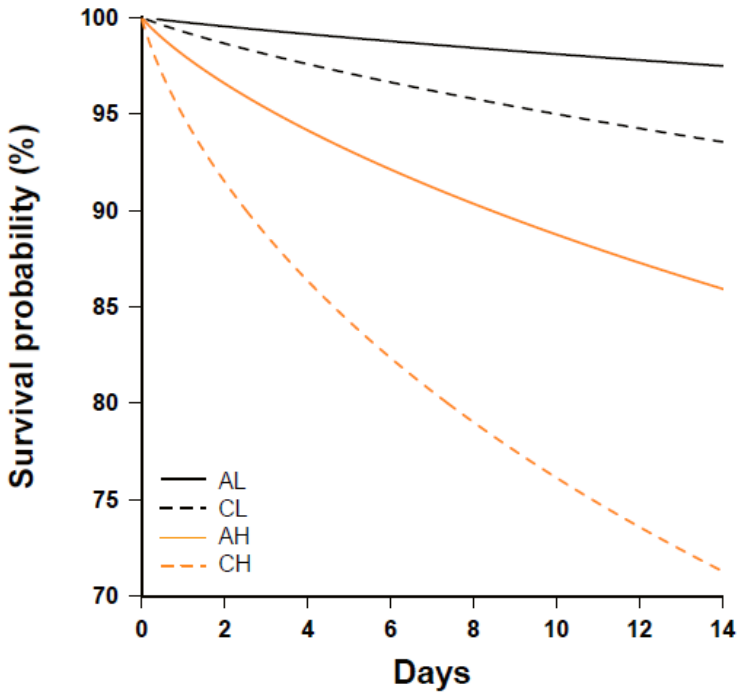

Figure 4.2 Estimated survival probability of *A. digitifera* larvae from different treatments over time. The fitted survival probabilities under the Weibull proportional hazard model for each treatment group (n=300 larvae), averaged across replicate tubes (n= 24 tubes). Survival probabilities declined rapidly with both temperature and symbiosis, but there was no interaction of these treatments. Solid line = aposymbiotic, dashed line = colonized, black = 27 °C, orange = 32 °C.

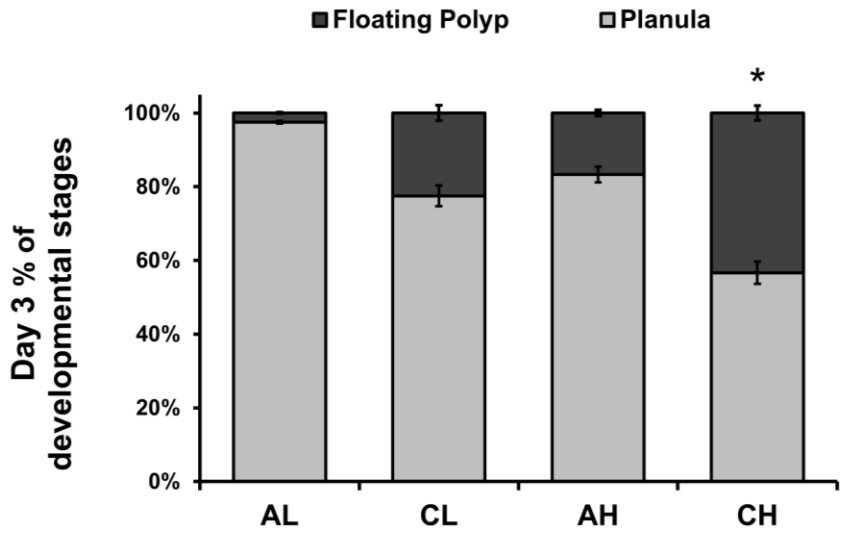

Figure 4.3 Percentage of metamorphosed floating polyps at day three in *A. digitifera* individuals used for RNASeq. Twenty individuals were randomly collected from each replicate tube (n=6 per group) and categorized into floating polyps (dark grey) or planula (light grey). The mean percentages for each group were compared to AL treatment group using a two-tailed Student's T-test. The bars represent standard error and the asterisk indicates significance, $p \leq 0.05$.

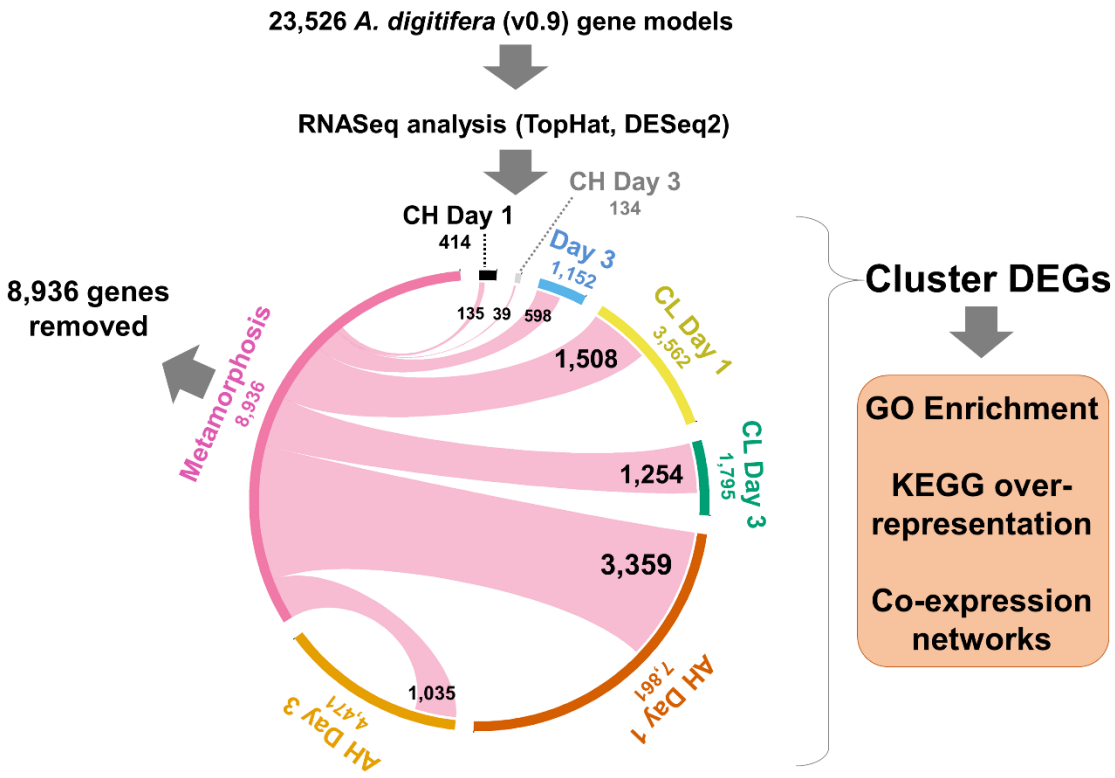

Figure 4.4 RNASeq analysis pipeline. Short reads were mapped to the *A. digitifera* v0.9 genome with 23,526 predicted gene models using TopHat (Trapnell *et al.*, 2009). The reads were summarized into counts by gene and tested for differential expression using DESeq2 (Love *et al.*, 2014). DEGs were identified for the time (day 3 compared to day 1), AH, CL, CH and metamorphosis. The colored segments outside the circle are the total number of DEGs for each category. The inner pink segments show the number of differential genes shared with metamorphosis. All 8,936 metamorphosis DEGs were removed from subsequent analyses. The remaining DEGs were analyzed using GO-term enrichment, KEGG over-representation and co-expression network tools.

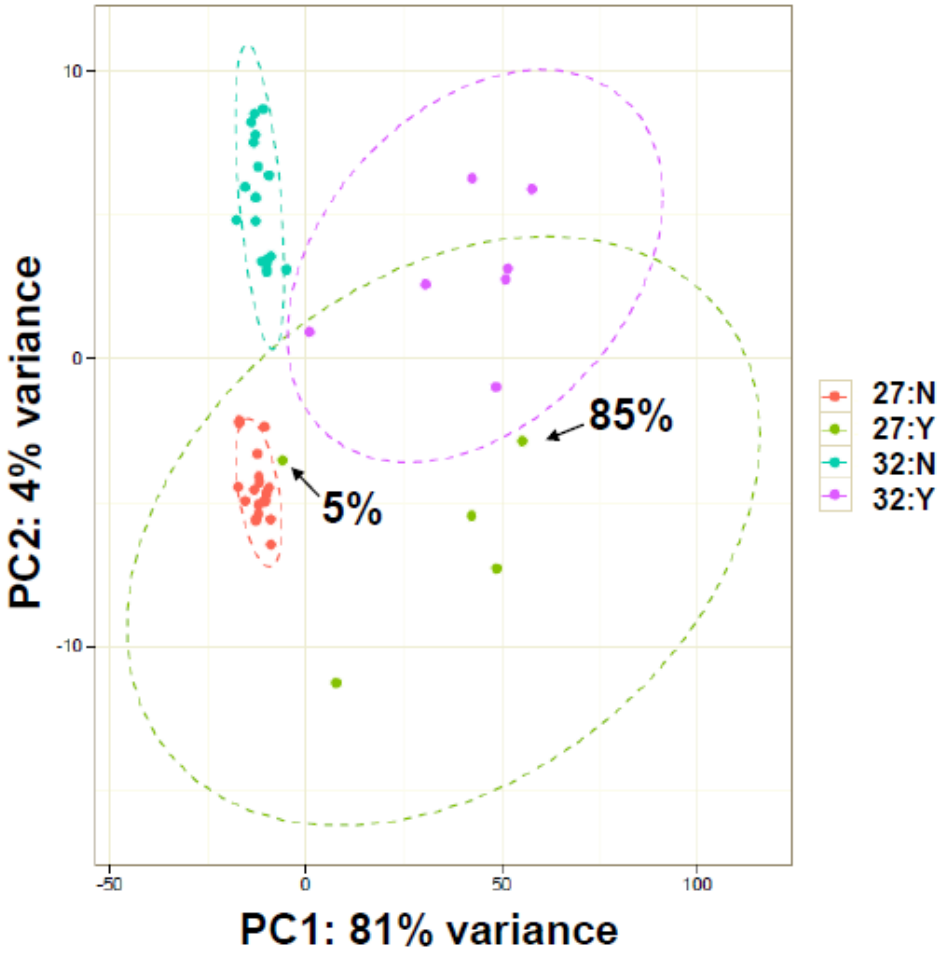

Figure 4.5 Principle component analysis of rlog transformed counts for each *A. digitifera* larval sample. Larval samples that did not undergo metamorphosis (N) formed tight groups with their respective temperature treatments (red = 27 °C, blue = 32 °C). The samples that had some level of metamorphosis (Y) ranging from 5 to 85% did not fall within the non-metamorphosed groups, but were also separated by temperature (green = 27 °C, purple = 32 °C). The greater the proportion of metamorphosis in a sample, the further the sample was from the planula group indicating unique transcriptional responses in these samples.

Table 4.2 Number of DEGs that were significant for each factor of the model, after excluding those shared with metamorphosis (Met.) and interaction terms. DEGs with expression (log_2) < 0.6 and > -0.6 were counted as stable expression.

Day	DEGs	AH* Time	CL* Time	CH	Met.	Time	AH	CL
1	**Total**	**634**	**138**	**279**	**8936**	**455**	**3848**	**1980**
	Up (> 0.6)	360	63	113	1835	69	1156	416
	Stable	178	37	78	6456	330	1943	1317
	Down (<0.6)	96	38	88	645	56	749	247
3	**Total**			**39**			**2064**	**468**
	Up (> 0.6)			16			594	191
	Stable			8			1154	165
	Down (<0.6)			15			316	112

AH = elevated *vs.* control temperatures in aposymbiotic larvae
CL = colonized *vs.* aposymbiotic larvae at control temperature
Time= day 1 *vs.* day 3 in aposymbiotic larvae at control temperature

Table 4.3 DEGs recovered on day one from the CH treatment group. The list was filtered by log_2 fold changes, including those that were ≥ 0.6 or ≤ -0.6.

Gene ID	UniProt Hit Description	Fold Change (log_2)	Adjusted p-value
aug_v2a.18327	Kinesin-like protein KIF13A	-1.649	1.31E-02
aug_v2a.06915		-1.585	7.17E-03
aug_v2a.15561		-1.453	1.19E-02
aug_v2a.15139		-1.441	2.95E-03
aug_v2a.08386	Nucleotide-binding oligomerization domain-containing protein 2	-1.234	1.19E-02
aug_v2a.03972	Ankyrin-1	-1.201	3.60E-02
aug_v2a.07006	Dynein intermediate chain 1, axonemal	-1.096	2.71E-02
aug_v2a.17788	PHD finger protein rhinoceros	-1.075	4.80E-02
aug_v2a.24541		-1.072	9.32E-03
aug_v2a.05987	Kinesin-like protein KIF13A	-1.068	2.71E-02
aug_v2a.00862	Endothelin-converting enzyme 1	-1.013	3.75E-02
aug_v2a.14857		-1.010	4.25E-02
aug_v2a.18192		-0.980	1.54E-02
aug_v2a.07529	Amiloride-sensitive sodium channel subunit alpha	-0.970	1.84E-02
aug_v2a.15768	Leucine-rich repeat-containing protein 48	-0.959	3.32E-02
aug_v2a.11296	UPF0704 protein C6orf165 homolog	-0.955	1.81E-02
aug_v2a.17051	FERM domain-containing protein 8	-0.952	1.19E-02
aug_v2a.24084	Tetratricopeptide repeat protein 24	-0.941	4.80E-02
aug_v2a.07231	GTP-binding protein RHO4	-0.936	1.81E-02
aug_v2a.23749		-0.935	2.93E-02
aug_v2a.06543	Eukaryotic translation initiation factor 5	-0.912	3.93E-02
aug_v2a.19366	DnaJ homolog subfamily C member 3	-0.911	2.75E-02
aug_v2a.04485	Zinc finger protein 474	-0.897	4.98E-02
aug_v2a.09356	Kinesin-like protein KIF17	-0.894	4.16E-02
aug_v2a.00874		-0.892	2.83E-02
aug_v2a.07772	Protein pelota homolog	-0.891	1.42E-02
aug_v2a.20154	Allene oxide synthase, chloroplastic	-0.885	9.99E-03
aug_v2a.03931	Intraflagellar transport protein 88 homolog	-0.885	6.26E-03
aug_v2a.06778	Coiled-coil domain-containing protein 103	-0.863	4.16E-02
aug_v2a.12080	Cyclic AMP-responsive element-binding protein 3-like protein 1	-0.861	5.66E-03
aug_v2a.08642		-0.855	4.72E-02
aug_v2a.05840		-0.846	3.49E-02
aug_v2a.12093	Potassium channel subfamily K member 3	-0.844	2.36E-02
aug_v2a.23726	Sorting nexin-27	-0.806	1.84E-02

Table 4.3 (Continued)

Gene ID	UniProt Hit Description	Fold Change (log_2)	Adjusted p-value
aug_v2a.23699	Uncharacterized protein C20orf152 homolog	-0.804	4.58E-02
aug_v2a.06524	Transmembrane prolyl 4-hydroxylase	-0.803	1.27E-03
aug_v2a.19049	Thioredoxin reductase 1, cytoplasmic	-0.801	2.49E-02
aug_v2a.11521	Synaptotagmin-7	-0.797	4.64E-02
aug_v2a.10664		-0.795	4.15E-02
aug_v2a.08205		-0.793	2.79E-02
aug_v2a.02353	Radial spoke head protein 3 homolog B	-0.793	8.04E-03
aug_v2a.16889	Eukaryotic peptide chain release factor GTP-binding subunit ERF3A	-0.789	2.16E-02
aug_v2a.10451	Toll-like receptor 1	-0.784	8.86E-03
aug_v2a.13466		-0.778	2.75E-02
aug_v2a.11913	Leucine-rich repeat-containing protein 34	-0.777	4.80E-02
aug_v2a.14559	Epidermal growth factor-like protein 6	-0.773	2.68E-02
aug_v2a.14456	Coiled-coil domain-containing protein 89	-0.772	1.19E-02
aug_v2a.13837	IQ domain-containing protein G	-0.771	1.19E-02
aug_v2a.13589	IQ domain-containing protein G	-0.764	2.78E-02
aug_v2a.23917	FERM domain-containing protein 8	-0.763	3.64E-02
aug_v2a.14164	Regulator of nonsense transcripts 3A	-0.747	4.80E-02
aug_v2a.16337	Exportin-1	-0.747	4.66E-02
aug_v2a.11629	UPF0396 protein CG6066	-0.745	1.84E-02
aug_v2a.14764	Putative serine/threonine-protein kinase F31E3.2	-0.737	3.43E-02
aug_v2a.22472	Coiled-coil domain-containing protein 75	-0.736	3.18E-02
aug_v2a.07451		-0.732	1.45E-02
aug_v2a.10148	Ubiquitin-specific peptidase-like protein 1	-0.730	4.59E-02
aug_v2a.22121	E3 ubiquitin-protein ligase TRIM23	-0.728	2.11E-02
aug_v2a.07427	Thyrotroph embryonic factor	-0.724	3.37E-02
aug_v2a.23579	Zinc finger protein 271	-0.723	3.16E-02
aug_v2a.06467	RIB43A-like with coiled-coils protein 2	-0.719	4.80E-02
aug_v2a.04697	Heme-binding protein 1	-0.718	9.32E-03
aug_v2a.21181	Macrophage-stimulating protein receptor	-0.714	4.99E-02
aug_v2a.03511	Probable protein disulfide-isomerase A6	-0.714	1.79E-03
aug_v2a.16138		-0.708	8.04E-03
aug_v2a.01884	Probable phospholipid-transporting ATPase IIA	-0.708	2.93E-02
aug_v2a.13346	WASH complex subunit 7 homolog	-0.705	4.73E-02
aug_v2a.01249		-0.703	2.78E-02
aug_v2a.00279	Methionine synthase reductase	-0.699	1.19E-02
aug_v2a.24400		-0.695	2.08E-02

Table 4.3 (Continued)

Gene ID	UniProt Hit Description	Fold Change (log_2)	Adjusted p-value
aug_v2a.07288		-0.691	2.35E-02
aug_v2a.16199	Probable phospholipid-transporting ATPase IIB	-0.684	2.80E-02
aug_v2a.04480	N-acetyl-beta-glucosaminyl-glycoprotein 4-beta-N-acetylgalactosaminyltransferase 1	-0.676	1.31E-02
aug_v2a.08157	Interferon-related developmental regulator 1	-0.671	4.66E-02
aug_v2a.17194	Testis-expressed sequence 9 protein	-0.663	4.75E-02
aug_v2a.02714	Intraflagellar transport protein 57 homolog	-0.657	3.73E-02
aug_v2a.19620		-0.652	4.10E-02
aug_v2a.04681	Protein FAM181B	-0.647	4.64E-02
aug_v2a.00464	Arachidonate 5-lipoxygenase	-0.645	4.62E-02
aug_v2a.20619		-0.640	4.80E-02
aug_v2a.17941	U2 small nuclear ribonucleoprotein auxiliary factor 35 kDa subunit-related protein 2	-0.637	3.60E-02
aug_v2a.01530	F-box/LRR-repeat protein 14	-0.636	1.88E-02
aug_v2a.02240		-0.634	4.66E-02
aug_v2a.17942	Leukocyte elastase inhibitor	-0.634	4.80E-02
aug_v2a.04696	Putative RNA polymerase II subunit B1 CTD phosphatase RPAP2	-0.621	2.36E-02
aug_v2a.00494	ATP-binding cassette sub-family A member 1	-0.621	3.37E-02
aug_v2a.07316	Charged multivesicular body protein 3	-0.614	5.66E-03
aug_v2a.07328	Serine/threonine-protein phosphatase 2A 55 kDa regulatory subunit B alpha isoform	-0.610	1.46E-02
aug_v2a.14756	UPF0557 protein C10orf119 homolog	0.614	4.38E-02
aug_v2a.09643	Dedicator of cytokinesis protein 1	0.617	2.26E-02
aug_v2a.17006		0.618	4.84E-02
aug_v2a.14953	Double-stranded RNA-specific adenosine deaminase	0.621	4.64E-02
aug_v2a.12331	Peptide transporter family 1	0.623	3.09E-02
aug_v2a.07409	B(0,+)-type amino acid transporter 1	0.624	4.16E-02
aug_v2a.00183	Histone acetyltransferase MYST4	0.629	4.38E-02
aug_v2a.05303		0.635	2.16E-02
aug_v2a.12808	Arf-GAP with SH3 domain, ANK repeat and PH domain-containing protein 1	0.637	4.80E-02
aug_v2a.00752	Bromodomain and WD repeat-containing protein 3	0.647	1.84E-02
aug_v2a.19785	Uncharacterized protein MJ1628	0.666	3.93E-02
aug_v2a.12786	UPF0562 protein v1g242151	0.678	4.22E-02
aug_v2a.23845	Heparanase	0.688	3.74E-03
aug_v2a.01728	Tubulin polyglutamylase TTLL5	0.690	3.49E-02

Table 4.3 (Continued)

Gene ID	UniProt Hit Description	Fold Change (log_2)	Adjusted p-value
aug_v2a.05691	Diamine acetyltransferase 2	0.697	4.15E-02
aug_v2a.09214	Pyruvate dehydrogenase phosphatase regulatory subunit, mitochondrial	0.698	4.80E-02
aug_v2a.23649	Metal tolerance protein 10	0.699	2.39E-02
aug_v2a.17701	Kinesin-like protein KIF22	0.710	4.80E-02
aug_v2a.19168	Arylsulfatase B	0.728	4.15E-02
aug_v2a.10302	Histone-lysine N-methyltransferase MLL5	0.730	2.57E-02
aug_v2a.06182	E3 ubiquitin-protein ligase HERC2	0.740	2.69E-02
aug_v2a.10607	Ubiquitin carboxyl-terminal hydrolase 25	0.748	3.93E-02
aug_v2a.09351	Large proline-rich protein BAT3	0.759	3.93E-02
aug_v2a.00696	SAM and SH3 domain-containing protein 1	0.759	3.60E-02
aug_v2a.00967	Protein sidekick-1	0.768	3.60E-02
aug_v2a.23953		0.774	1.46E-02
aug_v2a.06912	E3 ubiquitin-protein ligase Hakai	0.774	3.21E-02
aug_v2a.04340	Host cell factor 1	0.777	3.79E-02
aug_v2a.20459	Vinculin	0.777	1.84E-02
aug_v2a.14927	Putative E3 ubiquitin-protein ligase SH3RF1	0.782	1.84E-02
aug_v2a.21710		0.786	2.75E-02
aug_v2a.20381	F-box/LRR-repeat protein 2	0.801	1.19E-02
aug_v2a.15385	Rhombotin-1	0.803	2.16E-02
aug_v2a.10627		0.814	1.41E-02
aug_v2a.04903	Transmembrane protein 69	0.820	2.79E-02
aug_v2a.18302		0.820	4.80E-02
aug_v2a.08424	DDB1- and CUL4-associated factor-like 1	0.836	1.46E-02
aug_v2a.08061	Interleukin enhancer-binding factor 3-B	0.838	3.21E-02
aug_v2a.06078		0.844	4.80E-02
aug_v2a.16676		0.851	4.58E-02
aug_v2a.17722		0.852	3.12E-02
aug_v2a.01401	Calcium homeostasis endoplasmic reticulum protein	0.854	4.64E-02
aug_v2a.17193	Single-stranded DNA-binding protein, mitochondrial	0.856	3.11E-02
aug_v2a.06663	Homeobox protein homothorax	0.860	2.93E-02
aug_v2a.13068	39S ribosomal protein L11, mitochondrial	0.862	1.37E-02
aug_v2a.23510	D-inositol-3-phosphate glycosyltransferase	0.864	8.04E-03
aug_v2a.23695	39S ribosomal protein L17, mitochondrial	0.865	3.74E-03
aug_v2a.00613	DNA-directed RNA polymerase II subunit RPB1	0.866	4.66E-02
aug_v2a.10238	AT-rich interactive domain-containing protein 1A	0.867	3.21E-02

Table 4.3 (Continued)

Gene ID	UniProt Hit Description	Fold Change (log_2)	Adjusted p-value
aug_v2a.20573	Mediator of RNA polymerase II transcription subunit 12-like protein	0.899	4.66E-02
aug_v2a.08476	Acid trehalase-like protein 1	0.910	8.86E-03
aug_v2a.04659	Down syndrome cell adhesion molecule-like protein CG42256	0.912	4.80E-02
aug_v2a.14291	CAD protein	0.915	2.16E-02
aug_v2a.10311	Filamin-A	0.917	2.16E-02
aug_v2a.15306		0.920	1.41E-02
aug_v2a.17075	Bromodomain and WD repeat-containing protein 3	0.922	2.19E-02
aug_v2a.09800	Filamin-A	0.933	2.72E-02
aug_v2a.00878	Polycomb protein SUZ12	0.957	2.38E-02
aug_v2a.01040		0.990	1.45E-02
aug_v2a.22225	Ubiquitin carboxyl-terminal hydrolase 25	1.016	3.47E-02
aug_v2a.12807	Hemicentin-1	1.016	1.46E-02
aug_v2a.16164	RNA-binding protein with serine-rich domain 1	1.018	4.42E-02
aug_v2a.19414	Cytoplasmic dynein 1 heavy chain 1	1.026	4.48E-02
aug_v2a.10021	ETS-related transcription factor Elf-2	1.034	1.41E-02
aug_v2a.06384	Multiple PDZ domain protein	1.035	1.63E-02
aug_v2a.00753		1.039	4.59E-02
aug_v2a.06432	Delphilin	1.055	1.84E-02
aug_v2a.17461	Disco-interacting protein 2 homolog B	1.061	4.66E-02
aug_v2a.20411		1.061	2.75E-02
aug_v2a.18891	Storkhead-box protein 1	1.071	1.36E-02
aug_v2a.01426		1.075	1.41E-02
aug_v2a.14951	Splicing factor 3A subunit 1	1.094	2.83E-02
aug_v2a.06154	Histone-lysine N-methyltransferase, H3 lysine-79 specific	1.097	1.51E-02
aug_v2a.01394		1.101	3.73E-02
aug_v2a.14216	Amyloid beta A4 precursor protein-binding family B member 1-interacting protein	1.102	4.08E-02
aug_v2a.13530	Splicing factor 3A subunit 1	1.128	2.71E-02
aug_v2a.04111	Uncharacterized protein C3orf32 homolog	1.133	1.19E-02
aug_v2a.00993		1.138	3.74E-03
aug_v2a.03929	Serine/arginine repetitive matrix protein 1	1.138	1.31E-02
aug_v2a.16480	RNA-binding protein 16	1.140	4.59E-02
aug_v2a.18078	Protein sidekick-1	1.144	4.77E-02
aug_v2a.17559	Ankyrin repeat and KH domain-containing protein mask	1.151	1.54E-02

Table 4.3 (Continued)

Gene ID	UniProt Hit Description	Fold Change (log_2)	Adjusted p-value
aug_v2a.13910		1.153	2.09E-02
aug_v2a.05531	E3 ubiquitin-protein ligase SHPRH	1.163	1.45E-02
aug_v2a.17226	Ankyrin repeat and KH domain-containing protein mask	1.164	2.39E-02
aug_v2a.18883		1.166	3.32E-02
aug_v2a.08521	Abl interactor 1	1.171	1.41E-02
aug_v2a.08622	PDZ and LIM domain protein 3	1.180	1.51E-02
aug_v2a.22999		1.187	1.59E-02
aug_v2a.08509		1.200	2.78E-02
aug_v2a.14468		1.205	2.15E-02
aug_v2a.23779	UPF0606 protein C11orf41	1.207	3.21E-02
aug_v2a.19504		1.211	2.00E-02
aug_v2a.22693		1.214	4.62E-02
aug_v2a.22921	SWI/SNF complex subunit SMARCC1	1.223	3.95E-02
aug_v2a.22371	RNA-binding protein 16	1.223	4.10E-02
aug_v2a.23753	CAD protein	1.234	1.60E-02
aug_v2a.18348	Multiple PDZ domain protein	1.278	2.56E-02
aug_v2a.05530		1.321	8.86E-03
aug_v2a.13992		1.321	4.80E-02
aug_v2a.18019		1.336	1.84E-02
aug_v2a.01229	Phosphotidylinositol phosphatase PTPRQ	1.337	4.49E-02
aug_v2a.15287	Scm-like with four MBT domains protein 1	1.368	1.08E-02
aug_v2a.04538		1.450	4.80E-02
aug_v2a.20475		1.473	2.16E-02
aug_v2a.06038		1.500	1.84E-02
aug_v2a.08911		1.508	1.19E-02
aug_v2a.16259		1.540	4.49E-02
aug_v2a.17022	Collagen alpha-2(IV) chain	1.601	2.75E-02
aug_v2a.03233	Filamin-A	1.669	1.19E-02
aug_v2a.11752	Peroxidasin homolog	1.824	4.80E-02
aug_v2a.08967	Chymotrypsinogen A	1.889	1.31E-02
aug_v2a.20375	Hemicentin-1	2.088	3.03E-02

Table 4.4 DEGs recovered on day three from the CH treatment group.

Gene ID	UniProt Hit Description	Fold Change (log_2)	Adjusted p-value
aug_v2a.16069	CUB and sushi domain-containing protein 3	-2.38742	0.021266
aug_v2a.02777	Synaptotagmin-6	-2.08325	0.030878
aug_v2a.07455	Plastin-3	-1.65853	0.040585
aug_v2a.21003		-1.52674	0.038524
aug_v2a.01768		-1.39994	0.017829
aug_v2a.06228	Long-chain-fatty-acid--CoA ligase ACSBG1	-1.35567	0.043407
aug_v2a.03817	Beta-glucuronidase	-1.33538	0.043407
aug_v2a.03150	Transcription factor AP-1	-1.13981	0.0437
aug_v2a.13116	WD repeat-containing protein 76	-0.97421	0.046659
aug_v2a.11740	Neural cell adhesion molecule 1	-0.89275	0.043407
aug_v2a.02416	Phosphoserine aminotransferase	-0.83773	5.93E-07
aug_v2a.14980	DnaJ homolog subfamily C member 17	-0.65316	0.043407
aug_v2a.19379	Galactosylceramide sulfotransferase	-0.63376	0.033237
aug_v2a.11353	Methionine synthase	-0.63314	0.025016
aug_v2a.04697	Heme-binding protein 1	-0.62229	0.045165
aug_v2a.04924	Oxysterol-binding protein 1	-0.50963	0.034036
aug_v2a.14630	ADP-ribosylation factor GTPase-activating protein 3	-0.50934	0.043407
aug_v2a.15940	FAS-associated factor 1	-0.5047	0.043407
aug_v2a.07840	Succinate dehydrogenase [ubiquinone] flavoprotein subunit, mitochondrial	-0.49868	0.017829
aug_v2a.07894	Dihydrolipoyl dehydrogenase, mitochondrial	-0.41144	0.026177
aug_v2a.13963	Ankyrin repeat domain-containing protein 6	0.445134	0.025901
aug_v2a.03847	RING1 and YY1-binding protein	0.477148	0.043594
aug_v2a.08262	H(+)/Cl(-) exchange transporter 7	0.549537	0.026177
aug_v2a.21013	10-formyltetrahydrofolate dehydrogenase	0.603208	0.010709
aug_v2a.21709		0.700852	0.043407
aug_v2a.08917	Short transient receptor potential channel 4	0.759575	0.043407
aug_v2a.16362	Microtubule-actin cross-linking factor 1, isoform 4	0.858845	0.043407
aug_v2a.03982		0.869231	0.040585
aug_v2a.06802		0.965639	0.014141
aug_v2a.16686	TNF receptor-associated factor 3	1.083368	0.022478
aug_v2a.21593		1.14044	0.001316
aug_v2a.06710	TNF receptor-associated factor 6	1.177952	0.042698
aug_v2a.10680		1.207356	0.001617

Table 4.4 (Continued)

Gene ID	UniProt Hit Description	Fold Change (log_2)	Adjusted p-value
aug_v2a.21057		1.237193	0.016618
aug_v2a.21176	Choloylglycine hydrolase	1.534791	0.048091
aug_v2a.19221		1.547065	0.035565
aug_v2a.00365	Protein NLRC3	1.550023	0.043407
aug_v2a.20323	C-type lectin	1.950702	0.010538
aug_v2a.01044		2.265903	0.01313

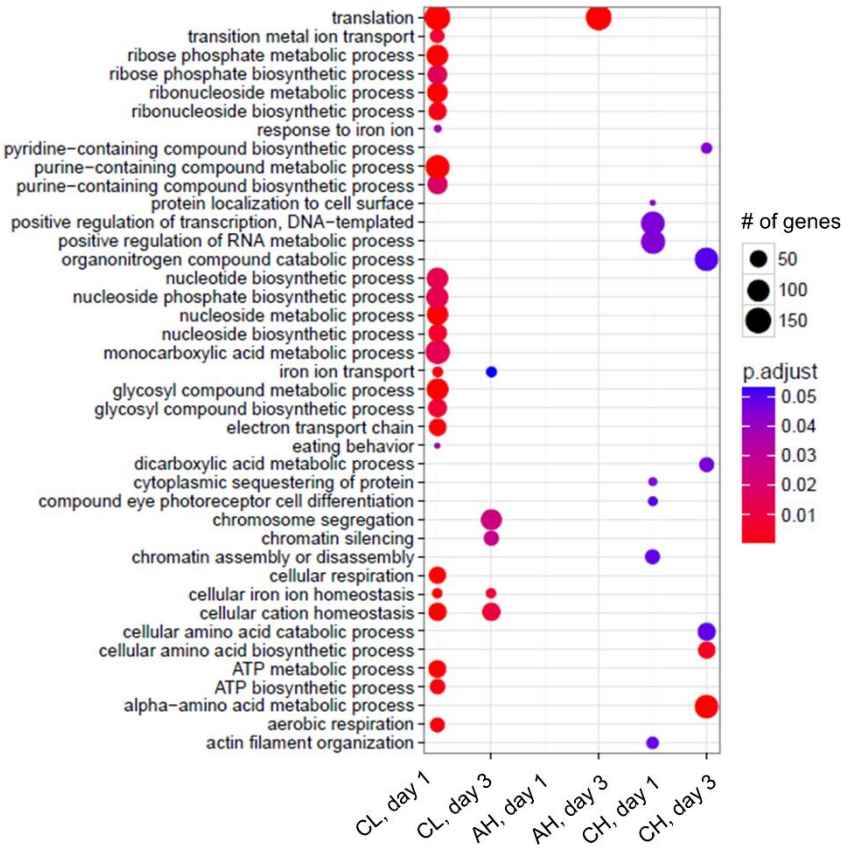

Figure 4.6 Enriched biological process GO-terms for each treatment by day in *A. digitifera* larval samples. GO-term enrichment was performed using ErmineJ gene score resampling method (Lee *et al.*, 2005) where negative-log-transformed p-values from all genes were used to compute a cumulative score for a gene set and significance of a specific gene is determined by random sampling of the data. The data were resampled 100,000 times and when more than one transcript was present, the best scoring replicate transcript was used. The size of the circle indicates the number of genes associated with the GO-term and color is the significance of that GO-term to be recovered from random sampling the gene set. The p-values were adjusted by a Benjamini-Hochberg correction (Benjamini *et al.*, 1995).

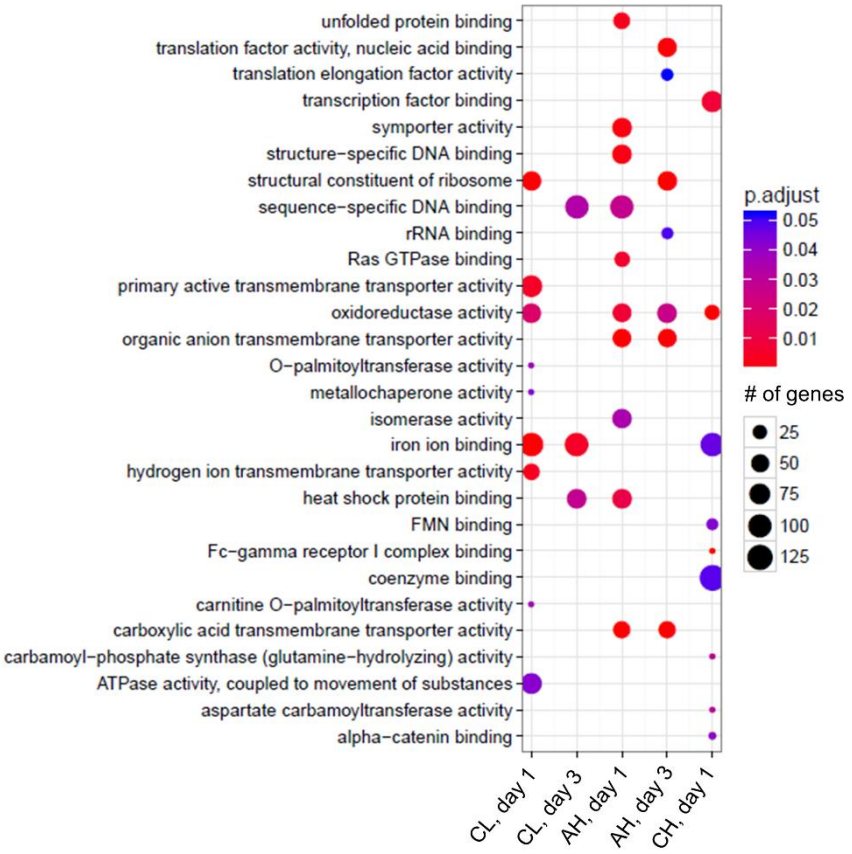

Figure 4.7 Enriched molecular function GO-terms for each treatment by day in *A. digitifera* larval samples. See Figure legend 4.6 for analysis details.

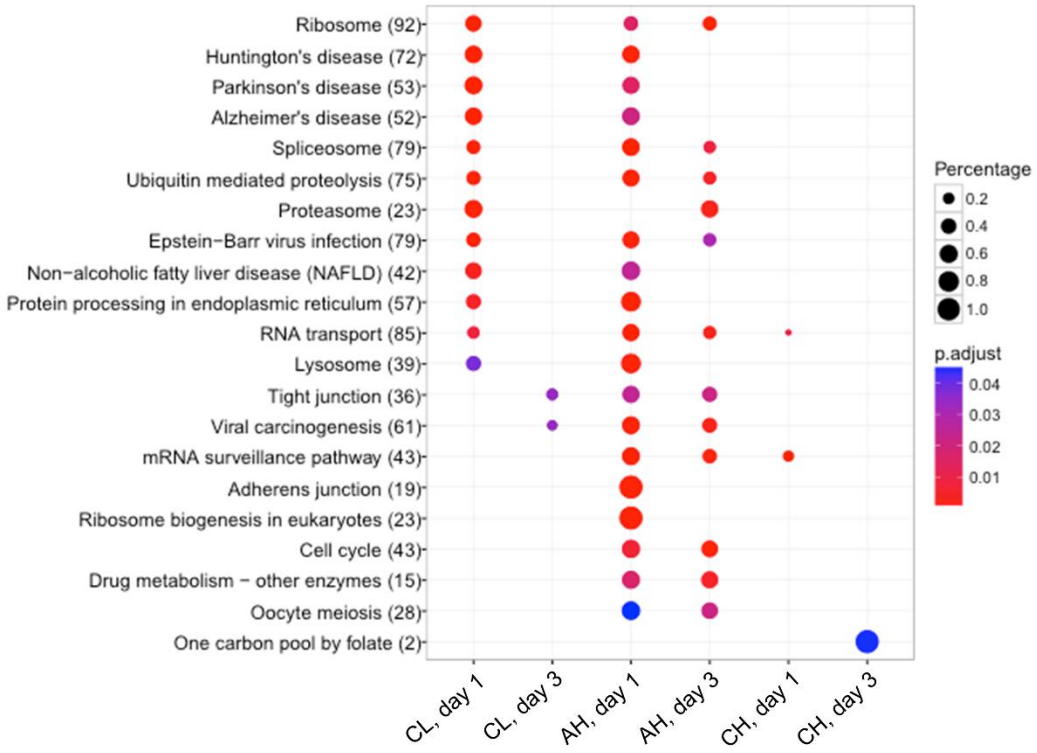

Figure 4.8 Top 20 KEGG pathways over-represented in colonization, high temperature and their interaction over time in *A. digitifera* larval samples. For each treatment group by day, a hypergeometric model was applied using clusterProfiler (Yu *et al.*, 2012) to determine if the number of KEGG-annotated genes associated with the group was larger than expected by chance based on the total number of KEGG annotations. The total number of KEGG-annotated genes for each pathway is presented in parentheses next to the pathway. The size of the circle is determined by the percentage of annotated genes in each treatment group compared to the total number of annotated genes from all treatment groups. The color of the circle is based on the significance using adjusted Benjamini-Hochberg p-values.

Table 4.5 KEGG pathways identified from the over-representation analysis by clusterProfiler (Yu *et al.*, 2012) of *A. digitifera* treatment groups.

Group	ID	Description	Gene Ratio	p-value	p.adjust
CL day one	ko03010	Ribosome	38/556	3.25E-17	9.61E-15
	ko05016	Huntington's disease	36/556	5.93E-15	8.77E-13
	ko05012	Parkinson's disease	28/556	2.48E-11	2.44E-09
	ko05010	Alzheimer's disease	25/556	7.77E-08	5.75E-06
	ko03040	Spliceosome	22/556	2.99E-07	1.77E-05
	ko04120	Ubiquitin mediated proteolysis	22/556	4.65E-07	2.29E-05
	ko03050	Proteasome	12/556	5.08E-06	0.000188
	ko05169	Epstein-Barr virus infection	24/556	5.08E-06	0.000188
	ko04932	Non-alcoholic fatty liver disease (NAFLD)	18/556	8.50E-05	0.002796
	ko04141	Protein processing in endoplasmic reticulum	19/556	0.000137	0.004054
	ko04144	Endocytosis	22/556	0.000157	0.004216
	ko03020	RNA polymerase	10/556	0.00028	0.006898
	ko03013	RNA transport	18/556	0.000336	0.007657
	ko00230	Purine metabolism	28/556	0.000377	0.007978
	ko05131	Shigellosis	11/556	0.000468	0.009231
	ko00240	Pyrimidine metabolism	20/556	0.000503	0.009306
	ko03060	Protein export	8/556	0.000828	0.014414
	ko00190	Oxidative phosphorylation	23/556	0.000984	0.016187
	ko04146	Peroxisome	11/556	0.001298	0.020219
	ko05130	Pathogenic Escherichia coli infection	8/556	0.001381	0.020445
	ko04142	Lysosome	13/556	0.002685	0.037844
	ko00020	Citrate cycle (TCA cycle)	9/556	0.003145	0.042309
	ko05132	Salmonella infection	11/556	0.003739	0.048116
CL day three	ko04530	Tight junction	7/168	0.000219	0.033779
	ko05203	Viral carcinogenesis	9/168	0.000287	0.033779
AH day one	ko03040	Spliceosome	40/1133	2.93E-11	9.29E-09
	ko03013	RNA transport	40/1133	2.49E-09	3.94E-07
	ko03015	mRNA surveillance pathway	23/1133	1.38E-08	1.46E-06
	ko04141	Protein processing in endoplasmic reticulum	38/1133	4.43E-08	3.28E-06
	ko04120	Ubiquitin mediated proteolysis	35/1133	5.17E-08	3.28E-06
	ko05016	Huntington's disease	36/1133	2.15E-06	0.000114

Table 4.5 (Continued)

Group	ID	Description	Gene Ratio	p-value	p.adjust
AH day one	ko04520	Adherens junction	19/1133	9.51E-06	0.000392
	ko05203	Viral carcinogenesis	32/1133	1.01E-05	0.000392
	ko03008	Ribosome biogenesis in eukaryotes	23/1133	1.11E-05	0.000392
	ko04142	Lysosome	26/1133	2.00E-05	0.000624
	ko05169	Epstein-Barr virus infection	36/1133	2.16E-05	0.000624
	ko05210	Colorectal cancer	16/1133	3.11E-05	0.000823
	ko04721	Synaptic vesicle cycle	14/1133	4.05E-05	0.000988
	ko03018	RNA degradation	20/1133	0.000162	0.003667
	ko00240	Pyrimidine metabolism	34/1133	0.000176	0.003711
	ko04144	Endocytosis	35/1133	0.000257	0.005091
	ko04110	Cell cycle	24/1133	0.000349	0.006506
	ko04915	Estrogen signaling pathway	17/1133	0.000382	0.006734
	ko04071	Sphingolipid signaling pathway	19/1133	0.000475	0.007682
	ko00531	Glycosaminoglycan degradation	7/1133	0.000485	0.007682
	ko05231	Choline metabolism in cancer	16/1133	0.000544	0.008206
	ko05168	Herpes simplex infection	29/1133	0.000617	0.008884
	ko00480	Glutathione metabolism	12/1133	0.000724	0.009981
	ko05012	Parkinson's disease	25/1133	0.001097	0.014496
	ko03010	Ribosome	28/1133	0.001198	0.01519
	ko03460	Fanconi anemia pathway	14/1133	0.001343	0.016378
	ko00983	Drug metabolism - other enzymes	8/1133	0.001409	0.016547
	ko04212	Longevity regulating pathway - worm	14/1133	0.001627	0.017784
	ko04922	Glucagon signaling pathway	14/1133	0.001627	0.017784
	ko04745	Phototransduction - fly	7/1133	0.001793	0.018946
	ko05010	Alzheimer's disease	27/1133	0.002039	0.020658
	ko04150	mTOR signaling pathway	11/1133	0.002085	0.020658
	ko04152	AMPK signaling pathway	18/1133	0.002372	0.022787
	ko04140	Regulation of autophagy	8/1133	0.002666	0.02402
	ko05131	Shigellosis	15/1133	0.002728	0.02402
	ko04666	Fc gamma R-mediated phagocytosis	14/1133	0.002791	0.02402

Table 4.5 (Continued)

Group	ID	Description	Gene Ratio	p-value	p.adjust
AH day one	ko04391	Hippo signaling pathway - fly	13/1133	0.002804	0.02402
	ko04530	Tight junction	17/1133	0.002904	0.024224
	ko04932	Non-alcoholic fatty liver disease (NAFLD)	24/1133	0.003043	0.024735
	ko04919	Thyroid hormone signaling pathway	18/1133	0.003135	0.024848
	ko03420	Nucleotide excision repair	12/1133	0.003336	0.025793
	ko04668	TNF signaling pathway	18/1133	0.004654	0.034353
	ko00563	Glycosylphosphatidylinositol (GPI)-anchor biosynthesis	8/1133	0.00466	0.034353
	ko04114	Oocyte meiosis	16/1133	0.006208	0.044728
	ko04962	Vasopressin-regulated water reabsorption	9/1133	0.006635	0.046388
	ko04722	Neurotrophin signaling pathway	18/1133	0.006731	0.046388
	ko04921	Oxytocin signaling pathway	21/1133	0.007017	0.047324
AH day three	ko03010	Ribosome	26/567	3.71E-08	1.12E-05
	ko04110	Cell cycle	19/567	3.70E-06	0.000557
	ko03015	mRNA surveillance pathway	13/567	1.15E-05	0.001151
	ko05203	Viral carcinogenesis	20/567	3.05E-05	0.002208
	ko03050	Proteasome	11/567	3.67E-05	0.002208
	ko03013	RNA transport	20/567	4.70E-05	0.002359
	ko00983	Drug metabolism - other enzymes	7/567	0.000106	0.004104
	ko04120	Ubiquitin mediated proteolysis	18/567	0.000109	0.004104
	ko03040	Spliceosome	17/567	0.000251	0.008409
	ko04114	Oocyte meiosis	12/567	0.000696	0.020957
	ko04530	Tight junction	12/567	0.000785	0.021364
	ko00531	Glycosaminoglycan degradation	5/567	0.000852	0.021364
	ko05169	Epstein-Barr virus infection	19/567	0.001301	0.030133
	ko05131	Shigellosis	10/567	0.002069	0.042624
	ko00511	Other glycan degradation	5/567	0.002124	0.042624
CH day one	ko03015	mRNA surveillance pathway	7/86	4.59E-07	5.92E-05
	ko03013	RNA transport	7/86	0.00013	0.008364
CH day three	ko00670	One carbon pool by folate	2/12	0.000617	0.044414

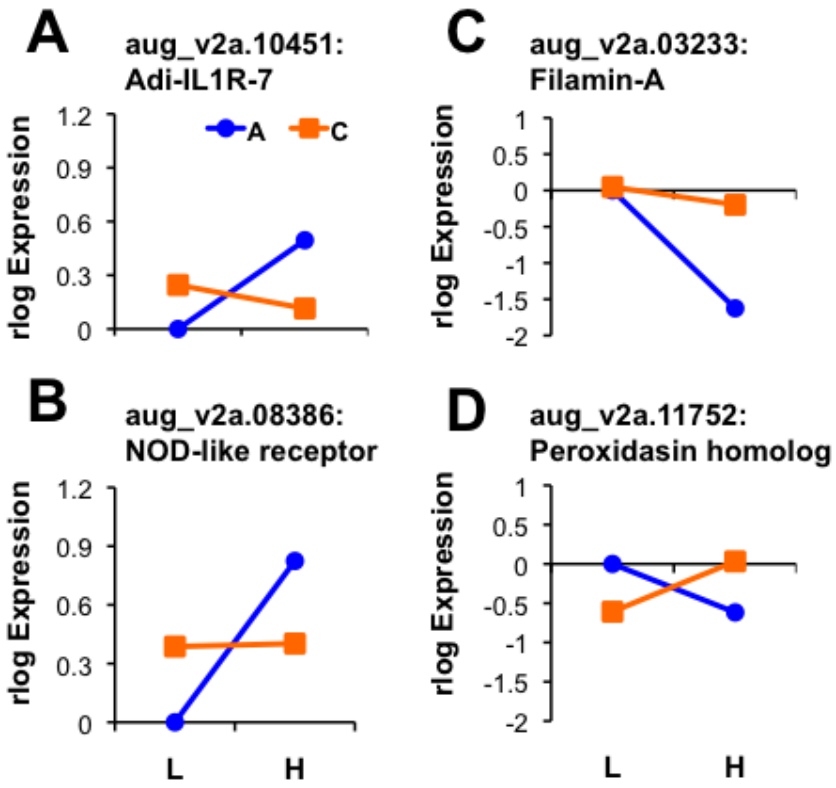

Figure 4.9 Four DEGs from *A. digitifera* larvae that differed in the CH compared to other treatments on day one. Average rlog transformed counts from the 6 replicates for each treatment were used to calculate fold changes, where treatment groups CL, AH and CH (see Table 4.1) expression was compared to the AL control treatment expression. Expression patterns of the genes (A) Adi-IL1R-7, (B) NOD-like receptor, (C) filamin-A, and (D) peroxidasin homolog are highlighted. Aposymbiotic = blue, colonized = orange.

Figure 4.10 Six DEGs from *A. digitifera* larvae that differed in the CH compared to other treatments on day three. Average rlog transformed counts from the 6 replicates for each treatment group were used to calculate fold changes, where treatment groups CL, AH and CH (see Table 4.1) expression was compared to the AL control treatment expression. Expression patterns of the genes (A) TRAF, (B) NLRC3, (C) transcription factor AP-1, (D) C-type lectin, (E) CUB and sushi domain containing protein, and (F) galatosylceramide sulfotransferase are highlighted. Aposymbiotic = blue, colonized = orange.

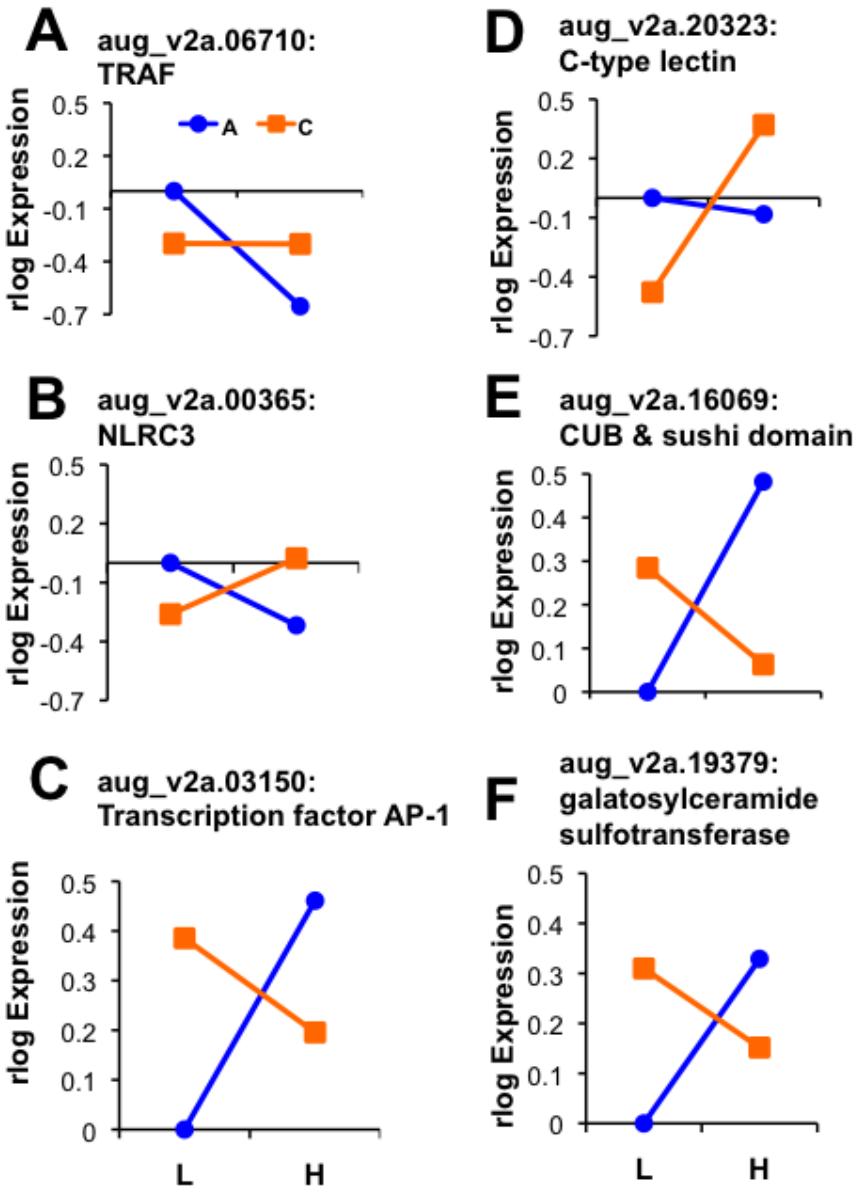
A
aug_v2a.06710:
TRAF
rlog Expression
0.5
0.2
-0.1
-0.4
-0.7
A
C
B
aug_v2a.00365:
NLRC3
C
aug_v2a.03150:
Transcription factor AP-1
0.4
0.3
0
L
H
D
aug_v2a.20323:
C-type lectin
E
aug_v2a.16069:
CUB & sushi domain
F
aug_v2a.19379:
galatosylceramide
sulfotransferase

Figure 4.10

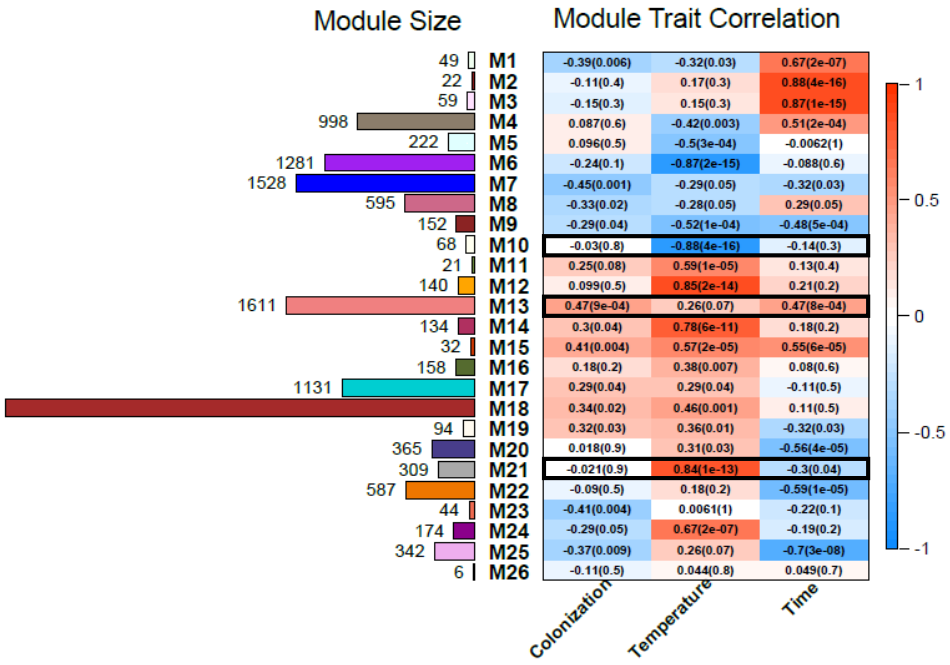

Figure 4.11 Module assignment and correlation to experimental treatments. Twenty six modules of genes with similar expression patterns were clustered using an adjacency matrix of VSD transformed counts in the R package WGCNA (Langfelder *et al.*, 2008a). The module size, or total number of genes clustered in each module, are represented by the colored bars on the left and the biweight midcorrelation (p-value) of each module to each treatment is presented on the right. The correlation strength is indicated by color, where strong positive correlations are red and strong negative correlations are blue. Three modules highlighted by the black box (ivory, light coral, and dark grey) are analyzed further in Figures 4.12 and 4.13.

Table 4.6 Functional enrichment analysis results for modules highly correlated with colonization, temperature or both treatment conditions.

Module Number	Term	Source	# of genes	Fischer's Exact test p-value	Benjamini correction
M6	DNA replication	David	10	7.3E-04	0.032
	mRNA transport	David	9	9.9E-04	0.036
	cofactor metabolic process	GO	18	1.3E-04	0.048
	Mitochondrion	GO	55	1.4E-04	0.012
M7	Mitochondrion	GO	109	1.2E-17	5.2E-15
	oxidative phosphorylation	GO	25	3.7E-13	8.5E-10
	ribonucleoprotein complex	GO	60	2.6E-12	3.9E-10
	cellular protein localization	GO	40	3.5E-07	7.4E-05
	positive regulation of ubiquitin-protein ligase	GO	15	4.7E-07	8.4E-05
M10	gated channel activity	GO	4	0.013	0.834
M12	glycoprotein	David	19	0.001	0.033
	apoptosis	David	6	0.001	0.038
	ubl conjugation	David	9	2.3E-05	0.002
M13	ATP-binding	David	101	6.0E-16	6.2E-14
	microtubule cytoskeleton	GO	52	1.3E-10	5.8E-08
	Endocytosis	GO	25	1.4E-06	7.3E-04
	EGF-like region, conserved site	InterPro	31	1.0E-07	3.5E-05
	Fibronectin, type III subdomain	InterPro	7	9.5E-04	0.030
	Dynein heavy chain	InterPro	9	1.8E-08	9.8E-06
	cell adhesion	GO	54	2.6E-07	2.2E-04
	HEAT domain	InterPro	12	2.1E-06	2.3E-04
	C-type lectin, conserved site	InterPro	10	0.002	0.046
	NACHT domain	David	8	7.4E-06	8.2E-04
	Thrombospondin, type 1 repeat	InterPro	9	0.002	0.043
	cholesterol metabolism	David	6	0.003	0.039
M14	DEATH-like domain	InterPro	8	2.7E-10	4.3E-08
	NOD-like receptor signaling pathway	KEGG	4	4.9E-04	0.005
	ABC transporters	KEGG	3	0.006	0.029
M21	Ankyrin 5	David	8	3.3E-05	0.019
	EGF-like, type 3	InterPro	9	9.0E-05	0.010
	Zinc finger, RING-type	InterPro	10	3.3E-04	0.016
	TNF receptor-associated factor TRAF	InterPro	3	7.8E-04	0.032

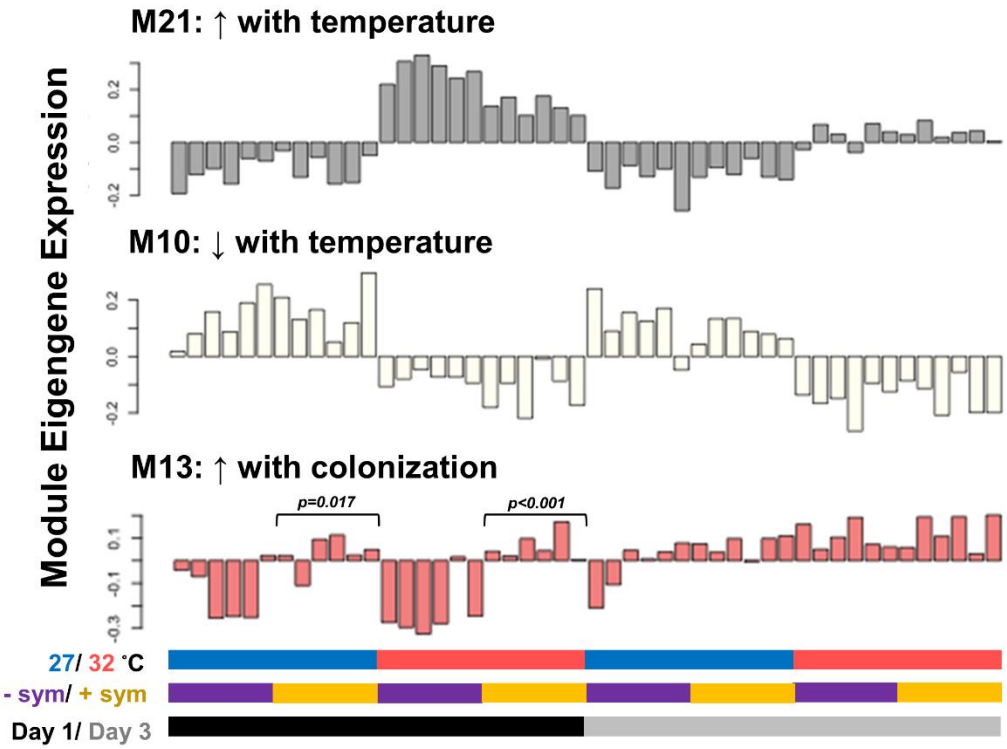

Figure 4.12 Summarized sample module eigengene expression for three modules highly correlated with temperature, colonization or both. For each module, an average sample eigengene value was calculated from the expression of all genes in that module. Colored bars at the bottom correspond to sample experimental conditions in the bar graphs above (temperature =27 or 32 °C; colonization = − sym or + sym; day = 1 or 3). M21 and M10 were both highly correlated with temperature, but in opposite directions. M13 was correlated with colonization and time on day one but not on day three. The results of a Student's T-test are presented above + sym samples that significantly differed with the –sym samples in each respective temperature.

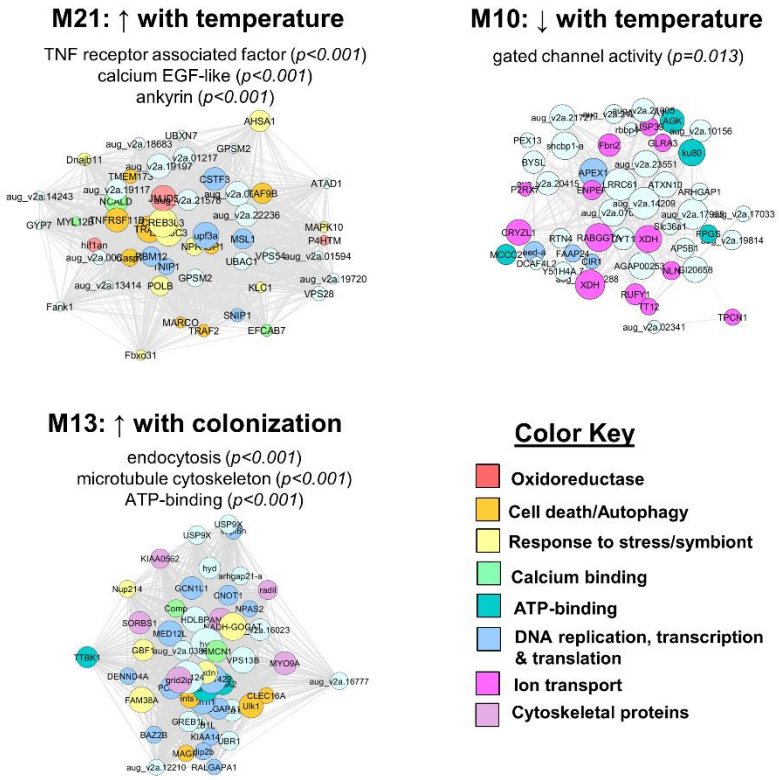

Figure 4.13 Network visualization of modules M21, M10 and M13. The top 50 genes with the highest MM, or intramodular connectivity, were isolated from the full network and visualized in Cytoscape v3.3.0 (Shannon *et al.*, 2003). The size of the nodes is based on their MM value and colored by generalized functional groups listed in the color key. Genes without annotation or which did not fit in the functional groups are light blue. The network layout was based on the spring embedded edge-weighted layout. The thickness of the edges is based on the weight, or strength of the connection between the two nodes. Select functional enrichment terms are presented for each module with full results listed in Table 4.6.

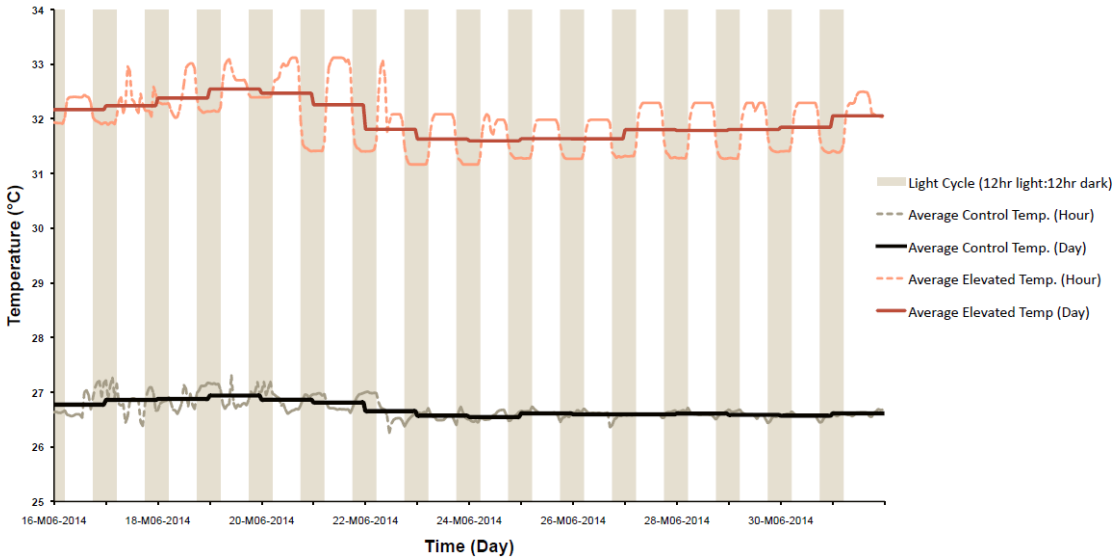

Figure 4.14 Experimental temperatures over 14 days. Temperature loggers submerged in water recorded temperature at 1 min intervals from each experimental chamber. Average temperatures by hour (dashed line) and by day (solid line) are displayed with the 12 h light: 12 h dark cycle indicated by shaded bars. Light cycle caused approximately 0.5 °C oscillation in temperature in the 32 °C treatment group, but with control temperature. Control treatment = black; elevated treatment = red.

4.3 References

Abrego, D., Van Oppen, M.J. and Willis, B.L. (2009). Highly infectious symbiont dominates initial uptake in coral juveniles. *Mol. Ecol.* **18,** 3518-3531.

Akira, S. and Takeda, K. (2004). Toll-like receptor signalling. *Nat. Rev. Immunol.* **4,** 499-511.

Andrews, S. (2010) FastQC: A quality control tool for high throughput sequence data. In *Reference Source*.

Anguera, M.C., Field, M.S., Perry, C., Ghandour, H., Chiang, E.-P., Selhub, J., *et al.* (2006). Regulation of folate-mediated one-carbon metabolism by 10-formyltetrahydrofolate dehydrogenase. *J. Biol. Chem.* **281,** 18335-18342.

Babcock, R. and Heyward, A. (1986). Larval development of certain gamete-spawning scleractinian corals. *Coral Reefs* **5,** 111-116.

Baird, A.H., Gilmour, James P., Kamiki, Takayuki M., Nonaka, Masanori, Pratchett, Morgan S., Yamamoto, Hiromi H., and Yamasaki, Hideo (2006) Temperature tolerance of symbiotic and non-symbiotic coral larvae. In *Proceedings of the 10th International Coral Reef Symposium In: 10th International Coral Reef Symposium*. Okinawa, Japan.

Benjamini, Y. and Hochberg, Y. (1995). Controlling the false discovery rate: a practical and powerful approach to multiple testing. *J. Roy. Stat. Soc. Ser. B. (Stat. Method.),* 289-300.

Blom, H.J. and Smulders, Y. (2011). Overview of homocysteine and folate metabolism. With special references to cardiovascular disease and neural tube defects. *J. Inherit. Metab. Dis.* **34,** 75-81.

Bowman, K.G. and Bertozzi, C.R. (1999). Carbohydrate sulfotransferases: mediators of extracellular communication. *Chem. Biol.* **6,** R9-R22.

Carter, S.L., Brechbühler, C.M., Griffin, M. and Bond, A.T. (2004). Gene co-expression network topology provides a framework for molecular characterization of cellular state. *Bioinformatics* **20,** 2242-2250.

Coffroth, M.A., Santos, S.R. and Goulet, T.L. (2001). Early ontogenetic expression of specificity in a cnidarian-algal symbiosis. *Mar. Ecol. Prog. Ser.* **222,** 85-96.

Cumbo, V., Baird, A. and van Oppen, M. (2013). The promiscuous larvae: flexibility in the establishment of symbiosis in corals. *Coral Reefs* **32,** 111-120.

Davy, S.K., Allemand, D. and Weis, V.M. (2012). Cell biology of cnidarian-dinoflagellate symbiosis. *Microbiol. Mol. Biol. Rev.* **76,** 229-261.

DeSalvo, M.K., Voolstra, C.R., Sunagawa, S., Schwarz, J.A., Stillman, J.H., Coffroth, M.A., *et al.* (2008). Differential gene expression during thermal stress and bleaching in the Caribbean coral *Montastraea faveolata*. *Mol. Ecol.* **17,** 3952-3971.

Edmunds, P., Gates, R. and Gleason, D. (2001). The biology of larvae from the reef coral *Porites astreoides*, and their response to temperature disturbances. *Mar. Biol.* **139,** 981-989.

Edmunds, P.J., Gates, R.D., Leggat, W., Hoegh-Guldberg, O. and Allen-Requa, L. (2005). The effect of temperature on the size and population density of dinoflagellates in larvae of the reef coral *Porites astreoides*. *Invertebr. Biol.* **124,** 185-193.

Feng, Y. and Walsh, C.A. (2004). The many faces of filamin: a versatile molecular scaffold for cell motility and signalling. *Nat. Cell Biol.* **6,** 1034-1038.

Flannagan, R.S., Jaumouillé, V. and Grinstein, S. (2012). The cell biology of phagocytosis. *Annu. Rev. Pathol.* **7,** 61-98.

Glynn, P.W. (1983). Extensive 'bleaching'and death of reef corals on the Pacific coast of Panama. *Environ. Conserv.* **10,** 149-154.

Grasso, L., Negri, A., Foret, S., Saint, R., Hayward, D., Miller, D. and Ball, E. (2011). The biology of coral metamorphosis: Molecular responses of larvae to inducers of settlement and metamorphosis. *Dev. Biol.* **353,** 411-419.

Hamada, M., Shoguchi, E., Shinzato, C., Kawashima, T., Miller, D.J. and Satoh, N. (2012). The complex NOD-like receptor repertoire of the coral *Acropora digitifera* includes novel domain combinations. *Mol. Biol. Evol.* **30,** 167-176.

Harii, S., Yasuda, N., Rodriguez-Lanetty, M., Irie, T. and Hidaka, M. (2009). Onset of symbiosis and distribution patterns of symbiotic dinoflagellates in the larvae of scleractinian corals. *Mar. Biol.* **156,** 1203-1212.

Hayward, D.C., Hetherington, S., Behm, C.A., Grasso, L.C., Forêt, S., Miller, D.J. and Ball, E.E. (2011). Differential gene expression at coral settlement and metamorphosis—a subtractive hybridization study. *PLoS One* **6,** e26411.

Heyward, A. and Negri, A. (2010). Plasticity of larval pre-competency in response to temperature: observations on multiple broadcast spawning coral species. *Coral Reefs* **29,** 631-636.

Hoegh-Guldberg, O. (1999). Climate change, coral bleaching and the future of the world's coral reefs. *Marine and Freshwater Research* **50,** 839-866.

Hofmann, G.E. and Todgham, A.E. (2010). Living in the now: physiological mechanisms to tolerate a rapidly changing environment. *Annu. Rev. Physiol.* **72,** 127-145.

Huang, D., Sherman, B., Tan, Q., Collins, J., Alvord, G., Roayaei, J., *et al.* (2007). The DAVID Gene Functional Classification Tool: a novel biological module-centric algorithm to functionally analyze large gene lists. *Genome Biol.* **8,** 183.

Hume, B., D'Angelo, C., Smith, E., Stevens, J., Burt, J. and Wiedenmann, J. (2015). *Symbiodinium thermophilum* sp. nov., a thermotolerant symbiotic alga prevalent in corals of the world's hottest sea, the Persian/Arabian Gulf. *Sci. Rep.* **5**.

Jenkins, G. (2003). The emerging role for sphingolipids in the eukaryotic heat shock response. *Cell. Mol. Life Sci.* **60,** 701-710.

Jeon, S.-B., Yoon, H.J., Park, S.-H., Kim, I.-H. and Park, E.J. (2008). Sulfatide, a major lipid component of myelin sheath, activates inflammatory responses as an endogenous stimulator in brain-resident immune cells. *J. Immunol.* **181,** 8077-8087.

Kvennefors, E.C.E., Leggat, W., Kerr, C.C., Ainsworth, T.D., Hoegh-Guldberg, O. and Barnes, A.C. (2010). Analysis of evolutionarily conserved innate immune components in coral links immunity and symbiosis. *Dev. Comp. Immunol.* **34,** 1219-1229.

Langfelder, P. and Horvath, S. (2008a). WGCNA: an R package for weighted correlation network analysis. *BMC Bioinformatics* **9,** 559.

Langfelder, P., Zhang, B. and Horvath, S. (2008b). Defining clusters from a hierarchical cluster tree: the Dynamic Tree Cut package for R. *Bioinformatics* **24,** 719-720.

Langmead, B. and Salzberg, S.L. (2012). Fast gapped-read alignment with Bowtie 2. *Nat. Methods* **9,** 357-359.

Lee, H.K., Braynen, W., Keshav, K. and Pavlidis, P. (2005). ErmineJ: tool for functional analysis of gene expression data sets. *BMC Bioinformatics* **6,** 269.

Lee, S.Y., Jeong, H.J., Kang, N.S., Jang, T.Y., Jang, S.H. and Lajeunesse, T.C. (2015). *Symbiodinium tridacnidorum* sp. nov., a dinoflagellate common to Indo-Pacific giant clams, and a revised morphological description of *Symbiodinium microadriaticum* Freudenthal, emended Trench & Blank. *Eur. J. Phycol.* **50,** 155-172.

Lesser, M.P. (1996). Elevated temperatures and ultraviolet radiation cause oxidative stress and inhibit photosynthesis in symbiotic dinoflagellates. *Limnol. Oceanogr.* **41,** 271-283.

Libro, S., Kaluziak, S.T. and Vollmer, S.V. (2013). RNA-seq profiles of immune related genes in the staghorn coral *Acropora cervicornis* infected with White Band Disease. *PLoS One* **8,** e81821.

Little, A.F., Van Oppen, M.J. and Willis, B.L. (2004). Flexibility in algal endosymbioses shapes growth in reef corals. *Science* **304,** 1492-1494.

Love, M.I., Huber, W. and Anders, S. (2014). Moderated estimation of fold change and dispersion for RNA-seq data with DESeq2. *Genome Biol.* **15,** 550.

Loya, Sakai, Yamazato, Nakano, Sambali and Van, W. (2001). Coral bleaching: the winners and the losers. *Ecol. Lett.* **4,** 122-131.

Luo, F., Yang, Y., Zhong, J., Gao, H., Khan, L., Thompson, D.K. and Zhou, J. (2007). Constructing gene co-expression networks and predicting functions of unknown genes by random matrix theory. *BMC Bioinformatics* **8,** 299.

Martin, M. (2011). Cutadapt removes adapter sequences from high-throughput sequencing reads. *EMBnet. journal* **17,** pp. 10-12.

Meng, X., Yuan, Y., Maestas, A. and Shen, Z. (2004). Recovery from DNA damage-induced G2 arrest requires actin-binding protein filamin-A/actin-binding protein 280. *J. Biol. Chem.* **279,** 6098-6105.

Meyer, E., Aglyamova, G.V. and Matz, M.V. (2011). Profiling gene expression responses of coral larvae (*Acropora millepora*) to elevated temperature and settlement inducers using a novel RNA-Seq procedure. *Mol. Ecol.* **20,** 3599-3616.

Meyer, E. and Weis, V.M. (2012). Study of cnidarian-algal symbiosis in the "omics" age. *Biol. Bull.* **223,** 44-65.

Müller, W.A. and Leitz, T. (2002). Metamorphosis in the Cnidaria. *Can. J. Zool.* **80,** 1755-1771.

Munday, P., Leis, J., Lough, J., Paris, C., Kingsford, M., Berumen, M. and Lambrechts, J. (2009). Climate change and coral reef connectivity. *Coral Reefs* **28,** 379-395.

Nelson, R., Fessler, L., Takagi, Y., Blumberg, B., Keene, D., Olson, P., *et al.* (1994). Peroxidasin: a novel enzyme-matrix protein of *Drosophila* development. *EMBO J.* **13,** 3438.

Nii, C.M. and Muscatine, L. (1997). Oxidative stress in the symbiotic sea anemone *Aiptasia pulchella* (Carlgren, 1943): contribution of the animal to superoxide ion production at elevated temperature. *Biol. Bull.* **192,** 444-456.

Nozawa, Y. and Harrison, P.L. (2007). Effects of elevated temperature on larval settlement and post-settlement survival in scleractinian corals, *Acropora solitaryensis* and *Favites chinensis*. *Mar. Biol.* **152,** 1181-1185.

Palmer, C.V. and Traylor-Knowles, N. (2012). Towards an integrated network of coral immune mechanisms. *Proc. R. Soc. Lond., Ser. B: Biol. Sci.* **279,** 4106-4114.

Pinzón, J.H., Kamel, B., Burge, C.A., Harvell, C.D., Medina, M., Weil, E. and Mydlarz, L.D. (2015). Whole transcriptome analysis reveals changes in expression of immune-

related genes during and after bleaching in a reef-building coral. *R. Soc. Open Sci.* **2,** 140214.

Polato, N.R., Voolstra, C.R., Schnetzer, J., DeSalvo, M.K., Randall, C.J., Szmant, A.M., *et al.* (2010). Location-specific responses to thermal stress in larvae of the reef-building coral *Montastraea faveolata*. *PLoS One* **5,** e11221.

Poole, A.Z., Kitchen, S.A., Dow, E.G. and Weis, V.M. (submitted). The role of complement in cnidarian-dinoflagellate symbiosis and immune challenge in the sea anemone *Aiptasia pallida*. *Front. Microbiol.*

Poole, A.Z. and Weis, V.M. (2014). TIR-domain-containing protein repertoire of nine anthozoan species reveals coral–specific expansions and uncharacterized proteins. *Dev. Comp. Immunol.* **46,** 480-488.

Portune, K.J., Voolstra, C.R., Medina, M.n. and Szmant, A.M. (2010). Development and heat stress-induced transcriptomic changes during embryogenesis of the scleractinian coral *Acropora palmata*. *Mar. Genomics* **3,** 51-62.

Putnam, H.M., Edmunds, P.J. and Fan, T.-Y. (2008). Effect of temperature on the settlement choice and photophysiology of larvae from the reef coral *Stylophora pistillata*. *Biol. Bull.* **215,** 135-142.

Quinlan, A.R. and Hall, I.M. (2010). BEDTools: a flexible suite of utilities for comparing genomic features. *Bioinformatics* **26,** 841-842.

Randall, C. and Szmant, A. (2009a). Elevated temperature reduces survivorship and settlement of the larvae of the Caribbean scleractinian coral, *Favia fragum* (Esper). *Coral Reefs* **28,** 537-545.

Randall, C.J. and Szmant, A.M. (2009b). Elevated temperature affects development, survivorship, and settlement of the elkhorn coral, *Acropora palmata* (Lamarck 1816). *Biol. Bull.* **217,** 269-282.

Rasband, W. (1997-2015) ImageJ. Bethesda, Maryland, USA, U. S. National Institutes of Health

Richier, S., Sabourault, C., Courtiade, J., Zucchini, N., Allemand, D. and Furla, P. (2006). Oxidative stress and apoptotic events during thermal stress in the symbiotic sea anemone, *Anemonia viridis*. *FEBS J.* **273,** 4186-4198.

Richmond, R.H. (1990). Reproduction and recruitment of corals : comparisons among the Caribbean, the tropical Pacific, and the Red Sea. *Mar. Ecol. Prog. Ser.* **60,** 185-203.

Rodriguez-Lanetty, M., Harii, S. and Hoegh-Guldberg, O.V.E. (2009). Early molecular responses of coral larvae to hyperthermal stress. *Mol. Ecol.* **18,** 5101-5114.

Schnitzler, C., Hollingsworth, L., Krupp, D. and Weis, V. (2011). Elevated temperature impairs onset of symbiosis and reduces survivorship in larvae of the Hawaiian coral, *Fungia scutaria*. *Mar. Biol.* **159,** 633-642.

Schnitzler, C.E. and Weis, V.M. (2010). Coral larvae exhibit few measurable transcriptional changes during the onset of coral-dinoflagellate endosymbiosis. *Mar. Genomics* **3,** 107-116.

Schwarz, J.A., Krupp, D.A. and Weis, V.M. (1999). Late larval development and onset of symbiosis in the scleractinian coral *Fungia scutaria*. *Biol. Bull.* **196,** 70-79.

Seneca, F.O., Forêt, S., Ball, E.E., Smith-Keune, C., Miller, D.J. and van Oppen, M.J. (2010). Patterns of gene expression in a scleractinian coral undergoing natural bleaching. *Mar. Biotechnol.* **12,** 594-604.

Shannon, P., Markiel, A., Ozier, O., Baliga, N.S., Wang, J.T., Ramage, D., *et al.* (2003). Cytoscape: a software environment for integrated models of biomolecular interaction networks. *Genome Res.* **13,** 2498-2504.

Shinzato, C., Shoguchi, E., Kawashima, T., Hamada, M., Hisata, K., Tanaka, M., *et al.* (2011). Using the *Acropora digitifera* genome to understand coral responses to environmental change. *Nature* **476,** 320-323.

Silverstein, R.N., Cunning, R. and Baker, A.C. (2015). Change in algal symbiont communities after bleaching, not prior heat exposure, increases heat tolerance of reef corals. *Glob. Chang. Biol.* **21,** 236-249.

Suwa, R., Nakamura, M., Morita, M., Shimada, K., Iguchi, A., Sakai, K. and Suzuki, A. (2010). Effects of acidified seawater on early life stages of scleractinian corals (Genus *Acropora*). *Fish. Sci.* **76,** 93-99.

Therneau, T. (2013) A package for survival analysis in S. R package version 2.37-4. pp. 23298-20032.

Trapnell, C., Pachter, L. and Salzberg, S.L. (2009). TopHat: discovering splice junctions with RNA-Seq. *Bioinformatics* **25,** 1105-1111.

van Oppen, M.J.H., Palstra, F.P., Piquet, A.M.T. and Miller, D.J. (2001). Patterns of coral-dinoflagellate associations in *Acropora*: significance of local availability and physiology of *Symbiodinium* strains and host-symbiont selectivity. *Proc. R. Soc. Lond., Ser. B: Biol. Sci.* **268,** 1759-1767.

Voolstra, C., Schnetzer, J., Peshkin, L., Randall, C., Szmant, A. and Medina, M. (2009a). Effects of temperature on gene expression in embryos of the coral *Montastraea faveolata*. *BMC Genomics* **10,** 627.

Voolstra, C.R., Schwarz, J.A., Schnetzer, J., Sunagawa, S., Desalvo, M.K., Szmant, A.M., *et al.* (2009b). The host transcriptome remains unaltered during the establishment of coral–algal symbioses. *Mol. Ecol.* **18,** 1823-1833.

Weis, V.M. (2008). Cellular mechanisms of Cnidarian bleaching: stress causes the collapse of symbiosis. *J. Exp. Biol.* **211,** 3059-3066.

Weis, V.M. (2010). The susceptibility and resilience of corals to thermal stress: adaptation, acclimatization or both? *Mol. Ecol.* **19,** 1515-1517.

Weis, V.M., Reynolds, W.S., deBoer, M.D. and Krupp, D.A. (2001a). Host-symbiont specificity during onset of symbiosis between the dinoflagellates *Symbiodinium* spp. and planula larvae of the scleractinian coral *Fungia scutaria*. *Coral Reefs* **20,** 301-308.

Winkler, N.S., Pandolfi, J.M. and Sampayo, E.M. (2015). *Symbiodinium* identity alters the temperature-dependent settlement behaviour of *Acropora millepora* coral larvae before the onset of symbiosis. *Proc. R. Soc. Lond. B. Biol. Sci.* **282,** 20142260.

Yakovleva, I.M., Baird, A.H., Yamamoto, H.H., Bhagooli, R., Nonaka, M. and Hidaka, M. (2009). Algal symbionts increase oxidative damage and death in coral larvae at high temperatures. *Mar. Ecol. Prog. Ser.* **378,** 105-112.

Yu, G., Wang, L.-G., Han, Y. and He, Q.-Y. (2012). clusterProfiler: an R package for comparing biological themes among gene clusters. *OMICS: J. Integrative Biol.* **16,** 284-287.

Yuyama, I., Harii, S. and Hidaka, M. (2012). Algal symbiont type affects gene expression in juveniles of the coral *Acropora tenuis* exposed to thermal stress. *Mar. Environ. Res.* **76,** 41-47.

5. CONCLUSION

The work presented here reveals new information about the cellular and molecular determinants of symbiosis at three different phases of cnidarian-dinoflagellate symbiosis: (1) onset, (2) maintenance and (3) breakdown. In Chapter 2, the molecular and cellular characterization of the sphingosine rheostat supported its hypothesized role in symbiosis maintenance. In addition, a new role in symbiont recognition and selection was proposed based on sphingosine rheostat expression and sphingolipid quantification during a recolonization experiment in *A. pallida*. In Chapter 3, modulation of the sphingosine rheostat was revealed to have two phases with heat stress, leading to the development of its predicted role in the cnidarian HSR, but not symbiosis breakdown. Finally, the last chapter looked at the combination of the onset of symbiosis and hyperthermal stress on aposymbiotic coral larvae from *A. digitifera*. From this study, dramatic phenotypes and global transcriptomic patterns emerged. These two events in concert cause immune suppression in the larvae by day three that could underlie the distinct colonization phenotypes observed. Taken together, these studies identify shared processes and further our understanding of the dynamic process of symbiosis in a changing world.

5.1 Sphingolipid metabolism contributes to the colonization and heat stress response in two model cnidarians at different developmental stages

The sphinogsine rheostat mediates phagocytosis of pathogenic and beneficial microbes (Heung *et al.*, 2006, Prakash *et al.*, 2010, Bryan *et al.*, 2015), and plays a role in establishment and maintenance of cnidarian-dinoflagellate symbiosis. The cnidarian sphingosine rheostat model was first proposed in 2006 by the Rodriguez-Lanetty and coworkers, and has been investigated over the last decade (this dissertation and Detournay *et al.* (2011). In Chapters 2 and 4, I looked at the onset of symbiosis in two cnidarian symbiosis model systems. In *A. pallida*, the sphingosine rheostat differed in different symbiotic states and at the onset of symbiosis, with a shift in the rheostat toward cell-survival symbiotic and newly colonized animals (Figure 5.1). To explore the expression patterns of genes in sphingolipid metabolism from the *A. digitifera* larvae

visually, I created a heatmap of the normalized expression (z-score) (Figure 5.2). Genes were categorized based on their function, either increasing pro-apoptotic ceramide or decreasing ceramide. The expression of SPHK and SGPP was upregulated in the colonization (CL) treatment. Moreover, *A. digitifera* larvae showed opposing pattern of expression in the aposymbiotic larvae with downregulation of SPHK coinciding with upreguation of SGPP (Figure 5.2). These results support the differences observed between symbiotic, aposymbiotic and newly recolonized *A. pallida* (Figure 5.1).

In Chapters 3 and 4, I investigated the effect of hyperthermal stress on *A. pallida* and *A. digitifera* at different developmental stages. In both cnidarians, sphingolipid metabolism was altered with the onset of a heat stress. In *A. pallida*, acute heat stress (Phase I) repressed transcription and activity of the sphingosine rheostat enzyme thereby reducing sphingolipid levels. With chronic heat stress (Phase II), the pro-apoptotic AP-SGPP expression and Sph lipid concentrations increased. These patterns suggest that sphingosine rheostat plays a role in longer-term acclimation to heat stress in cnidarians. From the KEGG over-representation analysis on the DEGs from *A. digitifera* larvae, 19 DEGs were enriched in the sphingolipid signaling pathway on day one (p-value =0.007; Table 4.5, pg. 152). Heat stress caused an upregulation of SPHK in the elevated temperature (AH) and combination of elevated temperature with colonization (CH) treatment compared to the control. In contrast, SGPP was downregulated in the AH and CH treatments. These results support the differences observed in symbiotic *A. pallida* (Figure 5.1) and points to a common HSR of cnidarians in the presence of symbionts.

Other physiological changes documented in the cnidarian HSR include increased NO production and host apoptosis. Interestingly, sphingolipids directly or indirectly modifies each of these cellular defense mechanisms. I will discuss how sphingolipid metabolism can modify NO production in detail. High cellular NO in *A. pallida* exposed to hyperthermal temperatures remains elevated for four days before returning to basal levels (Hawkins *et al.*, 2013). The contribution of both partners to elevated NO levels is still poorly understood, but NO production by nitric oxide synthases (NOS) in the host has been documented in the gastrodermal tissue where the *Symbiodinium* spp. reside (Safavi-Hemami *et al.*, 2010). NO can have both pro-survival and pro-inflammatory

effects on the cell. The sequential activation of neutral sphingomyelinase (N-SMase) and then SPHK results in increased cellular S1P, that in turn activates protein kinase B (Akt) through receptor-mediated signaling, and phosphorylates and activates endothelial NOS (eNOS) (De Palma *et al.*, 2006). Both S1P and low NO are inhibitory to pro-inflammatory signaling. In contrast, immune elicitors and elevated ROS trigger inducible NOS (iNOS) resulting in high cellular NO, and NO-dependent elevations in ceramide through the activation of lysosomal acidic sphingomyelinases (A-SMase) (Perrotta *et al.*, 2008). Elevated ceramide can also activate eNOS independently of Akt leading to pro-inflammatory environment (Florio *et al.*, 2003). Therefore, NO production regulates ceramide levels, synthesis, and trafficking, and determines cell fate.

In a transcriptional study of the coral *Acropora palmata*, the NOS interacting protein, a negative modulator of eNOS, was downregulated with elevated temperature suggesting an active role of eNOS in the HSR. NO levels did not change with exogenous additions of pro-survival metabolite S1P (Detournay *et al.*, 2011), suggesting that the predominant NOS active during phase I of the HSR is pro-inflammatory iNOS. Furthermore, heat shock proteins that are part of Phase I are allosteric enhancers of iNOS and co-precipitate in heat stress corals (Ross, 2014).

Based on the characterized role of sphingolipids in activating NO production and apoptosis in mammalian model systems, I have added these proposed mechanisms to the sphingosine rheostat model with hyperthermal stress in Figure 5.1. At ambient temperature in symbiotic-state, S1P can be exported and initiate receptor-mediated cell signaling that activates the PI3K/Akt pathway which in turn activates eNOS, resulting in low constitutive NO production that promotes cellular N-SMase activity but inhibits A-SMase activity in the lysosome. From 12 h to one day after the onset of heat stress, the symbiotic animals have high cytosolic levels of ROS and NO, perhaps from coupled activity of eNOS and iNOS, as symbiont photosynthesis is disrupted. The high ROS and NO could activate N-SMase, lysosomal A-SMase and *de novo* synthesis to increase cellular ceramide. Heat and oxidative stress of mammal cell lines leads to ceramide accumulation as early as 30 min, but not other sphingosine rheostat lipids (Goldkorn *et al.*, 1991, Jenkins, 2003). Ceramides then assemble with cholesterol to form ceramide-

rich rafts in organelle membranes altering membrane fluidity and cellular signaling toward cell death (Balogh *et al.*, 2013), and could repress sphingosine rheostat expression and activity seen in *A. pallida* and *A. digitifera*. All these events lead to increased host apoptosis and 29-50% symbiosis loss during Phase I of the HSR. In Phase II of the HSR, the transcription and activity of the rheostat is resumed as ROS and NO levels are lowered, in favor of high Sph levels leading to a second round of host cell death observed in a study by Hawkins *et al.* (2013). In contrast, in aposymbiotic state the rheostat is active during Phase I of the HSR with the rheostat shifted toward increased SPHK expression in *A. pallida* and *A. digitifera*.

5.2 Establishment of symbiosis under elevated temperature corresponds with phenotypic and transcriptomic differences

From the CH treatment, I observed a dramatic reduction in survival, successful colonization and density of symbionts in *A. digitifera* larvae compared to the CL treatment. These phenotypic differences were consistent with previous studies (Baird, 2006, Yakovleva *et al.*, 2009, Schnitzler *et al.*, 2011). Another consequence of the CH treatment was the acceleration of development from larvae to polyp. Settlement of competent larvae typically requires a substrate cue, like crustose coralline algae (Müller *et al.*, 2002). However, temperature is known to expedite development in other corals (Heyward *et al.*, 2010). The RNASeq analysis on *A. digitifera* larvae resulted in 64.6% of the genome being differentially expressed in the treatment conditions, many of which were associated with metamorphosis and temperature. I explored the CH expression patterns in more detail, and revealed that this treatment cause immune suppression by day three of the experiment. From the co-expression analysis I identified three modules that were significantly correlated with my experimental treatments. From these, I found genes responsive to stress and cell death upregulated with temperature while genes involved in ion transport were downregulated. The genes associated with the CL treatment on day one were linked to endocytosis and cytoskeletal remodeling, which is consistent with the process of acquiring symbionts. Collectively, the observed changes in host phenotype and transcriptome suggest that the undergoing colonization at an elevated temperature is stressful to *A. digitifera* larvae.

5.3 Future studies

5.3.1 Further exploration of sphingolipid signaling in cnidarian model systems

The data collected in Chapters 2 and 3 contributes to our understanding of the cnidarian sphingosine rheostat as a regulator of symbiont colonization dynamics and heat stress response, two important biological processes in these organisms (Figure 5.1). From the genomic survey, I identified one G protein-coupled receptor with homology to a S1P receptor. This would allow for extracellular S1P signaling, that thus far has been thought to evolve later in animal evolution. Cnidarians genomes share a surprising amount of homology with higher metazoans that has been lost in other invertebrate taxa (Putnam *et al.*, 2007, Reitzel *et al.*, 2008, Shinzato *et al.*, 2011). Functionally characterizing the molecular properties, localization and substrate-affinity of this receptor will contribute greatly to our sphingosine rheostat model, but also to the evolution of the sphingolipid gene repertoire in metazoans.

During symbiont colonization, the temporal patterns suggest that AP-SPHK and AP-SGPP enzymatic activity and their metabolites could contribute to the symbiont recognition and winnowing process *in situ*. In this study, I measured sphingolipid concentrations as an indirect measure of enzyme activity. To add to these findings, the enzymatic activity of AP-SPHK should be directly measured. Moreover, the transcription and metabolites were quantified from the whole animal, however, the intracellular symbionts are only found in the gastrodermal tissue. To gain a higher resolution of establishment and stable cnidarian symbiosis, methods that can isolate expression to the gastrodermal tissue should be tested in different symbiotic states, and when applicable in anemones taking up symbionts. These would include laser capture micro-dissection coupled with qPCR, *in situ* hybridization of AP-SPHK and AP-SGPP probes to look at tissue-specific expression, and quantification of fluorescently-labeled anti-SPHK1 used in Chapter 2 from anemone cross-sections. In addition, lipid metabolism could be monitored using live-cell imaging of fluorescently-labeled Sph and S1P (Hakogi *et al.*, 2003) on cell macerates from *A. pallida* (Gates *et al.*, 1992a).

From the heat stress experiment, I identified two phases of sphingosine rheostat regulation in the cnidarian HSR. As mentioned in Chapter 3, expanding the sphingosine

rheostat-mediated HSR to other non-symbiotic cnidarian model systems is needed to understand the temporal patterns of this biphasic response across the Phylum. In this study, I found that the rheostat might not contribute to symbiont loss and host apoptosis during Phase I (Figure 3.8) as previously predicted by Detournay and Weis (2011). Earlier time points from 30 min to three hours should be sampled to quantify gene expression, enzyme activity and sphingolipid concentrations. This would illuminate early sphingolipid signaling that could contribute to symbiont loss. Comparison with the mammalian HSR (discussed above) also points to other potential candidate genes that warrant further investigation. These include N-SMase, A-SMase, and genes involved in ceramide biosynthesis and recycling. Furthermore, the temporal patterns of ceramide concentrations should be quantified and overlaid with the cnidarian HSR model I proposed in Figure 3.8.

Another continuation of research on sphingolipid signaling in cnidarians should address the role of intracellular calcium ($[Ca^{2+}]_c$) that is mobilized by changes in cellular sphingolipid concentrations. During phagocytosis, early $[Ca^{2+}]_c$ elevations activates SPHK that creates a positive feedback loop, with elevated S1P causing sustained Ca2+ release (Maceyka *et al.*, 2002). Changes in $[Ca^{2+}]_c$ have been observed in bleaching corals (Fang *et al.*, 1997, Fang *et al.*, 1998, Huang *et al.*, 1998, Sandeman, 2006) and are associated with host cell detachment in *A. pallida* (Sawyer *et al.*, 2001). Given that intracellular Ca^{2+} initiates the fusion of the phagosome-lysosome in microbial phagocytosis (Nunes *et al.*, 2010), elevated Ca^{2+} could be a signaling precursor to symbiont removal. The downregulation of SGPP and calmodulin, a calcium-binding protein involved in the immune response, in the symbiotic state (Rodriguez-Lanetty *et al.*, 2006) sets up testable hypotheses that S1P levels increases and Ca^{2+} signaling decreases in the symbiotic state. Measuring the $[Ca^{2+}]_c$ in the model *A. pallida* and correlating Ca^{2+} signaling patterns to S1P-mediated responses during onset of symbiosis and heat stress would provide insights on potential downstream signaling cascades from these important secondary messengers. To isolate the effect of intracellular S1P on $[Ca^{2+}]_c$, caged S1P probes could be used (Meyer zu Heringdorf *et al.*, 2003). Caged S1P is a derivative of S1P that is inactive due to the presence of a photo-labile group on an

S1P functional group. Photo-activation with UV illumination cleaves the photo-labile group releasing biologically active S1P within the cell. The use of fluorescent Ca^{2+} indicator dyes would capture the temporal Ca^{2+} changes with S1P release.

5.3.2 Future work on the interaction of the onset of symbiosis and elevated temperature

In Chapter 4, I focused on the significant DEGs with the colonization-by-temperature interaction. However, there are many interesting patterns that emerged in the AH and CL treatments that should be addressed. Shared DEGs between these two treatments showed a positive correlation (Pearson's correlation r^2 =0.539), suggesting that the expression was very similar between these two treatment groups. However, what is more striking about this study is the number of DEGs recovered from the CL treatment alone (1,980 on day one and 468 on day three). Previous studies that have tried to capture symbiosis-influenced patterns during the onset of symbiosis in coral larvae recovered very few DEGs (Voolstra *et al.*, 2009b, Schnitzler *et al.*, 2010). This dramatic difference could be the result of the sensitivity of the RNASeq technology over the microarrays used in the previous experiments or the fact that I used different symbiont type (type A3) from the parental colony (type C1). To follow up on this study, the symbiont colonization dynamics, larval survival and gene expression should be measured using the homologous C1.

An unexpected outcome from the AH, CL and CH treatments was the inducement of metamorphosis. This result is not novel to *A. digitifera* larvae and has been noted in other coral studies (Edmunds *et al.*, 2001, Nozawa *et al.*, 2007, Putnam *et al.*, 2008, Randall *et al.*, 2009b, Heyward *et al.*, 2010), however, the high prevalence with the combination of colonization and temperature should be addressed further. The premature development of these individuals could have grave consequences for the recruitment and resilience of these species on the reef. Testing combinations of different temperature and symbiont concentrations will help reveal the effect of these two treatments on coral development.

As a consequence of metamorphosis occurring in my samples, I had to exclude more than half of the DEGs recovered from the RNASeq analysis. Using traditional clustering tools it was not possible to separate out the treatment effects on the gene

expression, however, by using the co-expression network analysis I was able to separate them for temperature, colonization and time. Using the same approach on the full dataset could identify genes associated with symbiosis, temperature and development that were previously discarded. By targeting functionally annotated genes, highly interconnected lineage-specific candidate genes could be identified. The function of these candidate genes could then be addressed in *A. digitifera* using molecular tools for gene knockdown such as morpholinos and CRISPR interference.

Figure 5.1 Expanded cnidarian sphingosine rheostat model between symbiotic states exposed to hyperthermal stress. Here I added my findings from Chapters 2 and 3 to the original cnidarian sphingosine rheostat model proposed by Rodriguez-Lanetty *et al.* (2006). At ambient temperature (25 °C) in symbiotic-state, the rheostat shifts toward upreguation of SPHK and increased S1P in symbiotic animals, but not in aposymbiotic animals (1). In both states, S1P can be exported and initiate receptor-mediated cell signaling (2) that activates the PI3K/Akt pathway (3) which in turn activates eNOS, resulting in low constitutive NO production that promotes cellular N-SMase activity but inhibits A-SMase activity in the lysosome. From 12 h to one day after the onset of heat stress (33 °C), the symbiotic animals have high cytosolic levels of ROS and NO, perhaps from coupled activity of eNOS and iNOS, as symbiont photosynthesis is disrupted (1). The high ROS and NO could activate N-SMase, lysosomal A-SMase and *de novo* synthesis to increase cellular ceramide (2). The ceramide accumulation could form ceramide-rich lipid platforms (3), and repress sphingosine rheostat expression and activity (4). All these events lead to increased host apoptosis and 29-50% symbiosis loss during Phase I of the HSR. In Phase II of the HSR from days four to seven of heat stress, the transcription and activity of the rheostat is resumed (1) as ROS and NO levels are lowered (2), in favor of high Sph levels leading to a second round of host cell death (3) observed in a study by Hawkins *et al.* (2013) From day four to seven, total symbiont loss increases slightly by approximately 17-19%. In contrast, in aposymbiotic state the rheostat is active during Phase I of the HSR with the rheostat shifted toward increased SPHK expression. Several aposymbiotic animals died before day four, so Phase II HSR was not recorded. Solid lines show direct evidence collected in this dissertation and dashed lines are predictions based on previous studies.

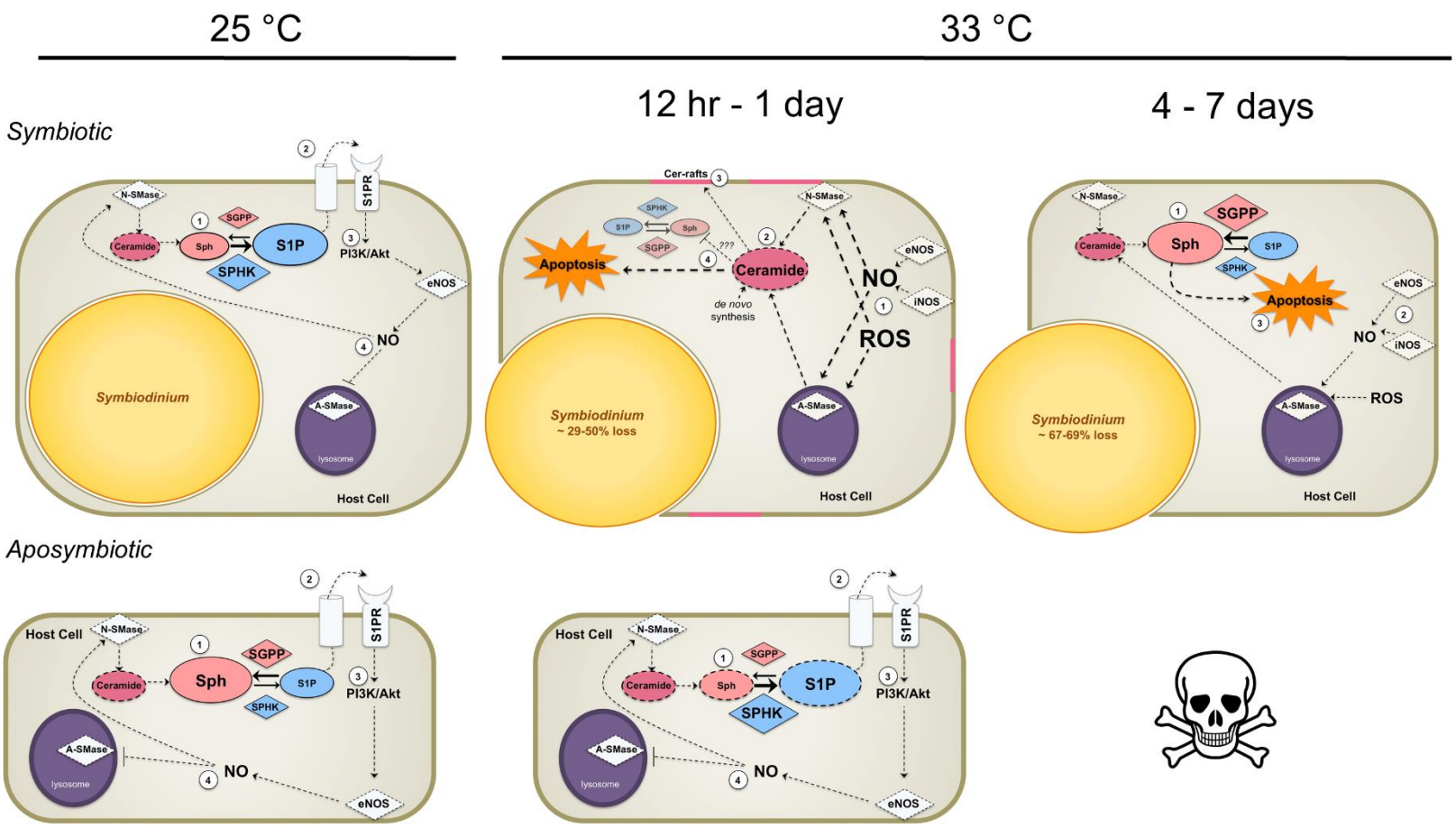
25 °C
33 °C
12 hr - 1 day
4 - 7 days
Symbiotic
Aposymbiotic
N-SMase
SGPP
Ceramide
Sph
S1P
SPHK
S1PR
PI3K/Akt
eNOS
NO
iNOS
ROS
Apoptosis
Cer-rafts
de novo
synthesis
???
A-SMase
lysosome
Symbiodinium
~ 29-50% loss
~ 67-69% loss
Host Cell

Figure 5.1

Figure 5.2 Differential expression of genes involved in sphingolipid signaling and metabolism from *A. digitifera* larvae in AL, AH, CL and CH treatments on day one. A cluster heatmap showing the correlation between rlog normalized counts for each gene (row) by sample (column). Row z-score, or scaled expression value, of each gene is plotted on a purple to cyan scale. Black tiles represent mean expression. The purple tiles indicate low expression from the mean expression whereas the cyan tiles indicate high expression. The colored column next to the heatmap on the left indicates the activity of that enzyme into two broad categories. The enzymatic activity of that gene leads to increased ceramide concentrations through *de novo* synthesis and salvage pathway (red), or decreased ceramide in the complex hydrolysis and sphingosine rheostat pathway (blue) (see Table 2.1 in Chapter 2). Genes with an asterisk next to their name were significant with metamorphosis on day three, and excluded from the original analysis in Chapter 4.

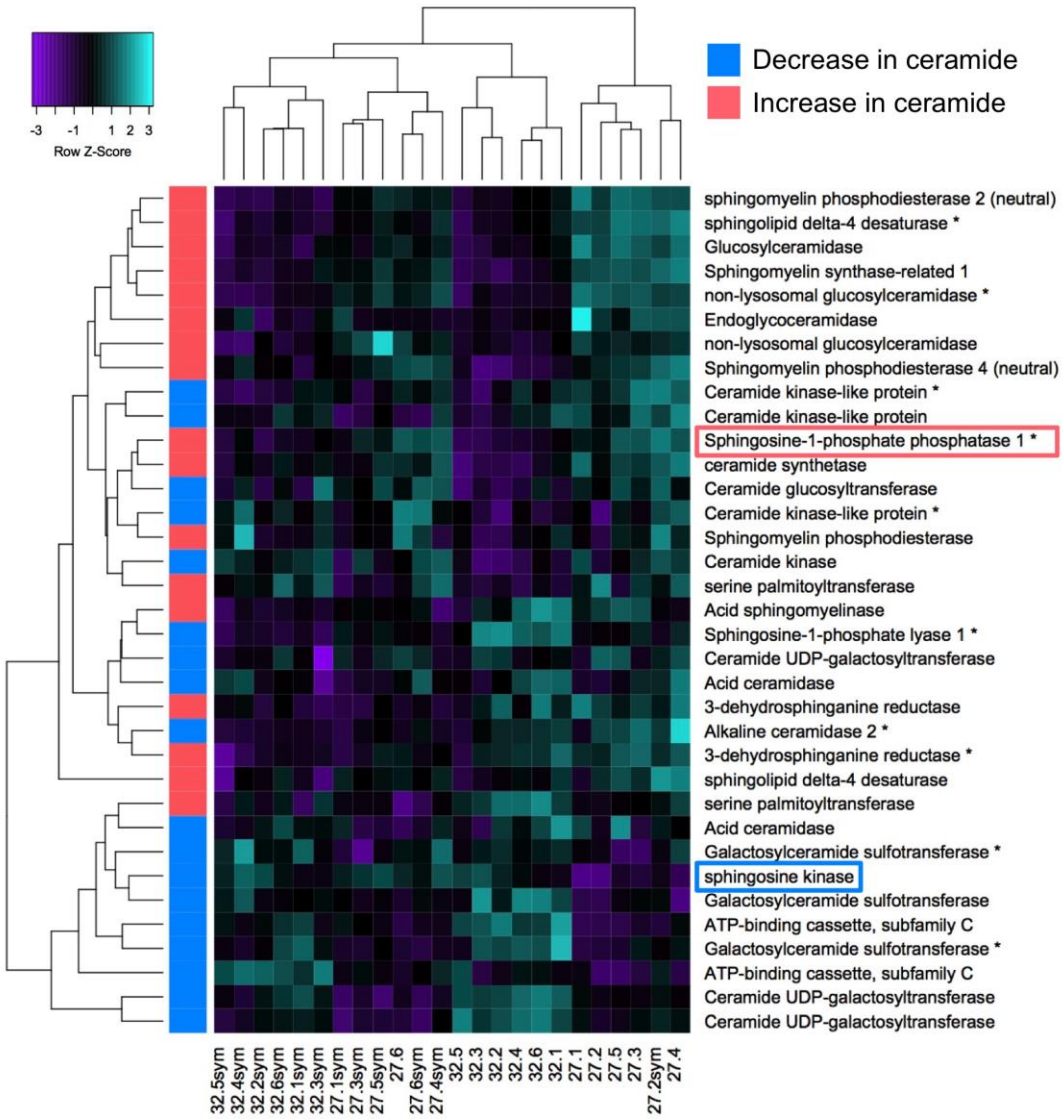
Row Z-Score
-3
-1
1
2
3
Decrease in ceramide
Increase in ceramide
sphingomyelin phosphodiesterase 2 (neutral)
sphingolipid delta-4 desaturase *
Glucosylceramidase
Sphingomyelin synthase-related 1
non-lysosomal glucosylceramidase *
Endoglycoceramidase
non-lysosomal glucosylceramidase
Sphingomyelin phosphodiesterase 4 (neutral)
Ceramide kinase-like protein *
Ceramide kinase-like protein
Sphingosine-1-phosphate phosphatase 1 *
ceramide synthetase
Ceramide glucosyltransferase
Ceramide kinase-like protein *
Sphingomyelin phosphodiesterase
Ceramide kinase
serine palmitoyltransferase
Acid sphingomyelinase
Sphingosine-1-phosphate lyase 1 *
Ceramide UDP-galactosyltransferase
Acid ceramidase
3-dehydrosphinganine reductase
Alkaline ceramidase 2 *
3-dehydrosphinganine reductase *
sphingolipid delta-4 desaturase
serine palmitoyltransferase
Acid ceramidase
Galactosylceramide sulfotransferase *
sphingosine kinase
Galactosylceramide sulfotransferase
ATP-binding cassette, subfamily C
Galactosylceramide sulfotransferase *
ATP-binding cassette, subfamily C
Ceramide UDP-galactosyltransferase
Ceramide UDP-galactosyltransferase
32.5sym
32.4sym
32.2sym
32.6sym
32.1sym
32.3sym
27.1sym
27.3sym
27.5sym
27.6
27.6sym
27.4sym
32.5
32.3
32.2
32.4
32.6
32.1
27.1
27.2
27.5
27.3
27.2sym
27.4

Figure 5.2

5.4 References

Baird, A.H., Gilmour, James P., Kamiki, Takayuki M., Nonaka, Masanori, Pratchett, Morgan S., Yamamoto, Hiromi H., and Yamasaki, Hideo (2006) Temperature tolerance of symbiotic and non-symbiotic coral larvae. In *Proceedings of the 10th International Coral Reef Symposium In: 10th International Coral Reef Symposium*. Okinawa, Japan.

Balogh, G., Péter, M., Glatz, A., Gombos, I., Török, Z., Horváth, I., *et al.* (2013). Key role of lipids in heat stress management. *FEBS Lett.* **587,** 1970-1980.

Bryan, A.M., Del Poeta, M. and Luberto, C. (2015). Sphingolipids as regulators of the phagocytic response to fungal infections. *Mediators Inflamm.* **2015,** 640540.

De Palma, C., Meacci, E., Perrotta, C., Bruni, P. and Clementi, E. (2006). Endothelial nitric oxide synthase activation by tumor necrosis factor α through neutral sphingomyelinase 2, sphingosine kinase 1, and sphingosine 1 phosphate receptors a novel pathway relevant to the pathophysiology of endothelium. *Arterioscler. Thromb. Vasc. Biol.* **26,** 99-105.

Detournay, O. and Weis, V.M. (2011). Role of the sphingosine rheostat in the regulation of cnidarian-dinoflagellate symbioses. *Biol. Bull.* **221,** 261-269.

Edmunds, P., Gates, R. and Gleason, D. (2001). The biology of larvae from the reef coral *Porites astreoides*, and their response to temperature disturbances. *Mar. Biol.* **139,** 981-989.

Fang, L.-S., Wang, J.-T. and Lin, K.-L. (1998). The subcellular mechanism of the release of zooxanthellae during coral bleaching. *Proc. Natl. Sci. Counc. Rep. China Pt. B Life Sci.* **22,** 150-158.

Fang, L.S., Huang, S.P. and Lin, K.L. (1997). High temperature induces the synthesis of heat-shock proteins and the elevation of intracellular calcium in the coral *Acropora grandis*. *Coral Reefs* **16,** 127-131.

Florio, T., Arena, S., Pattarozzi, A., Thellung, S., Corsaro, A., Villa, V., *et al.* (2003). Basic fibroblast growth factor activates endothelial nitric-oxide synthase in CHO-K1 cells via the activation of ceramide synthesis. *Mol. Pharmacol.* **63,** 297-310.

Gates, R. and Muscatine, L. (1992a). Three methods for isolating viable anthozoan endoderm cells with their intracellular symbiotic dinoflagellates. *Coral Reefs* **11,** 143-145.

Goldkorn, T., Dressler, K.A., Muindi, J., Radin, N.S., Mendelsohn, J., Menaldino, D., *et al.* (1991). Ceramide stimulates epidermal growth factor receptor phosphorylation in A431 human epidermoid carcinoma cells. Evidence that ceramide may mediate sphingosine action. *J. Biol. Chem.* **266,** 16092-16097.

Hakogi, T., Shigenari, T., Katsumura, S., Sano, T., Kohno, T. and Igarashi, Y. (2003). Synthesis of fluorescence-labeled sphingosine and sphingosine 1-phosphate; effective tools for sphingosine and sphingosine 1-phosphate behavior. *Biorg. Med. Chem. Lett.* **13,** 661-664.

Hawkins, T.D., Bradley, B.J. and Davy, S.K. (2013). Nitric oxide mediates coral bleaching through an apoptotic-like cell death pathway: evidence from a model sea anemone-dinoflagellate symbiosis. *FASEB J.* **27,** 4790-4798.

Heung, L.J., Luberto, C. and Del Poeta, M. (2006). Role of sphingolipids in microbial pathogenesis. *Infect. Immun.* **74,** 28-39.

Heyward, A. and Negri, A. (2010). Plasticity of larval pre-competency in response to temperature: observations on multiple broadcast spawning coral species. *Coral Reefs* **29,** 631-636.

Huang, S.P., Lin, K.L. and Fang, L.S. (1998). The involvement of calcium in heat-induced coral bleaching. *Zool. Stud.* **37,** 89-94.

Jenkins, G. (2003). The emerging role for sphingolipids in the eukaryotic heat shock response. *Cell. Mol. Life Sci.* **60,** 701-710.

Jenkins, G.M., Cowart, L.A., Signorelli, P., Pettus, B.J., Chalfant, C.E. and Hannun, Y.A. (2002). Acute activation of de novo sphingolipid biosynthesis upon heat shock causes an accumulation of ceramide and subsequent dephosphorylation of SR proteins. *J. Biol. Chem.* **277,** 42572-42578.

Jenkins, G.M., Richards, A., Wahl, T., Mao, C., Obeid, L. and Hannun, Y. (1997). Involvement of yeast sphingolipids in the heat stress response of *Saccharomyces cerevisiae*. *J. Biol. Chem.* **272,** 32566-32572.

Maceyka, M., Payne, S.G., Milstien, S. and Spiegel, S. (2002). Sphingosine kinase, sphingosine-1-phosphate, and apoptosis. *Biochim. Biophys. Acta* **1585,** 193 - 201.

Meyer zu Heringdorf, D., Liliom, K., Schaefer, M., Danneberg, K., Jaggar, J.H., Tigyi, G. and Jakobs, K.H. (2003). Photolysis of intracellular caged sphingosine-1-phosphate causes Ca2+ mobilization independently of G-protein-coupled receptors. *FEBS Lett.* **554,** 443-449.

Müller, W.A. and Leitz, T. (2002). Metamorphosis in the Cnidaria. *Can. J. Zool.* **80,** 1755-1771.

Nozawa, Y. and Harrison, P.L. (2007). Effects of elevated temperature on larval settlement and post-settlement survival in scleractinian corals, *Acropora solitaryensis* and *Favites chinensis*. *Mar. Biol.* **152,** 1181-1185.

Nunes, P. and Demaurex, N. (2010). The role of calcium signaling in phagocytosis. *J. Leukoc. Biol.* **88,** 57-68.

Perrotta, C., De Palma, C. and Clementi, E. (2008). Nitric oxide and sphingolipids: mechanisms of interaction and role in cellular pathophysiology. *Biol. Chem.* **389,** 1391-1397.

Prakash, H., Luth, A., Grinkina, N., Holzer, D., Wadgaonkar, R., Gonzalez, A.P., *et al.* (2010). Sphingosine kinase-1 (SphK-1) regulates *Mycobacterium smegmatis* infection in macrophages. *PLoS One* **5,** e10657.

Putnam, H.M., Edmunds, P.J. and Fan, T.-Y. (2008). Effect of temperature on the settlement choice and photophysiology of larvae from the reef coral *Stylophora pistillata*. *Biol. Bull.* **215,** 135-142.

Putnam, N.H., Srivastava, M., Hellsten, U., Dirks, B., Chapman, J., Salamov, A., *et al.* (2007). Sea anemone genome reveals ancestral eumetazoan gene repertoire and genomic organization. *Science* **317,** 86-94.

Randall, C.J. and Szmant, A.M. (2009b). Elevated temperature affects development, survivorship, and settlement of the elkhorn coral, *Acropora palmata* (Lamarck 1816). *Biol. Bull.* **217,** 269-282.

Reitzel, A.M., Sullivan, J.C., Traylor-Knowles, N. and Finnerty, J.R. (2008). Genomic survey of candidate stress-response genes in the estuarine anemone *Nematostella vectensis*. *Biol. Bull.* **214,** 233-254.

Rodriguez-Lanetty, M., Phillips, W. and Weis, V. (2006). Transcriptome analysis of a cnidarian - dinoflagellate mutualism reveals complex modulation of host gene expression. *BMC Genomics* **7,** 23.

Ross, C. (2014). Nitric oxide and heat shock protein 90 co-regulate temperature-induced bleaching in the soft coral *Eunicea fusca*. *Coral Reefs* **33,** 513-522.

Safavi-Hemami, H., Young, N.D., Doyle, J., Llewellyn, L. and Klueter, A. (2010). Characterisation of nitric oxide synthase in three cnidarian-dinoflagellate symbioses. *PLoS One* **5,** e10379-e10379.

Sandeman, I. (2006). Fragmentation of the gastrodermis and detachment of zooxanthellae in symbiotic cnidarians: a role for hydrogen peroxide and Ca2+ in coral bleaching and algal density control. *Rev. Biol. Trop.* **54,** 79-96.

Sawyer, S.J. and Muscatine, L. (2001). Cellular mechanisms underlying temperature-induced bleaching in the tropical sea anemone A*iptasia pulchella*. *J. Exp. Biol.* **204,** 3443-3456.

Schnitzler, C., Hollingsworth, L., Krupp, D. and Weis, V. (2011). Elevated temperature impairs onset of symbiosis and reduces survivorship in larvae of the Hawaiian coral, *Fungia scutaria*. *Mar. Biol.* **159,** 633-642.

Schnitzler, C.E. and Weis, V.M. (2010). Coral larvae exhibit few measurable transcriptional changes during the onset of coral-dinoflagellate endosymbiosis. *Mar. Genomics* **3,** 107-116.

Shinzato, C., Shoguchi, E., Kawashima, T., Hamada, M., Hisata, K., Tanaka, M., *et al.* (2011). Using the *Acropora digitifera* genome to understand coral responses to environmental change. *Nature* **476,** 320-323.

Voolstra, C.R., Schwarz, J.A., Schnetzer, J., Sunagawa, S., Desalvo, M.K., Szmant, A.M., *et al.* (2009b). The host transcriptome remains unaltered during the establishment of coral–algal symbioses. *Mol. Ecol.* **18,** 1823-1833.

Yakovleva, I.M., Baird, A.H., Yamamoto, H.H., Bhagooli, R., Nonaka, M. and Hidaka, M. (2009). Algal symbionts increase oxidative damage and death in coral larvae at high temperatures. *Mar. Ecol. Prog. Ser.* **378,** 105-112.

APPENDIX

6. APPENDIX: A SIMPLE QPCR METHOD FOR QUANTIFICATION OF DINOFLAGELLATES DURING REESTABLISHMENT OF SYMBIOSIS WITH THE SEA ANEMONE *AIPTASIA PALLIDA*

Sheila A. Kitchen

Angela Z. Poole

Virginia M. Weis

6.1 Abstract

Mutualistic symbioses between cnidarians, such as corals and sea anemones, and dinoflagellates in the genus *Symbiodinium* are of great ecological importance due to their roles in coral reef ecosystem diversity and productivity. Studying the establishment of symbiosis is essential for understanding the underlying mechanisms that regulate symbiont recognition, specificity, and the ability of symbionts to persist in host cells. In the laboratory, the symbiotic sea anemone *Aiptasia pallida* (= *Aiptasia pallida*) can be rendered symbiont-free (aposymbiotic) and experimentally recolonized to investigate the dynamics of this mutualistic partnership at early stages of symbiosis establishment. A variety of methods have been developed to measure *Symbiodinium* abundance during onset and breakdown of symbiosis in cnidarians, however most of these traditional techniques are not capable of detecting low symbiont numbers during early time points in recolonization experiments. In this study, we present a simple relative quantitative PCR assay to determine successful reestablishment of symbiosis over a period of three days. Relative levels of symbiont ribosomal large subunit 28S DNA were compared across different symbiotic states. Differences in relative quantities of symbionts were detected between aposymbiotic and recolonized *A. pallida* one day after inoculation, whereas traditional quantification methods proved unreliable under the same time course. This quick and sensitive qPCR assay can be applied to other cnidarian hosts to monitor symbiosis establishment and to studies on symbiosis breakdown.

6.2 Introduction

Cnidarians, such as sea anemones and corals, engage in mutualistic relationships with intracellular photosynthetic dinoflagellates in the genus *Symbiodinium*. Initiation of cnidarian-dinoflagellate symbiosis involves complex interpartner communication including host-symbiont contact, symbiont colonization (also referred to as infection) of host tissues and subsequent symbiont sorting within the host gastrodermal tissue (Davy *et al.*, 2012). This symbiosis forms the basis for the high productivity and diversity of coral reef ecosystems and therefore, the breakdown of this intimate partnership negatively impacts corals and coral reef health (Jones *et al.*, 2004, Pratchett *et al.*, 2009, Weis *et al.*, 2009). The cellular and physiological factors that are involved in the initiation and

breakdown of symbiosis are therefore of ecological importance and have been a focused research area in the study of cnidarian-dinoflagellate symbiosis.

Experimentation on the dynamics of onset or breakdown of cnidarian-dinoflagellate symbiosis often requires the measurement of *Symbiodinium* density within a host to determine treatment effect. Symbiont density is commonly measured in studies investigating colonization success at the onset of symbiosis (Weis *et al.*, 2001b, Hambleton *et al.*, 2014), symbiont loss during symbiosis breakdown (also referred to as cnidarian bleaching) (Ganot *et al.*, 2011, Hill *et al.*, 2014), or quantification of different *Symbiodinium* spp. types within host tissue (Correa *et al.*, 2009, Coffroth *et al.*, 2010, Arif *et al.*, 2014, McIlroy *et al.*, 2014). Although there are several methods used for quantifying *Symbiodinium* density, each technique was developed for particular life-stages (adult *vs.* larvae), monitoring time frames, or desired quantification outcomes (absolute *vs.* relative) (summarized in Table 1). Many of these techniques lack the sensitivity needed to detect low symbiont abundance at early time points during onset of symbiosis, and those that can detect low symbiont abundance are only applicable to studies in larvae (Table 1). Therefore, the goal of this study was to develop a simple relative quantitative PCR method (qPCR) for symbiont detection in the adult sea anemone *A. pallida*, an established laboratory model organism. *A. pallida* is a good laboratory model for the study of cnidarian-dinoflagellate symbiosis because it can be maintained in the aposymbiotic state (without symbionts) (Weis *et al.*, 2008, Sunagawa *et al.*, 2009, Lehnert *et al.*, 2012, Voolstra, 2013). Here, we monitored successful symbiosis establishment in *A. pallida* at different time points during a short recolonization experiment in which aposymbiotic anemones were inoculated with *Symbiodinium*.

Prior to developing the qPCR assay presented in this study, hemocytometer cell counts and Chl *a* quantification were tested in our experimental system. For hemocytometer cell counts, symbionts are isolated by homogenization of host tissue and pelleted through centrifugation (Coffroth *et al.*, 2001, Coffroth *et al.*, 2010, Hill *et al.*, 2014), but at the time points used in this study (1 and 3 days post-inoculation) there were too few symbionts to form a pellet. Instead, the entire homogenate was used for counting without washing away animal debris. The algal cells in the homogenate remained

clumped despite vigorous mixing preventing a uniform suspension, a problem encountered in other studies (Weis *et al.*, 2001b, Weis *et al.*, 2002) and making accurate cell counts difficult. From our pilot study, the estimated counts were highly variable across replicates within a treatment group (ex. estimated range of 5,660 to 28,094 algal cells per animal at 1 day post-inoculation). Thus, it was determined that hemocytometer cell counts were not an accurate way to quantify *Symbiodinium* for the time points used in this study.

Chl *a* quantification was also attempted. Chl *a* is a major photosynthetic pigment within *Symbiodinium* chloroplasts (Jeffrey *et al.*, 1968, Venn *et al.*, 2006). Total Chl *a* in host tissue can be used as a proxy for *Symbiodinium* cell number and has been used to determine symbiont abundance with seasonal temperature fluxes (Fitt *et al.*, 2000), bleaching events (Lesser, 1996, Jones, 1997, Warner *et al.*, 1999, Belda-Baillie *et al.*, 2002, Dove *et al.*, 2006, Hill *et al.*, 2014), and recolonization (Berner *et al.*, 1993). Chlorophyll extraction and spectrophotometric quantification were performed on aposymbiotic and symbiotic *A. pallida* and Chl *a* quantities of 0.11 and 2.20 μg per animal were obtained, respectively. The detection limit of spectrophotometric measurements of Chl *a* is approximately 0.1 mg L^{-1} (Aminot *et al.*, 2000), which is approximately the value obtained for our aposymbiotic anemone. This method has lower sensitivity than other techniques (fluorometric and HPLC) and is known to have errors in Chl *a* recovery when concentrations of photosynthetic pigments are low (Jeffrey *et al.*, 1975). In addition, a recolonization experiment performed in *A. pallida* in which whole animal fluorescence was measured, revealed that Chl *a* per *Symbiodinium* cell was undetectable at low symbiont density (~$1.8x10^4$ cells) (Berner *et al.*, 1993). Furthermore, this study documented a decrease in fluorescence readings per 10^4 *Symbiodinium* cells during the first ten days of the experiment indicating that there may have been a decrease in Chl *a* levels per *Symbiodinium* cell (Berner *et al.*, 1993). In order for Chl *a* content to be a reliable proxy for symbiont abundance, the concentration per cell must remain constant during the treatment. We concluded, therefore, that this technique was not sensitive or precise enough to differentiate between early time points during symbiosis establishment.

Given the limitations of the traditional methods, we chose to develop a qPCR method that would allow detection of small numbers of symbionts in adult hosts. qPCR-based techniques for *Symbiodinium* have been developed for the characterization of symbiont assemblages (Coffroth *et al.*, 2010, Byler *et al.*, 2013), quantifying relative amounts of two different symbiont types (Mieog *et al.*, 2007, Correa *et al.*, 2009) and determining symbiont-to-host cell ratios (Mieog *et al.*, 2009, Cunning *et al.*, 2013). These existing qPCR assays amplify multicopy loci, such as nuclear 28S ribosomal DNA (rDNA), internal transcribed spacer (ITS), or chloroplast 23S rDNA that are useful for delineating *Symbiodinium* types but vary in gene number between types (Mieog *et al.*, 2007, Arif *et al.*, 2014, Quigley *et al.*, 2014), making it difficult to translate an amplification cycle threshold value (C_t) into absolute numbers of cells. These assays also often involve complicated analyses that require extensive knowledge of qPCR. Lastly, none of these techniques has been used for quantification of symbionts at the onset of symbiosis. Therefore we developed a simple qPCR assay to quantify relative levels of symbionts in adult *A. pallida* at early time points during the establishment of symbiosis that does not require knowledge of numbers of gene copies. Relative qPCR was performed in which amplification of symbiont 28S rDNA was normalized to host ribosomal protein 10 (L10) amplification, to account for variation in host size. Following this, the Livak method (Livak *et al.*, 2001) was used to calculate relative differences in *Symbiodinium* abundance across symbiotic states and time points during the recolonization experiment.

6.3 Materials and Methods

6.3.1 Maintenance of A. pallida *and* Symbiodinium *cultures*

Symbiotic *A. pallida* from the Weis Lab (VWA: clade B1-containing) population were maintained in artificial seawater (ASW) at room temperature (~25°C) on a 40 μmol quanta m^{-2} s^{-1} 12 h light :12 h dark photoperiod. To obtain aposymbiotic *A. pallida*, symbiotic anemones were incubated at 4 °C for 6 h twice a week over six weeks to remove algal symbionts (Muscatine *et al.*, 1991). Between and after the series of cold-shock treatments, the anemones were kept in the dark until the beginning of the

experiments to prevent re-population with symbionts. Anemones were also cleaned regularly to remove expelled symbionts. Both symbiotic and aposymbiotic *A. pallida* were fed freshly hatched *Artemia* sp. nauplii twice a week. For the recolonization experiment, aposymbiotic anemones were inoculated with the homologous symbiont type, clade B1 *Symbiodinium minutum* (CCMP830), during exponential growth. The algae were grown in f/2 media at 25 °C with light intensity at 40 μmol quanta m^{-2} s^{-1} on a 12 h:12 h light-dark cycle.

6.3.2 Recolonization experiment

In preparation for the experiment, aposymbiotic *A. pallida* were plated into sterile 6-well plates containing 10 ml of filtered artificial seawater (FASW). The anemones were given daily water changes, and starved for 1 week prior to the start of the experiment. To prepare the *S. minutum* inoculum, CCMP830 cultures were concentrated with two rounds of centrifugation at 5,500 rpm for 6 min followed by 0.45 μm FASW washes. *S. minutum* concentration was quantified with replicate hemocytometer counts (n=8). A high inoculum of symbionts were pipetted over the oral disc of the anemones at a concentration of 2.19 x 10^5 ml^{-1} with 40 μl of homogenized and 0.4 μm filtered *Artemia* sp., a known feeding stimulus in other cnidarians (Schwarz *et al.*, 1999, Weis *et al.*, 2002, Harii *et al.*, 2009). The anemones were then placed in an incubator at 25 °C on a 12 h:12 h light-dark cycle at a light intensity of 20 μmol quanta m^{-2} s^{-1}. After 1 day, the anemones were washed with FASW to remove residual symbionts. At 1 and 3 days post-inoculation three anemones were washed with FASW, flash-frozen in liquid nitrogen, and stored at -80°C for DNA extraction.

6.3.3 DNA extraction and relative qPCR

DNA was extracted from the frozen anemones (n=3, except aposymbiotic group where n=4) using a modified CTAB protocol described by Coffroth et al. (1992). Briefly, anemones (average oral disc = 3.84 ± 0.14 mm) were homogenized in 2% CTAB using a plastic dounce to break up host tissue. Then, a small amount of 0.6 mm glass beads was added to the homogenate and vortexed for 5 min to break open the cell walls of the *S. minutum*. One hundred twenty μg/ml of Protinease K (Thermo Scientific, Waltham, MA)

was added to the homogenate and incubated for 3 h at 65 °C with a brief vortex every 30 min. After incubation, chloroform:isoamyl alcohol (24:1) was added for phase separation. For DNA precipitation, 1 ml cold 95% ethanol and 200 mM sodium acetate were added to the aqueous phase (top layer) and the solution was incubated overnight at -20 °C. The final DNA pellet was washed twice with 70% ethanol, dried, and resuspended in 10 mM Tris Base, pH 8.0.

To estimate relative symbiont density in each anemone, a qPCR assay was designed to compare gene copies of a region within domain 2 of 28S from symbiont nuclear rDNA using clade B1-specific primers that were previously developed by Correa et al. 2009 (2009). rDNA genes are useful for detecting *Symbiodinium* clades from complex assemblages *in hospite* (Correa *et al.*, 2009, Arif *et al.*, 2014), however these multicopy genes present challenges for absolute quantification. The gene copy number of 28S in CCMP830 is currently unknown and therefore the underlying assumption of this assay is that 28S gene copy number is the same for each clonal *S. minutum* cell. In studies that quantify mixed *Symbiodinium* assemblages within a host, accounting for variation in copy number between symbionts strains is important to obtain accurate results, but it is unnecessary in this study since the levels of just one symbiont type are quantified. Thus, as symbiont numbers increase during early stages of symbiosis establishment, the 28S gene copies will increase proportionally resulting in greater PCR amplification. To account for differences in the *A. pallida* size, primers were designed to the exon coding sequence of nuclear ribosomal protein L10. Primers were designed to the L10 gene in the *A. pallida* transcriptome (Lehnert *et al.*, 2012) using Primer 3 software through Geneious v 5.4.3 (Lloyd-Evans *et al.*, 2008, Kearse *et al.*, 2012, Untergasser *et al.*, 2012) (forward: 5' ACG TTT CTG CCG TGG TGT CCC 3', reverse: 5' CGG GCA GCT TCA AGG GCT TCA 3'). To confirm that the L10 primers amplified the correct sequence, the product was cloned using the pGEM T-easy kit (Promega, Madison, WI) and plasmids isolated using the QiaPrep Spin Miniprep Kit (Qiagen, Valencia, CA). Plasmids were checked for the correct insert size using the FastDigest EcoRI (Fermentas, Waltham, MA) and sent for sequencing on the ABI 3730 capillary sequence machine in the Center for Genome Research and Biocomputing at Oregon State University. The L10 primer set was also

validated for high PCR efficiency and amplification specificity of *A. pallida* DNA. Each sample was run in triplicate on the MasterCycler RealPlex^4 real-time PCR machine (Eppendorf, Hamburg, Germany). For each primer set, 15 µl volume qPCR reactions were prepared as follows: 20 ng μl^{-1} genomic DNA, 0.4 µM of the forward and reverse primers, 7.5 µl of 2x SensiFAST SYBR Hi-ROX master mix (Bioline USA, Boston, MA), and enough molecular grade H_2O to reach final volume. No-template negative controls were run for each primer pair to check for reagent contamination. The profile for the qPCR run was as follows: 95 °C for 2 min for initial denaturing, followed by 40 cycles of 95 °C for 5s, 60 °C for 10s, and 72 °C for 20s. A dissociation curve (95 °C for 15s, 60 °C for 15s, ramping temperature gradient (60-95 °C) for 20 min, and 95 °C for 15s) on the final PCR product was performed to confirm single amplicon detection.

The fluorescence baseline and threshold set by the RealPlex^4 machine was used to calculate C_t values, or the first reaction cycle in which fluorescent detection exceeds baseline. Following the Livak $2^{\Delta\Delta Ct}$ method (Livak *et al.*, 2001), the symbiont 28S C_t from each anemone was normalized to the corresponding anemone reference L10 C_t. The normalized values (ΔC_t) were subtracted from the maximum ΔC_t (lowest amplification) to obtain the ratio of relative quantities of 28S rDNA per anemone ($\Delta\Delta C_t$). All values are expressed as mean relative quantity on the $\log_2$ scale ± standard error. Relative quantities of 28S rDNA in symbiotic, aposymbiotic and recolonized anemones were compared using a 2-tailed Student's t-test with unequal variance at a significance threshold of $p \leq 0.05$.

6.4 Results and Discussion

Cellular and molecular signaling events associated with symbiont recognition and specificity occur within hours of symbiosis onset (Davy *et al.*, 2012). However, connecting these signaling events with successful symbiont acquisition can be difficult when symbiont numbers are low. Previous methods developed to measure symbiont abundance, such as cell counts, photosynthetic pigment quantification, and quantification of symbiont chlorophyll autofluorescence using fluorescence microscopy lack the sensitivity required to reliably detect symbiosis reestablishment at early time points in

adult *A. pallida* (Table 1). Therefore, we developed a relative qPCR assay to track acquisition of symbionts by hosts during recolonization.

The assay revealed differences in the relative amounts of symbiont 28S rDNA between aposymbiotic, symbiotic, and recolonized *A. pallida* (Fig 1). The relative $\log_2$ quantities of 28S rDNA ranged from 0-3.43 in aposymbiotic anemones, indicating that in some cold-shock-treated anemones, residual symbionts were still present, but at very low abundance (Fig. 1). This is not uncommon as it is difficult to obtain completely symbiont-free anemones with the cold-shock or chemical treatments (Berner *et al.*, 1993, Matthews *et al.*, 2015). The mean relative $\log_2$ quantity of the symbiotic anemones was 8.26 times larger than aposymbiotic anemones (t-test, $p < 0.001$).

During the recolonization experiment, the mean relative $\log_2$ quantities at days 1 and 3 post-inoculation were 6.73 ± 2.14 and 10.15 ± 0.52, respectively, both of which were significantly different from the aposymbiotic (t-test, $p = 0.050$ and $p < 0.001$) and symbiotic samples (t-test, $p = 0.039$ and $p=0.015$), but not from each other (Fig. 1). The lack of significance between day 1 and day 3 is likely due to the high variability observed within the day 1 treatment group. This suggests differential temporal responses of individual *A. pallida* to symbiont acquisition. However, despite the lack of significance, a trend of increasing 28S rDNA levels can be observed between day 1 and 3, indicating successful uptake and establishment of symbiosis. Since anemones were washed 1 day post-inoculation, increased symbiont densities at day 3 could be a result of symbiont proliferation within the host tissue, which also suggests successful establishment of symbiosis. However, since three anemones were chosen at random for each time point, variation in the ability to establish symbiosis in the *A. pallida* population cannot be completely ruled out as a reason for differences between time points. Methods that allow for repeated sampling from the same animal over multiple time points would allow for better resolution of this temporal variation.

This study provides a simple qPCR assay designed to detect relative levels of *S. minutum* at early time points during the reestablishment of symbiosis in adult *A. pallida*. This technique is much simpler than other qPCR-based symbiont quantification techniques due to the use of one symbiont and one host strain. Therefore, it is not

necessary to calculate gene copy numbers for either the symbiont or host. In addition, by indexing to a host gene locus, differences in animal size can be accounted for directly through established qPCR quantification methods. This technique has the potential to be applied to other cnidarians harboring *Symbiodinium* and in experiments tracking the bleaching response.

Table 6.1 Summary of *Symbiodinium* quantification techniques and application for studying the onset of cnidarian-dinoflagellate symbiosis.

Technique	Absolute numbers	Low symbiont density	Temporal scale	Life Stage	Attempted in this study
Hemocytometer cell counts	✓	×	Days to months	Adult	✓
Flow cytometry cell counts	✓	✓	1 month	Adult	
Cell counts in whole mounts	✓	✓	Hours to days	Larvae	
Stereo-microscope: total autofluorescence of symbionts	×	×	Within a week	Adult	
Confocal microscopy: total autofluorescence of symbionts	×	✓	Within a day	Adult tentacle	
Chl-*a* content	×	×	2 days	Adult	✓
FISH ^	✓	✓	N/A	Adult	
HTS ^	✓	✓	N/A	Adult	
qPCR ^	✓	✓	N/A	Adult	✓

^ These quantification methods have been applied to studies that describe proportion of different *Symbiodinium* types within a host (Fitt *et al.*, 2000, Loram *et al.*, 2007, Correa *et al.*, 2009, Mayfield *et al.*, 2009, Mieog *et al.*, 2009, Fay *et al.*, 2012, Byler *et al.*, 2013, Arif *et al.*, 2014, Hill *et al.*, 2014, McIlroy *et al.*, 2014, Quigley *et al.*, 2014) or loss of symbionts during a natural or laboratory-induced bleaching event (Jones, 1997, Warner *et al.*, 1999, Belda-Baillie *et al.*, 2002, Venn *et al.*, 2006, Ganot *et al.*, 2011, Cunning *et al.*, 2013, Hill *et al.*, 2014), but have not yet been applied to onset of symbiosis studies.

FISH = Fluorescence *in situ* hybridization; HTS = high-throughput sequencing.

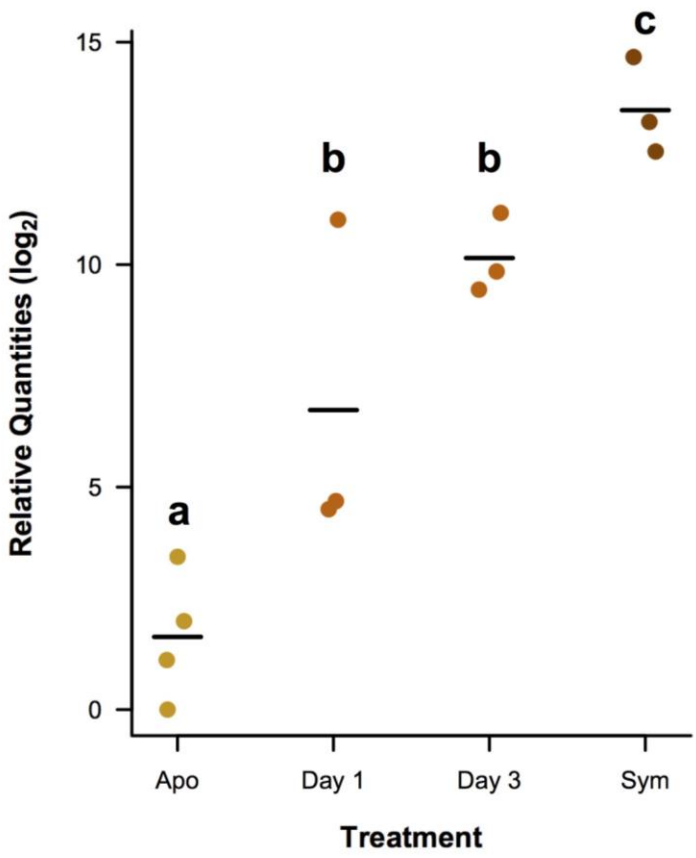

Figure 6.1 Comparison of relative quantities of symbiont 28S rDNA between aposymbiotic, symbiotic and recolonized *A. pallida*. For each treatment group, replicate relative quantities are presented by l with the mean relative $\log_2$ quantity indicated by the bar. Points are slightly offset for clarity. Groups not sharing a letter (a, b, or c) significantly differ ($p \leq 0.05$).

6.5 References

Aminot, A. and Rey, F. (2000) Standard procedure for the determination of chlorophyll a by spectroscopic methods. In *International Council for the Exploration of the Sea*. Denmark.

Arif, C., Daniels, C., Bayer, T., Banguera-Hinestroza, E., Barbrook, A., Howe, C.J., *et al.* (2014). Assessing *Symbiodinium* diversity in scleractinian corals via next-generation sequencing-based genotyping of the ITS2 rDNA region. *Mol. Ecol.* **23,** 4418-4433.

Belda-Baillie, C.A., Baillie, B.K. and Maruyama, T. (2002). Specificity of a model cnidarian-dinoflagellate symbiosis. *Biol. Bull.* **202,** 74-85.

Berner, T., Baghdasarian, G. and Muscatine, L. (1993). Repopulation of a sea anemone with symbiotic dinoflagellates: analysis by *in vivo* fluorescence. *J. Exp. Mar. Bio. Ecol.* **170,** 145-158.

Byler, K.A., Carmi-Veal, M., Fine, M. and Goulet, T.L. (2013). Multiple symbiont acquisition strategies as an adaptive mechanism in the coral *Stylophora pistillata*. *PLoS One* **8,** e59596.

Coffroth, M.A., Lasker, H.R., Diamond, M.E., Bruenn, J.A. and Bermingham, E. (1992). DNA fingerprints of a gorgonian coral: a method for detecting clonal structure in a vegetative species. *Mar. Biol.* **114,** 317-325.

Coffroth, M.A., Poland, D.M., Petrou, E.L., Brazeau, D.A. and Holmberg, J.C. (2010). Environmental symbiont acquisition may not be the solution to warming seas for reef-building corals. *PLoS One* **5,** e13258.

Coffroth, M.A., Santos, S.R. and Goulet, T.L. (2001). Early ontogenetic expression of specificity in a cnidarian-algal symbiosis. *Mar. Ecol. Prog. Ser.* **222,** 85-96.

Correa, A.M., McDonald, M.D. and Baker, A.C. (2009). Development of clade-specific *Symbiodinium* primers for quantitative PCR (qPCR) and their application to detecting clade D symbionts in Caribbean corals. *Mar. Biol.* **156,** 2403-2411.

Cunning, R. and Baker, A.C. (2013). Excess algal symbionts increase the susceptibility of reef corals to bleaching. *Nat. Clim. Change* **3,** 259-262.

Davy, S.K., Allemand, D. and Weis, V.M. (2012). Cell biology of cnidarian-dinoflagellate symbiosis. *Microbiol. Mol. Biol. Rev.* **76,** 229-261.

Dove, S., Ortiz, J.C., Enriquez, S., Fine, M., Fisher, P., Iglesias-Prieto, R., *et al.* (2006). Response of holosymbiont pigments from the scleractinian coral *Montipora monasteriata* to short-term heat stress. *Limnol. Oceanogr.* **51,** 1149-1158.

Fay, S.A. and Weber, M.X. (2012). The occurrence of mixed infections of *Symbiodinium* (Dinoflagellata) within individual hosts. *J. Phycol.* **48,** 1306-1316.

Fitt, W., McFarland, F., Warner, M. and Chilcoat, G. (2000). Seasonal patterns of tissue biomass and densities of symbiotic dinoflagellates in reef corals and relation to coral bleaching. *Limnol. Oceanogr.* **45,** 677-685.

Ganot, P., Moya, A., Magnone, V., Allemand, D., Furla, P. and Sabourault, C. (2011). Adaptations to endosymbiosis in a cnidarian-dinoflagellate association: differential gene expression and specific gene duplications. *PLoS Genet.* **7,** e1002187.

Hambleton, E.A., Guse, A. and Pringle, J.R. (2014). Similar specificities of symbiont uptake by adults and larvae in an anemone model system for coral biology. *J. Exp. Biol.* **217,** 1613-1619.

Harii, S., Yasuda, N., Rodriguez-Lanetty, M., Irie, T. and Hidaka, M. (2009). Onset of symbiosis and distribution patterns of symbiotic dinoflagellates in the larvae of scleractinian corals. *Mar. Biol.* **156,** 1203-1212.

Hill, R., Fernance, C., Wilkinson, S.P., Davy, S.K. and Scott, A. (2014). Symbiont shuffling during thermal bleaching and recovery in the sea anemone *Entacmaea quadricolor*. *Mar. Biol.* **161,** 2931-2937.

Jeffrey, S. and Haxo, F. (1968). Photosynthetic pigments of symbiotic dinoflagellates (zooxanthellae) from corals and clams. *Biol. Bull.* **135,** 149-165.

Jeffrey, S. and Humphrey, G. (1975). New spectrophotometric equations for determining chlorophylls *a*, *b*, *c1* and *c2* in higher plants, algae and natural phytoplankton. *Biochem Physiol Pflanz BPP***,** 191-194.

Jones, G.P., McCormick, M.I., Srinivasan, M. and Eagle, J.V. (2004). Coral decline threatens fish biodiversity in marine reserves. *Proc. Natl. Acad. Sci. USA* **101,** 8251-8253.

Jones, R.J. (1997). Changes in zooxanthellar densities and chlorophyll concentrations in corals during and after a bleaching event. *Mar. Ecol. Prog. Ser.* **158,** 51-59.

Kearse, M., Moir, R., Wilson, A., Stones-Havas, S., Cheung, M., Sturrock, S., *et al.* (2012). Geneious Basic: an integrated and extendable desktop software platform for the organization and analysis of sequence data. *Bioinformatics* **28,** 1647-1649.

Lehnert, E.M., Burriesci, M.S. and Pringle, J.R. (2012). Developing the anemone *Aiptasia* as a tractable model for cnidarian-dinoflagellate symbiosis: the transcriptome of aposymbiotic *A. pallida*. *BMC Genomics* **13,** 271.

Lesser, M.P. (1996). Elevated temperatures and ultraviolet radiation cause oxidative stress and inhibit photosynthesis in symbiotic dinoflagellates. *Limnol. Oceanogr.* **41,** 271-283.

Livak, K.J. and Schmittgen, T.D. (2001). Analysis of relative gene expression data using real-time quantitative PCR and the $2^{-\Delta\Delta CT}$ method. *Methods* **25,** 402-408.

Lloyd-Evans, E., Morgan, A.J., He, X., Smith, D.A., Elliot-Smith, E., Sillence, D.J., *et al.* (2008). Niemann-Pick disease type C1 is a sphingosine storage disease that causes deregulation of lysosomal calcium. *Nat. Med.* **14,** 1247-1255.

Loram, J.E., Boonham, N., O'Toole, P., Trapido-Rosenthal, H.G. and Douglas, A.E. (2007). Molecular quantification of symbiotic dinoflagellate algae of the genus *Symbiodinium*. *Biol. Bull.* **212,** 259-268.

Matthews, J.L., Sproles, A.E., Oakley, C.A., Grossman, A.R., Weis, V.M. and Davy, S.K. (2015). Menthol-induced bleaching rapidly and effectively provides experimental aposymbiotic sea anemones (*Aiptasia* sp.) for symbiosis investigations. *J. Exp. Biol.***,** jeb.128934.

Mayfield, A.B., Hirst, M.B. and Gates, R.D. (2009). Gene expression normalization in a dual-compartment system: a real-time quantitative polymerase chain reaction protocol for symbiotic anthozoans. *Mol. Ecol. Resour.* **9,** 462-470.

McIlroy, S., Smith, G. and Geller, J. (2014). FISH-Flow: a quantitative molecular approach for describing mixed clade communities of *Symbiodinium*. *Coral Reefs* **33,** 157-167.

Mieog, J.C., van Oppen, M.J., Berkelmans, R., Stam, W.T. and Olsen, J.L. (2009). Quantification of algal endosymbionts (*Symbiodinium*) in coral tissue using real-time PCR. *Mol. Ecol. Resour.* **9,** 74-82.

Mieog, J.C., van Oppen, M.J., Cantin, N.E., Stam, W.T. and Olsen, J.L. (2007). Real-time PCR reveals a high incidence of *Symbiodinium* clade D at low levels in four scleractinian corals across the Great Barrier Reef: implications for symbiont shuffling. *Coral Reefs* **26,** 449-457.

Muscatine, L., Grossman, D. and Doino, J. (1991). Release of symbiotic algae by tropical sea anemones and corals after cold shock. *Mar. Ecol. Prog. Ser.* **77,** 233-243.

Pratchett, M.S., Wilson, S.K., Graham, N.A.J., Munday, P.L., Jones, G.P. and Polunin, N.V.C. (2009) Coral bleaching and consequences for motile reef organisms: past, present, and uncertain future effects. In *Coral Bleching: patterns and processes, causes and consequences*. Heidelberg, Springer, pp. 139-158.

Quigley, K.M., Davies, S.W., Kenkel, C.D., Willis, B.L., Matz, M.V. and Bay, L.K. (2014). Deep-sequencing method for quantifying background abundances of *Symbiodinium* types: exploring the rare *Symbiodinium* biosphere in reef-building corals. *PLoS One* **9,** e94297.

Schwarz, J.A., Krupp, D.A. and Weis, V.M. (1999). Late larval development and onset of symbiosis in the scleractinian coral *Fungia scutaria*. *Biol. Bull.* **196,** 70-79.

Sunagawa, S., Wilson, E.C., Thaler, M., Smith, M.L., Caruso, C., Pringle, J.R., *et al.* (2009). Generation and analysis of transcriptomic resources for a model system on the rise: the sea anemone *Aiptasia pallida* and its dinoflagellate endosymbiont. *BMC Genomics* **10,** 258.

Untergasser, A., Cutcutache, I., Koressaar, T., Ye, J., Faircloth, B.C., Remm, M. and Rozen, S.G. (2012). Primer3—new capabilities and interfaces. *Nucleic Acids Res.* **40,** e115.

Venn, A.A., Wilson, M.A., Trapido-Rosenthal, H.G., Keely, B.J. and Douglas, A.E. (2006). The impact of coral bleaching on the pigment profile of the symbiotic alga, *Symbiodinium*. *Plant, Cell Environ.* **29,** 2133-2142.

Voolstra, C.R. (2013). A journey into the wild of the cnidarian model system *Aiptasia* and its symbionts. *Mol. Ecol.* **22,** 4366-4368.

Warner, M.E., Fitt, W.K. and Schmidt, G.W. (1999). Damage to photosystem II in symbiotic dinoflagellates: a determinant of coral bleaching. *Proc. Natl. Acad. Sci. USA* **96,** 8007-8012.

Weis, V.M. and Allemand, D. (2009). What determines coral health? *Science* **324,** 1153-1155.

Weis, V.M., Davy, S.K., Hoegh-Guldberg, O., Rodriguez-Lanetty, M. and Pringle, J.R. (2008). Cell biology in model systems as the key to understanding corals. *Trends Ecol. Evol.* **23,** 369-376.

Weis, V.M., Reynolds, W.S. and Krupp, D.A. (2001b). Host-symbiont specificity during onset of symbiosis between the dinoflagellates Symbiodinium spp. and planula larvae of the scleractinian coral Fungia scutaria. *Coral Reefs* **20,** 301-308.

Weis, V.M., Verde, E.A., Pribyl, A. and Schwarz, J.A. (2002). Aspects of the larval biology of the sea anemones *Anthopleura elegantissima* and *A. artemisia*. *Invertebr. Biol.* **121,** 190-201.

7. COMBINED BIBLIOGRAPHY

Abrego, D., Van Oppen, M.J. and Willis, B.L. (2009). Highly infectious symbiont dominates initial uptake in coral juveniles. *Mol. Ecol.* **18,** 3518-3531.

Ader, I., Brizuela, L., Bouquerel, P., Malavaud, B. and Cuvillier, O. (2008). Sphingosine kinase 1: a new modulator of hypoxia inducible factor 1α during hypoxia in human cancer cells. *Cancer Res.* **68,** 8635-8642.

Akira, S. and Takeda, K. (2004). Toll-like receptor signalling. *Nat. Rev. Immunol.* **4,** 499-511.

Al-Lihaibi, S.S., Ayyad, S.-E.N., Shaher, F. and Alarif, W.M. (2010). Antibacterial sphingolipid and steroids from the black coral *Antipathes dichotoma*. *Chem. Pharm. Bull. (Tokyo)* **58,** 1635-1638.

Alemany, R., van Koppen, C.J., Danneberg, K., Ter Braak, M. and Meyer zu Heringdorf, D. (2007). Regulation and functional roles of sphingosine kinases. *Naunyn-Schmiedeberg's Arch. Pharmacol.* **374,** 413-428.

Ali, H.Z., Harding, C.R. and Denny, P.W. (2011). Endocytosis and sphingolipid scavenging in *Leishmania mexicana* amastigotes. *Biochemistry Research International* **2012**.

Altschul, S.F., Gish, W., Miller, W., Myers, E.W. and Lipman, D.J. (1990). Basic local alignment search tool. *J. Mol. Biol.* **215,** 403-410.

Amar, K.-O., Douek, J., Rabinowitz, C. and Rinkevich, B. (2008). Employing of the amplified fragment length polymorphism (AFLP) methodology as an efficient population genetic tool for symbiotic cnidarians. *Mar. Biotechnol.* **10,** 350-357.

Aminot, A. and Rey, F. (2000) Standard procedure for the determination of chlorophyll a by spectroscopic methods. In *International Council for the Exploration of the Sea*. Denmark.

An, D., Na, C., Bielawski, J., Hannun, Y.A. and Kasper, D.L. (2011). Membrane sphingolipids as essential molecular signals for *Bacteroides* survival in the intestine. *Proc. Natl. Acad. Sci. USA* **108,** 4666-4671.

An, D., Oh, S.F., Olszak, T., Neves, J.F., Avci, F.Y., Erturk-Hasdemir, D., *et al.* (2014). Sphingolipids from a symbiotic microbe regulate homeostasis of host intestinal natural killer T cells. *Cell* **156,** 123-133.

An, S., Bleu, T., Huang, W., Hallmark, O.G., Coughlin, S.R. and Goetzl, E.J. (1997). Identification of cDNAs encoding two G protein-coupled receptors for lysosphingolipids. *FEBS Lett.* **417,** 279-282.

Andersen, C.L., Jensen, J.L. and Ørntoft, T.F. (2004). Normalization of real-time quantitative reverse transcription-PCR data: A model-based variance estimation approach to identify genes suited for normalization, applied to bladder and colon cancer data sets. *Cancer Res.* **64,** 5245-5250.

Andrews, S. (2010) FastQC: A quality control tool for high throughput sequence data. In *Reference Source*.

Anguera, M.C., Field, M.S., Perry, C., Ghandour, H., Chiang, E.-P., Selhub, J., *et al.* (2006). Regulation of folate-mediated one-carbon metabolism by 10-formyltetrahydrofolate dehydrogenase. *J. Biol. Chem.* **281,** 18335-18342.

Arif, C., Daniels, C., Bayer, T., Banguera-Hinestroza, E., Barbrook, A., Howe, C.J., *et al.* (2014). Assessing *Symbiodinium* diversity in scleractinian corals via next-generation sequencing-based genotyping of the ITS2 rDNA region. *Mol. Ecol.* **23,** 4418-4433.

Babcock, R. and Heyward, A. (1986). Larval development of certain gamete-spawning scleractinian corals. *Coral Reefs* **5,** 111-116.

Baird, A.H., Gilmour, James P., Kamiki, Takayuki M., Nonaka, Masanori, Pratchett, Morgan S., Yamamoto, Hiromi H., and Yamasaki, Hideo (2006) Temperature tolerance of symbiotic and non-symbiotic coral larvae. In *Proceedings of the 10th International Coral Reef Symposium In: 10th International Coral Reef Symposium*. Okinawa, Japan.

Balogh, G., Péter, M., Glatz, A., Gombos, I., Török, Z., Horváth, I., *et al.* (2013). Key role of lipids in heat stress management. *FEBS Lett.* **587,** 1970-1980.

Bartke, N. and Hannun, Y.A. (2009). Bioactive sphingolipids: metabolism and function. *J. Lipid Res.* **50,** S91-S96.

Baumgarten, S., Simakov, O., Esherick, L.Y., Liew, Y.J., Lehnert, E.M., Michell, C.T., *et al.* (2015). The genome of *Aiptasia*, a sea anemone model for coral symbiosis. *Proc. Natl. Acad. Sci. USA* **112,** 11893-11898.

Belda-Baillie, C.A., Baillie, B.K. and Maruyama, T. (2002). Specificity of a model cnidarian-dinoflagellate symbiosis. *Biol. Bull.* **202,** 74-85.

Bellantuono, A.J., Hoegh-Guldberg, O. and Rodriguez-Lanetty, M. (2011). Resistance to thermal stress in corals without changes in symbiont composition. *Proc. R. Soc. Lond., Ser. B: Biol. Sci.* **279,** 1100-1107.

Bellwood, D.R. and Hughes, T.P. (2001). Regional-scale assembly rules and biodiversity of coral reefs. *Science* **292,** 1532-1535.

Benjamini, Y. and Hochberg, Y. (1995). Controlling the false discovery rate: a practical and powerful approach to multiple testing. *J. Roy. Stat. Soc. Ser. B. (Stat. Method.),* 289-300.

Berner, T., Baghdasarian, G. and Muscatine, L. (1993). Repopulation of a sea anemone with symbiotic dinoflagellates: analysis by *in vivo* fluorescence. *J. Exp. Mar. Bio. Ecol.* **170,** 145-158.

Black, N.A., Voellmy, R. and Szmant, A.M. (1995). Heat shock protein induction in *Montastraea faveolata* and *Aiptasia pallida* exposed to elevated temperatures. *Biol. Bull.* **188,** 234-240.

Black, R.E. and Bloom, L. (1984). Heat shock proteins in *Aurelia* (Cnidaria, Scyphozoa). *J. Exp. Zool.* **230,** 303-307.

Bligh, E.G. and Dyer, W.J. (1959). A rapid method of total lipid extraction and purification. *Can. J. Biochem. Physiol.* **37,** 911-917.

Blom, H.J. and Smulders, Y. (2011). Overview of homocysteine and folate metabolism. With special references to cardiovascular disease and neural tube defects. *J. Inherit. Metab. Dis.* **34,** 75-81.

Bosch, T., Krylow, S.M., Bode, H.R. and Steele, R.E. (1988). Thermotolerance and synthesis of heat shock proteins: these responses are present in *Hydra attenuata* but absent in *Hydra oligactis*. *Proc. Natl. Acad. Sci. USA* **85,** 7927-7931.

Bouchard, J.N. and Yamasaki, H. (2009). Implication of nitric oxide in the heat-stress-induced cell death of the symbiotic alga *Symbiodinium microadriaticum*. *Mar. Biol.* **156,** 2209-2220.

Bowman, K.G. and Bertozzi, C.R. (1999). Carbohydrate sulfotransferases: mediators of extracellular communication. *Chem. Biol.* **6,** R9-R22.

Brekhman, V., Malik, A., Haas, B., Sher, N. and Lotan, T. (2015). Transcriptome profiling of the dynamic life cycle of the scypohozoan jellyfish *Aurelia aurita*. *BMC Genomics* **16,** 74.

Brown, B., Le Tissier, M. and Bythell, J. (1995). Mechanisms of bleaching deduced from histological studies of reef corals sampled during a natural bleaching event. *Mar. Biol.* **122,** 655-663.

Bryan, A.M., Del Poeta, M. and Luberto, C. (2015). Sphingolipids as regulators of the phagocytic response to fungal infections. *Mediators Inflamm.* **2015,** 640540.

Bryan, A.M., Farnoud, A.M., Mor, V. and Del Poeta, M. (2014). Macrophage cholesterol depletion and its effect on the phagocytosis of *Cryptococcus neoformans*. *J. Vis. Exp.***,** e52432-e52432.

Burge, C.A., Mouchka, M.E., Harvell, C.D. and Roberts, S. (2013). Immune response of the Caribbean sea fan, *Gorgonia ventalina*, exposed to an *Aplanochytrium* parasite as revealed by transcriptome sequencing. *Front. Physiol.* **4**.

Byler, K.A., Carmi-Veal, M., Fine, M. and Goulet, T.L. (2013). Multiple symbiont acquisition strategies as an adaptive mechanism in the coral *Stylophora pistillata*. *PLoS One* **8,** e59596.

Carter, S.L., Brechbühler, C.M., Griffin, M. and Bond, A.T. (2004). Gene co-expression network topology provides a framework for molecular characterization of cellular state. *Bioinformatics* **20,** 2242-2250.

Chan, H. and Pitson, S.M. (2013). Post-translational regulation of sphingosine kinases. *Biochim. Biophys. Acta* **1831,** 147-156.

Chang, Y., Abe, A. and Shayman, J.A. (1995). Ceramide formation during heat shock: a potential mediator of alpha B-crystallin transcription. *Proc. Natl. Acad. Sci. USA* **92,** 12275-12279.

Chapman, J.A., Kirkness, E.F., Simakov, O., Hampson, S.E., Mitros, T., Weinmaier, T., *et al.* (2010). The dynamic genome of *Hydra*. *Nature* **464,** 592-596.

Chen, H.-K., Song, S.-N., Wang, L.-H., Mayfield, A.B., Chen, Y.-J., Chen, W.-N.U. and Chen, C.-S. (2015). A compartmental comparison of major lipid species in a coral-*Symbiodinium* endosymbiosis: Evidence that the coral host regulates lipogenesis of its cytosolic lipid bodies. *PLoS One* **10,** e0132519.

Chen, M.-C., Cheng, Y.-M., Hong, M.-C. and Fang, L.-S. (2004). Molecular cloning of Rab5 (ApRab5) in Aiptasia pulchella and its retention in phagosomes harboring live zooxanthellae. *Biochem. Biophys. Res. Commun.* **324,** 1024-1033.

Chen, M.-C., Cheng, Y.-M., Sung, P.-J., Kuo, C.-E. and Fang, L.-S. (2003). Molecular identification of Rab7 (ApRab7) in Aiptasia pulchella and its exclusion from phagosomes harboring zooxanthellae. *Biochem. Biophys. Res. Commun.* **308,** 586-595.

Chen, M.C., Hong, M.C., Huang, Y.S., Liu, M.C., Cheng, Y.M. and Fang, L.S. (2005). ApRab11, a cnidarian homologue of the recycling regulatory protein Rab11, is involved in the establishment and maintenance of the *Aiptasia* - *Symbiodinium* endosymbiosis. *Biochem. Biophys. Res. Commun.* **338,** 1607 - 1616.

Chen, P.-W., Fonseca, L.L., Hannun, Y.A. and Voit, E.O. (2013). Coordination of rapid sphingolipid responses to heat stress in yeast. *PLoS Comp. Biol.* **9,** e1003078.

Chen, Y., Liu, Y., Sullards, M.C. and Merrill Jr, A.H. (2010). An introduction to sphingolipid metabolism and analysis by new technologies. *Neuromolecular Med.* **12,** 306-319.

Cheng, S., Wen, Z., Chiou, S., Tsai, C., Wang, S., Hsu, C., *et al.* (2009). Ceramide and cerebrosides from the octocoral *Sarcophyton ehrenbergi*. *J. Nat. Prod.* **72,** 465-468.

Cherukuri, A., Dykstra, M. and Pierce, S.K. (2001). Floating the raft hypothesis: lipid rafts play a role in immune cell activation. *Immunity* **14,** 657-660.

Chun, J., Goetzl, E.J., Hla, T., Igarashi, Y., Lynch, K.R., Moolenaar, W., *et al.* (2002). International union of pharmacology. XXXIV. Lysophospholipid receptor nomenclature. *Pharmacol. Rev.* **54,** 265-269.

Cinque, B., Di Marzio, L., Centi, C., Di Rocco, C., Riccardi, C. and Cifone, M.G. (2003). Sphingolipids and the immune system. *Pharmacol. Res.* **47,** 421-437.

Coffroth, M.A., Lasker, H.R., Diamond, M.E., Bruenn, J.A. and Bermingham, E. (1992). DNA fingerprints of a gorgonian coral: a method for detecting clonal structure in a vegetative species. *Mar. Biol.* **114,** 317-325.

Coffroth, M.A., Poland, D.M., Petrou, E.L., Brazeau, D.A. and Holmberg, J.C. (2010). Environmental symbiont acquisition may not be the solution to warming seas for reef-building corals. *PLoS One* **5,** e13258.

Coffroth, M.A., Santos, S.R. and Goulet, T.L. (2001). Early ontogenetic expression of specificity in a cnidarian-algal symbiosis. *Mar. Ecol. Prog. Ser.* **222,** 85-96.

Correa, A.M., McDonald, M.D. and Baker, A.C. (2009). Development of clade-specific *Symbiodinium* primers for quantitative PCR (qPCR) and their application to detecting clade D symbionts in Caribbean corals. *Mar. Biol.* **156,** 2403-2411.

Cowart, L.A. and Obeid, L.M. (2007). Yeast sphingolipids: recent developments in understanding biosynthesis, regulation, and function. *Biochim. Biophys. Acta* **1771,** 421-431.

Cumbo, V., Baird, A. and van Oppen, M. (2013). The promiscuous larvae: flexibility in the establishment of symbiosis in corals. *Coral Reefs* **32,** 111-120.

Cunning, R. and Baker, A.C. (2013). Excess algal symbionts increase the susceptibility of reef corals to bleaching. *Nat. Clim. Change* **3,** 259-262.

Cuvillier, O., Pirianov, G., Kleuser, B., Vanek, P.G., Coso, O.A., Gutkind, J.S. and Spiegel, S. (1996). Suppression of ceramide-mediated programmed cell death by sphingosine-1-phosphate. *Nature* **381,** 800-803.

Davy, S.K., Allemand, D. and Weis, V.M. (2012). Cell biology of cnidarian-dinoflagellate symbiosis. *Microbiol. Mol. Biol. Rev.* **76,** 229-261.

de Nadal, E., Ammerer, G. and Posas, F. (2011). Controlling gene expression in response to stress. *Nature Reviews Genetics* **12,** 833-845.

De Palma, C., Meacci, E., Perrotta, C., Bruni, P. and Clementi, E. (2006). Endothelial nitric oxide synthase activation by tumor necrosis factor α through neutral

sphingomyelinase 2, sphingosine kinase 1, and sphingosine 1 phosphate receptors a novel pathway relevant to the pathophysiology of endothelium. *Arterioscler. Thromb. Vasc. Biol.* **26,** 99-105.

Deng, X., Yin, X., Allan, R., Lu, D.D., Maurer, C.W., Haimovitz-Friedman, A., *et al.* (2008). Ceramide biogenesis is required for radiation-induced apoptosis in the germ line of *C. elegans*. *Science* **322,** 110-115.

DeSalvo, M.K., Sunagawa, S., Voolstra, C.R. and Medina, M. (2010). Transcriptomic responses to heat stress and bleaching in the elkhorn coral *Acropora palmata*. *Mar. Ecol. Prog. Ser.* **402,** 97-113.

DeSalvo, M.K., Voolstra, C.R., Sunagawa, S., Schwarz, J.A., Stillman, J.H., Coffroth, M.A., *et al.* (2008). Differential gene expression during thermal stress and bleaching in the Caribbean coral *Montastraea faveolata*. *Mol. Ecol.* **17,** 3952-3971.

Detournay, O., Schnitzler, C.E., Poole, A. and Weis, V.M. (2012). Regulation of cnidarian–dinoflagellate mutualisms: Evidence that activation of a host TGFβ innate immune pathway promotes tolerance of the symbiont. *Dev. Comp. Immunol.* **38,** 525-537.

Detournay, O. and Weis, V.M. (2011). Role of the sphingosine rheostat in the regulation of cnidarian-dinoflagellate symbioses. *Biol. Bull.* **221,** 261-269.

Dobson, L., Reményi, I. and Tusnády, G.E. (2015). CCTOP: a Consensus Constrained TOPology prediction web server. *Nucleic Acids Res.* **43,** W408-412.

Döll, F., Pfeilschifter, J. and Huwiler, A. (2005). The epidermal growth factor stimulates sphingosine kinase-1 expression and activity in the human mammary carcinoma cell line MCF7. *Biochim. Biophys. Acta* **1738,** 72-81.

Douglas, A.E. (2003). Coral bleaching - how and why? *Mar. Pollut. Bull.* **46,** 385-392.

Dove, S., Ortiz, J.C., Enriquez, S., Fine, M., Fisher, P., Iglesias-Prieto, R., *et al.* (2006). Response of holosymbiont pigments from the scleractinian coral *Montipora monasteriata* to short-term heat stress. *Limnol. Oceanogr.* **51,** 1149-1158.

Dunn, S.R. (2009). Immunorecognition and immunoreceptors in the Cnidaria. *Isj* **6,** 7-14.

Dunn, S.R., Schnitzler, C.E. and Weis, V.M. (2007). Apoptosis and autophagy as mechanisms of dinoflagellate symbiont release during cnidarian bleaching: every which way you lose. *Proc. R. Soc. Lond., Ser. B: Biol. Sci.* **274,** 3079-3085.

Dunn, S.R., Thomas, M.C., Nette, G.W. and Dove, S.G. (2012). A lipidomic approach to understanding free fatty acid lipogenesis derived from dissolved inorganic carbon within cnidarian-dinoflagellate symbiosis. *PLoS One* **7,** e46801.

Dunn, S.R., Thomason, J.C., Le Tissier, M.D.A. and Bythell, J.C. (2004). Heat stress induces different forms of cell death in sea anemones and their endosymbiotic algae depending on temperature and duration. *Cell Death Differ.* **11,** 1213-1222.

Dunn, S.R. and Weis, V.M. (2009). Apoptosis as a post-phagocytic winnowing mechanism in a coral-dinoflagellate mutualism. *Environ. Microbiol.* **11,** 268-276.

Dykstra, M., Cherukuri, A., Sohn, H.W., Tzeng, S.-J. and Pierce, S.K. (2003). Location is everything: lipid rafts and immune cell signaling. *Annu. Rev. Immunol.* **21,** 457-481.

Edgar, R.C. (2004). MUSCLE: multiple sequence alignment with high accuracy and high throughput. *Nucleic Acids Res.* **32,** 1792-1797.

Edmunds, P., Gates, R. and Gleason, D. (2001). The biology of larvae from the reef coral *Porites astreoides*, and their response to temperature disturbances. *Mar. Biol.* **139,** 981-989.

Edmunds, P.J., Gates, R.D., Leggat, W., Hoegh-Guldberg, O. and Allen-Requa, L. (2005). The effect of temperature on the size and population density of dinoflagellates in larvae of the reef coral *Porites astreoides*. *Invertebr. Biol.* **124,** 185-193.

Fallon, J., Kelly, J. and Kavanagh, K. (2012) *Galleria mellonella* as a model for fungal pathogenicity testing. In *Host-Fungus Interactions*. Springer, pp. 469-485.

Fang, L.-S., Wang, J.-T. and Lin, K.-L. (1998). The subcellular mechanism of the release of zooxanthellae during coral bleaching. *Proc. Natl. Sci. Counc. Rep. China Pt. B Life Sci.* **22,** 150-158.

Fang, L.S., Huang, S.P. and Lin, K.L. (1997). High temperature induces the synthesis of heat-shock proteins and the elevation of intracellular calcium in the coral *Acropora grandis*. *Coral Reefs* **16,** 127-131.

Fay, S.A. and Weber, M.X. (2012). The occurrence of mixed infections of *Symbiodinium* (Dinoflagellata) within individual hosts. *J. Phycol.* **48,** 1306-1316.

Feng, Y. and Walsh, C.A. (2004). The many faces of filamin: a versatile molecular scaffold for cell motility and signalling. *Nat. Cell Biol.* **6,** 1034-1038.

Fitt, W., McFarland, F., Warner, M. and Chilcoat, G. (2000). Seasonal patterns of tissue biomass and densities of symbiotic dinoflagellates in reef corals and relation to coral bleaching. *Limnol. Oceanogr.* **45,** 677-685.

Flannagan, R.S., Jaumouillé, V. and Grinstein, S. (2012). The cell biology of phagocytosis. *Annu. Rev. Pathol.* **7,** 61-98.

Florio, T., Arena, S., Pattarozzi, A., Thellung, S., Corsaro, A., Villa, V., *et al.* (2003). Basic fibroblast growth factor activates endothelial nitric-oxide synthase in CHO-K1 cells via the activation of ceramide synthesis. *Mol. Pharmacol.* **63,** 297-310.

Ganot, P., Moya, A., Magnone, V., Allemand, D., Furla, P. and Sabourault, C. (2011). Adaptations to endosymbiosis in a cnidarian-dinoflagellate association: differential gene expression and specific gene duplications. *PLoS Genet.* **7,** e1002187.

Garrett, T.A., Schmeitzel, J.L., Klein, J.A., Hwang, J.J. and Schwarz, J.A. (2013). Comparative lipid profiling of the cnidarian *Aiptasia pallida* and its dinoflagellate symbiont. *PLoS One* **8,** e57975.

Gates, R. and Muscatine, L. (1992a). Three methods for isolating viable anthozoan endoderm cells with their intracellular symbiotic dinoflagellates. *Coral Reefs* **11,** 143-145.

Gates, R.D., Baghdasarian, G. and Muscatine, L. (1992b). Temperature stress causes host cell detachment in symbiotic cnidarians: Implications for coral bleaching. *Biol. Bull.* **182,** 324-332.

Gates, R.D. and Edmunds, P.J. (1999). The physiological mechanisms of acclimatization in tropical reef corals. *Am. Zool.* **39,** 30-43.

Glynn, P.W. (1983). Extensive 'bleaching'and death of reef corals on the Pacific coast of Panama. *Environ. Conserv.* **10,** 149-154.

Goetzl, E.J. and An, S. (1998). Diversity of cellular receptors and functions for the lysophospholipid growth factors lysophosphatidic acid and sphingosine 1-phosphate. *The FASEB Journal* **12,** 1589-1598.

Goldkorn, T., Dressler, K.A., Muindi, J., Radin, N.S., Mendelsohn, J., Menaldino, D., *et al.* (1991). Ceramide stimulates epidermal growth factor receptor phosphorylation in A431 human epidermoid carcinoma cells. Evidence that ceramide may mediate sphingosine action. *J. Biol. Chem.* **266,** 16092-16097.

Gomez-Brouchet, A., Pchejetski, D., Brizuela, L., Garcia, V., Altie, M.-F., Maddelein, M.-L., *et al.* (2007). Critical role for sphingosine kinase-1 in regulating survival of neuroblastoma cells exposed to amyloid-β peptide. *Mol. Pharmacol.* **72,** 341-349.

Grajales, A. and Rodriguez, E. (2014). Morphological revision of the genus *Aiptasia* and the family Aiptasiidae (Cnidaria, Actiniaria, Metridioidea). *Zootaxa* **3826,** 55-100.

Grajales, A. and Rodríguez, E. (2016). Elucidating the evolutionary relationships of the Aiptasiidae, a widespread cnidarian–dinoflagellate model system (Cnidaria: Anthozoa: Actiniaria: Metridioidea). *Mol. Phylogenet. Evol.* **94,** 252-263.

Graner, M.W., Cumming, R.I. and Bigner, D.D. (2007). The heat shock response and chaperones/heat shock proteins in brain tumors: surface expression, release, and possible immune consequences. *J. Neurosci.* **27,** 11214-11227.

Grasso, L., Negri, A., Foret, S., Saint, R., Hayward, D., Miller, D. and Ball, E. (2011). The biology of coral metamorphosis: Molecular responses of larvae to inducers of settlement and metamorphosis. *Dev. Biol.* **353,** 411-419.

Guillard, R.R.L. and Ryther, J.H. (1962). Studies of marine planktonic diatoms I. *Cyclotella nana* Hustedt and *Detonula confervacea* Cleve. . *Can. J. Microbiol.* **8,** 229-239.

Hakogi, T., Shigenari, T., Katsumura, S., Sano, T., Kohno, T. and Igarashi, Y. (2003). Synthesis of fluorescence-labeled sphingosine and sphingosine 1-phosphate; effective tools for sphingosine and sphingosine 1-phosphate behavior. *Biorg. Med. Chem. Lett.* **13,** 661-664.

Hakomori, S.I., Yamamura, S. and Handa, K. (1998). Signal transduction through glyco (sphingo) lipids: Introduction and recent studies on glyco (sphingo) lipid‐enriched microdomains. *Ann. N.Y. Acad. Sci.* **845,** 1-10.

Hamada, M., Shoguchi, E., Shinzato, C., Kawashima, T., Miller, D.J. and Satoh, N. (2012). The complex NOD-like receptor repertoire of the coral *Acropora digitifera* includes novel domain combinations. *Mol. Biol. Evol.* **30,** 167-176.

Hambleton, E.A., Guse, A. and Pringle, J.R. (2014). Similar specificities of symbiont uptake by adults and larvae in an anemone model system for coral biology. *J. Exp. Biol.* **217,** 1613-1619.

Hanes, S.D. and Kempf, S.C. (2013). Host autophagic degradation and associated symbiont loss in response to heat stress in the symbiotic anemone, *Aiptasia pallida*. *Invertebr. Biol.* **132,** 95-107.

Hannun, Y.A. and Obeid, L.M. (2008). Principles of bioactive lipid signalling: lessons from sphingolipids. *Nat. Rev. Mol. Cell Biol.* **9,** 139-150.

Harii, S., Yasuda, N., Rodriguez-Lanetty, M., Irie, T. and Hidaka, M. (2009). Onset of symbiosis and distribution patterns of symbiotic dinoflagellates in the larvae of scleractinian corals. *Mar. Biol.* **156,** 1203-1212.

Hawkins, T., Krueger, T., Becker, S., Fisher, P. and Davy, S. (2014). Differential nitric oxide synthesis and host apoptotic events correlate with bleaching susceptibility in reef corals. *Coral Reefs* **33,** 141-153.

Hawkins, T.D., Bradley, B.J. and Davy, S.K. (2013). Nitric oxide mediates coral bleaching through an apoptotic-like cell death pathway: evidence from a model sea anemone-dinoflagellate symbiosis. *FASEB J.* **27,** 4790-4798.

Hawkins, T.D. and Davy, S.K. (2012). Nitric oxide production and tolerance differ among *Symbiodinium t*ypes exposed to heat stress. *Plant Cell Physiol.* **53,** 1889-1898.

Hayward, D.C., Hetherington, S., Behm, C.A., Grasso, L.C., Forêt, S., Miller, D.J. and Ball, E.E. (2011). Differential gene expression at coral settlement and metamorphosis—a subtractive hybridization study. *PLoS One* **6,** e26411.

Hemond, E.M., Kaluziak, S.T. and Vollmer, S.V. (2014). The genetics of colony form and function in Caribbean Acropora corals. *BMC Genomics* **15,** 1133.

Henikoff, S. and Henikoff, J.G. (1992). Amino acid substitution matrices from protein blocks. *Proc. Natl. Acad. Sci. USA* **89,** 10915-10919.

Heung, L.J., Luberto, C. and Del Poeta, M. (2006). Role of sphingolipids in microbial pathogenesis. *Infect. Immun.* **74,** 28-39.

Heyward, A. and Negri, A. (2010). Plasticity of larval pre-competency in response to temperature: observations on multiple broadcast spawning coral species. *Coral Reefs* **29,** 631-636.

Hill, R., Fernance, C., Wilkinson, S.P., Davy, S.K. and Scott, A. (2014). Symbiont shuffling during thermal bleaching and recovery in the sea anemone *Entacmaea quadricolor*. *Mar. Biol.* **161,** 2931-2937.

Hill, R., Ulstrup, K.E. and Ralph, P.J. (2009). Temperature induced changes in thylakoid membrane thermostability of cultured, freshly isolated, and expelled zooxanthellae from scleractinian corals. *Bull. Mar. Sci.* **85,** 223-244.

Hoegh-Guldberg, O. (1999). Climate change, coral bleaching and the future of the world's coral reefs. *Marine and Freshwater Research* **50,** 839-866.

Hoegh-Guldberg, O., Mumby, P.J., Hooten, A.J., Steneck, R.S., Greenfield, P., Gomez, E., *et al.* (2007). Coral reefs under rapid climate change and ocean acidification. *Science* **318,** 1737-1742.

Hoffmann, J.A., Kafatos, F.C., Janeway, C.A. and Ezekowitz, R.A.B. (1999). Phylogenetic perspectives in innate immunity. *Science* **284,** 1313-1318.

Hofmann, G.E. and Todgham, A.E. (2010). Living in the now: physiological mechanisms to tolerate a rapidly changing environment. *Annu. Rev. Physiol.* **72,** 127-145.

Huang, D., Sherman, B., Tan, Q., Collins, J., Alvord, G., Roayaei, J., *et al.* (2007). The DAVID Gene Functional Classification Tool: a novel biological module-centric algorithm to functionally analyze large gene lists. *Genome Biol.* **8,** 183.

Huang, S.P., Lin, K.L. and Fang, L.S. (1998). The involvement of calcium in heat-induced coral bleaching. *Zool. Stud.* **37,** 89-94.

Hughes, T.P., Baird, A.H., Bellwood, D.R., Card, M., Connolly, S.R., Folke, C., *et al.* (2003). Climate change, human impacts, and the resilience of coral reefs. *Science* **301,** 929-933.

Hume, B., D'Angelo, C., Smith, E., Stevens, J., Burt, J. and Wiedenmann, J. (2015). *Symbiodinium thermophilum* sp. nov., a thermotolerant symbiotic alga prevalent in corals of the world's hottest sea, the Persian/Arabian Gulf. *Sci. Rep.* **5**.

Igarashi, N., Okada, T., Hayashi, S., Fujita, T., Jahangeer, S. and Nakamura, S.-i. (2003). Sphingosine kinase 2 is a nuclear protein and inhibits DNA synthesis. *J. Biol. Chem.* **278,** 46832-46839.

Imbs, A.B. (2014). Lipid class and fatty acid compositions of the zoanthid *Palythoa caesia* (Anthozoa: Hexacorallia: Zoanthidea) and its chemotaxonomic relations with corals. *Biochem. Syst. Ecol.* **54,** 213-218.

Imbs, A.B., Yakovleva, I.M. and Pham, L.Q. (2010). Distribution of lipids and fatty acids in the zooxanthellae and host of the soft coral *Sinularia* sp. *Fish. Sci.* **76,** 375-380.

Iwaki, S., Kihara, A., Sano, T. and Igarashi, Y. (2005). Phosphorylation by Pho85 cyclin-dependent kinase acts as a signal for the down-regulation of the yeast sphingoid long-chain base kinase Lcb4 during the stationary phase. *J. Biol. Chem.* **280,** 6520-6527.

Jeffrey, S. and Haxo, F. (1968). Photosynthetic pigments of symbiotic dinoflagellates (zooxanthellae) from corals and clams. *Biol. Bull.* **135,** 149-165.

Jeffrey, S. and Humphrey, G. (1975). New spectrophotometric equations for determining chlorophylls *a, b, c1* and *c2* in higher plants, algae and natural phytoplankton. *Biochem Physiol Pflanz BPP***,** 191-194.

Jenkins, G. (2003). The emerging role for sphingolipids in the eukaryotic heat shock response. *Cell. Mol. Life Sci.* **60,** 701-710.

Jenkins, G.M., Cowart, L.A., Signorelli, P., Pettus, B.J., Chalfant, C.E. and Hannun, Y.A. (2002). Acute activation of de novo sphingolipid biosynthesis upon heat shock causes an accumulation of ceramide and subsequent dephosphorylation of SR proteins. *J. Biol. Chem.* **277,** 42572-42578.

Jenkins, G.M. and Hannun, Y.A. (2001). Role for de novo sphingoid base biosynthesis in the heat-induced transient cell cycle arrest of *Saccharomyces cerevisiae*. *J. Biol. Chem.* **276,** 8574-8581.

Jenkins, G.M., Richards, A., Wahl, T., Mao, C., Obeid, L. and Hannun, Y. (1997). Involvement of yeast sphingolipids in the heat stress response of *Saccharomyces cerevisiae*. *J. Biol. Chem.* **272,** 32566-32572.

Jeon, S.-B., Yoon, H.J., Park, S.-H., Kim, I.-H. and Park, E.J. (2008). Sulfatide, a major lipid component of myelin sheath, activates inflammatory responses as an endogenous stimulator in brain-resident immune cells. *J. Immunol.* **181,** 8077-8087.

Jones, G.P., McCormick, M.I., Srinivasan, M. and Eagle, J.V. (2004). Coral decline threatens fish biodiversity in marine reserves. *Proc. Natl. Acad. Sci. USA* **101,** 8251-8253.

Jones, P., Binns, D., Chang, H.-Y., Fraser, M., Li, W., McAnulla, C., *et al.* (2014). InterProScan 5: genome-scale protein function classification. *Bioinformatics* **30,** 1236-1240.

Jones, R.J. (1997). Changes in zooxanthellar densities and chlorophyll concentrations in corals during and after a bleaching event. *Mar. Ecol. Prog. Ser.* **158,** 51-59.

Juliano, C.E., Reich, A., Liu, N., Götzfried, J., Zhong, M., Uman, S., *et al.* (2014). PIWI proteins and PIWI-interacting RNAs function in *Hydra* somatic stem cells. *Proc. Natl. Acad. Sci. USA* **111,** 337-342.

Kassmer, S.H., Rodriguez, D., Langenbacher, A.D., Bui, C. and De Tomaso, A.W. (2015). Migration of germline progenitor cells is directed by sphingosine-1-phosphate signalling in a basal chordate. *Nat. Commun.* **6,** 8565.

Kawamura, H., Tatei, K., Nonaka, T., Obinata, H., Hattori, T., Ogawa, A., *et al.* (2009). Ceramide induces myogenic differentiation and apoptosis in *Drosophila* Schneider cells. *J. Radiat. Res. (Tokyo)* **50,** 161-169.

Kearse, M., Moir, R., Wilson, A., Stones-Havas, S., Cheung, M., Sturrock, S., *et al.* (2012). Geneious Basic: an integrated and extendable desktop software platform for the organization and analysis of sequence data. *Bioinformatics* **28,** 1647-1649.

Kelley, D.R. and Salzberg, S.L. (2010). Detection and correction of false segmental duplications caused by genome mis-assembly. *Genome Biol.* **11,** R28.

Kellogg, R.B. and Patton, J.S. (1983). Lipid droplets, medium of energy exchange in the symbiotic anemone *Condylactis gigantea*: a model coral polyp. *Mar. Biol.* **75,** 137-149.

Kenkel, C., Meyer, E. and Matz, M. (2013). Gene expression under chronic heat stress in populations of the mustard hill coral (*Porites astreoides*) from different thermal environments. *Mol. Ecol.* **22,** 4322-4334.

Kihara, A., Kurotsu, F., Sano, T., Iwaki, S. and Igarashi, Y. (2005). Long-chain base kinase Lcb4 Is anchored to the membrane through its palmitoylation by Akr1. *Mol. Cell. Biol.* **25,** 9189-9197.

Kitchen, S.A., Crowder, C.M., Poole, A.Z., Weis, V.M. and Meyer, E. (2015). *De novo* assembly and characterization of four anthozoan (Phylum Cnidaria) transcriptomes. *G3: Genes| Genomes| Genetics* **5,** 2441-2452.

Kohama, T., Olivera, A., Edsall, L., Nagiec, M.M., Dickson, R. and Spiegel, S. (1998). Molecular cloning and functional characterization of murine sphingosine kinase. *J. Biol. Chem.* **273,** 23722-23728.

Koles, K., Irvine, K.D. and Panin, V.M. (2004). Functional characterization of *Drosophila* sialyltransferase. *J. Biol. Chem.* **279,** 4346-4357.

Koul, A., Herget, T., Klebl, B. and Ullrich, A. (2004). Interplay between mycobacteria and host signalling pathways. *Nat Rev Micro* **2,** 189-202.

Kvennefors, E.C.E., Leggat, W., Kerr, C.C., Ainsworth, T.D., Hoegh-Guldberg, O. and Barnes, A.C. (2010). Analysis of evolutionarily conserved innate immune components in coral links immunity and symbiosis. *Dev. Comp. Immunol.* **34,** 1219-1229.

Langfelder, P. and Horvath, S. (2008a). WGCNA: an R package for weighted correlation network analysis. *BMC Bioinformatics* **9,** 559.

Langfelder, P., Zhang, B. and Horvath, S. (2008b). Defining clusters from a hierarchical cluster tree: the Dynamic Tree Cut package for R. *Bioinformatics* **24,** 719-720.

Langmead, B. and Salzberg, S.L. (2012). Fast gapped-read alignment with Bowtie 2. *Nat. Methods* **9,** 357-359.

Lanterman, M. and Saba, J. (1998). Characterization of sphingosine kinase (SK) activity in *Saccharomyces cerevisiae* and isolation of SK-deficient mutants. *Biochem. J* **332,** 525-531.

Le Stunff, H., Milstien, S. and Spiegel, S. (2004). Generation and metabolism of bioactive sphingosine-1-phosphate. *J. Cell. Biochem.* **92,** 882 - 899.

Le Stunff, H., Peterson, C., Thornton, R., Milstien, S., Mandala, S.M. and Spiegel, S. (2002). Characterization of murine sphingosine-1-phosphate phosphohydrolase. *J. Biol. Chem.* **277,** 8920-8927.

Lee, H.K., Braynen, W., Keshav, K. and Pavlidis, P. (2005). ErmineJ: tool for functional analysis of gene expression data sets. *BMC Bioinformatics* **6,** 269.

Lee, M.-J., Van Brocklyn, J.R., Thangada, S., Liu, C.H., Hand, A.R., Menzeleev, R., *et al.* (1998). Sphingosine-1-phosphate as a ligand for the G protein-coupled receptor EDG-1. *Science* **279,** 1552-1555.

Lee, S.Y., Jeong, H.J., Kang, N.S., Jang, T.Y., Jang, S.H. and Lajeunesse, T.C. (2015). *Symbiodinium tridacnidorum* sp. nov., a dinoflagellate common to Indo-Pacific giant clams, and a revised morphological description of *Symbiodinium microadriaticum* Freudenthal, emended Trench & Blank. *Eur. J. Phycol.* **50,** 155-172.

Lehnert, E.M., Burriesci, M.S. and Pringle, J.R. (2012). Developing the anemone *Aiptasia* as a tractable model for cnidarian-dinoflagellate symbiosis: the transcriptome of aposymbiotic *A. pallida*. *BMC Genomics* **13,** 271.

Lehnert, E.M., Mouchka, M.E., Burriesci, M.S., Gallo, N.D., Schwarz, J.A. and Pringle, J.R. (2014). Extensive differences in gene expression between symbiotic and aposymbiotic Cnidarians. *G3: Genes| Genomes| Genetics* **4,** 277-295.

Lesser, M.P. (1996). Elevated temperatures and ultraviolet radiation cause oxidative stress and inhibit photosynthesis in symbiotic dinoflagellates. *Limnol. Oceanogr.* **41,** 271-283.

Li, Y.-T. and Li, S.-C. (1999). Enzymatic hydrolysis of glycosphingolipids. *Anal. Biochem.* **273,** 1-11.

Libro, S., Kaluziak, S.T. and Vollmer, S.V. (2013). RNA-seq profiles of immune related genes in the staghorn coral *Acropora cervicornis* infected with White Band Disease. *PLoS One* **8,** e81821.

Lieser, B., Liebisch, G., Drobnik, W. and Schmitz, G. (2003). Quantification of sphingosine and sphinganine from crude lipid extracts by HPLC electrospray ionization tandem mass spectrometry. *J. Lipid Res.* **44,** 2209-2216.

Liew, Y.J., Aranda, M., Carr, A., Baumgarten, S., Zoccola, D., Tambutté, S., *et al.* (2014). Identification of microRNAs in the coral *Stylophora pistillata*. *PLoS One* **9,** e91101.

Little, A.F., Van Oppen, M.J. and Willis, B.L. (2004). Flexibility in algal endosymbioses shapes growth in reef corals. *Science* **304,** 1492-1494.

Liu, H., Sugiura, M., Nava, V.E., Edsall, L.C., Kono, K., Poulton, S., *et al.* (2000). Molecular cloning and functional characterization of a novel mammalian sphingosine kinase type 2 isoform. *J. Biol. Chem.* **275,** 19513-19520.

Livak, K.J. and Schmittgen, T.D. (2001). Analysis of relative gene expression data using real-time quantitative PCR and the $2^{-\Delta\Delta CT}$ method. *Methods* **25,** 402-408.

Lloyd-Evans, E., Morgan, A.J., He, X., Smith, D.A., Elliot-Smith, E., Sillence, D.J., *et al.* (2008). Niemann-Pick disease type C1 is a sphingosine storage disease that causes deregulation of lysosomal calcium. *Nat. Med.* **14,** 1247-1255.

Loram, J.E., Boonham, N., O'Toole, P., Trapido-Rosenthal, H.G. and Douglas, A.E. (2007). Molecular quantification of symbiotic dinoflagellate algae of the genus *Symbiodinium*. *Biol. Bull.* **212,** 259-268.

Love, M.I., Huber, W. and Anders, S. (2014). Moderated estimation of fold change and dispersion for RNA-seq data with DESeq2. *Genome Biol.* **15,** 550.

Loya, Sakai, Yamazato, Nakano, Sambali and Van, W. (2001). Coral bleaching: the winners and the losers. *Ecol. Lett.* **4,** 122-131.

Luo, F., Yang, Y., Zhong, J., Gao, H., Khan, L., Thompson, D.K. and Zhou, J. (2007). Constructing gene co-expression networks and predicting functions of unknown genes by random matrix theory. *BMC Bioinformatics* **8,** 299.

Maceyka, M., Milstien, S. and Spiegel, S. (2007). Shooting the messenger: oxidative stress regulates sphingosine-1-phosphate. *Circ. Res.* **100,** 7-9.

Maceyka, M., Payne, S.G., Milstien, S. and Spiegel, S. (2002). Sphingosine kinase, sphingosine-1-phosphate, and apoptosis. *Biochim. Biophys. Acta* **1585,** 193 - 201.

Maceyka, M., Sankala, H., Hait, N.C., Le Stunff, H., Liu, H., Toman, R., *et al.* (2005). SphK1 and SphK2, sphingosine kinase isoenzymes with opposing functions in sphingolipid metabolism. *J. Biol. Chem.* **280,** 37118-37129.

Malik, Z.A., Thompson, C.R., Hashimi, S., Porter, B., Iyer, S.S. and Kusner, D.J. (2003). Cutting edge: *Mycobacterium tuberculosis* blocks Ca2+ signaling and phagosome maturation in human macrophages via specific inhibition of sphingosine kinase. *J. Immunol.* **170,** 2811-2815.

Mandala, S.M., Thornton, R., Galve-Roperh, I., Poulton, S., Peterson, C., Olivera, A., *et al.* (2000). Molecular cloning and characterization of a lipid phosphohydrolase that degrades sphingosine-1-phosphate and induces cell death. *Proc. Natl. Acad. Sci. USA* **97,** 7859-7864.

Mandala, S.M., Thornton, R., Tu, Z., Kurtz, M.B., Nickels, J., Broach, J., *et al.* (1998). Sphingoid base 1-phosphate phosphatase: a key regulator of sphingolipid metabolism and stress response. *Proc. Natl. Acad. Sci. USA* **95,** 150-155.

Mañes, S., del Real, G. and Martínez-A, C. (2003). Pathogens: raft hijackers. *Nat. Rev. Immunol.* **3,** 557-568.

Mao, C., Saba, J. and Obeid, L. (1999). The dihydrosphingosine-1-phosphate phosphatases of *Saccharomyces cerevisiae* are important regulators of cell proliferation and heat stress responses. *Biochem. J* **342,** 667-675.

Martin, M. (2011). Cutadapt removes adapter sequences from high-throughput sequencing reads. *EMBnet. journal* **17,** pp. 10-12.

Matthews, J.L., Sproles, A.E., Oakley, C.A., Grossman, A.R., Weis, V.M. and Davy, S.K. (2015). Menthol-induced bleaching rapidly and effectively provides experimental aposymbiotic sea anemones (*Aiptasia* sp.) for symbiosis investigations. *J. Exp. Biol.***,** jeb.128934.

Mayfield, A.B., Hirst, M.B. and Gates, R.D. (2009). Gene expression normalization in a dual‐compartment system: a real‐time quantitative polymerase chain reaction protocol for symbiotic anthozoans. *Mol. Ecol. Resour.* **9,** 462-470.

Mayfield, A.B., Wang, L.-H., Tang, P.-C., Fan, T.-Y., Hsiao, Y.-Y., Tsai, C.-L. and Chen, C.-S. (2011). Assessing the impacts of experimentally elevated temperature on the biological composition and molecular chaperone gene expression of a reef coral. *PLoS One* **6,** e26529.

McGinty, E.S., Pieczonka, J. and Mydlarz, L.D. (2012). Variations in reactive oxygen release and antioxidant activity in multiple *Symbiodinium* types in response to elevated temperature. *Microb. Ecol.* **64,** 1000-1007.

McIlroy, S., Smith, G. and Geller, J. (2014). FISH-Flow: a quantitative molecular approach for describing mixed clade communities of *Symbiodinium*. *Coral Reefs* **33,** 157-167.

Mendel, J., Heinecke, K., Fyrst, H. and Saba, J.D. (2003). Sphingosine phosphate lyase expression is essential for normal development in *Caenorhabditis elegans*. *J. Biol. Chem.* **278,** 22341-22349.

Meng, X., Yuan, Y., Maestas, A. and Shen, Z. (2004). Recovery from DNA damage-induced G2 arrest requires actin-binding protein filamin-A/actin-binding protein 280. *J. Biol. Chem.* **279,** 6098-6105.

Metpally, R.P. and Sowdhamini, R. (2005). Cross genome phylogenetic analysis of human and *Drosophila* G protein-coupled receptors: application to functional annotation of orphan receptors. *BMC Genomics* **6,** 106.

Meyer, E., Aglyamova, G.V. and Matz, M.V. (2011). Profiling gene expression responses of coral larvae (*Acropora millepora*) to elevated temperature and settlement inducers using a novel RNA-Seq procedure. *Mol. Ecol.* **20,** 3599-3616.

Meyer, E. and Weis, V.M. (2012). Study of cnidarian-algal symbiosis in the "omics" age. *Biol. Bull.* **223,** 44-65.

Meyer zu Heringdorf, D., Liliom, K., Schaefer, M., Danneberg, K., Jaggar, J.H., Tigyi, G. and Jakobs, K.H. (2003). Photolysis of intracellular caged sphingosine-1-phosphate causes Ca2+ mobilization independently of G-protein-coupled receptors. *FEBS Lett.* **554,** 443-449.

Mieog, J.C., van Oppen, M.J., Berkelmans, R., Stam, W.T. and Olsen, J.L. (2009). Quantification of algal endosymbionts (*Symbiodinium*) in coral tissue using real-time PCR. *Mol. Ecol. Resour.* **9,** 74-82.

Mieog, J.C., van Oppen, M.J., Cantin, N.E., Stam, W.T. and Olsen, J.L. (2007). Real-time PCR reveals a high incidence of *Symbiodinium* clade D at low levels in four scleractinian corals across the Great Barrier Reef: implications for symbiont shuffling. *Coral Reefs* **26,** 449-457.

Miller, D.J., Hemmrich, G., Ball, E.E., Hayward, D.C., Khalturin, K., Funayama, N., *et al.* (2007). The innate immune repertoire in Cnidaria-ancestral complexity and stochastic gene loss. *Genome Biol.* **8,** R59.

Miyazaki, Y., Oka, S., Yamaguchi, S., Mizuno, S. and Yano, I. (1995). Stimulation of phagocytosis and phagosome-lysosome fusion by glycosphingolipids from *Sphingomonas paucimobilis*. *J. Biochem.* **118,** 271-277.

Monick, M.M., Cameron, K., Powers, L.S., Butler, N.S., McCoy, D., Mallampalli, R.K. and Hunninghake, G.W. (2004). Sphingosine kinase mediates activation of extracellular signal–related kinase and Akt by Respiratory Syncytial Virus. *Am. J. Respir. Cell Mol. Biol.* **30,** 844-852.

Morimoto, R. (1993). Cells in stress: transcriptional activation of heat shock genes. *Science (New York, NY)* **259,** 1409.

Müller, W.A. and Leitz, T. (2002). Metamorphosis in the Cnidaria. *Can. J. Zool.* **80,** 1755-1771.

Munday, P., Leis, J., Lough, J., Paris, C., Kingsford, M., Berumen, M. and Lambrechts, J. (2009). Climate change and coral reef connectivity. *Coral Reefs* **28,** 379-395.

Murate, T., Banno, Y., Keiko, T., Watanabe, K., Mori, N., Wada, A., *et al.* (2001). Cell type-specific localization of sphingosine kinase 1a in human tissues. *J. Histochem. Cytochem.* **49,** 845-855.

Muscatine, L. and Cernichiari, E. (1969). Assimilation of photosynthetic products of zooxanthellae by a reef coral. *Biol. Bull.* **137,** 506-523.

Muscatine, L., Grossman, D. and Doino, J. (1991). Release of symbiotic algae by tropical sea anemones and corals after cold shock. *Mar. Ecol. Prog. Ser.* **77,** 233-243.

Nagai, K.-i., Takahashi, N., Moue, T. and Niimura, Y. (2011). Alteration of fatty acid molecular species in ceramide and glucosylceramide under heat stress and expression of sphingolipid-related genes. *Advances in Biological Chemistry* **1,** 35-48.

Nakanaga, K., Hama, K., Kano, K., Sato, T., Yukiura, H., Inoue, A., *et al.* (2014). Overexpression of autotaxin, a lysophosphatidic acid-producing enzyme, enhances cardia bifida induced by hypo-sphingosine-1-phosphate signaling in zebrafish embryo. *J. Biochem.* **155,** 235-241.

Nelson, R., Fessler, L., Takagi, Y., Blumberg, B., Keene, D., Olson, P., *et al.* (1994). Peroxidasin: a novel enzyme-matrix protein of *Drosophila* development. *EMBO J.* **13,** 3438.

Nii, C.M. and Muscatine, L. (1997). Oxidative stress in the symbiotic sea anemone *Aiptasia pulchella* (Carlgren, 1943): contribution of the animal to superoxide ion production at elevated temperature. *Biol. Bull.* **192,** 444-456.

Nordström, K.J., Fredriksson, R. and Schiöth, H.B. (2008). The amphioxus (*Branchiostoma floridae*) genome contains a highly diversified set of G protein-coupled receptors. *BMC Evol. Biol.* **8,** 9.

Nozawa, Y. and Harrison, P.L. (2007). Effects of elevated temperature on larval settlement and post-settlement survival in scleractinian corals, *Acropora solitaryensis* and *Favites chinensis*. *Mar. Biol.* **152,** 1181-1185.

Nunes, P. and Demaurex, N. (2010). The role of calcium signaling in phagocytosis. *J. Leukoc. Biol.* **88,** 57-68.

Nyholm, S.V. and McFall-Ngai, M. (2004). The winnowing: establishing the squid–*Vibrio* symbiosis. *Nat. Rev. Microbiol.* **2,** 632-642.

Ogawa, C., Kihara, A., Gokoh, M. and Igarashi, Y. (2003). Identification and characterization of a novel human sphingosine-1-phosphate phosphohydrolase, hSPP2. *J. Biol. Chem.* **278,** 1268-1272.

Olivera, A., Kohama, T., Edsall, L., Nava, V., Cuvillier, O., Poulton, S. and Spiegel, S. (1999). Sphingosine kinase expression increases intracellular sphingosine-1-phosphate and promotes cell growth and survival. *J. Cell Biol.* **147,** 545-558.

Olivera, A., Kohama, T., Tu, Z., Milstien, S. and Spiegel, S. (1998). Purification and characterization of rat kidney sphingosine kinase. *J. Biol. Chem.* **273,** 12576-12583.

Olivera, A., Rosenfeldt, H.M., Bektas, M., Wang, F., Ishii, I., Chun, J., *et al.* (2003). Sphingosine kinase type 1 induces G12/13-mediated stress fiber formation, yet promotes

growth and survival independent of G protein-coupled receptors. *J. Biol. Chem.* **278,** 46452-46460.

Olivera, A. and Spiegel, S. (2001). Sphingosine kinase: a mediator of vital cellular functions. *Prostaglandins Other Lipid Mediat.* **64,** 123-134.

Oren, M., Paz, G., Douek, J., Rosner, A., Amar, K.O. and Rinkevich, B. (2013). Marine invertebrates cross phyla comparisons reveal highly conserved immune machinery. *Immunobiology* **218,** 484-495.

Oskouian, B. and Saba, J.D. (2004). Death and taxis: what non-mammalian models tell us about sphingosine-1-phosphate. *Semin. Cell Dev. Biol.* **15,** 529-540.

Palmer, C.V. and Traylor-Knowles, N. (2012). Towards an integrated network of coral immune mechanisms. *Proc. R. Soc. Lond., Ser. B: Biol. Sci.* **279,** 4106-4114.

Pandolfi, J.M., Bradbury, R.H., Sala, E., Hughes, T.P., Bjorndal, K.A., Cooke, R.G., *et al.* (2003). Global trajectories of the long-term decline of coral reef ecosystems. *Science* **301,** 955-958.

Patton, J.S. and Burris, J.E. (1983). Lipid synthesis and extrusion by freshly isolated zooxanthellae (symbiotic algae). *Mar. Biol.* **75,** 131-136.

Paxton, C.W., Davy, S.K. and Weis, V.M. (2013). Stress and death of cnidarian host cells play a role in cnidarian bleaching. *J. Exp. Biol.* **216,** 2813-2820.

Pchejetski, D., Kunduzova, O., Dayon, A., Calise, D., Seguelas, M.-H., Leducq, N., *et al.* (2007). Oxidative stress–dependent sphingosine kinase-1 inhibition mediates monoamine oxidase A–associated cardiac cell apoptosis. *Circ. Res.* **100,** 41-49.

Peng, S.-E., Chen, W.-N.U., Chen, H.-K., Lu, C.-Y., Mayfield, A.B., Fang, L.-S. and Chen, C.-S. (2011). Lipid bodies in coral–dinoflagellate endosymbiosis: Proteomic and ultrastructural studies. *Proteomics* **11,** 3540-3555.

Perez, S. and Weis, V. (2006). Nitric oxide and cnidarian bleaching: an eviction notice mediates breakdown of a symbiosis. *J. Exp. Biol.* **209,** 2804-2810.

Perrotta, C., De Palma, C. and Clementi, E. (2008). Nitric oxide and sphingolipids: mechanisms of interaction and role in cellular pathophysiology. *Biol. Chem.* **389,** 1391-1397.

Phan, V.H., Herr, D.R., Panton, D., Fyrst, H., Saba, J.D. and Harris, G.L. (2007). Disruption of sphingolipid metabolism elicits apoptosis-associated reproductive defects in *Drosophila*. *Dev. Biol.* **309,** 329-341.

Pinzón, J.H., Kamel, B., Burge, C.A., Harvell, C.D., Medina, M., Weil, E. and Mydlarz, L.D. (2015). Whole transcriptome analysis reveals changes in expression of immune-

related genes during and after bleaching in a reef-building coral. *R. Soc. Open Sci.* **2,** 140214.

Pitson, S.M., Moretti, P.A., Zebol, J.R., Lynn, H.E., Xia, P., Vadas, M.A. and Wattenberg, B.W. (2003). Activation of sphingosine kinase 1 by ERK1/2‐mediated phosphorylation. *EMBO J.* **22,** 5491-5500.

Pitson, S.M., Moretti, P.A., Zebol, J.R., Xia, P., Gamble, J.R., Vadas, M.A., *et al.* (2000). Expression of a catalytically inactive sphingosine kinase mutant blocks agonist-induced sphingosine kinase activation A dominant-negative sphingosine kinase. *J. Biol. Chem.* **275,** 33945-33950.

Polato, N.R., Voolstra, C.R., Schnetzer, J., DeSalvo, M.K., Randall, C.J., Szmant, A.M., *et al.* (2010). Location-specific responses to thermal stress in larvae of the reef-building coral *Montastraea faveolata*. *PLoS One* **5,** e11221.

Poole, A.Z., Kitchen, S.A., Dow, E.G. and Weis, V.M. (submitted). The role of complement in cnidarian-dinoflagellate symbiosis and immune challenge in the sea anemone *Aiptasia pallida*. *Front. Microbiol.*

Poole, A.Z. and Weis, V.M. (2014). TIR-domain-containing protein repertoire of nine anthozoan species reveals coral–specific expansions and uncharacterized proteins. *Dev. Comp. Immunol.* **46,** 480-488.

Portune, K.J., Voolstra, C.R., Medina, M.n. and Szmant, A.M. (2010). Development and heat stress-induced transcriptomic changes during embryogenesis of the scleractinian coral *Acropora palmata*. *Mar. Genomics* **3,** 51-62.

Prakash, H., Luth, A., Grinkina, N., Holzer, D., Wadgaonkar, R., Gonzalez, A.P., *et al.* (2010). Sphingosine kinase-1 (SphK-1) regulates *Mycobacterium smegmatis* infection in macrophages. *PLoS One* **5,** e10657.

Pratchett, M.S., Wilson, S.K., Graham, N.A.J., Munday, P.L., Jones, G.P. and Polunin, N.V.C. (2009) Coral bleaching and consequences for motile reef organisms: past, present, and uncertain future effects. In *Coral Bleching: patterns and processes, causes and consequences*. Heidelberg, Springer, pp. 139-158.

Puill-Stephan, E., Seneca, F.O., Miller, D.J., van Oppen, M.J. and Willis, B.L. (2012). Expression of putative immune response genes during early ontogeny in the coral *Acropora millepora*. *PLoS One* **7,** e39099.

Putnam, H.M., Edmunds, P.J. and Fan, T.-Y. (2008). Effect of temperature on the settlement choice and photophysiology of larvae from the reef coral *Stylophora pistillata*. *Biol. Bull.* **215,** 135-142.

Putnam, N.H., Srivastava, M., Hellsten, U., Dirks, B., Chapman, J., Salamov, A., *et al.* (2007). Sea anemone genome reveals ancestral eumetazoan gene repertoire and genomic organization. *Science* **317,** 86-94.

Quigley, K.M., Davies, S.W., Kenkel, C.D., Willis, B.L., Matz, M.V. and Bay, L.K. (2014). Deep-sequencing method for quantifying background abundances of *Symbiodinium* types: exploring the rare *Symbiodinium* biosphere in reef-building corals. *PLoS One* **9,** e94297.

Quinlan, A.R. and Hall, I.M. (2010). BEDTools: a flexible suite of utilities for comparing genomic features. *Bioinformatics* **26,** 841-842.

Ramakers, C., Ruijter, J.M., Deprez, R.H. and Moorman, A.F. (2003). Assumption-free analysis of quantitative real-time polymerase chain reaction (PCR) data. *Neurosci. Lett.* **339,** 62 - 66.

Randall, C. and Szmant, A. (2009a). Elevated temperature reduces survivorship and settlement of the larvae of the Caribbean scleractinian coral, *Favia fragum* (Esper). *Coral Reefs* **28,** 537-545.

Randall, C.J. and Szmant, A.M. (2009b). Elevated temperature affects development, survivorship, and settlement of the elkhorn coral, *Acropora palmata* (Lamarck 1816). *Biol. Bull.* **217,** 269-282.

Rasband, W. (1997-2015) ImageJ. Bethesda, Maryland, USA, U. S. National Institutes of Health

RCoreTeam (2013) R: A language and environment for statistical computing. Vienna, Austria, R Foundation for Statistical Computing.

Reitzel, A.M., Sullivan, J.C., Traylor-Knowles, N. and Finnerty, J.R. (2008). Genomic survey of candidate stress-response genes in the estuarine anemone *Nematostella vectensis*. *Biol. Bull.* **214,** 233-254.

Ren, J., Wen, L., Gao, X., Jin, C., Xue, Y. and Yao, X. (2009). DOG 1.0: illustrator of protein domain structures. *Cell Res.* **19,** 271-273.

Renault, A.D., Starz-Gaiano, M. and Lehmann, R. (2002). Metabolism of sphingosine 1-phosphate and lysophosphatidic acid: a genome wide analysis of gene expression in *Drosophila*. *Mech. Dev.* **119,** S293-S301.

Revel, J., Massi, L., Mehiri, M., Boutoute, M., Mayzaud, P., Capron, L. and Sabourault, C. (2016). Differential distribution of lipids in epidermis, gastrodermis and hosted *Symbiodinium* in the sea anemone *Anemonia viridis*. *Comp. Biochem. Physiol., A: Mol. Integr. Physiol.* **191,** 140-151.

Richier, S., Sabourault, C., Courtiade, J., Zucchini, N., Allemand, D. and Furla, P. (2006). Oxidative stress and apoptotic events during thermal stress in the symbiotic sea anemone, *Anemonia viridis*. *FEBS J.* **273,** 4186-4198.

Richmond, R.H. (1990). Reproduction and recruitment of corals : comparisons among the Caribbean, the tropical Pacific, and the Red Sea. *Mar. Ecol. Prog. Ser.* **60,** 185-203.

Rivera, J., Proia, R.L. and Olivera, A. (2008). The alliance of sphingosine-1-phosphate and its receptors in immunity. *Nat. Rev. Immunol.* **8,** 753-763.

Roberts, C.M., McClean, C.J., Veron, J.E.N., Hawkins, J.P., Allen, G.R., McAllister, D.E., *et al.* (2002). Marine biodiversity hotspots and conservation priorities for tropical reefs. *Science* **295,** 1280-1284.

Rodriguez-Lanetty, M., Harii, S. and Hoegh-Guldberg, O.V.E. (2009). Early molecular responses of coral larvae to hyperthermal stress. *Mol. Ecol.* **18,** 5101-5114.

Rodriguez-Lanetty, M., Phillips, W. and Weis, V. (2006). Transcriptome analysis of a cnidarian - dinoflagellate mutualism reveals complex modulation of host gene expression. *BMC Genomics* **7,** 23.

Rodriguez-Lanetty, M., Phillips, W.S., Dove, S., Hoegh-Guldberg, O. and Weis, V.M. (2008). Analytical approach for selecting normalizing genes from a cDNA microarray platform to be used in q-RT-PCR assays: a cnidarian case study. *J. Biochem. Biophys. Methods* **70,** 985-991.

Roggentin, P., Schauer, R., Hoyer, L.L. and Vimr, E.R. (1993). The sialidase superfamily and its spread by horizontal gene transfer. *Mol. Microbiol.* **9,** 915-921.

Rosengarten, R.D. and Nicotra, M.L. (2011). Model systems of invertebrate allorecognition. *Curr. Biol.* **21,** R82-R92.

Rosic, N.N. and Hoegh-Guldberg, O. (2010). A method for extracting a high-quality RNA from *Symbiodinium* sp. *J. Appl. Phycol.* **22,** 139-146.

Ross, C. (2014). Nitric oxide and heat shock protein 90 co-regulate temperature-induced bleaching in the soft coral *Eunicea fusca*. *Coral Reefs* **33,** 513-522.

Rozen, S. and Skaletsky, H. (1999) Primer3 on the WWW for general users and for biologist programmers. In *Bioinformatics Methods and Protocols*. Springer, pp. 365-386.

Safavi-Hemami, H., Young, N.D., Doyle, J., Llewellyn, L. and Klueter, A. (2010). Characterisation of nitric oxide synthase in three cnidarian-dinoflagellate symbioses. *PLoS One* **5,** e10379-e10379.

Sandeman, I. (2006). Fragmentation of the gastrodermis and detachment of zooxanthellae in symbiotic cnidarians: a role for hydrogen peroxide and Ca2+ in coral bleaching and algal density control. *Rev. Biol. Trop.* **54,** 79-96.

Sanders, S.M., Shcheglovitova, M. and Cartwright, P. (2014). Differential gene expression between functionally specialized polyps of the colonial hydrozoan *Hydractinia symbiolongicarpus* (Phylum Cnidaria). *BMC Genomics* **15,** 406.

Sawyer, S.J. and Muscatine, L. (2001). Cellular mechanisms underlying temperature-induced bleaching in the tropical sea anemone A*iptasia pulchella*. *J. Exp. Biol.* **204,** 3443-3456.

Schnitzler, C., Hollingsworth, L., Krupp, D. and Weis, V. (2011). Elevated temperature impairs onset of symbiosis and reduces survivorship in larvae of the Hawaiian coral, *Fungia scutaria*. *Mar. Biol.* **159,** 633-642.

Schnitzler, C.E. and Weis, V.M. (2010). Coral larvae exhibit few measurable transcriptional changes during the onset of coral-dinoflagellate endosymbiosis. *Mar. Genomics* **3,** 107-116.

Schwab, S.R., Pereira, J.P., Matloubian, M., Xu, Y., Huang, Y. and Cyster, J.G. (2005). Lymphocyte sequestration through S1P lyase inhibition and disruption of S1P gradients. *Science* **309,** 1735-1739.

Schwarz, J.A., Krupp, D.A. and Weis, V.M. (1999). Late larval development and onset of symbiosis in the scleractinian coral *Fungia scutaria*. *Biol. Bull.* **196,** 70-79.

Seneca, F.O., Forêt, S., Ball, E.E., Smith-Keune, C., Miller, D.J. and van Oppen, M.J. (2010). Patterns of gene expression in a scleractinian coral undergoing natural bleaching. *Mar. Biotechnol.* **12,** 594-604.

Seo, Y.-J., Alexander, S. and Hahm, B. (2011). Does cytokine signaling link sphingolipid metabolism to host defense and immunity against virus infections? *Cytokine Growth Factor Rev.* **22,** 55-61.

Shaner, R.L., Allegood, J.C., Park, H., Wang, E., Kelly, S., Haynes, C.A., *et al.* (2009). Quantitative analysis of sphingolipids for lipidomics using triple quadrupole and quadrupole linear ion trap mass spectrometers. *J. Lipid Res.* **50,** 1692-1707.

Shannon, P., Markiel, A., Ozier, O., Baliga, N.S., Wang, J.T., Ramage, D., *et al.* (2003). Cytoscape: a software environment for integrated models of biomolecular interaction networks. *Genome Res.* **13,** 2498-2504.

Shinzato, C., Hamada, M., Shoguchi, E., Kawashima, T. and Satoh, N. (2012). The repertoire of chemical defense genes in the coral *Acropora digitifera* genome. *Zool. Sci.* **29,** 510-517.

Shinzato, C., Inoue, M. and Kusakabe, M. (2014). A snapshot of a coral "holobiont": a transcriptome assembly of the scleractinian coral, *Porites*, captures a wide variety of genes from both the host and symbiotic zooxanthellae. *PLoS One* **9,** e85182.

Shinzato, C., Shoguchi, E., Kawashima, T., Hamada, M., Hisata, K., Tanaka, M., *et al.* (2011). Using the *Acropora digitifera* genome to understand coral responses to environmental change. *Nature* **476,** 320-323.

Shpirer, E., Chang, E.S., Diamant, A., Rubinstein, N., Cartwright, P. and Huchon, D. (2014). Diversity and evolution of myxozoan minicollagens and nematogalectins. *BMC Evol. Biol.* **14,** 205.

Silverstein, R.N., Cunning, R. and Baker, A.C. (2015). Change in algal symbiont communities after bleaching, not prior heat exposure, increases heat tolerance of reef corals. *Glob. Chang. Biol.* **21,** 236-249.

Simon, G. and Rouser, G. (1967). Phospholipids of the sea anemone: Quantitative distribution; absence of carbon-phosphorus linkages in glycerol phospholipids; structural elucidation of ceramide aminoethylphosphonate. *Lipids* **2,** 55-59.

Spiegel, S. and Milstien, S. (2003). Sphingosine-1-phosphate: An enigmatic signaling lipid. *Nat. Rev. Mol. Cell Biol.* **4,** 397 - 407.

Spiegel, S. and Milstien, S. (2011). The outs and the ins of sphingosine-1-phosphate in immunity. *Nat. Rev. Immunol.* **11,** 403-415.

Starcevic, A., Dunlap, W.C., Cullum, J., Shick, J.M., Hranueli, D. and Long, P.F. (2010). Gene expression in the scleractinian Acropora microphthalma exposed to high solar irradiance reveals elements of photoprotection and coral bleaching. *PLoS One* **5,** e13975.

Starz-Gaiano, M., Cho, N.K., Forbes, A. and Lehmann, R. (2001). Spatially restricted activity of a *Drosophila* lipid phosphatase guides migrating germ cells. *Development* **128,** 983-991.

Steinberg, B.E. and Grinstein, S. (2008). Pathogen destruction versus intracellular survival: the role of lipids as phagosomal fate determinants. *J. Clin. Invest.* **118,** 2002-2011.

Stukey, J. and Carman, G.M. (1997). Identification of a novel phosphatase sequence motif. *Protein Sci.* **6,** 469-472.

Suggett, D.J., Warner, M.E., Smith, D.J., Davey, P., Hennige, S. and Baker, N.R. (2008). Photosynthesis and production of hydrogene perxoide by *Symbiodinim* (Pyrrophyta) phylotypes with different thermal tolerances *J. Phycol.* **44,** 948-956.

Sullivan, J., Kalaitzidis, D., Gilmore, T. and Finnerty, J. (2007). Rel homology domain-containing transcription factors in the cnidarian *Nematostella vectensis*. *Dev. Genes Evol.* **217,** 63-72.

Sunagawa, S., Wilson, E.C., Thaler, M., Smith, M.L., Caruso, C., Pringle, J.R., *et al.* (2009). Generation and analysis of transcriptomic resources for a model system on the rise: the sea anemone *Aiptasia pallida* and its dinoflagellate endosymbiont. *BMC Genomics* **10,** 258.

Suwa, R., Nakamura, M., Morita, M., Shimada, K., Iguchi, A., Sakai, K. and Suzuki, A. (2010). Effects of acidified seawater on early life stages of scleractinian corals (Genus *Acropora*). *Fish. Sci.* **76,** 93-99.

Tafesse, F.G., Rashidfarrokhi, A., Schmidt, F.I., Freinkman, E., Dougan, S., Dougan, M., *et al.* (2015). Disruption of sphingolipid biosynthesis blocks phagocytosis of *Candida albicans*. *PLoS Path.* **11,** e1005188.

Taris, N., Lang, R.P. and Camara, M.D. (2008). Sequence polymorphism can produce serious artefacts in real-time PCR assays: hard lessons from Pacific oysters. *BMC Genomics* **9,** 234.

Tchernov, D., Gorbunov, M.Y., de Vargas, C., Yadav, S.N., Milligan, A.J., Häggblom, M. and Falkowski, P.G. (2004). Membrane lipids of symbiotic algae are diagnostic of sensitivity to thermal bleaching in corals. *Proc. Natl. Acad. Sci. USA* **101,** 13531-13535.

Therneau, T. (2013) A package for survival analysis in S. R package version 2.37-4. pp. 23298-20032.

Thompson, C.R., Iyer, S.S., Melrose, N., VanOosten, R., Johnson, K., Pitson, S.M., *et al.* (2005). Sphingosine kinase 1 (SK1) is recruited to nascent phagosomes in human macrophages: inhibition of SK1 translocation by *Mycobacterium tuberculosis*. *J. Immunol.* **174,** 3551-3561.

Timmins-Schiffman, E. and Roberts, S. (2012). Characterization of genes involved in ceramide metabolism in the Pacific oyster (*Crassostrea gigas*). *BMC Res. Notes* **5,** 502.

Tolleter, D., Seneca, F.O., DeNofrio, J.C., Krediet, C.J., Palumbi, S.R., Pringle, J.R. and Grossman, A.R. (2013). Coral bleaching independent of photosynthetic activity. *Curr. Biol.* **23,** 1782-1786.

Trapnell, C., Pachter, L. and Salzberg, S.L. (2009). TopHat: discovering splice junctions with RNA-Seq. *Bioinformatics* **25,** 1105-1111.

Untergasser, A., Cutcutache, I., Koressaar, T., Ye, J., Faircloth, B.C., Remm, M. and Rozen, S.G. (2012). Primer3—new capabilities and interfaces. *Nucleic Acids Res.* **40,** e115.

van Brocklyn, J.R. and Williams, J.B. (2012). The control of the balance between ceramide and sphingosine-1-phosphate by sphingosine kinase: Oxidative stress and the seesaw of cell survival and death. *Comp. Biochem. Physiol. B Biochem. Mol. Biol.* **163,** 26-36.

van Oppen, M.J.H., Palstra, F.P., Piquet, A.M.T. and Miller, D.J. (2001). Patterns of coral-dinoflagellate associations in *Acropora*: significance of local availability and physiology of *Symbiodinium* strains and host-symbiont selectivity. *Proc. R. Soc. Lond., Ser. B: Biol. Sci.* **268,** 1759-1767.

van Woesik, R., Sakai, K., Ganase, A. and Loya, Y. (2011). Revisiting the winners and the losers a decade after coral bleaching. *Mar. Ecol. Prog. Ser.* **434,** 67-76.

Vandesompele, J., De Preter, K., Pattyn, F., Poppe, B., Van Roy, N., De Paepe, A. and Speleman, F. (2002). Accurate normalization of real-time quantitative RT-PCR data by geometric averaging of multiple internal control genes. *Genome Biol.* **3,** 1 - 11.

Venn, A.A., Loram, J.E. and Douglas, A.E. (2008). Photosynthetic symbioses in animals. *J. Exp. Bot.* **59,** 1069-1080.

Venn, A.A., Wilson, M.A., Trapido-Rosenthal, H.G., Keely, B.J. and Douglas, A.E. (2006). The impact of coral bleaching on the pigment profile of the symbiotic alga, *Symbiodinium*. *Plant, Cell Environ.* **29,** 2133-2142.

Vidal-Dupiol, J., Ladrière, O., Destoumieux-Garzón, D., Sautière, P.-E., Meistertzheim, A.-L., Tambutté, E., *et al.* (2011). Innate immune responses of a scleractinian coral to vibriosis. *J. Biol. Chem.* **286,** 22688-22698.

Voolstra, C., Schnetzer, J., Peshkin, L., Randall, C., Szmant, A. and Medina, M. (2009a). Effects of temperature on gene expression in embryos of the coral *Montastraea faveolata*. *BMC Genomics* **10,** 627.

Voolstra, C.R. (2013). A journey into the wild of the cnidarian model system *Aiptasia* and its symbionts. *Mol. Ecol.* **22,** 4366-4368.

Voolstra, C.R., Schwarz, J.A., Schnetzer, J., Sunagawa, S., Desalvo, M.K., Szmant, A.M., *et al.* (2009b). The host transcriptome remains unaltered during the establishment of coral–algal symbioses. *Mol. Ecol.* **18,** 1823-1833.

Wang, J., Meng, P., Sampayo, E., Tang, S. and Chen, C. (2011). Photosystem II breakdown induced by reactive oxygen species in freshly-isolated *Symbiodinium* from *Montipora* (Scleractinia; Acroporidae). *Mar. Ecol. Prog. Ser.* **422,** 51-62.

Warner, M.E., Fitt, W.K. and Schmidt, G.W. (1996). The effects of elevated temperature on the photosynthetic efficiency of zooxanthellae *in hospite* from four different species of reef coral: a novel approach. *Plant, Cell Environ.* **19,** 291-299.

Warner, M.E., Fitt, W.K. and Schmidt, G.W. (1999). Damage to photosystem II in symbiotic dinoflagellates: a determinant of coral bleaching. *Proc. Natl. Acad. Sci. USA* **96,** 8007-8012.

Wei, W.-C., Sung, P.-J., Duh, C.-Y., Chen, B.-W., Sheu, J.-H. and Yang, N.-S. (2013). Anti-inflammatory activities of natural products isolated from soft corals of Taiwan between 2008 and 2012. *Mar. Drugs* **11,** 4083-4126.

Weis, V.M. (2008). Cellular mechanisms of Cnidarian bleaching: stress causes the collapse of symbiosis. *J. Exp. Biol.* **211,** 3059-3066.

Weis, V.M. (2010). The susceptibility and resilience of corals to thermal stress: adaptation, acclimatization or both? *Mol. Ecol.* **19,** 1515-1517.

Weis, V.M. and Allemand, D. (2009). What determines coral health? *Science* **324,** 1153-1155.

Weis, V.M., Davy, S.K., Hoegh-Guldberg, O., Rodriguez-Lanetty, M. and Pringle, J.R. (2008). Cell biology in model systems as the key to understanding corals. *Trends Ecol. Evol.* **23,** 369-376.

Weis, V.M., Reynolds, W.S., deBoer, M.D. and Krupp, D.A. (2001a). Host-symbiont specificity during onset of symbiosis between the dinoflagellates *Symbiodinium* spp. and planula larvae of the scleractinian coral *Fungia scutaria*. *Coral Reefs* **20,** 301-308.

Weis, V.M., Reynolds, W.S. and Krupp, D.A. (2001b). Host-symbiont specificity during onset of symbiosis between the dinoflagellates Symbiodinium spp. and planula larvae of the scleractinian coral Fungia scutaria. *Coral Reefs* **20,** 301-308.

Weis, V.M., Verde, E.A., Pribyl, A. and Schwarz, J.A. (2002). Aspects of the larval biology of the sea anemones *Anthopleura elegantissima* and *A. artemisia*. *Invertebr. Biol.* **121,** 190-201.

Whitehead, L.F. and Douglas, A.E. (2003). Metabolite comparisons and the identity of nutrients translocated from symbiotic algae to an animal host. *J. Exp. Biol.* **206,** 3149-3157.

Wilson, W.H., Schroeder, D.C., Allen, M.J., Holden, M.T., Parkhill, J., Barrell, B.G., *et al.* (2005). Complete genome sequence and lytic phase transcription profile of a *Coccolithovirus*. *Science* **309,** 1090-1092.

Winkler, N.S., Pandolfi, J.M. and Sampayo, E.M. (2015). *Symbiodinium* identity alters the temperature-dependent settlement behaviour of *Acropora millepora* coral larvae before the onset of symbiosis. *Proc. R. Soc. Lond. B. Biol. Sci.* **282,** 20142260.

Wooldridge, S.A. (2010). Is the coral-algae symbiosis really 'mutually beneficial' for the partners? *Bioessays* **32,** 615-625.

Xia, P., Wang, L., Moretti, P.A., Albanese, N., Chai, F., Pitson, S.M., *et al.* (2002). Sphingosine kinase interacts with TRAF2 and dissects tumor necrosis factor-α signaling. *J. Biol. Chem.* **277,** 7996-8003.

Yabu, T., Imamura, S., Yamashita, M. and Okazaki, T. (2008). Identification of Mg2+-dependent neutral sphingomyelinase 1 as a mediator of heat stress-induced ceramide generation and apoptosis. *J. Biol. Chem.* **283,** 29971-29982.

Yadav, M., Clark, L. and Schorey, J.S. (2006). Macrophage's proinflammatory response to a mycobacterial infection is dependent on sphingosine kinase-mediated activation of phosphatidylinositol phospholipase C, protein kinase C, ERK1/2, and phosphatidylinositol 3-kinase. *J. Immunol.* **176,** 5494-5503.

Yakovleva, I.M., Baird, A.H., Yamamoto, H.H., Bhagooli, R., Nonaka, M. and Hidaka, M. (2009). Algal symbionts increase oxidative damage and death in coral larvae at high temperatures. *Mar. Ecol. Prog. Ser.* **378,** 105-112.

Yamashiro, H., Oku, H., Higa, H., Chinen, I. and Sakai, K. (1999). Composition of lipids, fatty acids and sterols in Okinawan corals. *Comp. Biochem. Physiol. B Biochem. Mol. Biol.* **122,** 397-407.

Yang, Y., Xiong, J., Zhou, Z., Huo, F., Miao, W., Ran, C., *et al.* (2014). The genome of the myxosporean *Thelohanellus kitauei* shows adaptations to nutrient acquisition within its fish host. *Genome Biol. Evol.* **6,** 3182-3198.

Yellowlees, D., Rees, T.A.V. and Leggat, W. (2008). Metabolic interactions between algal symbionts and invertebrate hosts. *Plant, Cell Environ.* **31,** 679-694.

Yeung, T. and Grinstein, S. (2007). Lipid signaling and the modulation of surface charge during phagocytosis. *Immunol. Rev.* **219,** 17-36.

Yu, G., Wang, L.-G., Han, Y. and He, Q.-Y. (2012). clusterProfiler: an R package for comparing biological themes among gene clusters. *OMICS: J. Integrative Biol.* **16,** 284-287.

Yuyama, I., Harii, S. and Hidaka, M. (2012). Algal symbiont type affects gene expression in juveniles of the coral *Acropora tenuis* exposed to thermal stress. *Mar. Environ. Res.* **76,** 41-47.

Zhang, H., Desai, N.N., Olivera, A., Seki, T., Brooker, G. and Spiegel, S. (1991). Sphingosine-1-phosphate, a novel lipid, involved in cellular proliferation. *J. Cell Biol.* **114,** 155-167.